

Synthesis and Antibacterial Profiling of Dehydroamino Acid Containing Argyrin Analogues

By Lei Yang, MSc

Thesis Submitted to the University of Nottingham for the degree of Doctor of Philosophy

Sept 2017

Abstract

The argyrins are a family of macrocyclic heptapeptides isolated from the marine myxobacterium *Archangium gephyra*. Among them, argyrin A **1.1** and B **1.2** displayed potent antibacterial activity against multidrug resistant Gram-negative human pathogen *Pseudomonas aeruginosa* and *Burkholderia multivorans*. The bacterial elongation factor G (EF-G) was identified as the conserved cellular target of argyrin A and B in *P. aeruginosa*.

The aim of this thesis was to synthesise argyrin analogues with improved antibacterial activity and therefore contributes to the structural activity relationship (SAR) of such analogues towards *P. aeruginosa* and *B. multivorans*. The total synthesis of argyrin analogues was achieved through a Fmoc/*t*Bu solid-phase peptide synthesis followed by a solution phase head-to-tail macrocyclisation.

The key building blocks, *N*-Boc-thiazole dipeptide **1.29**, substituted L-tryptophan analogues **1.44** and β-substituted Fmoc-dehydroamino acids were obtained by new synthetic procedures. In addition to the previously reported modified Hantzsch's approach, synthesis of the *N*-Boc-thiazole dipeptide **1.29** was also achieved by MnO_2-mediated oxidation of thiazolidine, pre-formed by condensation of L-cysteine with pyruvaldehyde, to thiazole. The asymmetric synthesis of substituted L-tryptophan analogues **1.44** was accomplished through the application of glycine-Ni(II) Schiff base **1.40**, which allowed the synthesis of argyrin analogues with various substituted L-tryptophans. The synthesis of Fmoc-dehydrobutyrine **1.55** and Fmoc-dehydrophenylalanine **1.56** were achieved through a pyridine mediated β-elimination of tosylated Fmoc-threonine and Fmoc-hydroxyphenylalanine, respectively. This thesis also reported a successful installation of four β-substituted Fmoc-dehydroamino

acids, Fmoc-dehydrobutyrine **1.55**, Fmoc-dehydrophenylalanine **1.56**, Fmoc-dehydrovaline **4.24** and Fmoc-dehydroleucine **4.25**, during Fmoc/*t*Bu solid-phase peptide synthesis for the replacement of dehydroalanine in argyrin.

The 4-Br-L-tryptophan dehydrobutyrine containing argyrin **4.42** was identified to have the most potent *in vitro* activity against *P. aeruginosa* and *B. multivorans*. Most importantly, the replacement of dehydroalanine residue with dehydrobutyrine improved the antibacterial activity of argyrin towards *P. aeruginosa* and *B. multivorans*. This finding indicates that dehydroamino acid not only control the planarity of the cyclic structure of argyrin but also play an important role in the interaction between argyrin and EF-G.

Acknowledgement

I am greatly thankful to my supervisor Dr. Weng Chan for his continuous supports, encouragements and guidance throughout my PhD study. Not only did he lead me to the field of peptide medicinal chemistry, but also provided me with useful advices regarding my project. I would like to thank Dr. Cristina De Matteis who gave me invaluable advices through my first year and second year viva.

I am especially thankful to all the present and past members of the medicinal chemistry division for their assistants. I am very grateful to Sivaneswary Genapathy for helping me understanding this project, helping me with the bioassay and organic reactions, and providing me with argyrin analogues for bioassay. I would like to thank all the present and past members of lab C22, Fabio Rui, Robert Hampson, Vivian Ng, and Paulina Bajko, who offered me invaluable suggestions and helped me every time when I came across problems with some reactions. I would like to thank all the members of lab C69, especially Ewan Murry, for helping me with bioassay. I would like to thank all the members from the Chemistry lab, Francesco Zamberlan, James Krupa, Alex Wichlaze, and Terry May, for their invaluable suggestions in some reactions.

I would like to express my grateful to my friends, Rosa Catina, Rui Gao, Zhimin Liu, Zhenyu Wang, Yidong Liu, Xue Wu, Xiaolu Pu, and Lili Shen. My life in Nottingham would not be colourful without them.

My PhD study could not be possible without the financial funding from my parents. I would like to express my greatly thankful to my parents, who raised me and encouraged me at every stage of my life.

Abbreviations

Acetone-d_6	Deuterated acetone
AMD	Activated manganese dioxide
AHL	Acyl homoserine lactone
Bcc	*Burkholderia cepacia* complex
BDSF	*Burkholderia* diffusible signal factor
Bn	Benzyl
Boc	*tert*-butoxycarbonyl
Boc_2O	Di-*tert*-butyl dicarbonate
br	broad
Cbz	Carboxybenzyl
CF	Cystic fibrosis
CGD	Chronic granulomatous disease
CFTR	Cystic fibrosis transmembrane regulator
CMD	Chemical manganese dioxide
COSY	Correlation spectroscopy
d	Doublet
DBU	1,8-Diazabicyclo[5.4.0]undec-7-ene
DCC	Dicyclohexylcarbodiimide
DCM	Dichloromethane
dd	Doublet of doublet
de	Diastereomeric excess
DEAD	Diethylazodicarboxylate
DhA	Dehydroalanine
DhB	Dehydrobutyrine
DhLeu	Dehydroleucine
DhPh	Dehydrophenylalanine

DhVal	Dehydrovaline
DIPEA	*N*,*N*-Diisopropylethylamine
DIW	Deionised water
DME	1,2, dimethoxyethane
DMF	*N,N*-dimethylformamide
DMSO	Dimethyl sulfoxide
DMSO-d_6	Deuterated dimethyl sulfoxide
dr	Diastereomeric ratio
dt	Doublet of triplet
ee	Enantiomeric excess
EF-G	Elongation factor G
EPS	Exopolysaccharide
equiv.	Molar equivalence
er	Enantiomeric ratio
ET12	Electrophoretic Type 12
FA	Fusidic acid
FDA	Food and Drug Administration
Fmoc	9-fluorenylmethoxycarbonyl
GDP	Guanosine diphosphate
GTP	Guanosine triphosphate
HATU	2-(1*H*-7-Azabenzotriazol-1-yl)-1,1,3,3-tetramethyl uronium hexafluorophosphate methanaminium
HBTU	*O*-Benzotriazole-*N*, *N*,*N*',*N*'-tetramethyl-uronium-hexafluoro-phosphate
HOBt	1-hydroxybenzotriazole
HPLC	High performance liquid chromatography
HSL	Homoserine lactone
iChip	Isolation Chip
IC	Initiation complex

IC_{50}	Median inhibition concentration (required to reduce the effect by 50%)
J	Coupling constant
m	Multiplet
MH media	Mueller-Hinton media
MIC	Minimum inhibitory concentration
MIC_{90}	Minimum inhibitory concentration that inhibits 90% of growth of organism
MBC	Minimum bactericidal concentration
mp	Melting point
mRNA	Messenger ribonucleic acid
MRSA	Methicillin-resistant *Staphylococcus aureus*
MS	Mass spectrometry
MsCl	Methanesulfonyl chloride
MW	Microwave
NADPH	Nicotinamide adenine dinucleotide phosphate
NMR	Nuclear magnetic resonance
ppm	Parts per million
PHDC	Philadelphia-District of Columbia
PTC	Peptidyl-transferase-centre
PyBOP	Benzotriazol-1-yloxytris(pyrrolidino)phosphonium hexafluorophosphate
q	Quadruplet
QS	Quorum sensing
R_f	Retention factor
RF	Release factor
RP-HPLC	Reverse-Phase high performance liquid chromatography
RRF	Ribosome recycling factor
rt	Room temperature

SAR	Structure-activity relationship
SEM	Scanning Electron Micrograph
SPPS	Solid-phase peptide synthesis
t	Triplet
TBTU	*O*-(Benzotriazol-1-yl)-*N*,*N*,*N*',*N*'-tetramethyluronium tetrafluoroborate
t-Bu	*tert*-butyl
TFA	Trifluoroacetic acid
TFAA	Trifluoro acetic anhydride
THF	Tetrahydrofuran
TLC	Thin layer chromatography
TNFR1	Tumour necrosis factor receptor 1
t_R	Retention time
TsCl	4-Toluenesulfonyl chloride
UP	Ubiquitin pathway
UTI	Urinary tract infection
UV	Ultra violet
v/v	Volume per volume

Content

Abstract i
Acknowledgement iii
Abbreviations iv
Content viii
Chapter 1 Introduction 1
1.1.1 *Burkholderia Cepacia* Complex 5
1.1.2 *Pseudomonas Aeruginosa* 14
1.2 Argyrin 26
1.2.1 Bacterial Protein Synthesis 28
1.2.2 Function of Elongation Factor G in Protein Synthesis 34
1.2.3 Argyrin Inhibits Elongation Factor G 40
1.3 Current Methods for Argyrin Total Synthesis 44
1.3.1 Ley's Method 45
1.3.2 Kalesse's Method 47
1.3.3 Jiang's Method 48
1.3.4 Chan's Method 49
1.4 Aim and Objectives 51
Chapter 2 Synthesis of Two Key Buildings Blocks of Argyrins 56
2.1 Thiazole Dipeptide 57
2.2 Synthetic Approach to Thiazole Dipeptides 57
2.3 Synthesis of 2-((tert-butoxycarbonyl)-1-amino-alkyl)thiazole-4-carboxylic Acid 61
2.3.1 Synthesis of 2-((tert-butoxycarbonyl)-1-amino-alkyl)-thiazole-4-carboxylic Acid Using Chan's Route 61
2.3.2 Synthesis of 2-((tert-butoxycarbonyl)-1-amino-alkyl)-thiazole-4-carboxylic Acid Using Ley's Route 69

2.4 Asymmetric Synthesis of Tryptophan Analogues 73
2.5 Reported Synthetic Approaches to Optically Pure Tryptophans 74
2.5.1 Ley's Approach to the Synthesis of (*S*)-4-methoxy-tryptophan 75
2.5.2 Nickeleit's Approach for the Synthesis of (*S*)-4-methoxy-Tryptophan 77
2.5.3 Jiang's Approach for the Synthesis of (*S*)-4-methyoxy-tryptophan 78
2.5.4 Chan's Approach for the Synthesis of Substituted Tryptophans 80
2.6 Asymmetric Synthesis of Substituted (*S*)-Tryptophans Through Alkylation of Belokon's Nucleophilic Glycines 82
2.6.1 Homologation of Chiral Glycine Ni(II) Schiff Base 83
2.6.2 General Preparation of BPB-Glycine Ni(II) Complex 85
2.6.3 Preparation of Indolemethyl Chloride for Alkylation 89
2.7 Conclusions 102
Chapter 3 Synthesis of α,β-Dehydroamino Acids 104
3.1 α,β-Dehydroamino Acids Containing Peptides 104
3.1.1 Lantibiotics 105
3.1.2 Thiopeptide Antibiotics 107
3.2 Conformational Property and Chemical Reactivity of the Dehydroamino Acid Residues 110
3.3 Installation of a Dehydroamino Acid into Argyrin 110
3.4 Previous Reports for Installing Dehydroamino Acids into Peptides 111
3.4.1 Elimination Reactions 111
3.4.2 Preparation of the Dehydroalanine Precursor, Phenylselenocysteine 116
3.4.3 Preparation of Dehydrobutyrine Precursor Methyl-

Phenylselenocysteine 117
3.5 Synthesis of *N*-Fmoc-Phenylselenocysteine 119
3.5.1 Synthesis of β-Lactone 120
3.5.2 β-Lactone Ring Opening 123
3.5.3 *N*-Boc Deprotection of Phenylselenocysteine 124
3.5.4 *N*-Fmoc Protection of Phenylselenocysteine 126
3.6 Synthesis of Dehydrobutyrine and Dehydrophenylalanine 126
3.6.1 Carboxyl Group Protection by Diphenylmethyl Ester 129
3.6.2 Conversion of Hydroxyl Group into a Tosylate Using Tosyl Chloride 131
3.6.3 Dpm Ester Deprotection by TFA 134
3.7 Applying an *O*-Tosylation Followed by Elimination for a Threonine-Containing Cyclic Peptide 138
3.8 Conclusions 140
Chapter 4 Fmoc Solid-Phase Peptide Synthesis of Argyrin Analogues 142
4.1 Solid-Phase Peptide Synthesis 143
4.1.1 Resins and Linkers 148
4.1.2 Activation of the Carboxyl Group of the Amino Acid 152
4.2 Total Synthesis of Argyrin Analogues Using Fmoc/*t*Bu SPPS 156
4.2.1 Resin Loading: Attachment of Fmoc-sarcosine 157
4.2.2 Peptide Assembly 158
4.2.3 Oxidative Elimination 160
4.2.4 Direct Application of *N*-Fmoc-dehydroamino Acid 163
4.2.5 Deprotection and Cleavage of Peptide from Solid Support 164
4.2.6 Macrocyclisation of Argyrin Linear Precursors 166
4.2.7 Chemical Stability of Argyrins 172
4.3 Conclusions 172
Chapter 5 Antibacterial Activity of the Argyrin Analogues 174
5.1 The Argyrin Susceptibility Assay Procedure 176

5.2 Activity of Argyrin Against *P. aeruginosa* 179
5.2.1 Activity of Substituted-L-Tryptophan Argyrins Against *P. aeruginosa* 180
5.2.2 Activity of Argyrins with Different Dehydroamino Acid Residues Against *P. aeruginosa* 184
5.2.3 Activity of Thaizole Side-Chain Modified Argyrins Against *P. aeruginosa* 188
5.3 Activity of Argyrins Against *B. multivorans* 189
5.4 The Activity of Argyrins Against Other Organisms 192
5.5 Molecular Target of Argyrins 194
5.6 Conclusions 196
Chapter 6 General Conclusion and Future Work 198
6.1 General Conclusion 198
6.1.1 Synthesis of Thiazole Dipeptide 200
6.1.2 Asymmetric Synthesis of Substituted Tryptophans 201
6.1.3 Synthesis of *N*-Fmoc-phenylselenocysteine 204
6.1.4 Synthesis of Dehydrobutyrine and Dehydrophenylalanine 204
6.1.5 Fmoc/*t*Bu Solid-Phase Peptide Synthesis of Argyrin Analogues 206
6.1.6 SAR Studies of Argyrins 209
6.2 Future Work 212
6.2.1 Optimisation of the Synthetic Procedure and Purification 212
6.2.2 Computational Studies 217
6.2.3 Cytotoxicity of Argyrin Analogues 217
6.2.4 MIC_{50} of Argyrin Analogues 217
Chapter 7 Experimental 219
7.1 Material 219
7.2 General methods 220
7.3 Instrumentation 220
7.4 Experimental for Chapter 2 222

7.4.1 Preparation of Thiazole Dipeptide 222
7.4.2 Preparation of Gycine-Ni(II) BPB Schiff Base 228
7.4.3 Preparation of 3-hydroxyethylindole 231
7.5 Experimental for Chapter 3 250
7.5.1 Preparation of Phenylselenocysteine 250
7.5.2 Preparation for Dehydrobutyrine 254
7.5.3 Preparation for Dehydrophenylalanine 259
7.6 Experimental for Chapter 4 263
7.6.1 Preparation of Linear Argyrin Precursors 263
7.6.2 General Procedure for On-resin Oxidation Elimination of Phenyl Selenide 266
7.6.2 General Procedure for Head-to-Tail Cyclisation 269
7.7 Antibacterial Assay 278
7.8 Chemical Stability of Argyrin Analogues 280
Chapter 8 References 281

Chapter 1
Introduction

For more than 60 years, antibacterial drugs, commonly known as antibiotics[1], have been regarded as panacea in the treatment of various infections. The major way that antibiotics save lives is through the treatment and prevention of severe infections.[2] However, most antibiotics used today are derivatives of classes of compounds discovered between the early-1900s and mid-1980s. Even though such antibiotics, beginning with penicillin and streptomycin, provide effective cure for most bacterial infections, there is a requirement of new and novel antibiotics.

As Alexander Fleming warned during his Nobel Prize speech in 1945, bacteria could become resistant to these antibiotics (penicillin).[3] Certainly, the development of each new antibiotic has been followed in time by the development of bacterial resistance.[4] The development of bacterial resistance is accelerated by the selective pressure posed by the appropriate, as well as inappropriate use of antibiotics.[5] The inevitable rise of resistance will limit the utility of today's antibiotics in the future. Consequently, the wide spread of resistant bacteria that causes untreatable infections is becoming one of the major threats to human and animal health worldwide in twenty first century. In the

United States, the Centres for Diseases Control and Prevention (CDC) estimates that more than 2 million people are infected by antibiotic-resistant bacteria each year, and at least 2% of patients failed to survive.[6]

In recent decades, the pace of discovery and development of new antibiotics has dropped dramatically. The 'golden era' (1940s-1960s)[7] (Figure 1.1) witnessed the discovery of most antibiotics used today through screening soil-dwelling bacteria[8], a process that was later named the Waksman platform[8]. The antibiotics discovery peaked in 1950s, which brought antibiotics such as vancomycin, streptogramin, and metronidazole.[9] However, after the initial rush of new compounds that were isolated from actinomycetes, new antibiotics became hard to identify using the Walkman platform, which led to a drop of antibiotics discovery from the 1980s onwards.[10] The number of antibiotics approved by Food and Drug Administration (FDA) fell from 29 during the 1980s to 9 in the first decade of the 2000s.[11] Major pharmaceutical companies are primarily focused on modifying existing classes of antibiotics discovered during 1930s to 1980s.[10] Such classes of antibiotics can be related to a limited number of chemical structures or scaffolds. Four such scaffolds, the penicillin, cephalosporins, quinolones and macrolides accounted for 73% of the chemical antibiotics reported between 1981 and 2005.[12] Increasingly, synthetic tailoring of these scaffolds has become the predominant mode of making new generations of antibiotics during that period. In addition, new generations are often designed to combat the bacterial resistance of previous generations. For example, second-[13] and third-generation[14] cephalosporins like cefaclor and ceftazidime are more resistant to destruction by the resistance enzyme β-lactamase. When new β-lactamases emerged that were resistant to third-generation cephalosporins, fourth-generation molecules, such as cefepime, were developed with less susceptible to cleavage by these enzymes[15]. Moreover, even more concerning than the dropping pace of drug approvals is that resistance to one antibiotic often leads to resistance to several antibiotics within the same class. For example,

Staphylococcus aureus that develops resistance towards methicillin are also resistant to other β-lactam antibiotics, such as oxacillin and cephalosporins.[16] In conclusion, making improvements to existing scaffolds is a good short-term strategy to develop new antibiotics, but it is generally agreed that the best way to combat the declining efficacy of approved antibiotics is to introduce new classes of antibiotics. Figure 1.1 illustrates the models of antibiotics discovery and development.

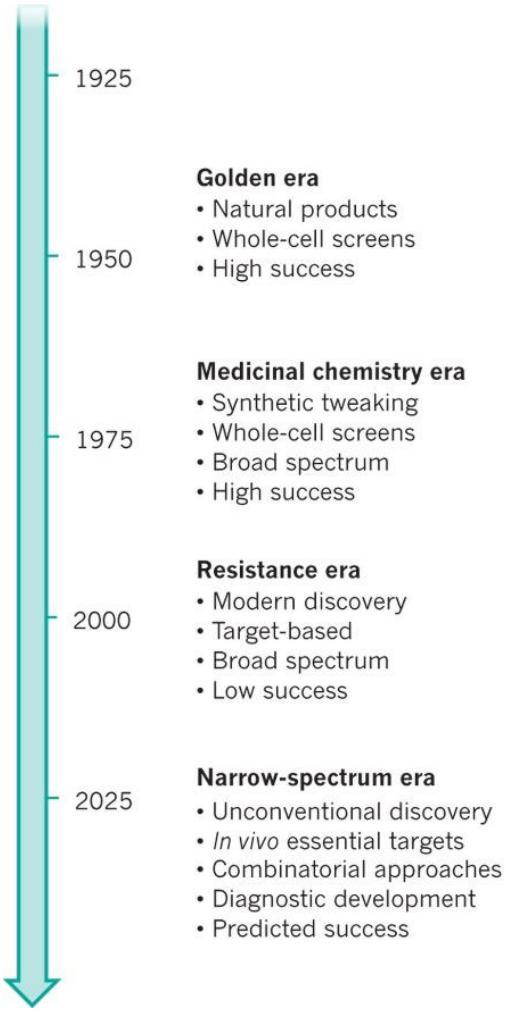


Figure 1.1: Models of antibiotics discovery and development.[7]

Many synthetic antibiotics also suffered from poor cell-membrane penetration and efflux issues. As mentioned above, most antibiotics in clinical use today were discovered by screening cultivable soil microorganisms. However, 99% of

all species in external environments are uncultured[17], which means they cannot be grown under laboratory conditions, resulting in an untapped source of new antibiotics[18]. A breakthrough has been made by Epstein *et al*. as they utilised a multi-channel device known as the isolation chip (iChip)[19], to simultaneously isolate and grow uncultured bacteria. Before the device was covered with two semi-permeable membranes and put back into soil, a sample of soil is diluted to deliver one bacterial cell to a given channel. Thus, nutrients and growth factors diffusing through chambers enables the uncultured bacteria to grow under the same conditions as they do under natural environment. The resulting bacteria extracts were screened for antibacterial activity. An extract, named as teixobactin[20], from a new species of Gram-negative β-proteobacteria *Eleftheria terrae* showed good antibacterial activity. Teixobactin shows promising inhibition against cell wall synthesis by binding to lipid II. When evaluated with *Staphylococcus aureus* or *Mycobacterium tuberculosis*, no resistance to teixobactin was detected.[20] The case of teixobactin revealed that more natural compounds with low susceptibility to resistance could be discovered.

This chapter consists of four sections. Section 1.1 focuses on the development of antibiotics and increasing attention on the antibacterial resistant superbugs. In addition, this section illustrates the pathogenesis and treatment methods of two intrinsically drug resistant bacteria, *Burkholderia cepacia* complex and *Pseudomonas aeruginosa*. Section 1.2 discusses the therapeutic potentials of a new class of macrocyclic peptide antibiotic argyrin and its mechanism of action. Argyrin displayed good antibacterial activity towards intrinsically drug resistant bacteria, including *Burkholderia cepacia* complex and *Pseudomonas aeruginosa*. In order to chemically synthesise argyrin and its analogues, a review of previous reported total synthesis methods is outlined in Section 1.3. This Chapter is concluded in Section 1.4 with the aim and objectives of the research work carried out in this thesis.

1.1.1 *Burkholderia Cepacia* Complex

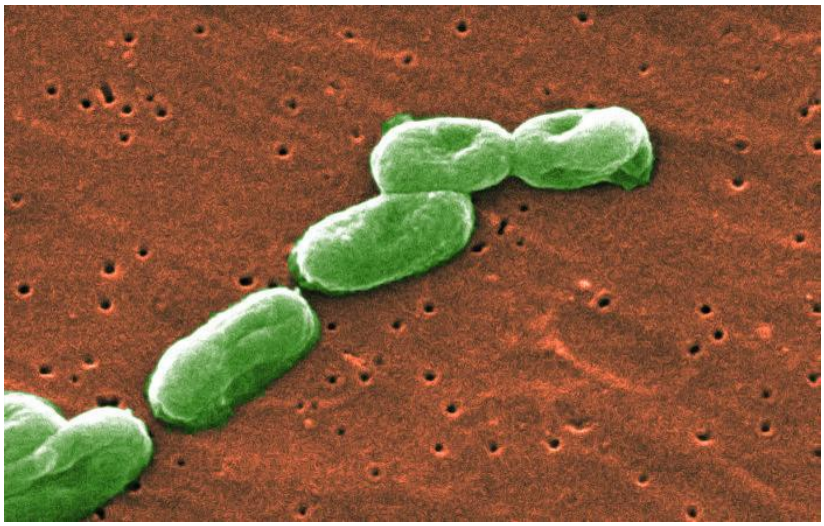


Figure 1.2: Scanning Electron Micrograph (SEM) of *Burkholderia cepacia*.[21]

The *Burkholderia cepacia* complex (Bcc) (Figure 1.2) is a group of motile, non-spore-forming, rod-shaped, metabolically diverse Gram-negative β-proteobacterium[22,23] widely spreading in the environment. In 1950, the *Burkholderia cepacia* (*B. cepacia*) was first described as *Pseudomonas cepacia* (*P. cepacia*) which is responsible for sour skin disease in onions.[24] In 1992, Yabuuchi *et al.* analysed molecular taxonomic of *P. cepacia* and related species collected from pathogens of plants, animals, and humans. Based on their studies, they reported a new genus *Burkholderia* based on the 16S rRNA sequences, cellular lipid and fatty acid composition, DNA-DNA homology values, and phenotypic characteristics.[25] The *B. cepacia* and related species are now known as Bcc which is comprised of 20 different but phenotypically related species, with 78% of their genes in common.[26] The genomes size of these bacteria ranged from 6.2 Mbp in *Burkholderia dolosa* AUO158 to 8.7 Mbp in *Burkholderia lata* 383[27], arranged in three chromosomes and a large plasmid. Based on the genetic variances, the Bcc are separated into nine different genomovars[22] as listed in Table 1.1.

Genomovar	Species name
I	*cepacia*
II	*multivorans*
III	none
IV	*stabilis*
V	*vietnamiensis*
VI	none
VII	*ambifaria*
VIII	*anthina*
IX	*pyrrocinia*

Table 1.1: *Bcc* complex genomovars and species names.[22]

The Bcc organisms live in diverse ecological niches[28], with either pathogenic or beneficial effects to other organisms[29] (Figure 1.3). Several strains can induce plant host-defence mechanisms and enhance disease resistance in plants by producing compounds that protect their host from bacteria[30], protozoa, pathogenic fungi[31] and nematodes[32]. Therefore, such strains have attracted significant commercial investment as bioremediation, plant growth promoting agents and biocontrol agents due to their ability to colonize the rhizosphere of crops, like maize, rice, corn and sunflower (Figure 1.3).[33]

Since the 1980s, the Bcc organisms have been regarded as important human opportunistic pathogens.[34] These bacteria cause life-threatening infections in immunocompromised patients, in patients with chronic granulomatous disease (CDG)[35], and especially in cystic fibrosis (CF) patients[36] (Figure 1.3). *B. cenocepacia* predominates in North America CF patients, while *Burkholderia multivorans* predominates in European CF patients.[37] The outbreaks caused by other Bcc species are spread globally. For instance, 85% of the Bcc isolates from patients of major CF centre in Lisbon are *B. cepacian* species.[38] These finding led to the conclusion that the prevalence of Bcc species differed geographically and regionally.

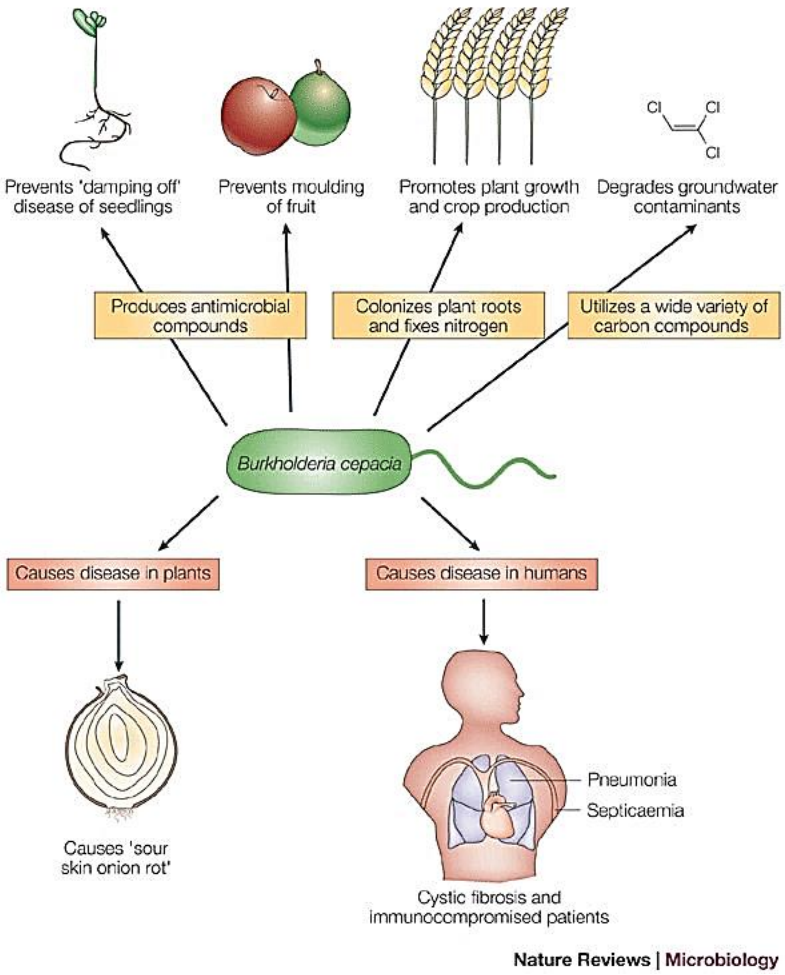


Figure 1.3: Beneficial and detrimental effects of the *Burkholderia cepacia* complex.[39]

Cystic fibrosis (CF) is the most common lethal inherited disorder among Caucasians, with a frequency of approximately 1 in 2500 livebirths.[40] The disease results from mutations in the CF transmembrane conductance regulator (CFTR) gene.[36] CFTR functions as a cAMP-regulated chloride channel[41], primarily found in the apical membranes of epithelial cells[42]. Although genetic defect affects several organs, the respiratory tract is the most affected which is the main cause of morbidity and mortality among CF patients. At least 90% of CF patients die from respiratory failure.

Pseudomonas aeruginosa strains account for the large majority of respiratory infections among CF patients while Bcc strains infect a small proportion of CF patients.[43] Approximately 3.5% of CF patients worldwide are affected by Bcc

infections.[44] However, Bcc infections are particularly concerning in CF patients and their caregivers as the clinical outcome is unpredictable and highly variable. Few Bcc infected patients are asymptomatic carriage[39], since most patients suffer from an increased decline in pulmonary function.[27] Thus, significant percentage of the Bcc infected patients develop a rapid and fatal combination of necrotizing pneumonia, bacteraemia and worsening respiratory failure characterised as the cepacia syndrome[34], resulting in early death. The cepacia syndrome does not occur with any of the other CF pathogen, such as *Pseudomonas aeruginosa*, *Haemophilus influenza*, *Staphylococcus aureus*, and *Stenotrophomonas maltophilia*. Additionally, several Bcc strains of the species *B. multivorans*, *B. cenocepacia*, *B. dolosa* and *B. cepacia* can be readily transmitted among CF patients.[45] In fact, highly epidemic lineages of the *B. cenocepacia* species have been discovered, including the Midwest epidemic lineages, the Philadelphia-District of Columbia (PHDC) and the Electrophoretic Type 12 (ET12).[46] Among them, the ET12 lineage was found to spread among CF patients from Europe to North America.[47]

The Bcc bacteria infects CF patients by first entering the respiratory tract. After that, the bacteria adhere to the host mucosal or epithelial surfaces. The mucus in CF lung is increased due to defective mucociliary clearance, abnormal submucosal gland function and enhanced inflammatory response.[48] Such mucus provides an ideal environment for bacterial colonization. Following penetration of Bcc in the mucus layer, the adhesion of the organism to epithelial surface is achieved through attachment to both protein and glycolipid receptors on the lung epithelial cells. A functional respiratory epithelium is essential for overcoming pathogens, through the production of numerous cytokines, chemokines, adhesion molecules and inflammatory enzymes.[49] However, the 55 kDa protein cytokeratin 13, which is abundant in CF epithelial cells, is identified as the protein receptor for the 22 kDa protein cable pili adhesion of certain *B. cenocepacia* strains.[50] A 55 kDa protein tumour necrosis factor receptor 1

(TNFR1), is also identified as a second protein receptor.[51] The generality of such receptor to Bcc species are not fully studied.

Apart from protein receptors, glycolipids including Asialo ganglioside (aGM1), aGM2,[52] Gb2, and Gb3[53] have been discovered in epithelial binding of Bcc as well. These glycolipids prompt inflammatory responses by elicit intracellular signalling. The invasion and survival of Bcc bacteria within epithelial cells is achieved through different routes, including invasion as a biofilm, penetration through the epithelium by paracytosis,[54] and rearrangement of the cytoskeleton.[55] The ability to penetrate the epithelial barrier and gain access to the blood stream to cause bacteraemia is a major contributor to death in Bcc infected CF patient. *In vitro* studies by Duff *et al*. show that four different Bcc species can break the intercellular tight junctions and translocate to the basolateral side of the epithelial layer.[56]

Bcc infections are also discovered in other immunocompromised patients, such as chronic granulomatous disease (CGD) patients, which is reported to be the second leading death of CGD patients.[35] The CGD disease is identified by mutations in the subunits of the nicotinamide adenine dinucleotide phosphate (NADPH) oxidase complex of the phagocytes. Such mutations cause reduced production of reactive oxygen species. Patients suffering from HIV and cancer are also reported to be Bcc infection targets.[57]

1.1.1.1 Virulence Factors of Bcc Bacteria

Several virulence factors are produced by Bcc to enhance their pathogenicity in both CF and non-CF patients. As mentioned earlier, Bcc bacteria contain large and complex genomes. The high genomic plasticity of Bcc genomes allows them to survive and thrive in various environments, including the human host.

Bacteria have cell-to-cell communication systems, known as quorum sensing systems, to coordinate multicellular behaviour. QS system regulated the gene expression based on the population of bacteria. Bacteria secrete signalling molecules that accumulate outside the cell. Once the concentration of the specific signal molecule reaches a threshold, the bacteria starts to induce or repress target gene expression.[58] For example, the LuxIR homolog CepIR quorum sensing system was first identified in a *B. cenocepacia* strain.[59] After that, similar QS systems were widely discovered in all Bcc species. The CepIR system depends on acyl homoserine lactone (AHL) synthase CepI and the transcriptional regulator CepR to produce the signalling molecule *N*-octanoyl homoserine lactone (C_8-HSL) and a by-product *N*-hexanoyl homoserine lactone (C_6-HSL) (Figure 1.4).[59] In Bcc, CepIR regulates the expression of various virulence factors, as disruption of which caused decreased extracellular protease and lipase activities and increased iron-chelating siderophore production.[60] Additionally, this system is also involved in the regulation of swarming motility and biofilm stability.[60] BvuIR was discovered in *Burkholderia vietnamiensis* that produce *N*-decanoyl homoserine lactone (C_{10}-HSL) (Figure 1.4).[61] Further studies on *B. cenocepacia* revealed two additional QS systems, AHL-type system CciIR[62] and an orphan LuxR homolog[63], CepR2. These systems often regulate reversely in the same way as CepIR does.

Non-homoserine lactone molecules are also used by *B. cenocepacia* as *Burkholderia* diffusible signal factor (BDSF).[64] The RpfFR QS system produce fatty acid molecule *cis*-2-dodecenoic acid (BDSF) as signalling molecule dependent on the cell density. Such BDSF changes some functions controlled by the CepIR, CciIR, and CepR2 systems.[64]

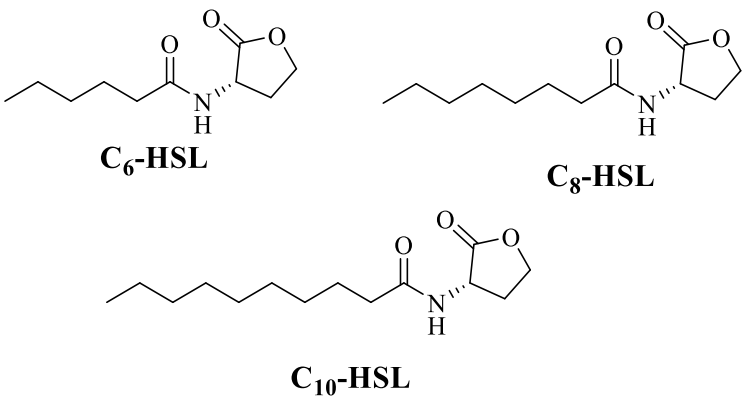


Figure 1.4: QS autoinducers C_6-HSL, C_8-HSL and C_{10}-HSL

Bcc bacteria employ special secretion systems to deliver molecules to the host cell that contribute to infection by destroying host cellular processes. These secretion systems are important for virulence and survival. In isolates of the *B. cenocepacia* ET12 and *B. vietnamiensis*, type I[65] and type II[66] secretion systems have been identified to deliver haemolytic proteins. A type III secretion system (T3SS) has been identified in *B. cenocepacia* that delivers virulence-associated protein to the host cell.[67] Type VI secretion system, present in *B. cenocepacia* K56-2, plays a role in virulence.[68] Two type IV secretion systems have been characterised in *B. cenocepacia* strains, being Ptw system and bc-VirB/D4 system. Ptw is responsible for intracellular survival in epithelial cells[69] while bc-VirB/D4 involves in DNA mobilisation[70].

Several proteins were produced by Bcc bacteria to cause virulence. Lipase was produced by many strains of Bcc, including *B. multivorans* and *B. cenocepacia*, under type II secretion system. Lipase plays a role in lung epithelial cell invasion, which is supported by the research that inhibition of lipase lead to reduced invasion.[71] Two distinct extracellular zinc metalloproteases, ZmpA[72] and ZmpB[73], were identified in many Bcc species, including *B. cenocepacia*, but not *B. multivorans* or *B. dolosa*. These two protein are response for proteolysis of many proteins found in the extracellular matrix, including their ability to degrade type IV collagen and fibronectin, showing the potential for

lung tissue damage.[73] Four siderophores, i.e. cepabactin, pyochelin, ornibactin and cepaciachelin, are synthesised by Bcc to acquire iron from the host environment.[74] In addition to siderophores, a serine protease has been identified as a virulence factor in *B*. *cenocepacia* strain K-562. This protease is responsible for proteolytic degradation of iron-binding protein ferritin, and thus enables *B. cenocepacia* to obtained iron from ferritin.[75]

Lipopolysaccharide (LPS) is a complex glycolipid, including lipid A, core oligosaccharide and o-antigen, present in the outer leaflet of the outer membrane of Gram-negative bacteria.[76] However, Bcc bacteria have distinctive LPS from other Gram-negative bacteria as they have different lipid A moiety and core oligosaccharide. Bcc bacteria have significant amounts of 4-amino-4-deoxy-L-arabinose (Ara4N) in the lipid A and inner core oligosaccharide instead of phosphate or 3-deoxy-D-manno-oct-2-ulosonic acid found in other Gram-negative bacteria.[77] Significantly, the Lipid A of Bcc shows reduced negative charge due to the positively charged ammonium group present in Ara4N. Such an important difference leads to decreased susceptibility of Bcc bacteria to cationic antimicrobial peptides and polymyxin.[78]

Exopolysaccharides (EPSs), mostly composed of polysaccharides, are high molecular weight polymers secreted by bacteria to extracellular environment.[79] The present of EPSs in Bcc infected CF patients is rare, as clinical isolated *B. cenocepacia* J2315 and *B. cenocepacia* K56-2 produce no or little EPSs.[80] However, some Bcc strains isolated from a subgroup of Portuguese CF patients was discovered to produce an EPS[81], cepacian. Cepacian was identified to inhibit neutrophil chemotaxis and neutrophil generation of reactive oxygen species, O_2^- and hydrogen peroxide.[82]

Bcc isolates have been found to form biofilm *in vitro* in the presence of AHL signalling molecules. Some Bcc species were discovered to detect the QS signals released by *P. aeruginosa* (see later in section 1.1.22) in biofilm, resulting in a mixed biofilm.[83] Various genes are required for the formation of biofilm. Those genes can be related to three classes: genes encoding regulatory factors that regulate AHL (C_8-HSL) production, gene involved in the biogenesis and maintenance of the outer membrane integrity, and genes encoding surface protein. Bcc can use biofilm to survive in the CF lung environment.[84] Therefore, new antibiotics will be developed to disrupt the biofilm as well as inhibit QS system responsible for the biofilm formation.

1.1.1.2 Resistance to Antibiotics

Bcc bacteria have intrinsic resistance to most of clinically used antimicrobials. Bcc bacteria are resistant to aminoglycosides; Bcc LPS block the binding of aminoglycosides leading to resistance.[85] In addition, an outer membrane efflux pump system has been identified in the Bcc that is responsible for elimination of quinolones, trimethoprim, and chloramphenicol.[86] The resistance of trimethoprim can be achieved through the production of trimethoprim-resistant dihydrofolate reductase, as well.[87] Some antibiotics failed to transport into cell due to the presence of Bcc outer membrane porin proteins. The resistance of Bcc to β-lactams depends on two mechanisms: degradation by periplasmic β-lactamases[88] and reduced susceptible due to specific penicillin-binding proteins[89].

1.1.1.3 Bcc Antibacterial Treatment

Current Bcc treatment is achieved through typically a combination of two or three antibiotics, including ceftazidime, chloramphenicol, rifampicin, cotrimoxazole and minocycline.[90] However, the elimination of the pathogen from patients was rare, particularly in patients with chronic infections. Ball *et al.* have recently reported nebulized amiloride and tobramycin could be an effective treatment within 2 months of initial infections.[91] In terms of CF patients, segregation remain the most successful prevention from Bcc infections.[92]

1.1.2 *Pseudomonas Aeruginosa*



Figure 1.5: SEM of *Pseudomonas aeruginosa*[93]

Pseudomonas is a genus of Gram-negative aerobic gammaproteobacteria comprising more than 120 species.[94] These bacteria are widely found in the soil and surfaces of the aqueous environment, as well as on humans, animals and plants.[95] A yellow-green fluorescent pigment, pyoverdine, and a blue-green

pigment, pyocyanin, are detected through laboratory incubation of *Pseudomonas* species on agar.[96] Among the *Pseudomonas* species, *P. aeruginosa* (Figure 1.5) is a major opportunistic pathogen that causes hospital and community-acquired infections.[97] Community-acquired infections caused by *P. aeruginosa* include, but are not limited to, skins and soft tissue infection (diabetic foot, burns and wounds), keratitis (contaminated contact lens), otitis externa (water blockage in ear canal) and otitis media folliculitis (contaminated hot tubs). Hospital-acquired infections include pneumonia, infection of burn wound, infections from surgical site, urinary tract infections (UTIs) and bloodstream infections (septicaemia). In terms of immunocompromised patients, bacteraemia caused by *P. aeruginosa* was discovered in patients with acute leukaemia, cancer, and patients infected with HIV.[98]

1.1.2.1 Airway Infection of *P. aeruginosa*

P. aeruginosa is one of the most common pathogens causing respiratory infections. Both acute and chronic airway infections caused by *P. aeruginosa* have been identified.[97] In terms of acute infections, *P. aeruginosa* is responsible for causing pneumonia among patients with poor health status, patients of old age, patients with neutropenia due to cancer therapy, and patients with immunosuppression due to organ transplant.[99] If the *P. aeruginosa* is not eliminated during acute infection, the bacteria will stay in the lung environment leading to a chronic and recurrent infection.[97]

The chronic pseudomonal lung infections are mostly discovered in the patients suffering from CF disease, resulting in decreased lung function and high morbidity and mortality rates. Like Bcc bacterial infection of CF patients, the *P. aeruginosa* can cause infection by colonization in the thickened mucus of CF

airways.[99] The phenotype of *P. aeruginosa* isolates from acute infections is distinct from isolates from chronic infections. To be specific, the bacterium isolated from chronic infection is less cytotoxic and inflammatory than the strain isolated during its initial acute infection phase.[100] The reason of such difference developed by *P. aeruginosa* is described in the section below.

1.1.2.2 The Virulence Factors of *P. aeruginosa*

Several virulence factors contribute to the survival of *P. aeruginosa* in humans. *P. aeruginosa* employs two different strategies to establish acute and chronic infections in patients. In case of acute infections of CF patients, *P. aeruginosa* breaks down lung defence and circulates in the bloodstream, resulting in death of patients within hours or days.[101] Virulence factors such as type III secretion system (T3SS) and various of extracellular toxins produced contribute to the establishment of acute infection.[102] However, in case of chronic infection of CF patients, *P. aeruginosa* can live in host for decades without reaching the bloodstream. Some clinical isolates of chronic CF lung infections were discovered to lack of some inflammatory bacterial features, like flagella and pili.[101] In contrast to acute infections, chronic infections were less studied due to less developed modelling of such infection *in vitro*.

Adhesion of bacteria to the host cell surface is the first step of infections.[103] The *P. aeruginosa* firstly attached to the sites in which the flagella and type 4 pili[104] are the main adhesions of *P. aeruginosa* to facilitate attachment to host cell surface. *P. aeruginosa* possesses one single polar flagellum that enables swimming motility in a rotating corkscrew motion.[97] The flagella bind to the glycolipid asialoGM1 on the lung epithelial cell surface and can eliminate inflammatory response by binding to Toll-like receptor 5 (TLR5).[105] The other

adhesion, Type 4 pili, are response for twitching[106] and swarming motility[107].

Once *P. aeruginosa* is attached to the host epithelia, the T3SS is activated to inject toxins directly into host cells. *P. aeruginosa* produces five secretion systems, type I, II, III, V, and VI.[108] The needle-like appendage of the T3SS allows bacteria to inject effector protein into epithelial cell through a pore formed in the epithelial cell membrane.[109] The four effectors, exoenzymes S (ExoS), ExoT, ExoU and ExoY, are identified in *P. aeruginosa*. The four effector proteins are variably expressed in different strains. Nearly all strains express at least one of the two major cytotoxins ExoU or ExoS,[110] while most strains express minor cytotoxins ExoY and ExoT.[109] ExoS and Exo T are bifunctional containing *N*-terminal GTPase-activating protein (GAP) activity and *C*-terminal ADP-ribosyltransferase (ADPRT) activity. Both activities maintain the actin cytoskeletal organization. In addition, ADPRT activity also plays a role in pathogenesis.[111]

Furthermore, *P. aeruginosa* secreted several proteases. These proteases can degrade immunoglobulins and fibrin, contribute to tissue damage in respiratory infections, and disrupt epithelial tight junctions.[106] For example, alkaline protease, a 50 kDa zinc metalloprotease, degrades host complement protein and host fibronectin.[112] It also degrades free flagellin monomers and therefore interferes with flagellin signalling through host TLR5.[113] *P. aeruginosa* secreted two elastases, LasA and LasB, through type 2 secretion system. This is regulated by the *lasI* QS system.[114] Serine protease LasA and LasB enable bacterial survival from host immune system by degrading elastin and collagen and inactivating immunoglobulin A and G.[115] Another serine protease, Protease IV, can degrade immunoglobulins, complement proteins, and fibrinogen.[116] It also inhibits the association of *P. aeruginosa* with macrophages through degradation of host surfactant protein A and D.[117]

The LPS of *P. aeruginosa* consists of a membrane-anchored lipid A, O-antigen, and polysaccharide core region.[118] Lipid A of *P. aeruginosa* contains a diglucosamine biphosphate backbone with *O*- and *N*- linked primary and secondary fatty acids.[119] Lipid A can bind to host cell receptor MD2 and CD14 to activate the TLR4 resulting in the inflammation, pro-inflammatory cytokines and chemokines production and endotoxic shock.[120] Penta-acylated lipid A (presence of a decanoic acid at the three-position) species was isolated from acute infections.[118] In contrast, hexa- and hepta- acylated species were isolated from chronic infections with increased inflammatory properties.[121] The reason might due to a distinct binding of lipid A to MD2.[122]

The QS systems are estimated to regulate approximately 10% of genes in the *P. aeruginosa* genome and at least 20% of the expressed bacterial proteome.[123] QS systems play a central role in biofilm formation, cell survival and virulence by initiation of specific genes in response to the autoinducers produced by the bacteria. *P. aeruginosa* produces at least three autoinducers, 3-oxo-dodecanoyl homoserine lactone (3-oxo-C_{12}-HSL) (Figure 1.6), butyryl homoserine lactone (C_4-HSL) (Figure 1.6), and 2-heptyl-3-hydroxy-4-quinolone (Figure 1.6),[124] and have three QS systems: *pqs*[125], *las*[126] and *rhl*[127] system. The *las* system is composed of a *lasI*-encoded acyl-HSL (AHL) synthase and the *lasR*-encoded transcriptional activator. 3-ox-C_{12}-HSL is synthesised by *lasI* AHL synthase, which is directed by *las*, and acts on the *lasR* AHL transcriptional activator. The *rhl* system is composed of an *rhlI*-encoded acyl-HSL synthase and an *rhlR*-encoded transcriptional activator. C_4-HSL is synthesised by *rhlR* AHL synthase, which is directed by *rhl*, and acts on the *rhlI* AHL transcriptional activator. For *pqs* system, the 2-heptyl-3-hydroxy-4-quinolone is synthesised through two operons, *pqs*ABCDE and *phn*AB, and three genes on these operons, *pqsR*, *pqsH*, and *pqsL*.[123] The *P. aeruginosa* QS systems function in a hierarchical manner, as the *las* system positively regulates *rhl* and production of quinolines.[128] The *P. aeruginosa* uses QS to regulate the production of virulence factors, including

proteases, adhesion, exotoxin A, elastase, motility, biofilm formation, the response to host immune signals, iron chelators and expression of efflux pump.[58]

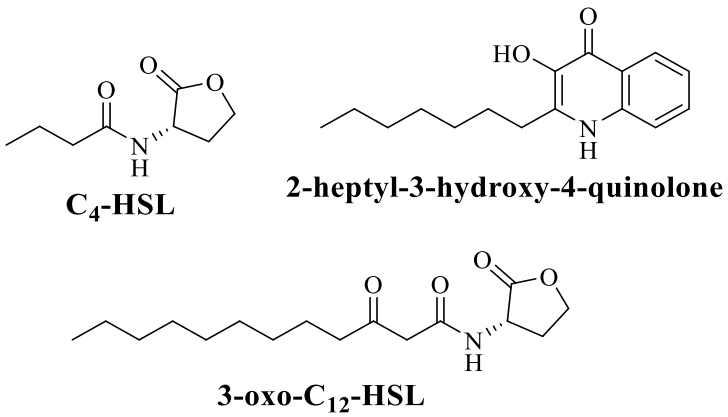


Figure 1.6: QS autoinducers C_4-HSL, 3-oxo-C_{12}-HSL and 2-heptyl-3-hydroxy-4-quinolone[124]

The adhered colonies form biofilms to protect themselves against the host immune response. The formation of biofilms is intricately related to the QS systems.[129] The communities of bacteria are encased in extracellular polymeric substances (EPS). Composed of lipids, proteins, polysaccharides, and extracellular DNA, the EPS matrix occupy up to 90% of the volume of the biofilm[130] and enhance the physical and chemical robustness of biofilm by decreasing the penetration of antibiotics[131] and host defence molecules[132]. Formation of biofilms is initiated by the reversible attachment of planktonic bacteria to the surface. After that, irreversible attachment of bacteria occurs and to microcolonies formed in EPS matrix.[133] Such attachments are contributed by type IV pili, flagella, alginate, extracellular DNA, and Pel and Psl polysaccharides. The production of Pel and Psl are regulated by the *las* system.[134] The QS systems regulates cell lysis in biofilm to release the extracellular DNA. Followed the irreversible attachment, biofilm maturation and growth of the three-dimensional community occurs. The maturation of

biofilm leads to mushroom-shaped structures with fluid-filled channels allowing the exchange of nutrients and wastes. After all the above steps, the planktonic bacteria are released from biofilm to colonize other surfaces.[135] Apart from the direct impact of biofilm, QS indirectly influences the biofilm formation through the control of swarming and twitching motilities.[58] The flagella-dependent form of bacterial translocation, warming motility, is regulated by the *rhl* system, and is implicated in the early stages of biofilm formation.[136]

Apart from QS systems, two-component regulatory systems also regulate the formation of biofilm. The *GacS*/*GacA* two-component system is one the 60 two-component systems found in the genome of *P. aeruginosa*. The *GacS*/*GacA* system plays a role in the production of virulence factors and biofilm formation. The transmembrane sensor kinase (*GacS*) transfers a phosphate group to its cognate regulator (*GacA*), which in turn promotes the transcription of two small regulatory RNAs, *RsmZ* and *RsmY*.[137] The two regulators then bind and inactivate the RNA-binding regulatory protein RsmA. Free RsmA negatively controls the synthesis of C_4-HSL and 3-oxo-C_{12}-HSL. Therefore, the *las* and *rhl* systems can control the extracellular virulence factors.[138]

The host environment has little free iron because it has sequestration molecules, like lactoferrin and transferrin.[97] *P. aeruginosa* secrets siderophore, pyochelin, and pyoverdine to scavenge iron from the host depots. Pyocyanin also causes oxidative stress to the host cell by disrupting host catalase and inhibiting mitochondrial electron transport. It protects bacteria from reactive oxygen and nitrogen species produced by phagocytic cells during infection because it is partly controlled by the oxidative stress RR.[139]

In conclusion, in terms of acute *P. aeruginosa* infections, an increased productions of extracellular virulence factors, such as elastases, proteases, or

cytotoxins, damages the host tissue, allowing the invasion and dissemination to blood vessel to cause a life-threatening bacteraemia. The virulence factors produced in the adhesion step are regulated by the QS systems. After the adhesion, the colonies form a biofilm which contains various virulence factors mentioned above. In the chronic infection scenario, *P. aeruginosa* undergoes a genetic adaptation to express high mucoidity and increased resistance towards host defence mechanisms.[140] Virulence mechanisms are essential for bacterial infection and persistence. Interfering with the biosynthesis, secretion, or specific virulence factors, or disturbing regulatory systems is becoming attractive strategy for antibiotic design. Therefore, antivirulence therapy can be a promising alternative to the classical antibiotic therapy.

1.1.2.3 Antimicrobial Resistance

P. aeruginosa infections are difficult to treat because it is intrinsically resistant to many classes of antibiotics.[141] General antibacterial resistance mechanisms, including blockage of entry, efflux pump, enzymatic degradation and target structure alteration, can be impacted by *P. aeruginosa* in the development of resistance.[142]

The outer membrane of *P. aeruginosa* consists of an asymmetric bilayer of lipopolysaccharide and phospholipids traversed by protein channels, porins.[143] The resistance to antibiotics is largely due to the low permeability of the outer membrane. The outer membrane blocks the penetration of large hydrophilic molecules and restricts the penetration of small hydrophilic molecules.[144] Penetration of small antibiotics, such as quinolones, through the outer membrane is achieved by passage through the aqueous channels provided by porin proteins. Two classes of porins are produced by general Gam-negative

bacteria: the general one allows most hydrophilic molecules to pass and the specific one only allows certain molecules to pass.[145] OprD is a specific porin responsible for penetration of carbapenem. The decreased expression of OprD in *P. aeruginosa* is the major mechanism for carbapenem resistance.[146]

Antibiotics may be eliminated from *P. aeruginosa* through multidrug efflux pumps. The functional efflux pumps systems span both the inner and outer membranes, and periplasmic space between the membranes.[145] These pumps are composed of three proteins, including a periplasmatic connective protein, an outer membrane porin, and a protein transporter of cytoplasmatic membrane.[147] High concentrations of antibiotics can upregulate the expression of efflux pumps.[147] For example, MexAB-OprM, MexCD-OprJ, MexEF-OprN and MexXY-Oprm efflux fluoroquinolones and β-lactams.[148] In terms of enzymatic degradation, *P. aeruginosa* produces various β-lactamases, such as the metallo-β-lactamases (MBL)[149], chromosomal cephalosporinase (AmpC)[150] and extended-spectrum β-lactamases (ESBL)[151]. For instance, when *P. aeruginosa* is exposed to penicillin, AmpC is induced, leading to resistance.

The intrinsic mechanism can be enhanced or stabilised by mutation, leading to acquired resistance.[145] Such acquired resistance is horizontal transfer of genetic elements and mutation of an existing resistance cassette in bacteria. The DNA elements, like plasmids, transposons, and integrons, with antibiotic resistance genes can be acquired by bacterial conjugation, transformation and transduction.[97] Mutation leading to overexpression of efflux pumps, reduced penetration of antibiotics, hyperproduction of β-lactamases and alteration of antibiotic targets made *P. aeruginosa* hard to treat. Mutation in *mexZ* causes an overexpression of MexXY-OprM, leading to fluoroquinolone resistance in clinical strains of *P. aeruginosa*.[152] Mutations in the porin OprD (either *mexT* or *mexS*) restrict the penetration of imipenem resulting in resistance.[153] The hyperproduction of β-lactamases takes place when an *ampC* β-lactamase factor,

AmpD, is mutated.[154] All the traits above are inheritable to *P. aeruginosa*.

A third type of resistance, adaptive resistance, occurs when the bacteria are continually exposed to an antibiotic or is under stressed environment.[155] Unlike the intrinsic and acquired resistance, the development of adaptive resistance highly depends on the environmental conditions around the bacteria. Several factors trigger the adaptive resistance, including environment cue, such as anaerobiosis, concentration of ions, carbon source, and polyamines, and social behaviour such biofilms and swarming motility.[156] All those factors have been related to an increased virulence to host and an increased resistance to antibiotics. Table 1.2 indicates the difference among the three types of resistance.

Type of resistance	**Intrinsic**	**Acquired**	**Adaptive**
Acquisition	Not acquired,	Mutation,	Changes in gene expression triggered by the environmental factors
Mechanisms	Low outer membrane permeability, β-lactamase and efflux pump	Horizontal transfer, mutations resulting in low uptake and overexpression of efflux pump	Changes of β-lactamase gene expression and expression of regulatory genes leading to efflux pump overexpression
Characteristics	Inheritable, stable, irreversible, independent of environment	Inheritable, stable, irreversible, independent of environment	Not inheritable, transient, revert upon removal of inducing signal, dependent on environment

Table 1.2: Type of resistance of *P. aeruginosa*

Multi-drug resistant (MDR) *P. aeruginosa* strains displayed several resistance mechanisms simultaneously. Different combinations of these mechanisms mediate resistance to specific antibiotics. For example, fluoroquinolone resistance is caused by both effective efflux pumps and mutations in the antibacterial targets.[157] Carbapenem resistance is caused primarily by decreased expression of the OprD porin, and marginally by efflux pumps and β-lactamases.[146]

1.1.2.4 Treatment of *P. aeruginosa* Infections

P. aeruginosa infections are currently treated with a number of antibiotics. However, there is no standard treatment for *P. aeruginosa* infections, a combination of at least two antibiotics is selected in most cases. Such antibiotics include β-lactams, fluoroquinolones, and aminoglycosides. For example, penicillins (piperacillin-tazobactam and ticarcillin-clavulanate)[158], cephalosporins (ceftazidime and cefepime)[159], aztreonam, and anti-pseudomonal carbapenems (doripenem, imipenem-cilastatin and meropenem)[159] (Figure 1.7) are β-lactams that are applied for *P. aeruginosa* infected CF patients.[160] The tobramycin inhalation solution (TOBI® Novartis Pharmaceuticals), approved in 1998, is an aminoglycoside that is accepted as a standard treatment for *P. aeruginosa* infected CF patients. The second-generation fluoroquinolone, ciprofloxacin and third-generation fluoroquinolone, levofloxacin (Figure 1.7) are administered to improve patient outcomes and to avoid drug resistance during the off cycle of tobramycin inhalation solution.[161]

Colistin, also known as polymyxin E, is a mixture of the cyclic polypeptides colistin A and B (Figure 1.8) has been brought back on stage as a last-lane antibiotic due to its activity against multi-resistant strains of *P. aeruginosa*,

though it has been reported to have nephrotoxicity and neurotoxicity.[162] The colistin methanesulphonate was given alone or in combination therapy to eliminate acute *P. aeruginosa* infections and to treat chronic *P. aeruginosa* infections.[163] The bactericidal antibiotic fosfomycin (Figure 1.8) was used in combination with other antibiotics for CF patients infected with multi-resistant *P. aeruginosa*.[164] The unique action mode, inhibition of the initial step in cell wall synthesis, prevents cross-resistance when it is co-administered with other antibiotics.[165]

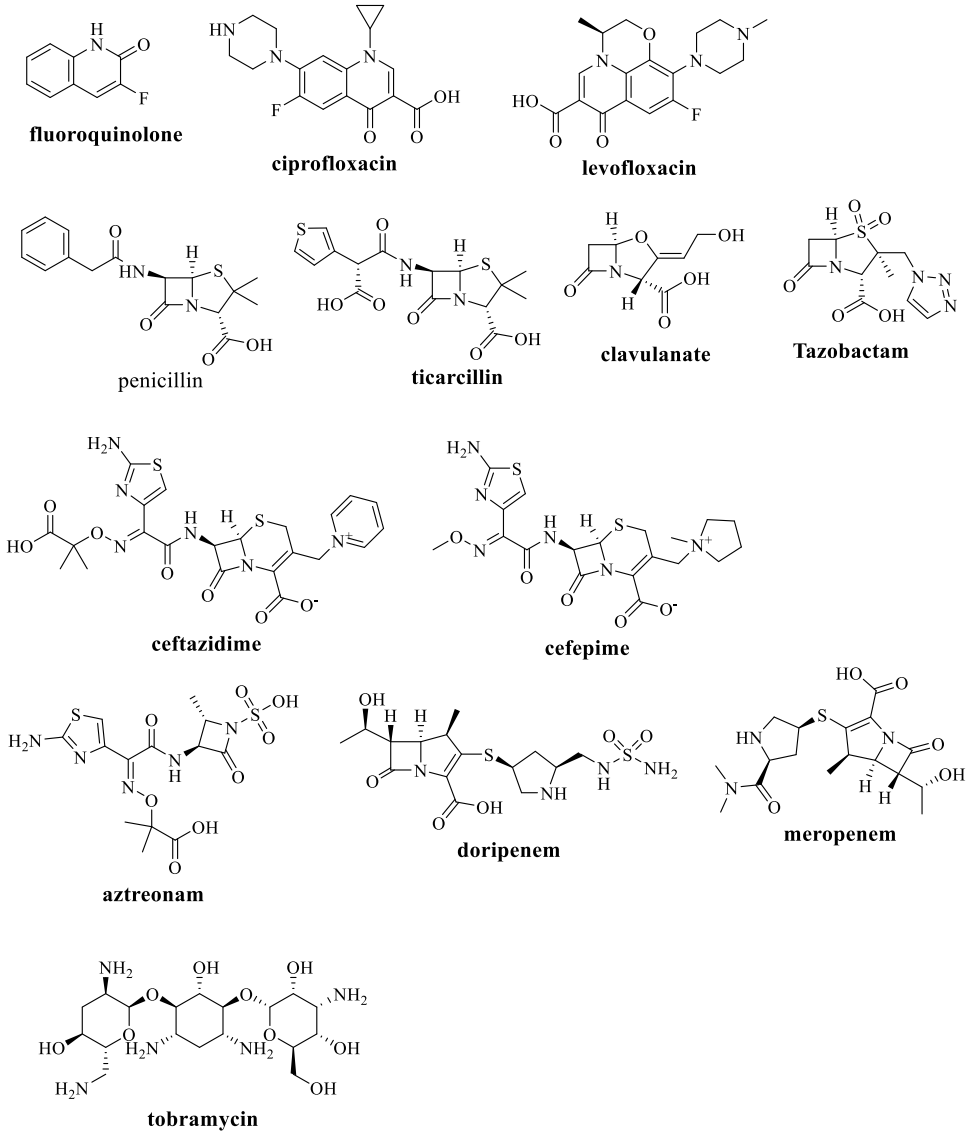
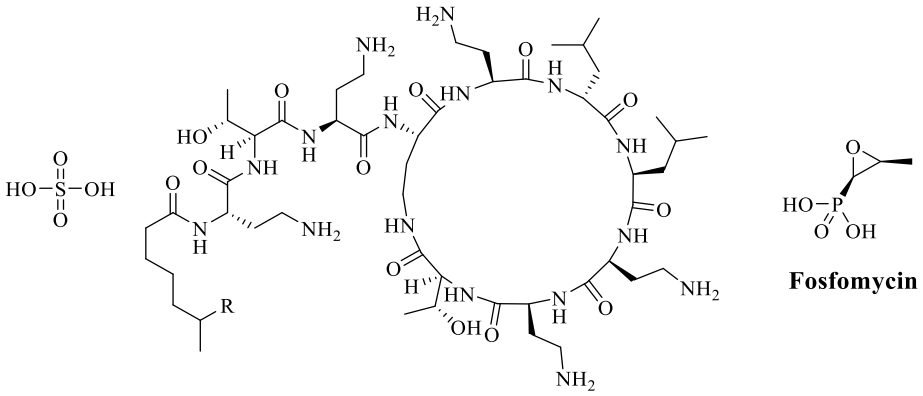


Figure 1.7: β-lactams, fluoroquinolones and aminoglycosides used for the treatment of *P. aeruginosa* infections

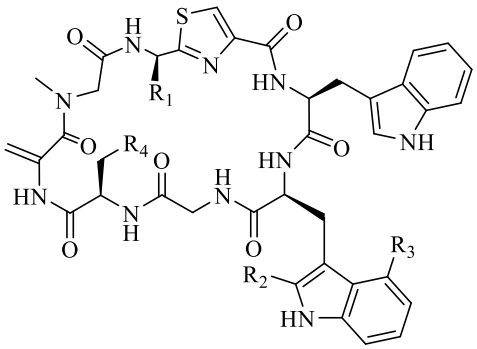


Colistin A R= CH_3
Colistin B R= H

Fosfomycin

Figure 1.8: Colistin A, Colistin B and Fosfomycin

1.2 Argyrin



Argyrin A **1.1**: R_1=CH_3, R_2=H, R_3=OCH_3, R_4=H
Argyrin B **1.2**: R_1=CH_3, R_2=H, R_3=OCH_3, R_4=CH_3
Argyrin C **1.3**: R_1=CH_3, R_2=CH_3, R_3=OCH_3, R_4=H
Argyrin D **1.4**: R_1=CH_3, R_2=CH_3, R_3=OCH_3, R_4=CH_3
Argyrin E **1.5**: R_1=CH_3, R_2=H, R_3=H, R_4=H
Argyrin F **1.6**: R_1=CH_2OH, R_2=H, R_3=OCH_3, R_4=H
Argyrin G **1.7**: R_1=CH_2OH, R_2=H, R_3=OCH_3, R_4=CH_3
Argyrin H **1.8**: R_1=H, R_2=H, R_3=OCH_3, R_4=H

Figure 1.9: The argyrin A-H **1.1-1.8**

The argyrins are a family of eight cyclic heptapeptides (Figure 1.9). The A21459 A and B, produced by a member of the genus *Actinoplanes* sp., were discovered by Selva *et al*. during a course of a screening program for new antibiotic agents.[166] The argyrin A and B showed similar biological activity. In fact,

argyrin A displayed a rather unusual spectrum of antibacterial activity (Table 1.3), being active against a few Gram-negative bacteria, including *P. aeruginosa*, and the Gram-positive bacteria *Clostridium difficile*.[166]

Later in 2002, Sasse *et al*. independently reported the screening for cytostatic compounds from a myxobacteria. They isolated a group of eight cyclic peptides from the culture broth of *Archangium gephyra* strain Ar 8082. The eight cyclic peptides were named as argyrin A to H (Figure 1.9).[167] Further structure study show that argyrin A and B are identical to A21459 A and B, respectively, with a revised position of the methoxy substituent in the methoxytryptophan residue.[168] Argyrin A was identified as a proteasome inhibitor[169], while argyrin B was found to be a potent inhibitor of T-cell independent antibody formation[167]. In terms of antibacterial and antifungal activity, argyrin A-H are show to be most potent against two species of the genus *Pseudomonas*.[167]

Although both Sasse *et al*. and Selva *et al*. discovered that the argyrins inhibit protein synthesis, the specific cellular target was not revealed until 2012 by the researchers from Novartis Pharmaceutical. Through mutant selection and whole genome sequencing studies, Nyeler *et al*. found that argyrin B inhibits bacterial protein synthesis by targeting the evolutionarily conserved elongation factor G (EF-G).[170] Additionally, argyrin B displayed potent antibacterial activity against multidrug-resistant Gram-negative bacteria *Pseudomonas aeruginosa* and *Burkholderia multivorans*.

To understand the antibacterial mechanism of argyrins, the procedure of bacterial protein synthesis, role of EF-G in protein translocation, and the binding interaction of EF-G with argyrin are described below.

Microorganism	MIC(μg/ml)
***Bacillus subtilis* ATCC 6633**	Inactive
Clostridium difficile	0.03
***Clostridium perfringens* L290**	8
***Enterobacter cloacae* LI349**	Inactive
***Enterococcus faecalis* ATCC7080**	In active
Escherichia coli	Inactive
***Enterococcus faecalis* ATCC7080**	Inactive
Haemophilus influenzae	16-64
***Klebsiella pneumoniae* L I 42**	Inactive
***Mycoplasma gallisepticum* L43 1**	2
***Neisseria caviae* ATCC14659**	0.13
Neisseria gonorrhoeae	64
Proteus mirabilis	16
***Proteus rettgeri* LI503**	32
***Proteus vulgaris* ATCC881**	4
Pseudomonas aeruginosa	4-32
***Salmonella typhimurium* L389**	Inactive
***S. typhimurium* TA1538 (hyperpermeable)**	8
***Shigella dysenteriae* L87**	Inactive
Staphylococcus aureus	32-64
***Staphylococcus pneumoniae* L44**	Inactive
***Streptococcus pyogenes* L49**	Inactive

Table 1.3: Antimicrobial activity of A21459 complex.[166]

1.2.1 Bacterial Protein Synthesis

Protein synthesis is performed by ribosomes in all living organisms. The ribosomes of both bacteria (2.5 MDa) and eukaryote (4 MDa) consist of approximately two-thirds RNA and one-third protein. To be specific, it contains three ribosomal RNAs (rRNA; 16S, 23S and 5S), which dominate the main functional sites, and 55 ribosomal proteins. All ribosomes in bacteria are composed of two subunits: a large 50S subunit (34 proteins and 23S, 5S RNA)

and a small 30S subunit (21 proteins and 16S RNA) (Figure 1.10 (A)). The large subunit contains the active site of the enzyme while the small subunit ensures fidelity. The two subunits can reversibly form the 70s ribosomes on the translation initiation region (TIR) of the messenger RNA (mRNA) during the initiation step of protein synthesis.

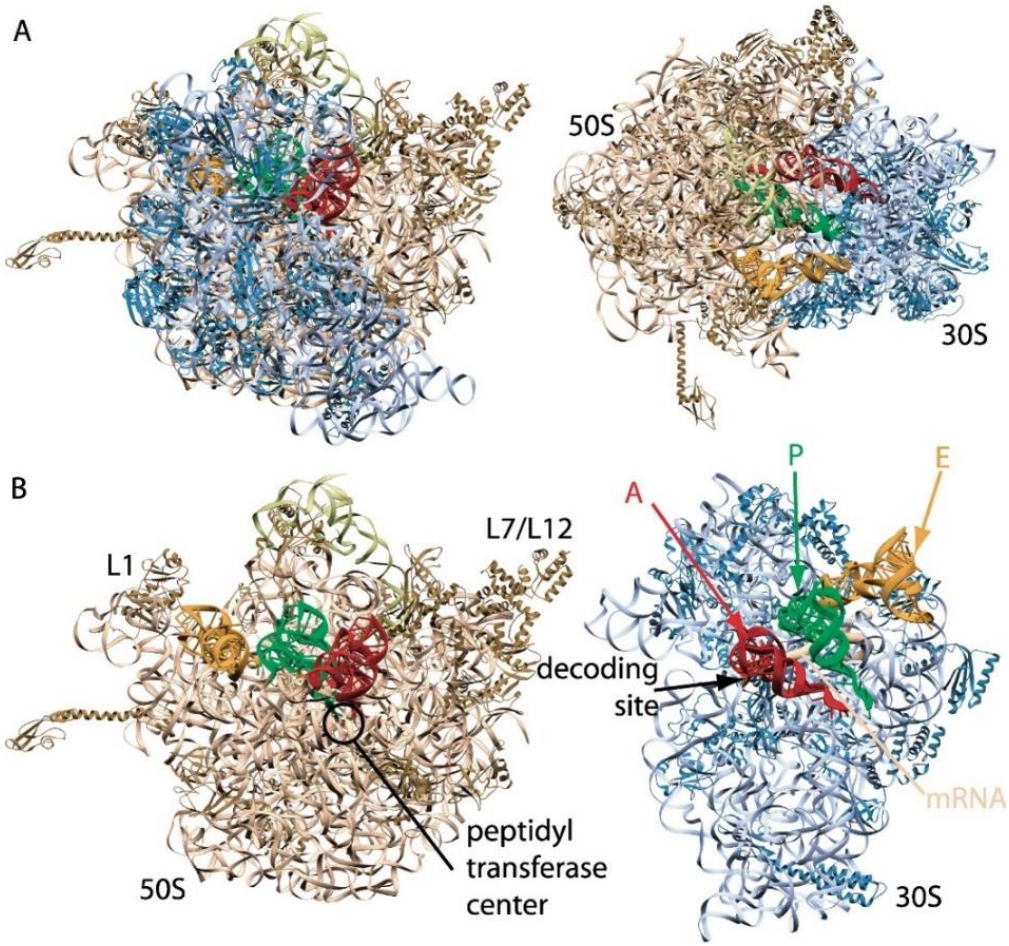


Figure 1.10: Crystal structure of the ribosome. (A) The 70S ribosome complexed with mRNA and tRNA; (B) Exploded view of the 50S and 30S subunits in the 70s ribosome with the location of A-, P-, and E-site tRNAs.[171]

The protein synthesis process, which is known as translation, takes place through binding of transfer RNAs (tRNAs) and their associated amino acids to the ribosome in an order determined by a messenger RNA (mRNA) template. The mRNA binds in a cleft between the 'head' and 'body' of the small 30S subunit, where its codons interact with the anticodons of tRNA. There are three

ribosomal binding sites for tRNA: the A (aminoacyl)-site, the P (peptidyl)-site and the E (exit)-site (Figure 1.10 (B)). The A-site binds the incoming aminoacyl-tRNA. The P site holds the peptidyl-tRNA attached to the growing polypeptide chain. The deacylated P-site tRNA moves to the E-site after formation of peptide-bond, and then leaves the ribosome. In the large 50S subunit, the 3' ends of P- and A-site tRNAs are in close proximity in the peptidyl-transferase centre (PTC) while the 3' end of the E-site tRNA is away from the PTC.

1.2.1.1 Initiation

The bacterial protein translation process can be divided into three steps, being initiation, elongation, and termination steps (Figure 1.11). Protein translation starts with the formation of a 70S complex on the mRNA. Such complex includes small 30S ribosome subunit, the mRNA template, three initiation factors (IF-1, IF-2 and IF-3), and an initiator tRNA, known as fMet-$tRNA^{fMet}$. The $tRNA^{fMet}$ is a tRNA that is attached to a modified methionine, with a formyl group bound to its amino group, formyl methionine (fMet). $tRNA^{fMet}$ contains anticodon sequence 5' CAU 3' that binds to a complementary start codon AUG. The mRNA and the tRNA interact by base-pairing rules to incorporate the small 30S subunit in the correct position. The 30S subunit attaches to the ribosome-binding site, which is known as Shine-Dalgarno sequence (AGGAGG). The IF-3 is responsible for recognition of the ribosome-binding site on the mRNA, while IF-2 recognizes $tRNA^{fMet}$ and binds it to the ribosome. $tRNA^{fMet}$ interacts with the AUG start codon, and the large 50S ribosomal subunit then attaches followed by the release of three IF and hydrolysis of GTP to GDP. The ribosome is orientated to move along the mRNA in the direction of 5' to 3'.

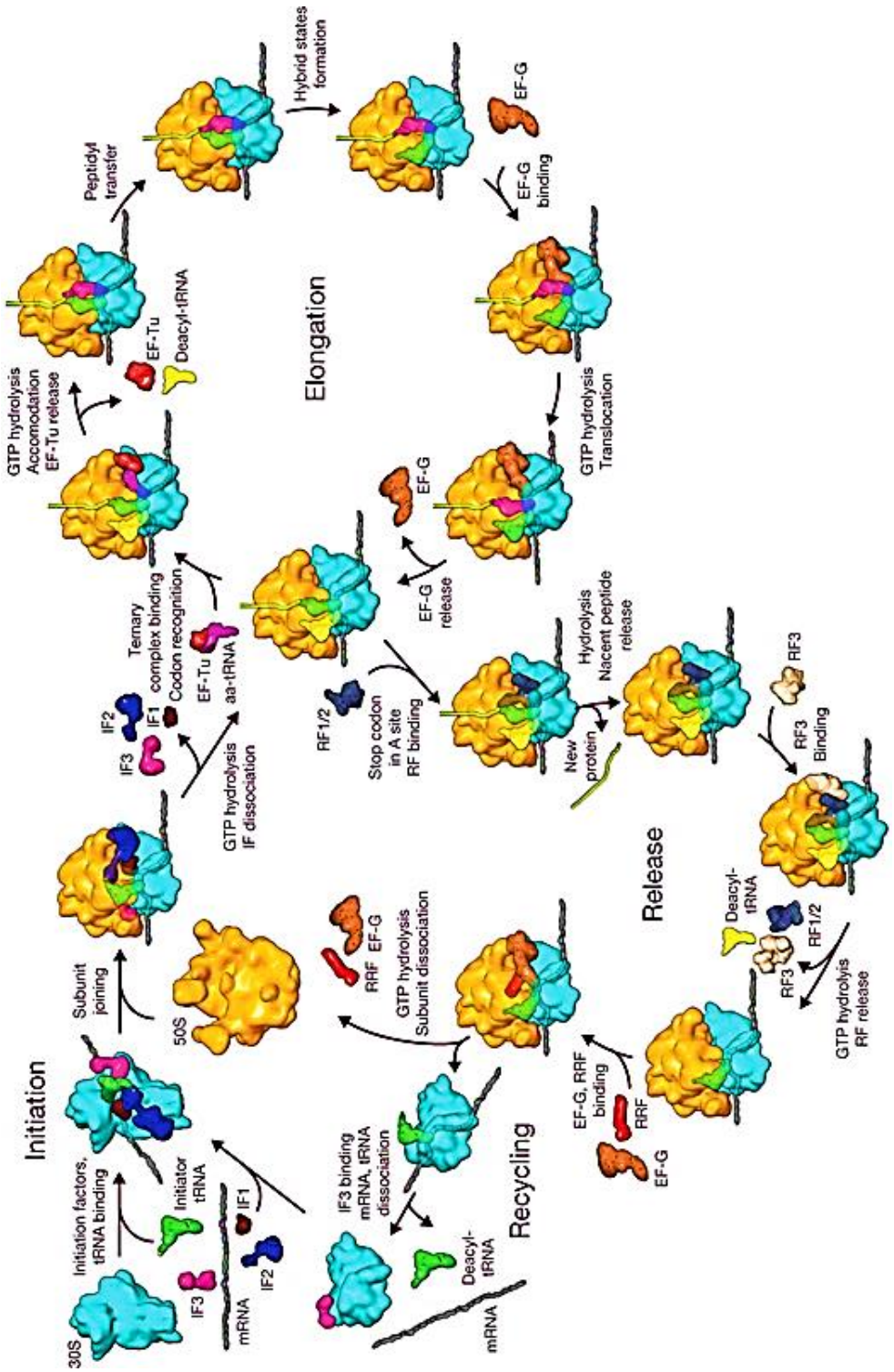


Figure 1.11: Overview of bacterial translation.[172]

1.2.1.2 The Elongation cycle

The elongation cycle can be divided into three steps: decoding, peptidyl transfer, and translocation as shown in Figure 1.12. During translation, elongation factors play a key role in the elongation of a polypeptide chain, as these proteins accelerate the protein synthesis. The elongation factor Tu (EF-Tu) facilitates decoding and delivers aminoacyl tRNA (aa-tRNA) to the A-site as part of a ternary complex with GTP. The attachment of the aa-tRNA is recognized by the codon on the mRNA as described above. EF-Tu is then activated to hydrolyse GTP to GDP, which stimulates the leaving of the acceptor end of aa-tRNA and moving of aa-tRNA to the 50S A-site. The leaving of GDP occurs with the help of elongation factor Ts (EF-Ts).

During protein synthesis, when aa-tRNA occupies the A site of both subunits, the ribosome catalyses the transfer of the peptidyl group on the P-site tRNA to the A-site aa-tRNA. Thus, this results in a complex consisting of peptidyl-tRNA in the A-site and deacylated tRNA in the P-site, which is known as a pre-translocation (PRE) complex.[173] Thus, the tRNA acceptor stems move within the 50S subunit to form a hybrid-state complex, in which the peptidyl-tRNA and deacylated tRNA are in the A/P and P/E sites, respectively.

After that, the codon-anticodon helices move within the 30S subunit to result in the post-translocation (POST) complex[173], where peptidyl-tRNA and deacylated tRNA are in the P and E sites of both subunits. The GDP-EF-G complex dissociates from the complex. The A-site is now free for next aa-tRNA to bind. The ribosome moves along the mRNA template precisely three nucleotides at a time relative to the mRNA.

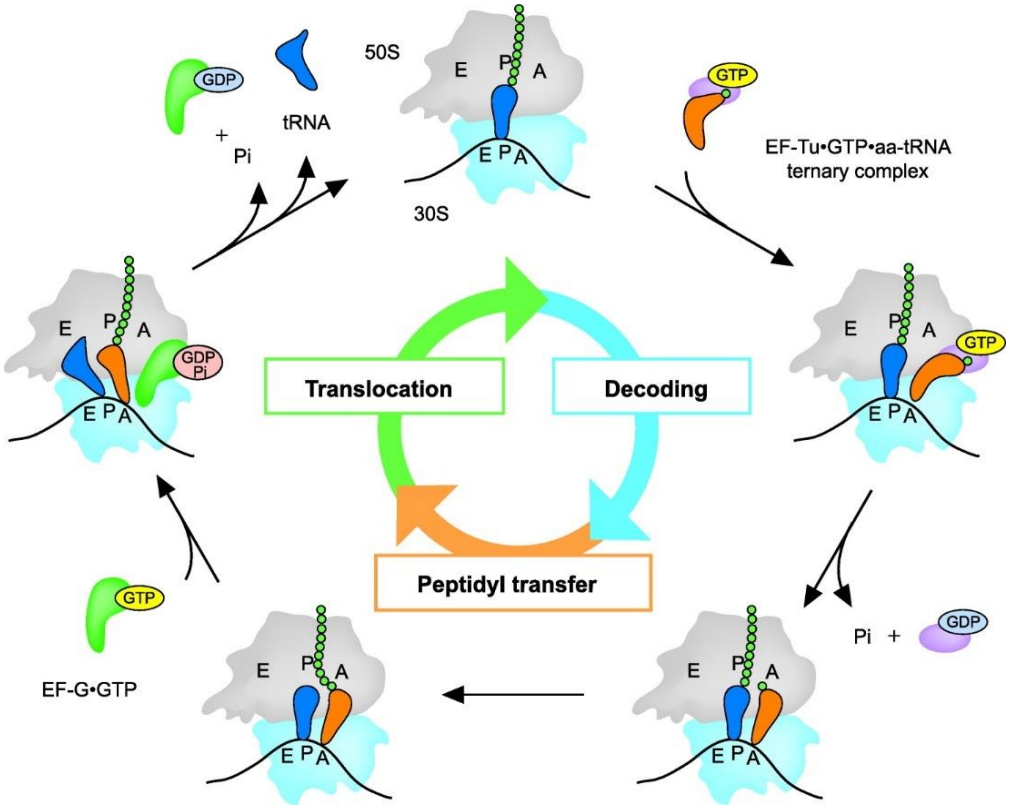


Figure 1.12: Translocation elongation cycle.[173]

1.2.1.3 Termination

There are three stop codons, UAG, UAA and UGA, that have no corresponding tRNA molecule. When the A-site is occupied by one of these three codons, the newly synthesised polypeptide chain leaves the ribosome, and the mRNA, tRNA, and the two ribosomal subunits complex breaks. Release factor 1 (RF1) promotes the leasing of polypeptide chain from UAA and UAG, while release factor 2 (RF2) stop chain with UAA and UGA. These two release factors are cooperated by release factor 3 (RF3) to stop protein synthesis. The RF3 accelerates the dissociation of RF1 and RF2 from the ribosome with the hydrolysis of GTP to GDP after peptide release. The release factor binds to the A-site and blocks the addition of amino acid to the growing polypeptide chain by peptidyl transferase. Instead, polypeptide chain and tRNA bond is

hydrolysed, and the resulting protein with carboxyl end free from tRNA is released. This is illustrated as the released part of Figure 1.11.

After hydrolysis of GTF by RF3, the mRNA and a deacylated tRNA is left in the P site. A ribosome recycling factor (RRF), together with the EF-G, process the recycle of ribosome into subunits for a new round of protein synthesis as shown in the Recycling part of Figure 1.11.

More than one polypeptide chain can be synthesised from one mRNA molecule. Once the start AUG codon is free due the beginning of ribosomal translocating along the mRNA, another ribosome can bind. A second initiation complex forms. A third ribosome can bind to the start codon when the second ribosome move along the mRNA molecule. Consequently, many protein molecules can be synthesised on the mRNA at a time.

1.2.2 Function of Elongation Factor G in Protein Synthesis

The 78 kDa bacterial peptide EF-G belongs to the GTPase superfamily of protein[174], which includes EF-Tu, IF2, and release factor 3 (RF3). The GTPase activity is turned on by binding to GTP, and is turned off by hydrolysing GTP to GDP.[175] Thus, this switch mechanism enables the GTPase to direct the synthesis and translocation of proteins. During the translocation of protein synthesis, the ribosome moves precisely one codon along the mRNA template. EF-G catalyses the movement of the deacylated tRNA and peptidyl-tRNA bound to the P- and A-sites of the ribosome to the E-and P-sites, respectively, followed by the tRNA dissociation from the E-site.

However, translation can take place in the absence EF-G. GTP hydrolysis is not required for translocation as translocation can occur slowly with non-hydrolysable GTP analogy β, γ-imidoguanosine 5'-triphosphate (GDPNP), but may be required for EF-G release.[176] Kinetic experiments by Rodnina *et al*. indicated that the energy of GTP hydrolysis drives the translocation.[177] Translocation occurs much slower with GDPNP than with GTP.

The crystallography of EF-G (Figure 1.13) show that it contains five domains, I (G), II, III, IV, and V. Domain I (G Domain), which is the largest domain, binds to GTP or GDP.[178] It is homologous to GTPases of the Ras superfamily[179], and can couple GTP hydrolysis to a conformational modification that change the functional state of the protein.[174] Domain II is an all-β structure as a twisted β-barrel. Domains III, IV, and V are specific to EF-G and form a unit that alter its orientation towards domain I and II. Domains III and V have a common protein motif, ribonucleoprotein (RNP) or RNA recognition motif (RRM).[180] Additionally, EF-G contains a unique 90-residue subdomain G', which is different from other elongation factors. Domain IV extends out from the rest of protein in a unique α-β fold. Domain IV has similar shape and overall charge distribution with the anticodon stem-loop of tRNA in the ternary complex.

Cryo-electron microscopy (cryo-EM) studies of the pre- and post-translocation EF-G bound to ribosomes show that binding of EF-G to ribosome resulted in a large conformational change in both ribosome and EF-G, most notably in the structure of the L7/L12 stalk.[182] The flexible switch I and switch II regions in the G domain are responsible for causing such conformational changes through contacts with other domains. A ratchet-like conformational change of ribosome occurs. EF-G-GTP binds to the ribosome, resulting in a counter-clockwise rotation in the small ribosomal subunit.[183] EF-G hydrolyses GTP to GDP and leave the ribosome, which causes a clockwise rotation of the small subunit back to original position.[184] This ratcheting movement enables the tRNAs to move

into A/P and P/E hybrid states bound to the A-and P-sites in the small subunit and the P- and E-sites in the large subunit. Most importantly, the ratchet movement happens when the aa-tRNA in the P site is released.[185] Cryo-EM structures also indicated that the EF-G was held in a position with both large and small subunits. The G domain, domain III and domain V all surround the sarcin-ricin loop (SRL). The domain II interacts with the shoulder of 16S RNA in the small subunits. Domain III contacts with both SRL in the large subunit and protein S12 and h5 of the small subunit. Domain V interacts with the L 11-RNA region of the large subunit. Domain IV occupies the A site of the small subunit and interacts with mRNA and P-site tRNA by inserting into the decoding centre of the small subunit.[186]

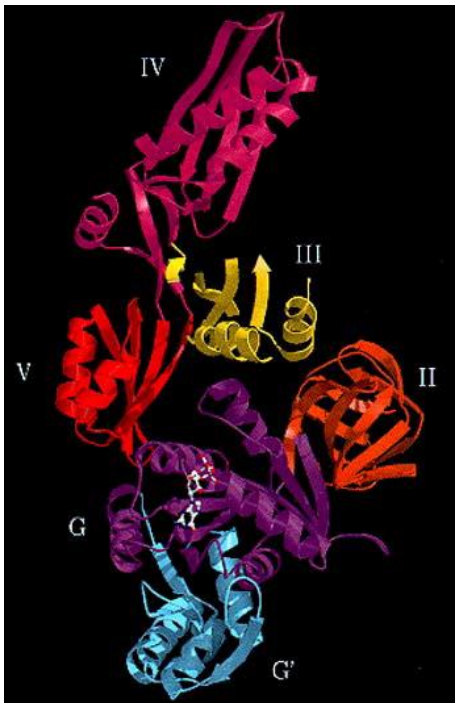


Figure 1.13: The overall structure of EF-G in complex with GDP (ball -and-stick model).[181]

Among the translation factors, EF-G is the only one that functions in two different steps during translation, the translocation and ribosome recycling (disassembly of the post-termination ribosome).[187] Ribosome recycling is the final step of protein synthesis, and it happens when the translating ribosome

reaches a stop codon. EF-G together with the ribosome recycling factor (RRF) drives the dissociation of the ribosomal post-termination complex into small and large subunits during the ribosome recycling with the help of GTP hydrolysis. Unlike the translocation, the GTP hydrolysis is strictly required in ribosomal disassembly by EF-G.

1.2.2.1 EF-G Inhibitor Fusidic Acid

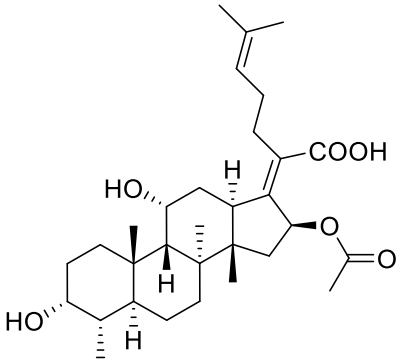


Figure 1.14: Fusidic Acid **1.9**

Fusidic acid (FA) **1.9** (Figure 1.14) is a narrow spectrum steroid antibiotic initially used to treat *Staphylococcus aureus* infections. FA targets EF-G on the ribosome and blocks its dissociation after GTP hydrolysis and translocation.[188] FA shows low affinity to free EF-G but forms a rigid complex with ribosome-bound EF-G.[189] To be specific, FA targets EF-G in three states of the ribosomal translocation process. Firstly, FA binds to EF-G in the early translocation state with high efficiency. A drug-stalled intermediate translocation state was proceeded by the FA- and EF-G-bound ribosome. Secondly, FA may repeatedly bind to EF-G in the intermediate translocation state and thus enhance the ribosome stalling time. Thirdly, FA binds to the EF-G in the post-translocation state of the ribosome resulting in an inhibited dissociation of the ribosome into small and large subunits after translocation.[190] The FA locks EF-G on the RRF-

free post-termination ribosome, blocking the binding of RRF until FA dissociates from EF-G and following EF-G dissociation from the ribosome. If the EF-G and RRF have bound to the ribosome in a splitting-competent complex, binding of FA can stop ribosome splitting by locking the EF-G in an intermediate state. Such ribosome complex, containing RRF and EF-G, is stalled by FA and remains assembled until FA is dissociated. In contrast, in terms of elongation process, the ribosomes are bound by FA in an early state of the translocation process. Wintermeyer *et al*. studied the effect of FA on EF-G/RRF-dependent ribosome disassembly by the light-scattering stopped-flow assay.[191] Their results indicated that the ribosome disassembly by the EF-G GTP/RFF was completely inhibited by FA at a concentration of 1 μM while the inhibition of EF-G turnover during translocation was 200 μM. Therefore, they concluded that the FA inhibits bacterial protein synthesis by blocking the ribosomal recycling rather than peptide elongation.

Gao *et al*. first reported the FA-binding site using a 3.6 Å crystal structure of EF-G and GDP bound to the *T. thermophiles* ribosome with cryo-EM (Figure 1.15 A) and single-particle reconstructions.[186] After that, Selmer *et al*. solved the apo crystal structure of *S. aureus* EF-G to 1.9 Å resolution.[192] The FA is in a pocket surrounded by the switch II region of the G domain, domains II and domain III. The switch II region has a Phe at its tip, F88 in *S. aureus* and F90 in *Thermus thermophiles*, and a T84 residues.[193] These two residues are important for transmitting the conformational changes of switch II between the GTP and GDP forms of EF-G. FA directly interacts with F90 and stops the switch II region of EF-G transmitting from its GTP binding conformation to its GDP binding conformation. Therefore, FA stops the releasing of GTP from its post-translocation complex by trapping it in an intermediate conformation between the GTP and GDP state as show in Figure 1.15 B.

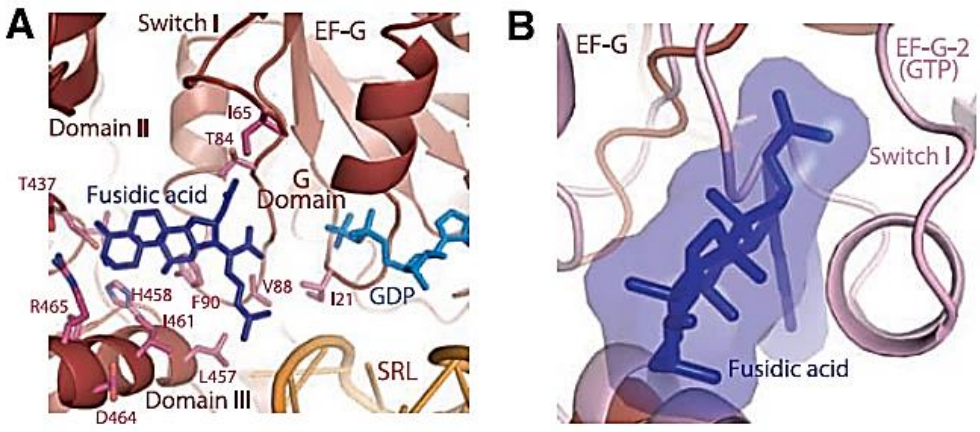


Figure 1.15: FA bound to EF-G in the ribosome. (A) Amino acids interaction of FA in a EF-G domain pocket; (B) Conformational changes of EF-G between the FA-bound form (red) with the GDP-bound form (grey)[186]

Although resistance frequencies of *S. aureus* against FA is generally low, the emerging resistance is a problem that would limit the use of FA for the treatment of staphylococcal infections.[194] There are three mechanistic classes of resistance to FA. The first class is associated with mutation of the *fusA* gene, encoding EF-G.[195] Among this class, a strong FA resistant clinical isolate is the F88L mutation. The F88L mutant strains displays a significantly reduced growth rate and colony size. Therefore, F88 is crucial for the normal and efficient formation of EF-G.[196] The second class, which includes *fusB*, *fusC*, and *fusD* mutants, is found in the chromosome.[197] These three are acquired FA resistant genes found in *Staphylococcus* spp.. The *fusB* and *fusC* are also found in coagulase-negative staphylococci. The gene *fusD* was also an intrinsic factor that caused FA resistance in *Staphylococcus saprophyticus*.[197] All these three mutants express EF-G proteins that protect against FA inhibition. The third class is related to *fusE* mutants, which encodes ribosome protein L6.[198] The first and third class alter the drug targeting site while the second class protects the drug targeting site.

1.2.3 Argyrin Inhibits Elongation Factor G

In 2012, Nyfeler *et al.* identified that argyrin B targets EF-G through resistant mutant selection and whole genome sequencing, biophysical binding study and x-ray crystallography.[170] The whole genome sequencing was carried out on the *P. aeruginosa* mutants with decreased susceptibility to argyrin B. Single point mutations in the *fusA1* gene were identified that caused the reduced sensitivity of *P. aeruginosa* against argyrin B. The observed point mutations in EF-G were P414S, S417L, S459F, P486S, T671A and Y683S (Figure 1.12). Similarly, mutations in *fusA1* was identified in argyrin B resistant-mutant *B. multivorans*. The research group also tested that the binding of argyrin B to purified *P. aeruginosa* EF-G in order to confirm that the argyrin B directly interacts with EF-G. Good binding was observed by measurement with isothermal titration calorimetry and surface plasmon resonance (SPR). However, the S459F mutant variant of EF-G was not able to bind to argyrin. They further studied the target binding pocket and mode of inhibition in a 2.9 Å crystal structure of *P. aeruginosa* EF-G in complex with argyrin B.[170] The overall domain structure of *P. aeruginosa* EF-G is similar to the previously reported *S.aureus* EF-G[192] and *Thermus thermophiles* EF-G[178]. The argyrin B was found to bind at the interface of domains III and V, which is different from the FA bind pocket (between II and III)[192], affording a novel allosteric binding site as shown in Figure 1.16 and 1.17. More importantly, the binding of argyrin B towards EF-G causes a rotation of domains III and V with respect to domains I and II comparing with previously resolved structure. The argyrin B-bound EF-G displays an extended conformation when comparing with previously described *Thermus thermophiles* EF-G in complex with GTP[186] or in complex with FA and the ribosome due to a ratcheting of domain IV. In conclusion, the argyrin B binding elongated the structure of the EF-G, and therefore make EF-G not compatible with ribosome binding.

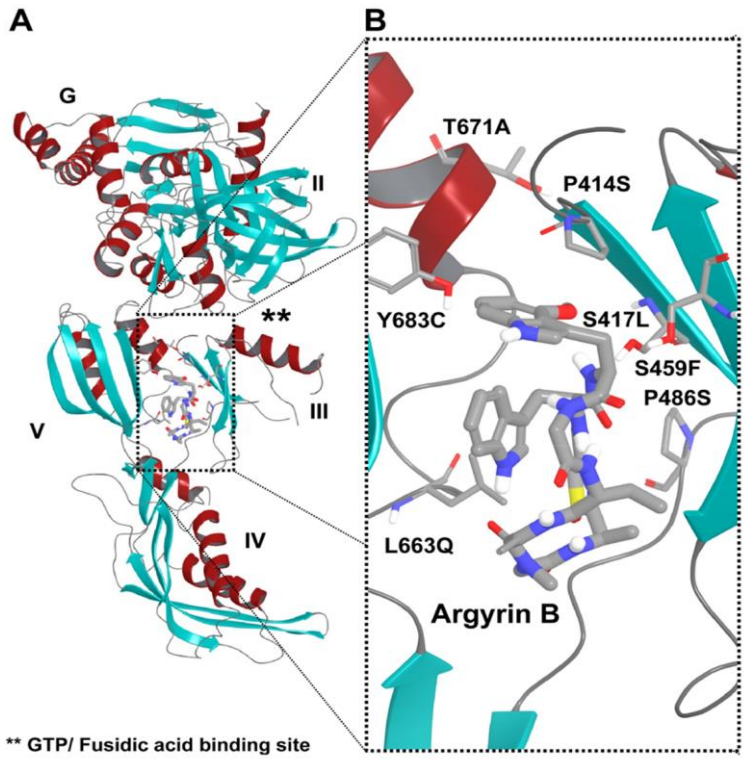


Figure 1.16: (A) The binding domain of argyrin B, which is distinct from the GTP/FA binding domain; (B) Inset view with key amino acids interactions between argyrin B and domain III of EF-G.[170]

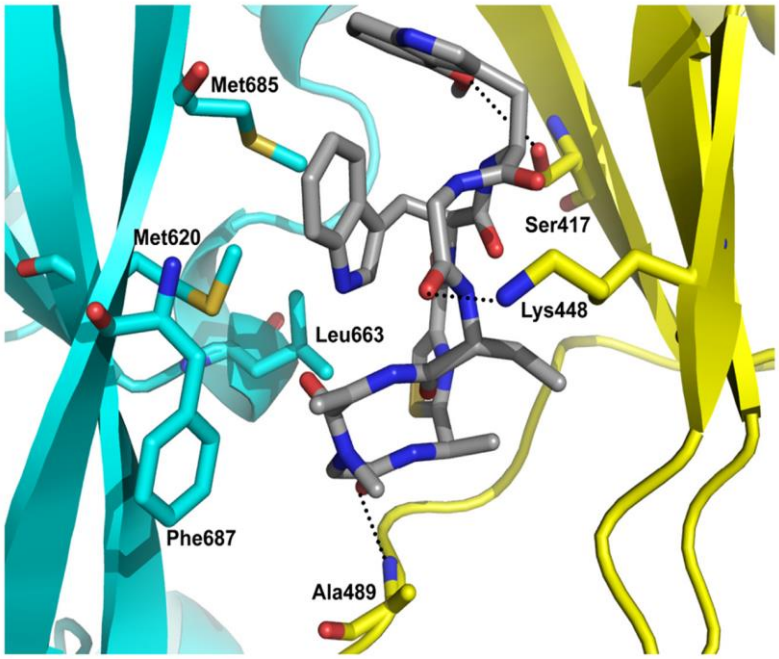


Figure 1.17: Interaction between *P. aeruginosa* EF-G (domain III in yellow and domain V in cyan) and argyrin B (gray).[170]

In the same year, Bielecki *et al*. determined that the mode of action of argyrin A was similar to argyrin B using whole genome sequencing technology.[199] A strong relationship between argyrin A resistance and mutation in EF-G was discovered, which suggested that EF-G is the target of argyrin A. Overall six mutations (in five amino acid positions in *fusA*) (Figure 1.18 (A) and (B)) that changed the amino acid sequence in the EF-G were identified. The previously identified S417L, S459F and L663Q responsible for argyrin B resistance in *P. aeruginosa* were also observed in the mutations responsible for the argyrin A resistance. The other three are I457T, L663M and M685R. Mapping of these mutations over the structural model of EF-G indicated that two of these mutations (L663M/Q and M685R) were located in domain V, and three mutations (S417L, S459F and I457T) were located in the domain III.

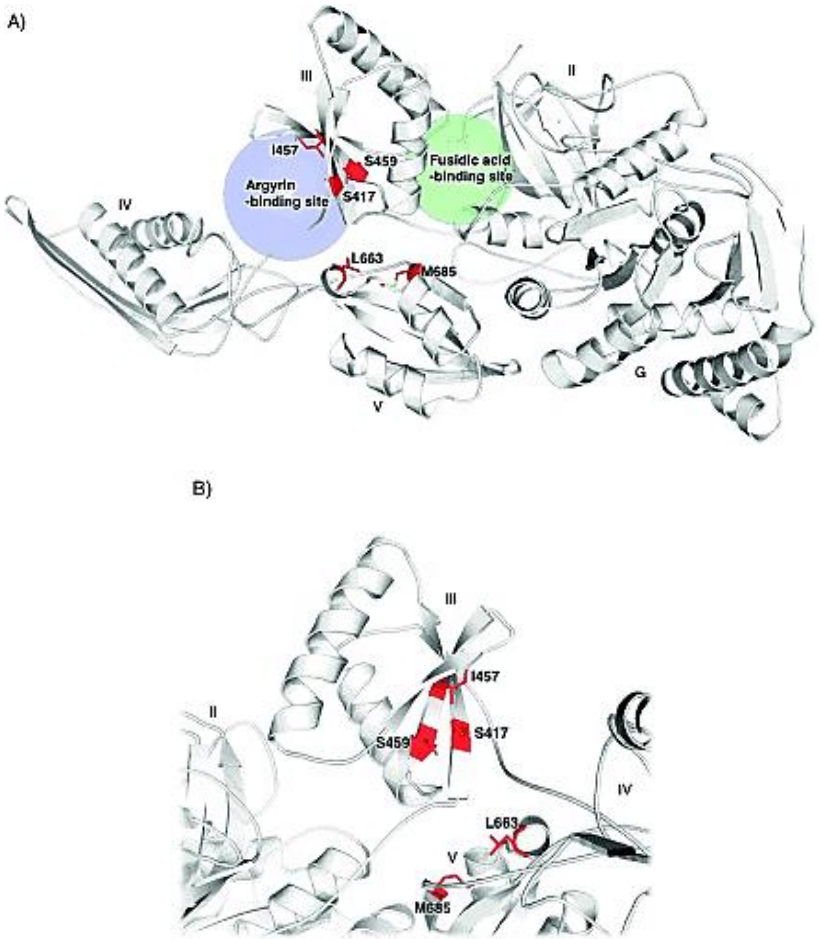


Figure 1.18: (A) Overview of argyrin A and fusidic acid binding site in EF-G; (B) The mutation residues causing argyrin resistance (red).[199]

1.2.3.1 Argyrin B Targets Mitochondrial EF-G in Mammalian Cell and Yeast

Apart from targeting bacterial EF-G, Nyfeler *et al* reported that argyrin B targets mitochondrial EF-G in eukaryotic cells.[170] They first determined argyrin B activity against yeast. Argyrin B that was inactive against wild type yeast *Saccharomyces cerevisiae* (BY4741) and strain BYΔ8 with eight deleted genes were grown in a rich medium with glucose as carbon source. However, argyrin B displayed a strong inhibition against BYΔ8 when glucose was substituted with ethanol/glycerol. Energy generation from ethanol/glycerol is strictly relying on oxidative phosphorylation in yeast while glucose is metabolised by anaerobic fermentation. Therefore, the result suggested that argyrin B affected mitochondrial function. Argyrin B was also a substrate for drug efflux pumps in yeast. A mutagenesis strategy[200], similar as what they used for bacteria, was used to identify the specific target of argyrin B in yeast. Using the whole genome sequencing, the *MEF1* gene, encoding mitochondrial elongation factor (mEF-G), was discovered in all resistant yeast strains tested. Four individual mutations S473L, S517F, G517D and P667L were identified, and G517D was further determined to be a passenger mutation that does not cause argyrin B resistance. Comparing with the *P. aeruginosa* EF-G mutations, P667L is novel while S473L and S517F of mEF-G was related to S417L and S459F of *P. aeruginosa* EF-G, respectively. The mEF-G in yeast *S. cerevisiae* is the closest homologue of bacterial EF-G, and thus suggested that argyrin B target exists in the eukaryotic cells.

Nyfeler *et al*. explored the argyrin B-sensitivity of mammalian cells.[170] Argyrin B inhibited cell viability in 18 human cancer cell lines with a maximum IC_{50} of 1 μM. Argyrin B displayed a similar effect as mitochondrial electron transport

inhibitors rotenone and antimycin A. Since electron transport complexes are translated by mitochondrial ribosomes[201], correlation of argyrin B to mitochondrial electron transport inhibitors suggested that argyrin B inhibited mitochondrial protein synthesis through mitochondrial elongation factor G (encoded by human *GFM*). The human mEF-G is the closest mammalian homologue to bacterial EF-G and yeast mEF-G. Although the overall sequence homology between *P. aeruginosa* EF-G and human mEF-G is only 40%, the research group found that human mEF-G contains amino acid residues that mediate argyrin B binding and bacterial resistance. Therefore, they applied corresponding *P. aeruginosa* EF-G point mutations (S452L, S494F, L693Q) to human mEF-G. Apparently, HCT116 (human colorectal cancer line) and RKO (human colon cancer line) with wild type mEF-G are sensitive to argyrin. While the mEF-G S452L and S494F showed minor reduction of sensitivity, mEF-G L693Q displayed 4- and 7-fold reduced susceptibility to argyrin B in HCT116 and RKO cells, respectively.

1.3 Current Methods for Argyrin Total Synthesis

The reported antibacterial activity of argyrin A and B made them potential drug candidates. In order to further determine their structure-activity relationship (SAR), several synthetic methods have been developed for the production of argyrin and its analogues.

In 2002, Ley *et al*. achieved the first solution phase total synthesis of argyrin B.[202] According to the structural complexity of argyrin B, the research group devised a route that could protect the stereogenic centres at crucial stages of the synthesis. Their route included synthesis of three protected fragments, containing one thiazole, one tripeptide with a 4-methoxytryptophan unit and one

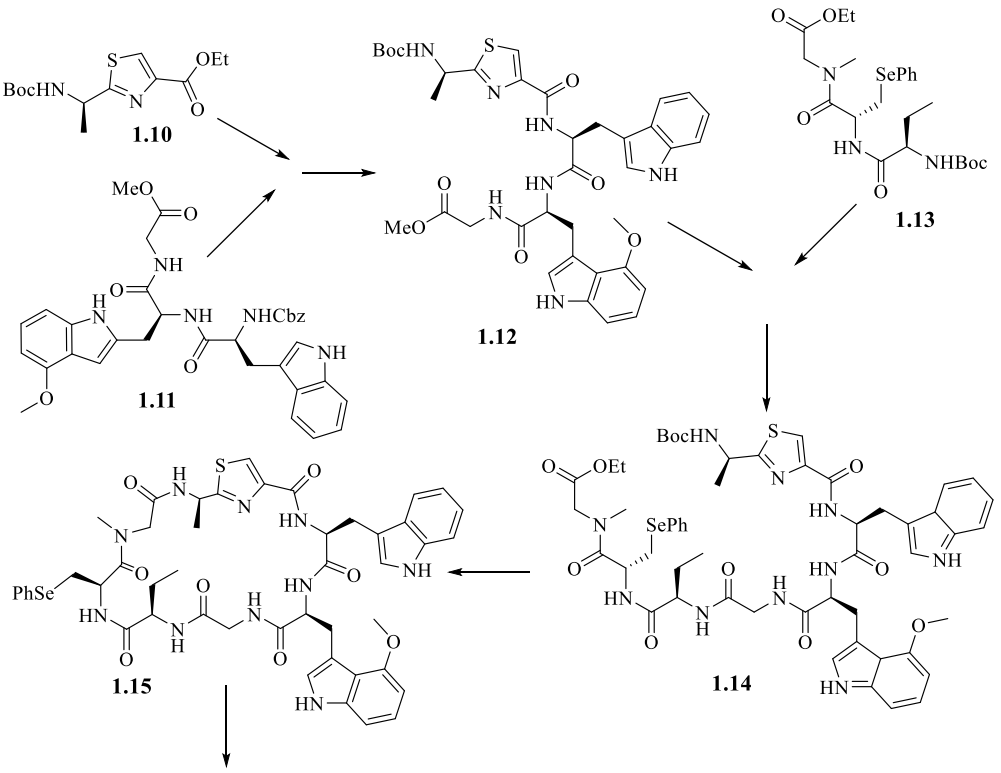
tripeptide with the dehydroalanine component. The challenges of the total synthesis of argyrin are making of unnatural amino acid residues, these being 4-methoxy-L-tryptophan, dehydroalanine and thiazole dipeptide, assembling of three fragments with proper coupling methods and final cyclising process. The α-centre to the *C*-terminus of all the three fragments is achiral so that epimerization during assembly could be avoided. Following Ley *et al.*, Wu *et al.*[203] and Bülow *et al*.[204] reported solution phase total synthesis of argyrin A and E, and argyrin F, respectively. However, the solution-phase macrocycle-assembly method used by those three research groups suffered from the inconvenient purification at every synthetic step resulting in compromised overall yield. To overcome these shortages, Chan and co-workers applied Fmoc/*t*Bu solid-phase peptide synthesis (SPPS) for stepwise assembly of the argyrin linear precursors.[205] Apart from the commercial available protected amino acid residues, they successfully synthesised the three unnatural building blocks, the thiazole dipeptide, the dehydroalanine residue, and various substituted L-tryptophan residue. The following sections outline a brief discussion of each of the reported methods.

1.3.1 Ley's Method

Ley *et al*. reported a synthetic route to achieve the total synthesis of argyrin B as shown in Scheme 1.1. As mentioned above, the route required preparation of three protected fragments. The first fragment is the thiazole dipeptide **1.10**. They followed the reported route from *N*-Boc-D-alanine using a modified Hantzsch thiazole formation.[206] The second fragment is the tripeptide containing 4-methoxy-L-tryptophan **1.11**. With the help of an enzyme mediated resolution route, i.e. an immobilized Penicillin G acylase, they successfully synthesised the key building block 4-methoxy-L-tryptophan. The final fragment **1.12** required synthesis of the phenylselenocysteine Sec(Ph) as the masked precursor

of dehydroalanine. The dehydroalanine is unstable and is prone to nucleophilic attack. The detailed synthesis route of the thiazole dipeptide, phenylselenocysteine, and various substituted L-tryptophan will be described in Chapters 2 and 3.

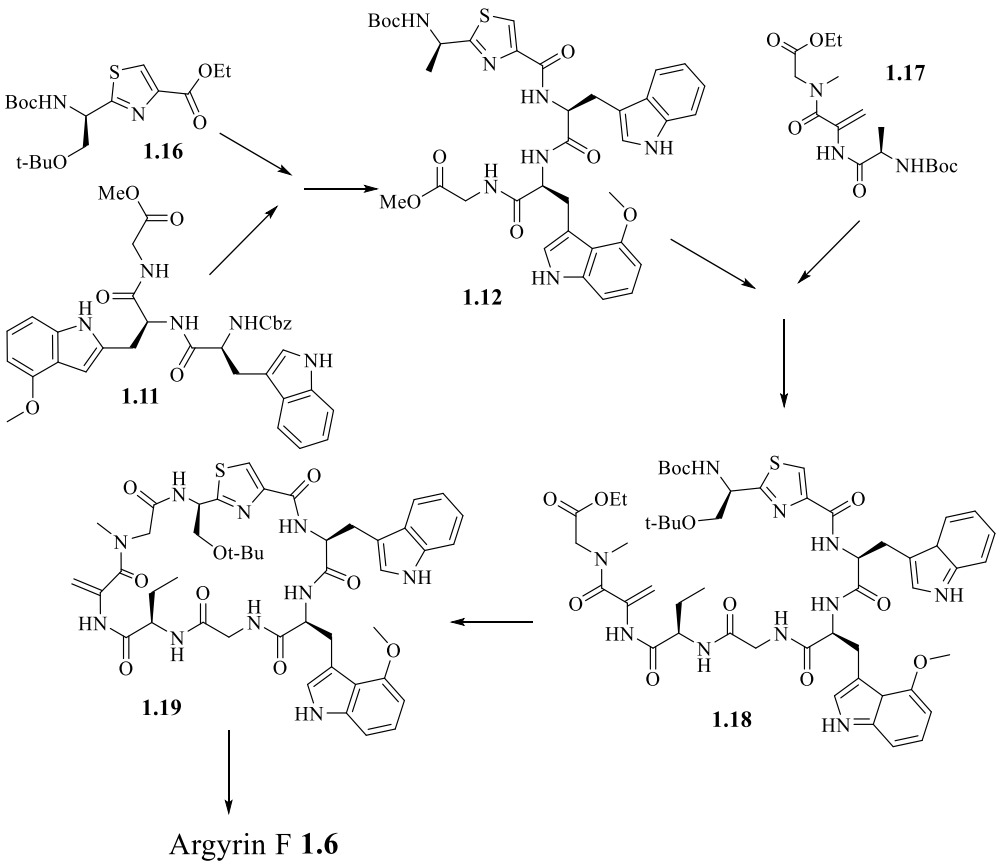
With all three fragments synthesised, the Cbz protection group in the tripeptide **1.11** is removed by hydrolysis, following coupling with the free acid from thiazole dipeptide **1.10** to generate pentapeptide **1.12**. The pentapeptide was hydrolysed and coupled with the Boc-deprotected Sec(Ph) containing fragment **1.13** to give the heptapeptide **1.14**. The *C*- and *N*- termini of the heptapeptide were deprotected and finally cyclised to give the fully assembled cyclic heptapeptide **1.15**. Finally, the *syn*-elimination of the selenide was carried out with sodium periodate and bicarbonate to afford argyrin B **1.2** in a total yield of 5.6%.



Scheme 1.1: Total synthesis of argyrin B through Ley's method.[202]

1.3.2 Kalesse's Method

Kalesse and co-workers took advantage of solution phase total synthesis method developed by Ley *et al*.[202] and synthesised argyrin A and its analogues (Scheme 1.2).[204] They dissected the argyrin in three complex segments as well. The thiazole dipeptide was synthesised using Hantzsch thiazole formation from *N*-Boc-D-alanine for argyrin A, B, C, D and E, and from *tert*-butyl protected serine to **1.16** for argyrin F and G. Unlike Ley *et al*., they utilised DuanPhos ligand in combination with $Rh(cod)_2BF_4$ as the chiral auxiliary for catalytic hydrogenation to provide the 4-methoxy-L-tryptophan in 99% *ee* to make tripeptide **1.11**.



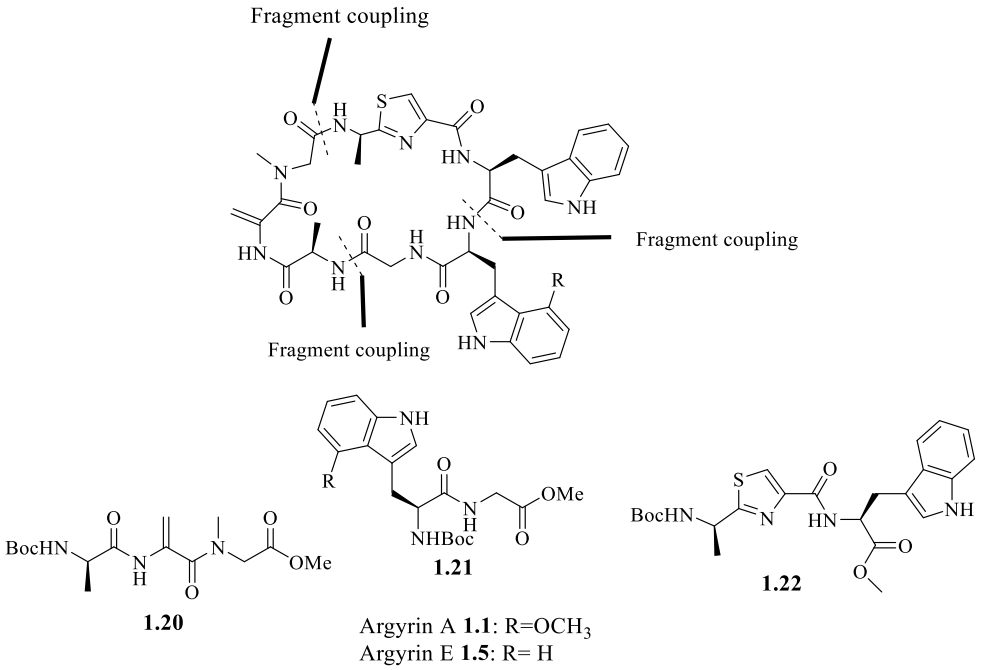
Scheme 1.2: Total synthesis of argyrin F using Kalesse's method.[204]

In contrast to the making masked precursor phenylselenocysteine described by Ley *et al.*, they performed a copper(I)-catalysed β-elimination of the serine hydroxy group to generate the dehydroalanine containing tripeptide **1.17** for direct usage. They hypothesised that the dehydroalanine moiety was chemically stable as long as the α-amino group was substituted by an electron-withdrawing group, which was amide of D-Ala or D-Abu residue.

1.3.3 Jiang's Method

Jiang and co-workers reported a convergent strategy by the condensation of a tripeptide and two dipeptide fragments to synthesise argyrin A and E (Scheme 1.3).[203] The achiral glycine was selected as the *C*-terminal end to avoid racemisation during backbone macrocyclisation. The thiazole, which was synthesised via Hantzsch thiazole formation from *N*-Boc-D-alanine, was coupled with the methyl ester of tryptophan to generate the dipeptide **1.22**. The synthesis of dehydroalanine containing tripeptide **1.20** was accomplished through mesylation followed by β-elimination of serine. Their method of synthesis of 4-methoxy-L-tryptophan containing dipeptide **1.21** included a palladium-catalysed heteroannulation reaction, which will be described in Chapter 2.

All the fragments (scheme 1.3) were coupled after *N*-Boc deprotection and saponified to generate the linear precursor. The linear heptapeptides were than cyclised after *C*-terminal methyl ester hydrolysed and *N*-terminal Boc deprotected.

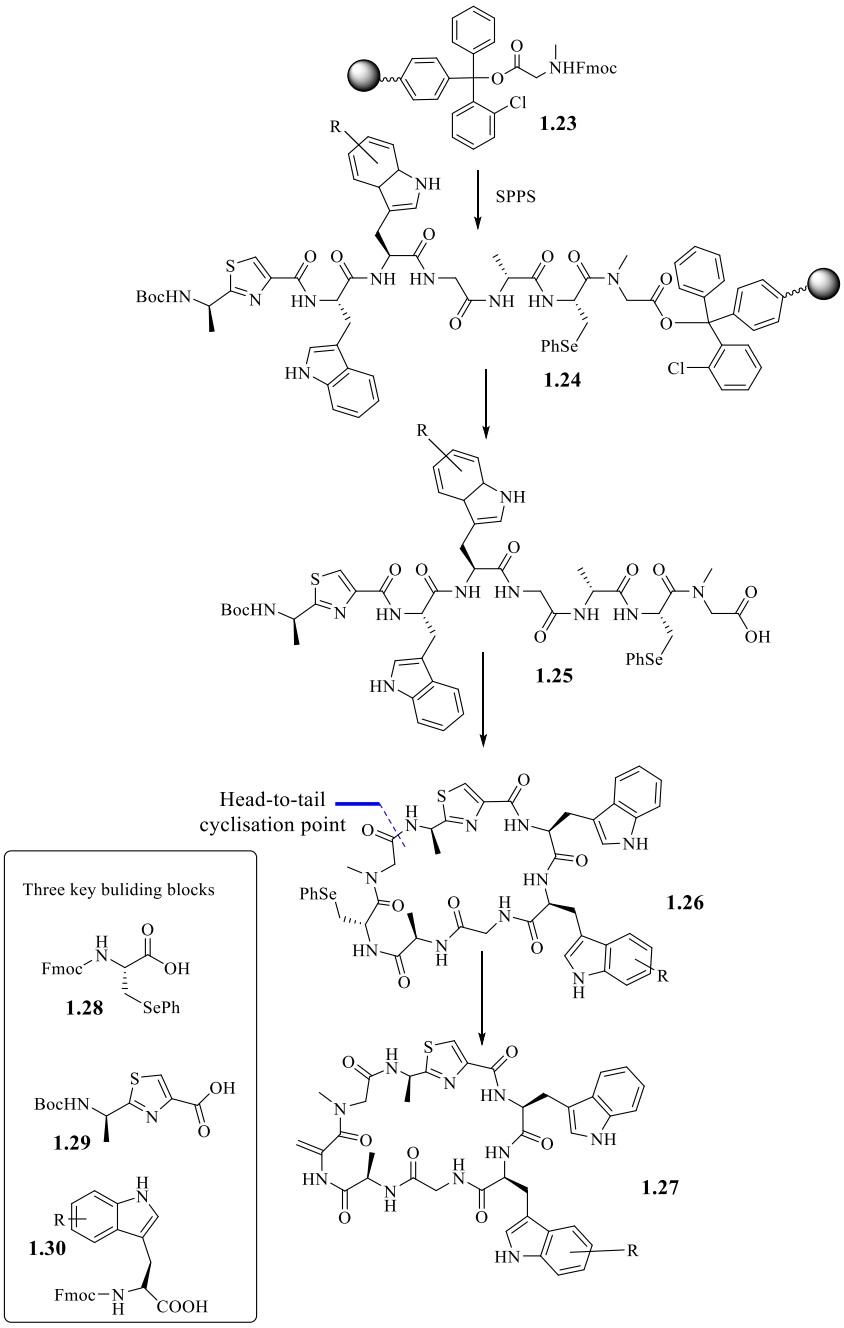


Scheme 1.3: Total synthesis of Argyrin A and E using Jing's method.[203]

1.3.4 Chan's Method

Chan and co-workers, for the first time, developed a Fmoc/*t*Bu solid-phase peptide (SPPS) followed by a solution-phase macrocyclisation strategy to achieve the total synthesis of the argyrins **1.27** as shown in Scheme 1.4. The amino acid residues for argyrin are sarcosine, dehydroalanine, D-Ala, Gly, L-Trp, and a thiazole dipeptide. The dehydroalanine, substituted L-Trp **1.30** and thiazole dipeptide **1.29** were synthesised. The masked precursor phenylselenocysteine **1.28** was synthesised and was unmasked to give the *exo*-methylene moiety at a later stage of the Fmoc/*t*Bu SPPS. The thiazole dipeptide **1.29** was synthesised following the method reported by Ley *et al*.[202]. The asymmetric synthesis of L-tryptophan analogues **1.30** was achieved with the help of a (*S*)-methylbenzylamine-based chiral auxiliary reagent[207]. With all the building blocks in hand, the total synthesis of the argyrin through Fmoc/*t*Bu SPPS, followed by solution phase macrocyclisation, and final unmasking of

phenylselenocysteine to give the dehydroalanine. The success of this strategy offered an alternative method for the total synthesis of argyrin analogues.



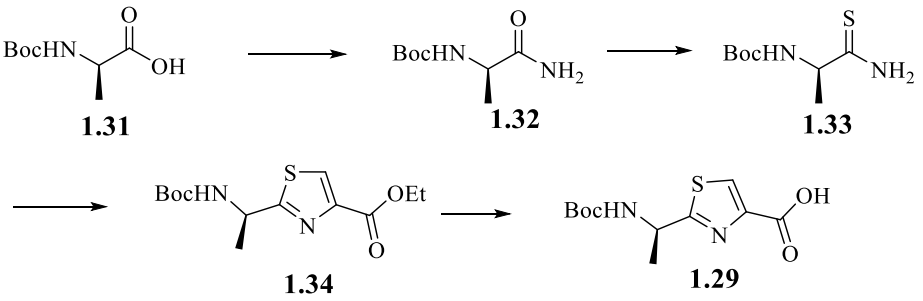
Scheme 1.4: Total synthesis of argyrin analogues and three key building blocks reported by Chan and co-workers.[205]

1.4 Aim and objectives

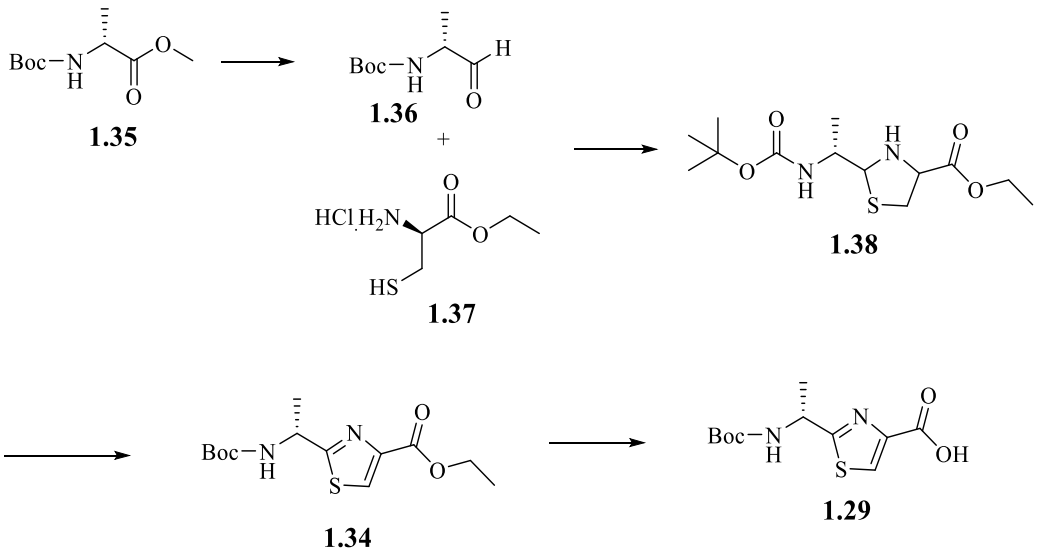
The above sections indicated that argyrin could be a novel antibacterial candidate due to its unique mechanism of action and synthetic accessibility. Their outstanding activity towards relevant clinical pathogens *P. aeruginosa* and *B. multivorans* has encouraged the research work carried out in this thesis. The primary aim of this thesis was to synthesise argyrin analogues with improved antibacterial activity. The evaluation of SARs of the argyrins towards *P. aeruginosa* and *B. multivorans* is presented in this thesis based on the early work carried by Chan and co-workers. The reported co-crystal complex of argyrin B-bound *P. aeruginosa* EF-G will guide rational design of a focused library of argyrin analogues. Chan and co-workers in their preliminary investigation into the structure-activity relationship (SAR) of argyrin that govern their antibacterial activity explored the role of (*S*)-4-methoxytryptophan. They found that the 4-methoxy functionality is crucial to maintain antibacterial activity, since shifting the methoxy functionality from 4-position to 5-position weakened its activity. The potential role of the dehydroalanine residue in the antibacterial activity of argyrin B will be considered. The dehydroalanine residue of the argyrin B is expected to constrain the cyclic conformation of argyrin, thereby governing the rigidity of the structure, which is likely to be essential for target binding affinity.

For the synthesis of argyrin analogues, the methodology of solid-phase peptide synthesis and macrocyclisation strategy is applied (Scheme 1.4). Among the seven amino acid building blocks of argyrin B, tryptophan analogues, thiazole dipeptide and dehydroalanine are not commercially available and are therefore synthesised. The sarcosine residue was selected as the *C*-terminal amino acid to avoid epimerisation of the *C*-terminus during the head-to-tail macrocyclisation.

Chapter 2 discusses the synthesis of two key building blocks, the *N*-Boc-thiazole dipeptide **1.29** and substituted L-tryptophan analogues **1.30**. The previously reported Hantzsch thiazole synthesis of thiazole was selected (Scheme 1.5) and an alternative thiazole dipeptide synthesis was also evaluated (Scheme 1.6). The alternative method was achieved by condensation of L-cysteine **1.37** with pyruvaldehyde **1.36** to form a thiazolidine **1.38** which was then oxidized to thiazole **1.34** by MnO_2.

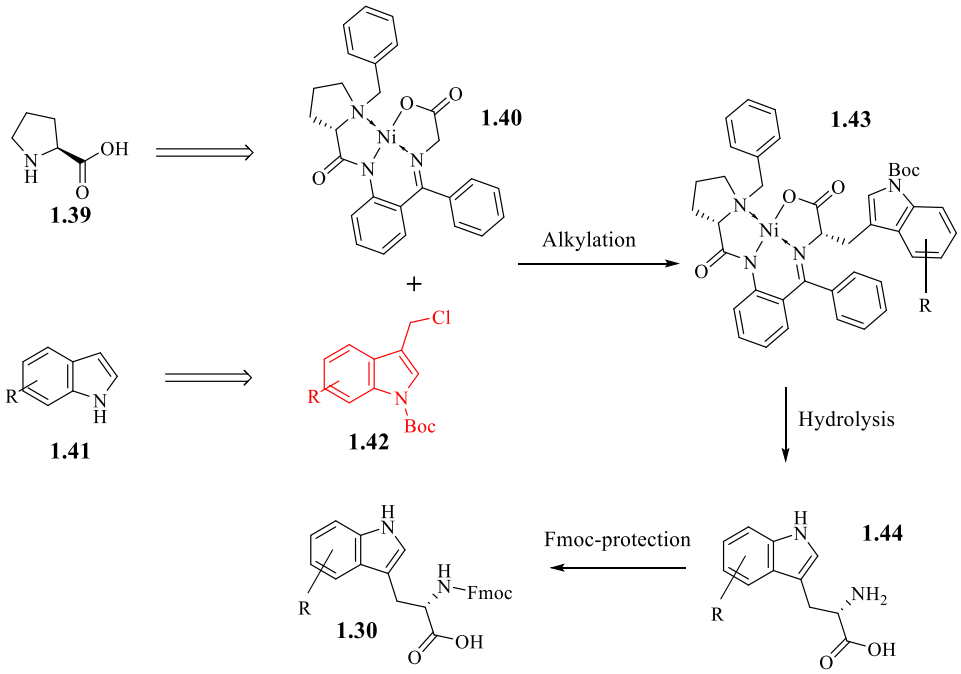


Scheme 1.5: Total synthesis of thiazole dipeptide using Schmidt's modified Hantzsch method



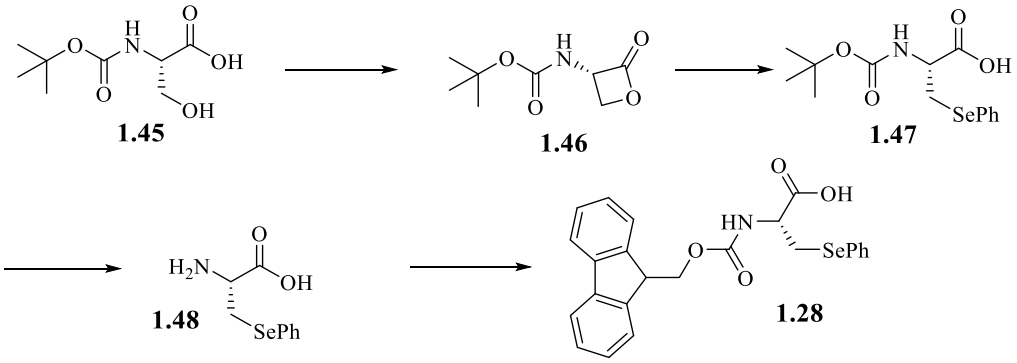
Scheme 1.6: Alternative total synthesis of thiazole dipeptide

The asymmetric synthesis of L-tryptophan analogues **1.30** was achieved by alkylation of an indole alkylhalide **1.42** with the BPB-(*S*)-glycine-Ni(II) Schiff base **1.40** following acid hydrolysis as illustrated in Scheme 1.7.

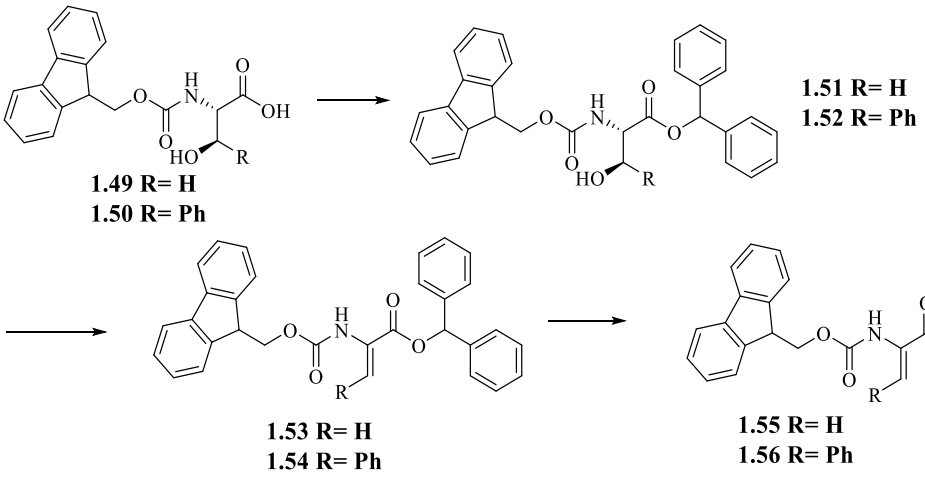


Scheme 1.7: Total synthesis of substituted L-Tryptophans *via* alkylation with BPB-(*S*)-glycine-Ni(II) Schiff base

Chapter 3 discussed the synthesis of the precursor *N*-Fmoc-Sec(Ph) (Scheme 1.8) **1.28** and a β-elimination method of threonine **1.49** to dehydrobutyrine **1.55** and hydroxy-phenylalanine **1.50** to dehydrophenylalanine **1.56** (Scheme 1.9). Inspired by the formation of the dehydrobutyrine from the tosylation of threonine, this thesis further investigated the application of the strategy at the cyclic peptide level. Accordingly, the direct conversion of the threonine residue containing cyclic peptide to dehydrobutyrine containing cyclic peptide under tosylation condition was investigated.



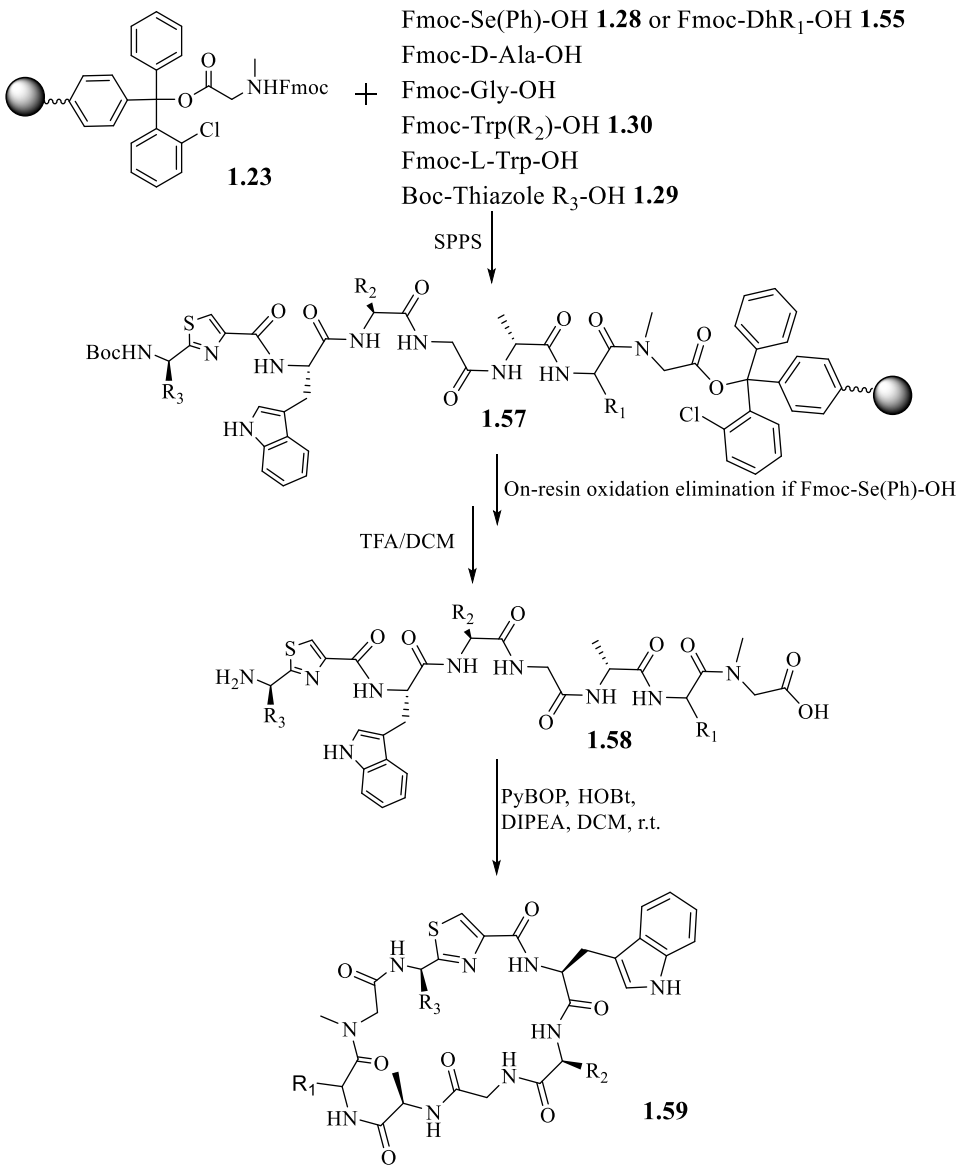
Scheme 1.8: Total synthesis of masked precursor Fmoc-Sec(Ph)



Scheme 1.9: Synthesis route for Fmoc-dehydroamino acids

Chapter 4 describes the total synthesis of the argyrins through Fmoc/*t*Bu SPPS and the final solution-phase macrocyclisation. Additionally, an on-resin oxidation elimination of phenylselenocysteine to dehydroalanine was operated (Scheme 1.10). This chapter also determined the NMR spectra of the dehydro amino residue containing argyrin analogues.

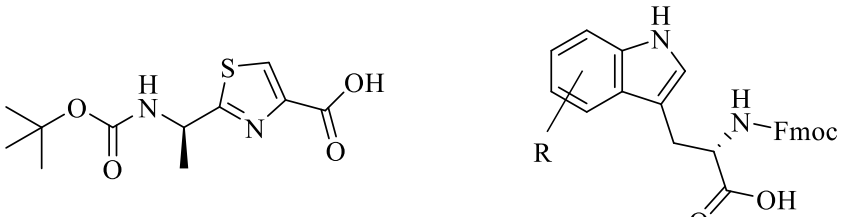
Chapter 5 reports the antibacterial activity profiling of the argyrin analogues against a panel of Gram-negative and Gram-positive bacteria. One most active dehydrobutyrine containing argyrin analogue was reported. Such an analogue displayed an improvement of antibacterial activity against *Pseudomonas aeruginosa* and *Burkholderia multivorans*.



Scheme 1.10: The Fmoc/*t*Bu-SPPS, on-resin oxidation elimination and solution-phase macrocyclisation of the linear precursors to argyrins.

Chapter 2
Synthesis of Two Key Building Blocks of Argyrins

The synthesis methods of two unusual amino acid building blocks (Figure 2.1) of argyrin, the *N*-Boc-thiazole dipeptide **1.29** and substituted L-tryptophan analogues **1.30**, are outlined in this chapter. Two approaches for the synthesis of *N*-Boc-thiazole dipeptide **1.29** are described in this chapter. This chapter also illustrates the asymmetric synthesis of L-tryptophan analogues **1.30** by alkylation of an indole alkylhalide **1.42** with the (*S*)-BPB-glycine-Ni(II) Schiff base followed by hydrolysis.



1.29 **1.30**

Figure 2.1: Two key building blocks **1.29** and **1.30**

2.1 Thiazole Dipeptide

Thiazole is a heterocyclic compound that contains a sulfur and a nitrogen. The aromaticity of thiazole is due to fully conjugated π electrons and a planar ring system. Thiazole moieties, typically as thiazole dipeptide fragments, are found in many naturally occurring cyclic peptides, such as Sanguinamide A[208] **2.1**, dendroamide A[209] **2.2**, and amythiamicin D[210] **2.3** (Figure 2.2).

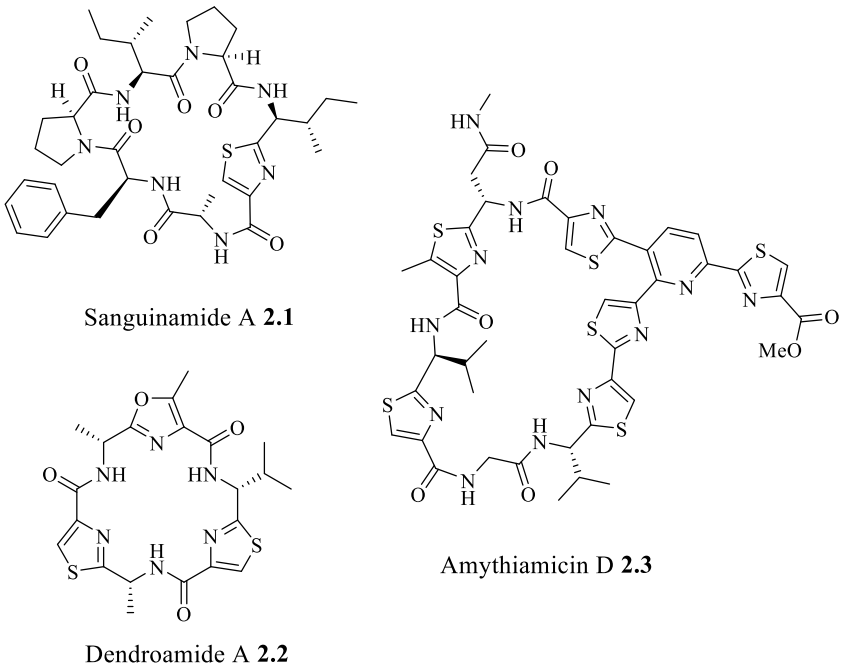
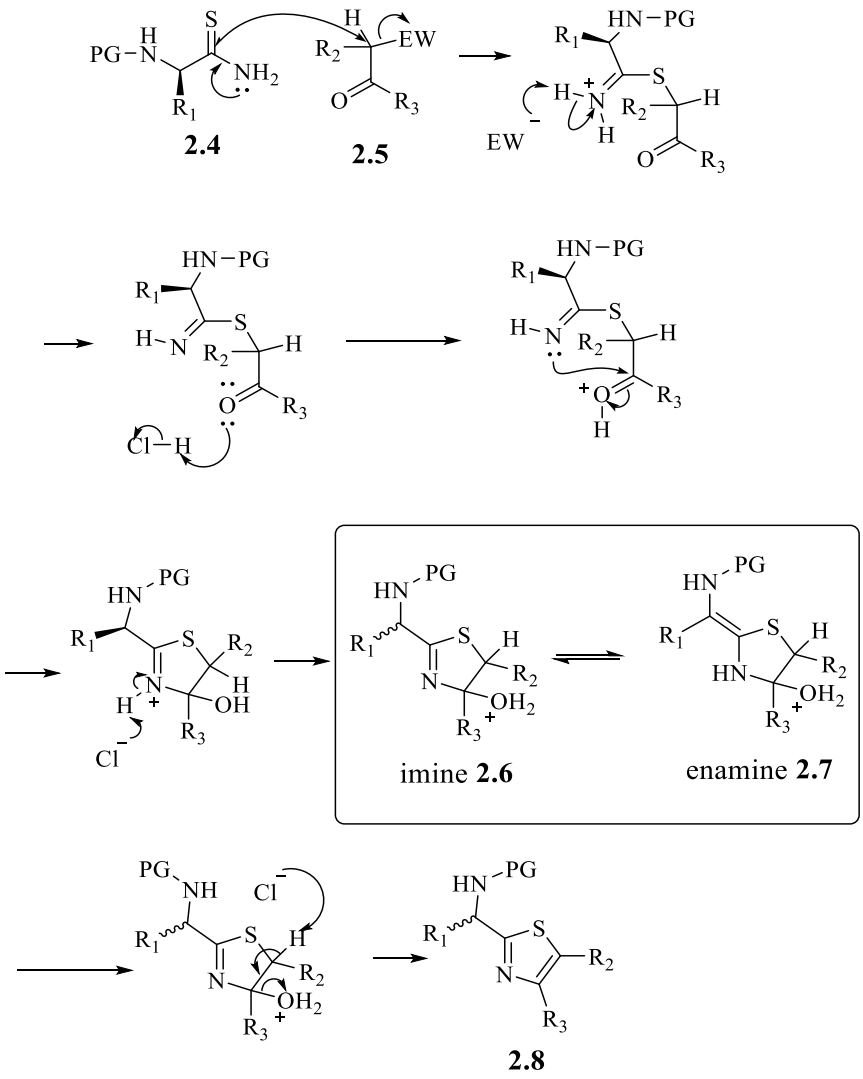


Figure 2.2: Thiazole containing cyclic peptides

2.2 Synthetic Approach to Thiazole Dipeptides

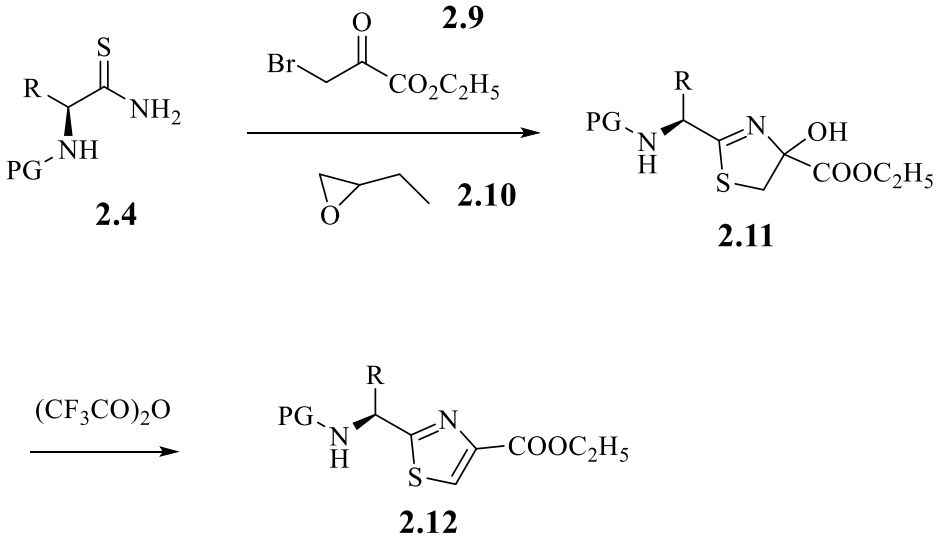
The therapeutic relevant thiazole containing compounds has maintained development of robust method for their construction by total chemical synthesis. The most widely adopted thiazole synthetic methods are based on a modified Hantzsch thiazole synthesis (Scheme 2.1), initially developed in 1889.[211] The

method involved condensation of a thioamide **2.4** with an α-haloketone **2.5** followed by acid-catalysed dehydration to generate the required thiazole **2.8**. This reaction is based on the strong nucleophilicity of the sulfur atom in the thioamides. However, this method generated C_2-exomethine racemised thiazole amino acids, even when starting with chiral precursors. This is due to the slow rate of the acid-catalysed aromatisation of a delta-thiazoline intermediate, which causes racemisation via an acid-catalysed imine **2.6**-enamine **2.7** type equilibration.



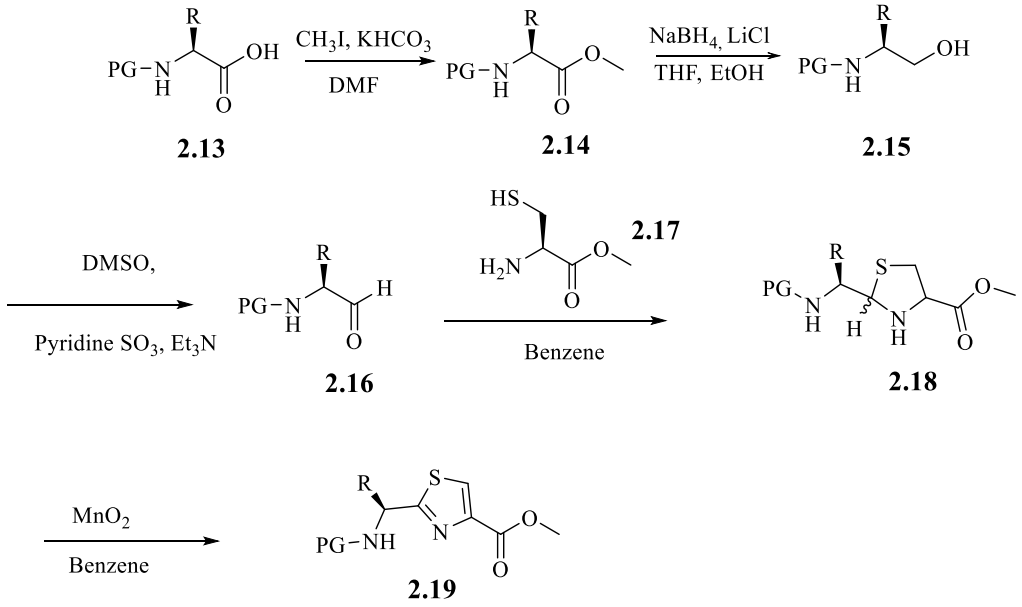
Scheme 2.1: Proposed mechanism of Hantzsch thiazole synthesis

In order to overcome the problem of racemic products, alternative reaction conditions have been developed. In 1986, Schmidt *et al.* reported a synthetic route to generate the enantiomerically pure thiazole amino acid by modifying the Hantzsch procedure (Scheme 2.2).[212] The starting component of the Hantzsch synthesis could be obtained by treating the amides with the Lawesson's reagent to generate the corresponding thioamides **2.4**. The thioamides were reacted then with ethyl bromopyruvate **2.9** in ethanol to form the thiazole compounds with 40-60% *ee*. The optical purity was enhanced by the addition of ethyloxirane (1,2-epoxybutane) **2.10** which traps the hydrobromic acid by-product and stops the reaction at the stage of the dihydrothiazole **2.11**. The dihydrothiazole intermediate is dehydrated with trifluoroacetic anhydride to generate the optical pure thiazole-4-carboxylic ester **2.12**. The choice of solvent is important to obtain high optical purity. A higher optical purity was observed when ethanol or acetone was selected as solvent in the condensation step. In addition, the choice of the *N*-protecting group contributes to the high optical purity. The phthaloylamino thiocarboxamides and *p*-nitrobenzyloxycarbonylamino derivatives mostly generate racemic thiazoles.



Scheme 2.2: Schmidt's modified Hantzsch thiazole synthesis

In 1987, Hamada *et al*. reported a robust synthetic route (Scheme 2.3) to generate enantiomerically pure thiazole amino acid using commercially available *N*-Boc or *N*-Z protected α-amino acids as starting material.[213] *N*-Boc or *N*-Z protected amino acids **2.13** were first converted to the corresponding methyl esters **2.14** by methyl iodide in dimethylformamide containing potassium hydrogen carbonate at room temperature. The methyl esters were then reduced to amino alcohol derivatives **2.15** with lithium chloride–sodium borohydride in ethanol–tetrahydrofuran. Selective Parikh-Doering oxidation of the *N*-protected amino alcohol was carried out using sulfur trioxide–pyridine complex in triethylamine to give the enantiomerically pure amino aldehyde derivatives **2.16**. A thiazolidine intermediate **2.18**, which is a mixture of C-3 epimers, was achieved via a condensation-cyclisation route using cysteine **2.17** and amino aldehyde. Finally, the oxidation of the thiazolidine using manganese dioxide yield desired thiazole **2.19**, activated manganese dioxide was preferred.



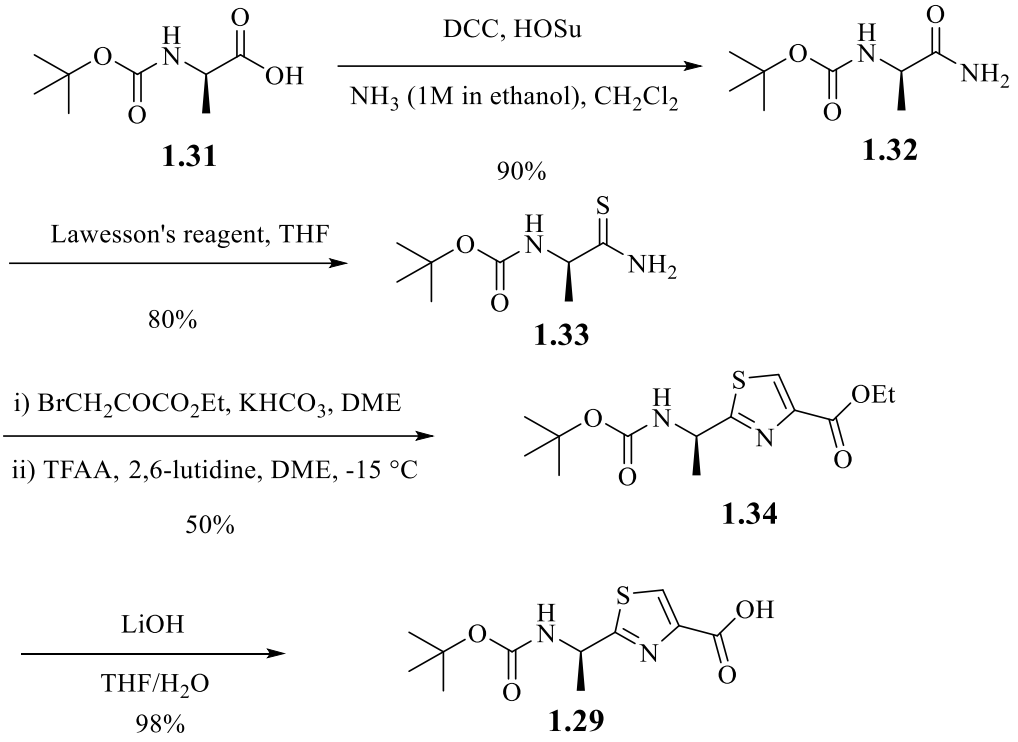
Scheme 2.3: Hamada's modified thiazole amino acid synthesis

2.3 Synthesis of 2-((*tert*-butoxycarbonyl)-1-amino-alkyl)thiazole-4-carboxylic Acid

Inspired by the previously developed thiazole synthesis methods, both Schmidt's modified Hantzsch and Hamada's route were evaluated and reported in this thesis. The Schmidt's modified Hantzsch route was adopted by many research groups during the synthesis of argyrin. In addition, Moody and co-workers also reported the application of Schmidt's modified Jantsch route with good yield and no racemization when synthesizing amythiamicin D.[210] In this thesis, the route reported by Chan and co-workers[205], which is similar to Moody's method, is used. In terms of Hamada's route, a modified route developed by Ley and co-worker during their synthesis of plantazolicin A[214] was attempted with modification.

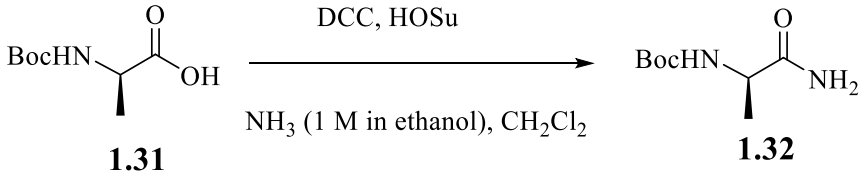
2.3.1 Synthesis of 2-((*tert*-butoxycarbonyl)-1-amino-alkyl)-thiazole-4-carboxylic Acid Using Chan's Route

The synthesis started from the transformation of *N*-Boc-protected D-alanine **1.31** to the corresponding thioamide **1.33** through the intermediate amide **1.32**. The resultant thioamide was condensed with ethyl bromopyruvate to generate an intermediate which was then reacted with trifluoroacetic anhydride in the presence of 2,6-lutidine to afford the *N*-Boc protected thiazole dipeptide ethyl ester **1.34**. The ethyl ester was hydrolysed with lithium hydroxide to give the *N*-Boc protected thiazole amino acid **1.29**. The detailed reaction procedure is described in Scheme 2.4.



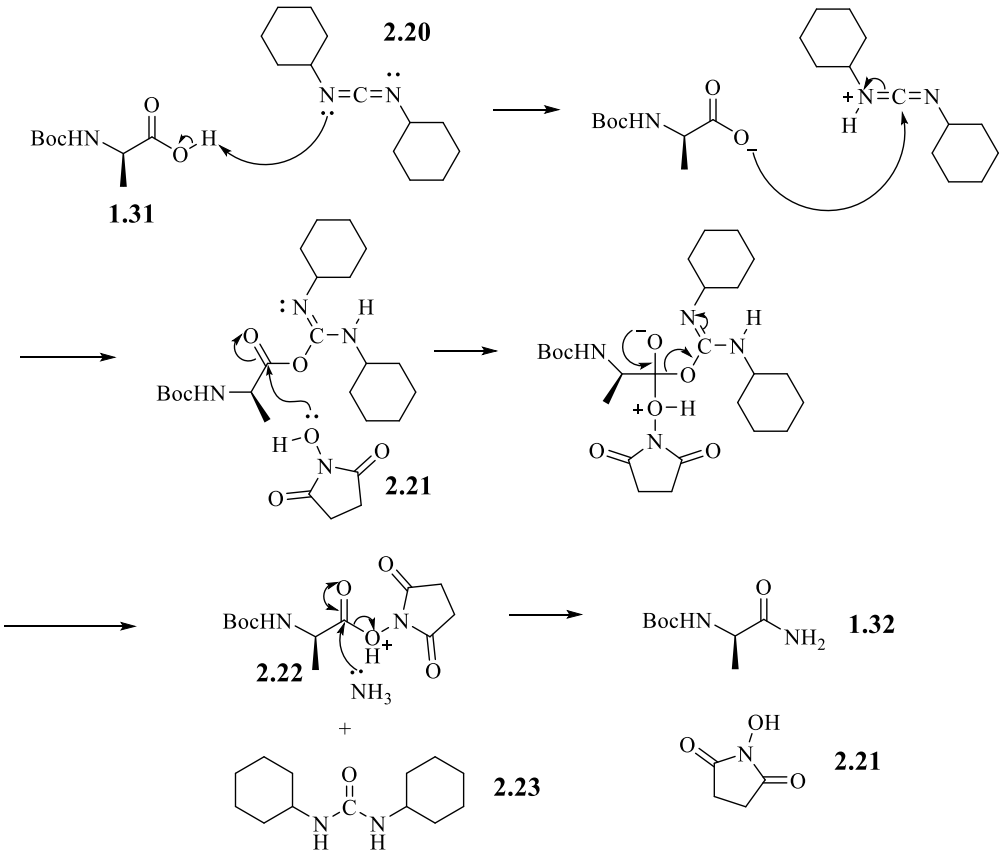
Scheme 2.4: Thiazole dipeptide synthesis starting from *N*-Boc-D-ala

2.3.1.1 Amidation of *N*-Boc-D-alanine



Scheme 2.5: Amidation of *N*-Boc-D-alanine

The amide was obtained by amidation of the carboxylic moiety of the *N*-Boc-D-alanine (Scheme 2.5). An active ester was formed using a standard carboxylic acid activation procedure, which was reacted with ammonia to yield the amide. The proposed reaction mechanism was displayed in Scheme 2.6.

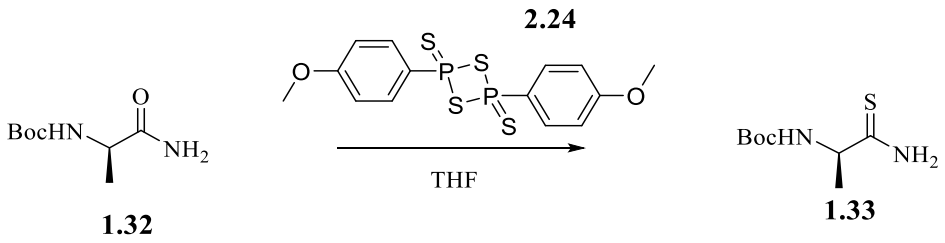


Scheme 2.6: Proposed mechanism of DCC and HO-Su mediated amide formation

The one-pot reaction can be divided into two steps. Firstly, the *N,N'*-dicyclohexylcarbodiimide (DCC) **2.20** and *N*-hydroxysuccinimide (HOSu) **2.21** were used as the coupling reagents to activate the carboxylic acid group of the *N*-Boc-D-alanine to a reactive acylating agent. The resultant succinimidyl ester **2.22** was stable and could be monitored using thin layer chromatography (TLC). Once the starting material was fully converted to the succinimidyl ester, which was monitored by TLC, 2 M ammonia in EtOH was added to the reaction mixture as the second step. The formation of a white solid before the addition of ammonia indicated the formation of the urea **2.23**. After addition of ammonia, the formation of the desired amide happened rapidly with the generation of HOSu **2.31**. The two by-products, HOSu and DCC-urea, generated from this reaction were mostly removed by filtration. In most cases, the crude was purified through column chromatography. However, when the reaction was scaled up to 10 g, the purification through column chromatography became

challenging. Therefore, an alternative purification method was attempted. After filtration, the crude white solid was suspended in dry acetone at 0 ºC. The resultant participate was DCC-urea which was filtered. The acetone was remove under *vacuo*, residual material was further treated with acetone if not pure enough. The reaction was monitored by TLC by staining with ninhydrin in butanol containing 3% acetic acid. The yields were typically higher than 90%.

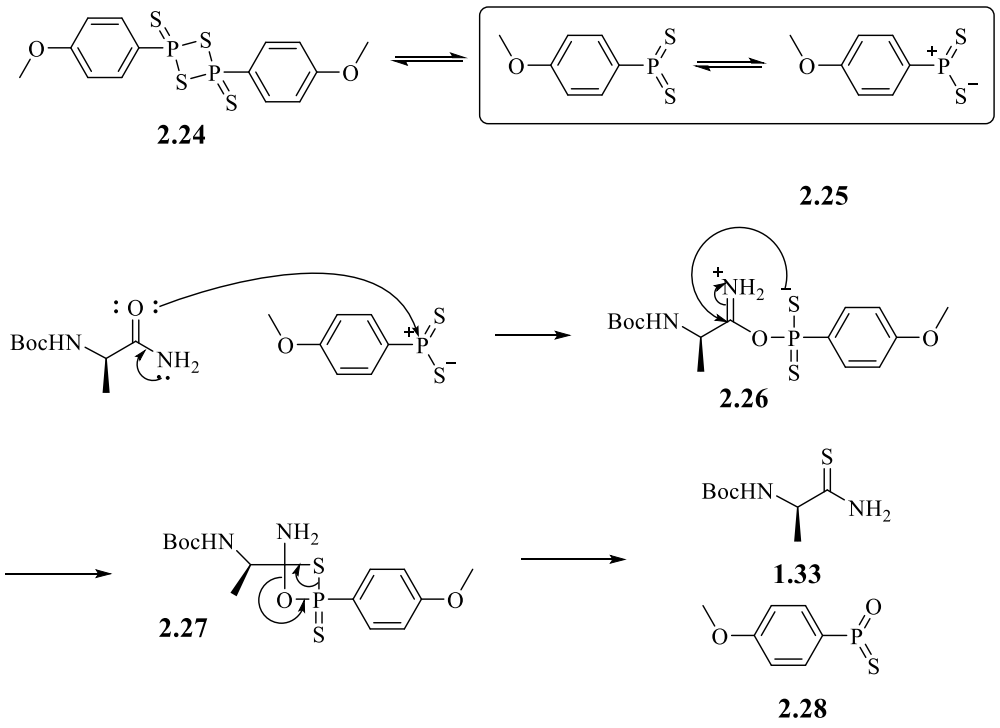
2.3.1.2 Thionation of *N*-Boc Amino Amides by Lawesson's Reagent



Scheme 2.7: Thionation using Lawesson's reagent

The second step of the synthesis was thionation (Scheme 2.7). The carbonyl functional group was converted into a thiocarbonyl by reaction with Lawesson's reagent **2.24**. Lawesson' reagent is a mild and convenient thionation agent for converting ketones, esters and amides to the corresponding thioketones, thioesters and thioamides in good yields. Before the invention of Lawesson's reagent in 1978, phosphorus pentasulfide (P_4S_{10}) was used as the thionation reagent.[215] Lawesson's reagent has advantages over P_4S_{10} longer reaction time, higher reaction temperature and since the use of P_4S_{10} requires excess amounts. Other thionation reagents, such as Belleau's reagent, provide alternative selections.[216] In this thesis, Lawesson's reagent was selected as described by Chan and co-workers.

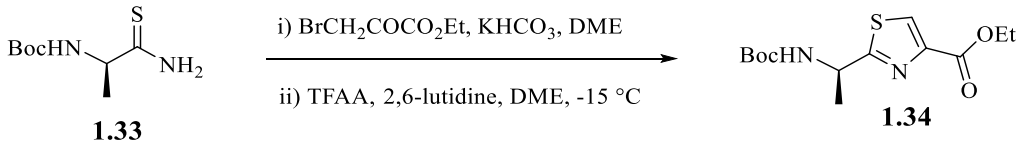
The usual method of thionation is performed in refluxing benzene, toluene or xylene. The Lawesson's reagent, in solution, is in equilibrium with a more reactive dithiophosphine yilde **2.25** as shown in Scheme 2.8.[217] The dithiophosphine yilde reacts with **1.32** to give a four-membered thiaoxaphosphetane intermediate **2.26**. A stable P=O bond was formed because the P=O bond is much thermodynamically stronger than the P=S bond. The thiaoxaphosphetane intermediate **2.27** then decomposed to form the desired thioamide.



Scheme 2.8: Proposed mechanism of thionation with Lawesson's reagent

Thus, the reaction was performed in THF at 0 ºC as described by Chan and co-workers.[205] After the addition Lawesson' reagent, the reaction was brought to room temperature and stirred for a further 1 hour. The reaction was monitored by TLC with ninhydrin staining. The reaction yield was 80%. However, the disadvantage in the usage of Lawesson's reagent was the unpleasant odour.

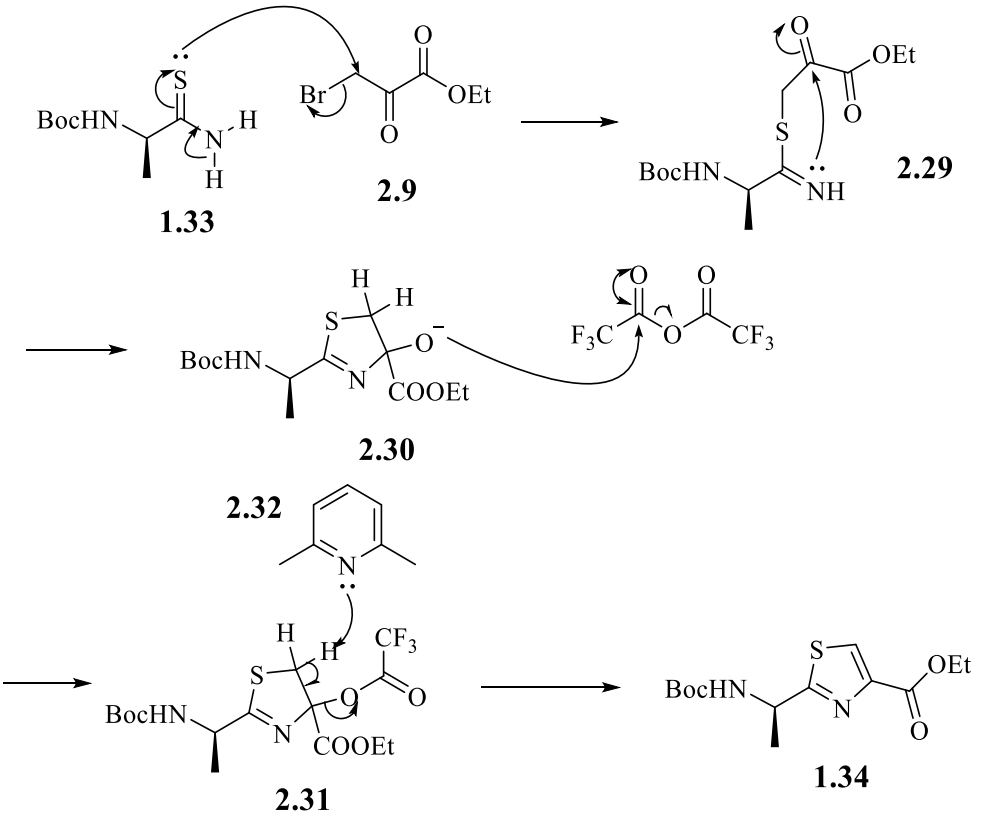
2.3.1.3 Schmidt's Modified Hantzsch Thiazole Formation



Scheme 2.9: Modified thiazole formation

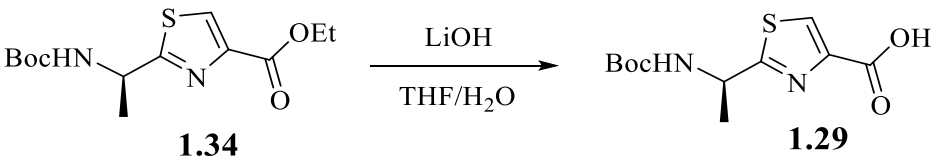
Chan *et al.* further investigated the Schmidt's modified Hantzsch thiazole formation based on the findings of Holzapfel *et al.*[218] and Meyers *et al*.[206], and developed a combination of a two-step reaction to synthesise the thiazole ethyl ester (Scheme 2.9). The thioamide was condensed with ethyl bromopyruvate **2.9** in the presence of potassium bicarbonate ($KHCO_3$) in 1,2-dimethoxy ethane (DME) as solvent to generate the 4-hydroxythiazoline intermediate. The usage of DME was first reported by Holzapfel *et al.*[218]. In their report, the resultant intermediate was treated with pyridine and TFAA to generate the desired thiazole with full protection of the stereogenic C_2-exomethine. It has been reported that the isolation of hydroxythiazoline leads to racemisation through imine-enamine equilibration (Scheme 2.1). Therefore, the TFAA was added to activate the hydroxyl group of hydroxythiazoline **2.30** to form a good leaving group without isolation. However, this method was limited by the choice of starting material. When thiazoles were derived from alanine, the resultant *ee* value was low. Meyer *et al.* replaced the pyridine with 2,6-lutidine **2.32** and lowered the reaction temperature to -15 ºC to avoid racemisation of the thiazole intermediate due to the imine-enamine equilibration (Scheme 2.10).[206] Chan *et al.* reported that the addition of TFAA and 2,6-lutidine **2.32** within 10 minutes resulted in no racemization.[205] Hence, the usage of the bulky base 2,6-lutidine and low reaction temperature enhanced the enantiomeric purity. The acid catalysed imine-enamine inter-conversion (Scheme 2.1) was prevented under such reaction condition.

Thus, the reaction was carried out by the addition of ethyl bromopyruvate in the presence of finely powdered potassium bicarbonate to the *N*-Boc-(*R*)-Ala-thioamide in dry DME at -15 ºC. The reaction mixture was stirred vigorously for 5 minutes, followed by the addition of a solution of 2,6-lutidine and TFAA in DME. The reaction was stirred for 1 hour at -15 ºC and monitored by TLC indicated the consumption of the thiazoline intermediate. The resulting reaction mixture was subjected to an aqueous work-up and column chromatography purification to yield the desired thiazole ester in 50% yield. In order to determine the optical purity of the product, the optical rotation analysis was applied. The optical rotation obtained $[\alpha]_D^{23} = +38.3$ (c=1.0, $CHCl_3$) was nearly identical to the reported value $[\alpha]_D^{25} = +40.8^o$ (*c* = 1.0, $CHCl_3$)[219].



Scheme 2.10: Proposed mechanism of thiazole formation from thioamide

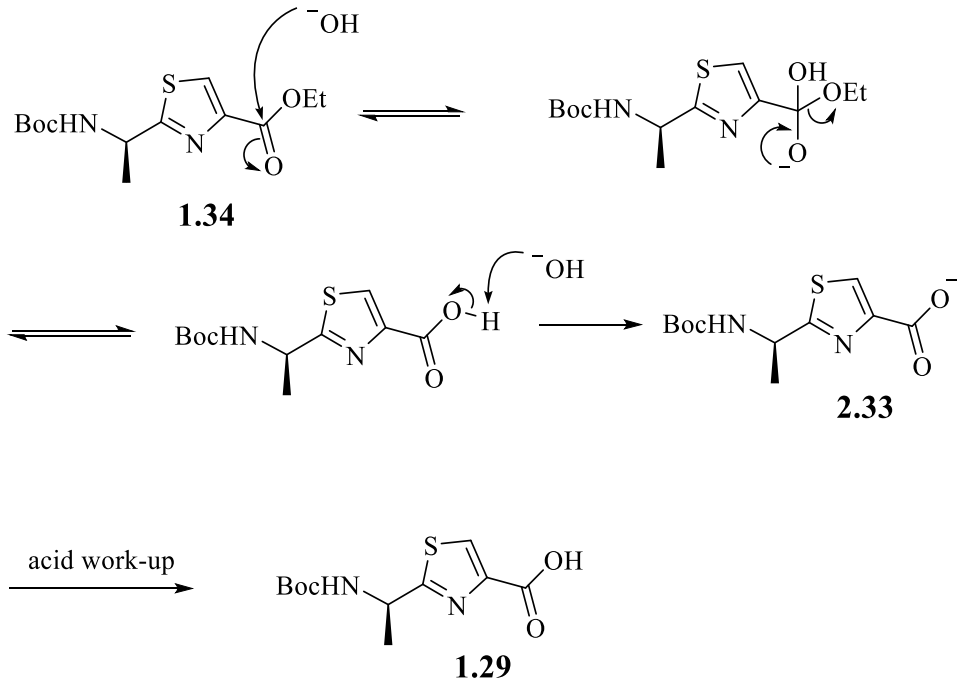
2.3.1.4 Saponification of Thiazole Ester to Carboxylic Acid



1.34 **1.29**

Scheme 2.11: Saponification of thiazole ester

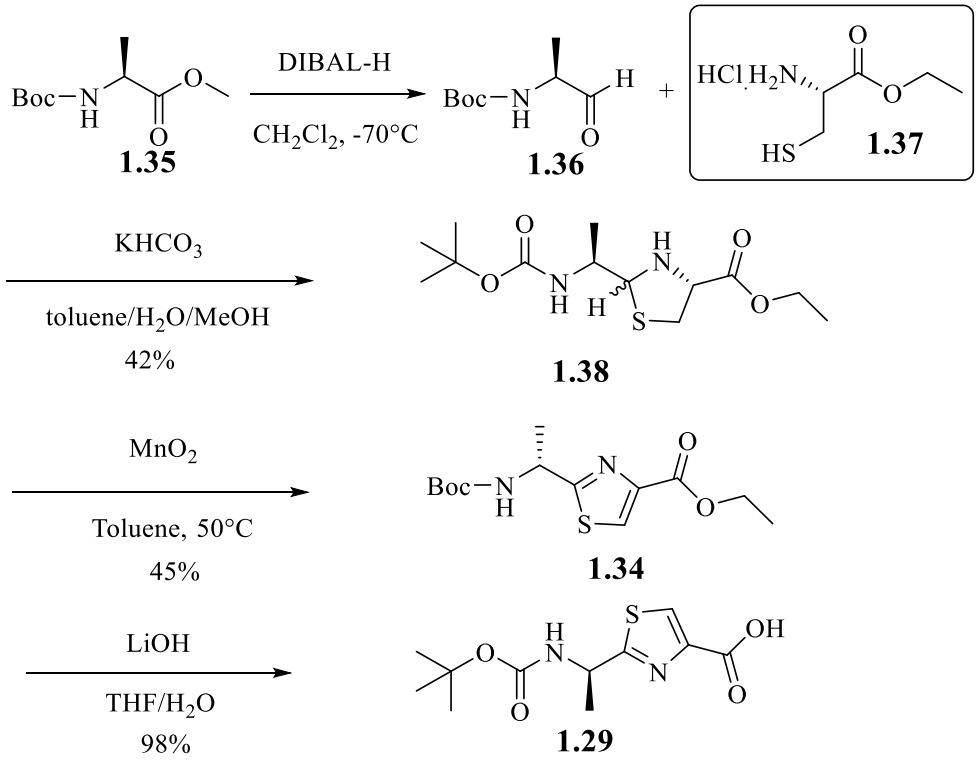
The final step was the hydrolysis of thiazole ethyl ester to generate the desired thiazole amino acid (Scheme 2.11). Hydrolysis of esters can be carried under both acidic and basic condition. In this case, basic conditions were applied because the *N*-Boc can be cleaved under acidic conditions. Saponification of ester was readily achieved with aqueous alkali, such as sodium hydroxide, lithium hydroxide or potassium hydroxide under reflux within hours. The mechanism is illustrated in Scheme 2.12.



Scheme 2.12: Mechanism of base catalysed hydrolysis of ester

Previously, THF/H_2O/MeOH was used as the solvent. The presence of MeOH catalysed the transesterification, resulting in the generation of the thiazole methyl ester by-product. The by-product was confirmed by ES-MS and ^1H NMR. In order to avoid the transesterification, THF/H_2O solvent system was applied. The aqueous solution of LiOH was added dropwise to the thiazole ethyl ester in THF at 0 ºC. The reaction was brought to room temperature and stirred for 15 h. Upon completion, the reaction was acidified with sat. $KHSO_4$ to pH = 2 and extracted with DCM to afford the desired thiazole dipeptide in 98% yield. The optical rotation obtained $[\alpha]_D^{23}$ = +29.1 (c=1.0, $CHCl_3$) was comparable with reported value $[\alpha]_D^{26}$ = +31° (*c* = 1.0, $CHCl_3$).[220]

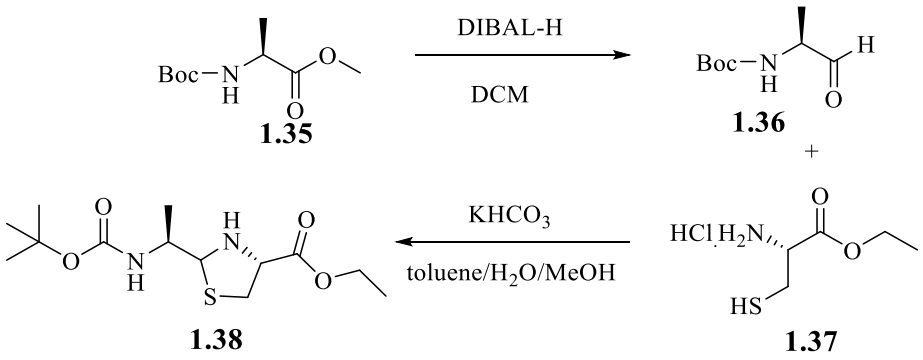
2.3.2 Synthesis of 2-((*tert*-butoxycarbonyl)-1-amino-alkyl)-thiazole-4-carboxylic Acid Using Ley's Route



Scheme 2.13: Modified Ley's route for thiazole synthesis

Owing to the unpleasant Lawesson' reagent, the alternative thiazolidine formation was attempted by condensation of cysteine methyl ester with an amino acid derived aldehyde. The resultant thiazolidine was oxidized by manganese dioxide to yield thiazole ethyl ester. The full reaction route was show in Scheme 2.13.

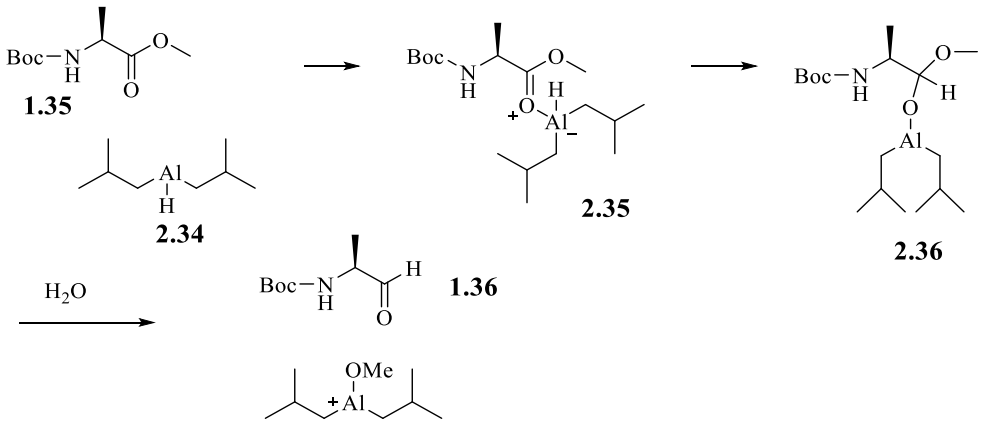
2.3.2.1 Formation of Thiazolidine Methyl Ester



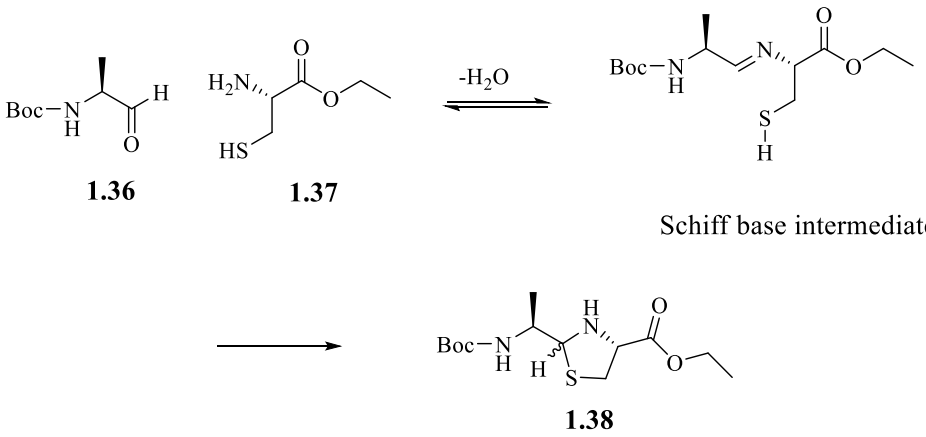
Scheme 2.14: Formation of Thiazolidine Methyl Ester

The first step involved the reduction of *N*-Boc-D-alanine methyl ester to afford the corresponding aldehyde (Scheme 2.14). Various reducing agents, such as lithium aluminium hydride and sodium borohydride, are available. However, the di-isobutyl aluminium hydride (DIBAL) **2.34** was selected. DIBAL is a strong, bulky reducing agent, and capable of reducing carboxylic acids and esters to aldehydes and alcohols, amides to amines and aldehydes, and nitriles to aldehydes and amines. In order to avoid further reduction of the desired aldehyde product to alcohol, the reaction temperature should be kept at -70 ºC and one equivalent of DIBAL is used. The proposed reaction route is illustrated in Scheme 2.15. The reaction starts from the coordination of a lone pair from the carbonyl oxygen to the aluminium from DIBAL. The DIBAL then delivers its hydride to the carbonyl carbon to form a neutral hemiacetal (tetrahedral)

intermediate **2.36** which is stable at low temperature. Subsequently, quenching of the reaction with water breaks down the hemiacetal to yield the desired aldehyde. The resultant aldehyde was used for condensation without further purification.



Scheme 2.15: DIBAL reduction

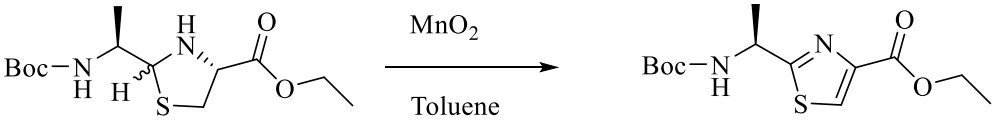


Scheme 2.16: Thiazolidine condensation

The proposed thiazolidine condensation route from aldehyde and (*R*)-cysteine ethyl ester is illustrated in Scheme 2.16. Thus, the reaction was carried out in a toluene/MeOH/H_2O solvent mixture, and potassium bicarbonate was selected as the base. According to the mechanism, a Schiff base intermediate **2.37** is formed. The reaction was stirred vigorously and monitored by TLC until all the starting material disappeared. An aqueous work up was carried out prior to

column chromatography purification. The isomer raised was due to the epimer at the Thi-C_2. Since next step is an oxidation of the thiazolidine moiety to a thiazole, the diastereomeric mixture was used without resolution of the isomers.

2.3.2.2 Oxidation of the Thiazolidine to Afford the Thiazole

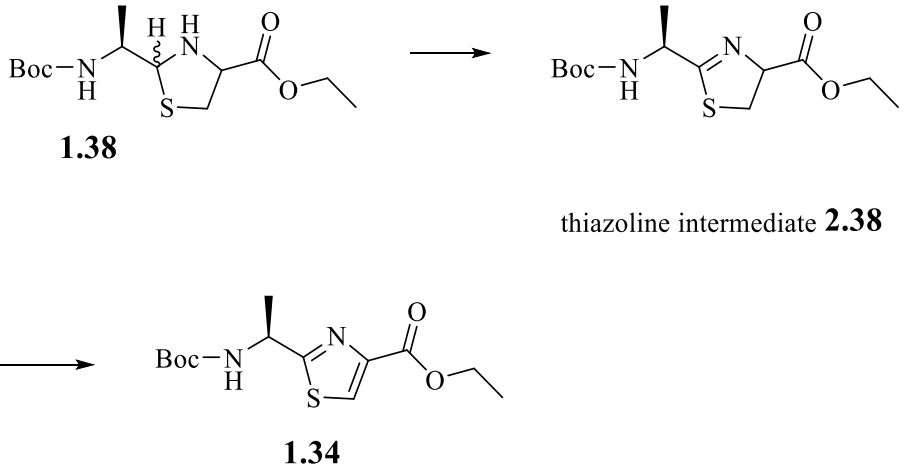


1.38 **1.34**

Scheme 2.17: Oxidation of the thiazolidine to thiazole

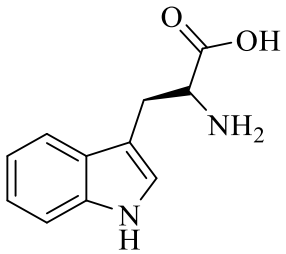
The oxidation of the thiazolidine to the thiazole was performed with chemical manganese dioxide in the presence of toluene or acetonitrile (Scheme 2.17). The proposed route of this reaction is outlined in Scheme 2.18. A thiazoline intermediate **2.38** migtht be formed, followed by further oxidation to yield the thiazole. The manganese dioxide mediated oxidation might occur via a stepwise removal of hydrogen atoms in a radical mediated process.

The activated manganese dioxide was used since the normal manganese dioxide failed to react. The usage of either solvents, acetonitrile or toluene, displayed no difference in yield, the yields were 45% and 47%, respectively. The enantiomeric purity of the resultant thiazole ethyl ester was determined by the optical rotation value and ^{1}H NMR spectroscopy. The optical rotation $[\alpha]_D^{23}$ = +39.0 (c = 1.0, $CHCl_3$) was nearly identical to $[\alpha]_D^{22}$ = +40.8° (*c* = 1.0, $CHCl_3$)[205] previously synthesised thiazole using Chan's method (Section 2.3.1.3). The final saponification was carried out using the same procedure as previously described in Section 2.3.1.4. Thus, the hydrolysis of the thiazole ethyl ester afforded the desired thiazole amino acid **1.29** in 95% yield.



Scheme 2.18: Proposed reaction route of oxidation

2.4 Asymmetric Synthesis of Tryptophan Analogues



2.39

Figure 2.2 L-Tryptophan **2.39**

The (*S*)-4-methoxy-tryptophan is an unusual amino acid residue found in argyrin. L-Tryptophan **2.39** is a neutral aromatic amino acid widely found in living organisms. It is one of the 20 L-amino acid incorporated into proteins during translation. Additionally, it is one of the nine essential amino acids that cannot be endogenously synthesised and needs to be obtained by human from diet.

Tryptophan is derived from indole, a bicyclic ring comprising a benzene and a pyrrole moiety, which is linked via a methylene group to the α-carbon of an α-

amino acid structure. The high hydrophobicity of tryptophan is dependent on the presence of the indole ring. The N-H group of the indole ring can form hydrogen bonds while the aromaticity of the benzene ring enables non-polar interactions. The extensive π-electron system of the aromatic indole side-chain displays a significant quadrupole moment. The negatively charged π-electron system of tryptophan can interact with various cationic species, which accounts for the key π–cationic interactions found in ligand-receptor interactions. Chan and co-workers in their preliminary investigations into the SAR of argyrin that govern their antibacterial activity explored the role of the (*S*)-4-methoxytryptophan residue.[205] They found that the 4-methoxy functionality was crucial to maintain antibacterial activity, where shifting the methoxy from 4- to 5-position weakened its activity. They synthesised a number of argyrin analogues in which the strategic 4-methoxy group was replaced with halogens or other substituents in various positions of Trp.

This chapter includes a brief description of current synthetic approaches to optically pure tryptophan derivatives during total synthesis of argyrins. The advantages and disadvantages of each approach are outlined. An alternative route recently adopted in our research group is also outlined for the synthesis of 4- and 5-substituted tryptophans.

2.5 Reported Synthetic Approaches to Optically Pure Tryptophans

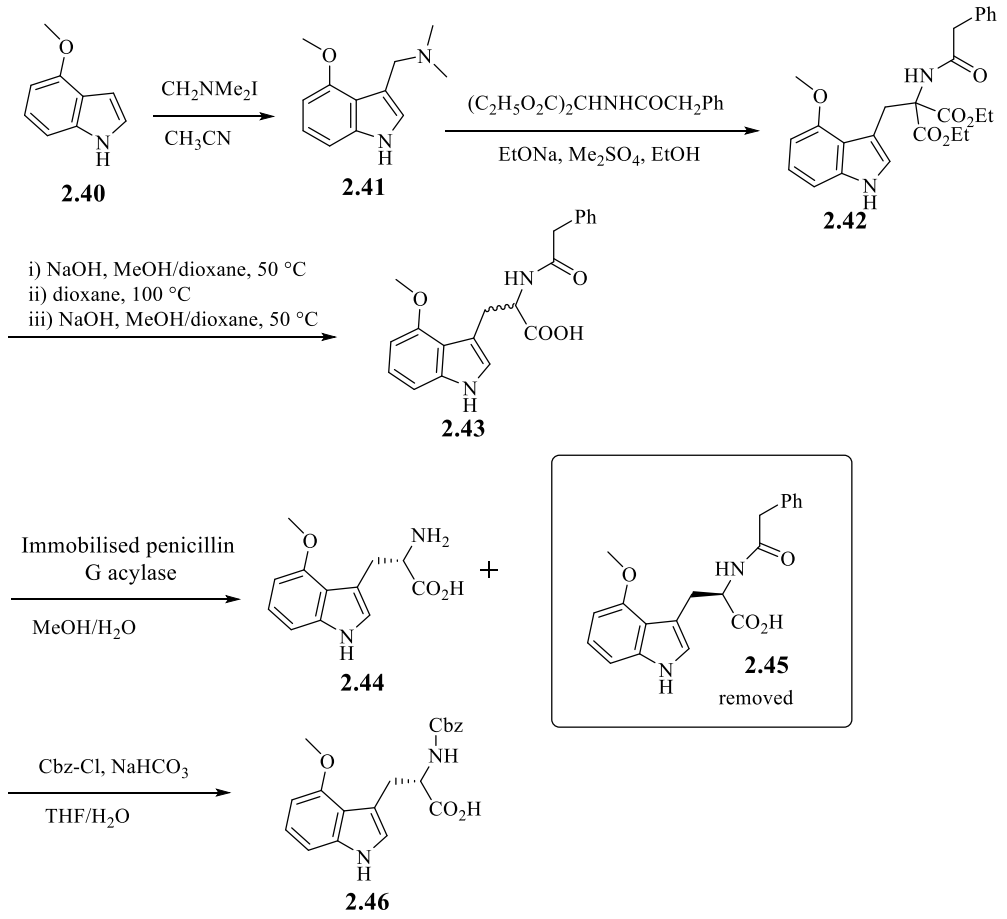
The current methods for obtaining enantiomerically pure (*S*)-tryptophan derivatives are based on either chemical or enzymatic approach. In the enzymatic approach, an *N*-acylase enzyme is frequently used in the final step to achieve the resolution of the racemates, in which racemic *N*-acetyl-tryptophan

is used as the substrate. The chemical approach requires multi-step processes which allows access to a wide range of indole-substituted tryptophans. Stereoselectivity of reactions and stability of intermediates are two major challenges for the chemical approaches. Frequently, chiral auxiliary reagents are used. For example, Nickeleit's approach[204] requires DuanPhos as ligand, while Ley's approach[202] requires Schollkopf chiral auxiliary reagent. Both approaches also apply a catalytic hydrogenation route. Previously, in Chan's group, an operationally flexible α-substituted benzylamine-facilitated asymmetric Strecker synthesis of (*S*)-Trp analogues was reported.[205] These various synthetic approaches to (*S*)-tryptophan analogues are discussed in detail below.

2.5.1 Ley's Approach to the Synthesis of (*S*)-4-methoxy-tryptophan

The main feature of the method reported by Ley *et al*.[202] is an enzyme resolution step using immobilized Penicillin G acylase[221] (Scheme 2.19). Penicillin acylase is a serine hydrolase with a catalytic mechanism similar to serine proteases. Specifically, the acyl donor-binding site of penicillin acylase shows high affinity for a phenylacetyl moiety or a phenoxyacetyl moiety. In the preparation of the appropriate penicillin acylase substrate, the 4-methoxy-indole **2.40** was converted quantitatively to the derivative **2.41** by aminoalkylation reaction, followed by condensation with the enolate of 2-phenylacetylaminomalonic acid diethyl ester to give **2.42**. Saponification of the diester and mono-decarboxylation of the carboxylic acid afforded racemic 4-methoxy phenylacetamide **2.43** in 56% yield. The enzymatic kinetic resolution of the racemic phenylacetamide was achieved with Penicillin G acylase.

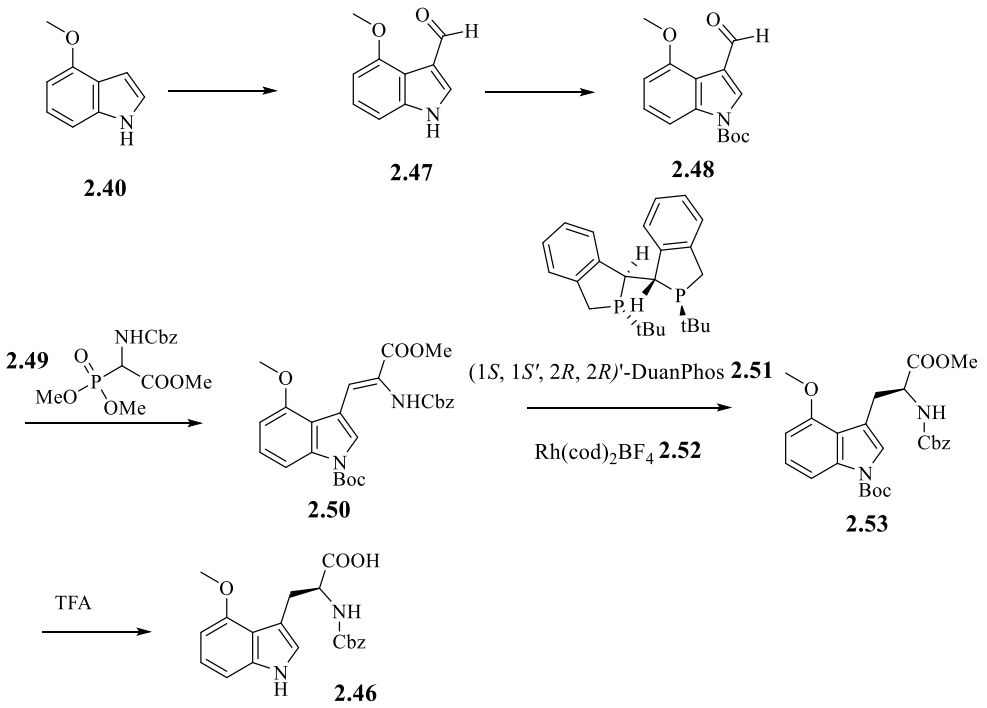
The enzymatic kinetic resolution depends on the ability of the enzyme to discriminate the substrate enantiomers, in which the two enantiomers are converted into the corresponding product at substantially different reaction rates. Subsequently, the unchanged starting material **2.45** was removed from the enzymatic reaction mixture and the desired free amino acid **2.44** was *N*-protected with CbzCl to yield optical pure *N*-Cbz-4-MeO-(*S*)-tryptophan **2.46** in 44% yield. However, the penicillin G acylase is now no longer commercially available.



2.40 **2.41** **2.42** **2.43** **2.44** **2.45** **2.46**

Scheme 2.19: Synthesis of (*S*)-4-methyoxy- tryptophan reported by Ley *et al*.[202]

2.5.2 Nickeleit's Approach for the Synthesis of (*S*)-4-methoxy-Tryptophan



Scheme 2.20: Nickeleit's approach for (*S*)-4-methyoxy- tryptophan synthesis

In order to prepare the 4-methoxy-L-tryptophan for the synthesis of argyrin F, Nickeleit *et al.* analysed different chiral auxiliaries for their usage in catalytic hydrogenation.[204] They identified the DuanPhos ligand **2.51**, in combination with $Rh(cod)_2BF_4$ **2.52** [222]to afford the required amino acid in quantitative yield (99%) and 99% *ee*. Their synthetic procedure is outlined in Scheme 2.20. The asymmetric hydrogenation was acknowledged by the 2001 Nobel Prize in Chemistry to William Knowles and Royji Noyori.[223] The rhodium-based catalysts in complex with a chiral phosphorus ligand formed the main basis of many asymmetric hydrogenations.

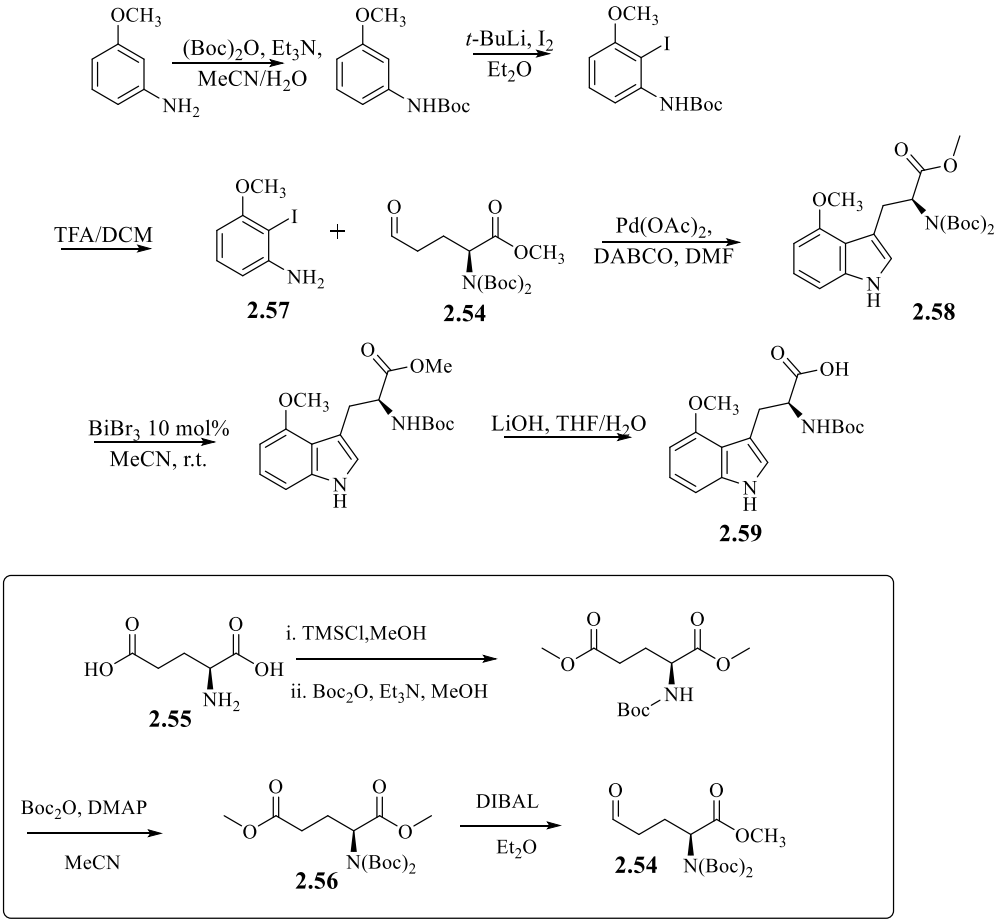
The α-dehydrotryptophan derivative is the precursor for the asymmetric hydrogenation of tryptophan. In Nickeleit's approach, the α-dehydrotryptophan was synthesised in three steps. The starting material 4-methyoxy-indole **2.40** was converted to corresponding aldehyde **2.47** through Vilsmeier formylation. The resultant aldehyde was *N*-Boc protected on the indole NH. The *N*-Boc protected indole-3-carboxyaldehyde **2.48** was subjected to Horner-Wadsworth-Emmons reaction using phosphonoglycine **2.49** and DBU to afford the (*Z*)-dehydrotryptophan **2.50** as a single isomer. The usage of DuanPhos in combination with catalytic $Rh(cod)_2BF_4$ under 10 bars of hydrogen gave the enantiomerically pure protected tryptophan **2.53**. This procedure was first reported by Moody *et al.* in 2004.[210] Finally, the desired *N*-Cbz protected tryptophan **2.46** was obtained by TFA-mediated acidolysis of the Boc group and saponification of the methyl ester.

Although this method benefits from short reaction time and high enantioselectivity, its application is restricted to specific tryptophan analogues. The selection of suitable catalyst-ligand combination is also time-consuming.

2.5.3 Jiang's Approach for the Synthesis of (*S*)-4-methyoxy-tryptophan

Jiang *et al*.[203] adopted a ligand-less palladium-catalysed one-pot annulation reaction reported by Zhu *et al*.[224] in 2006 to synthesise 4-methoxy-L-tryptophan during the total synthesis of argyrin A. Specially, the approach utilises a chiral amino acid substrate in order to afford the appropriate tryptophan analogues. The full synthetic route is shown in Scheme 2.21.

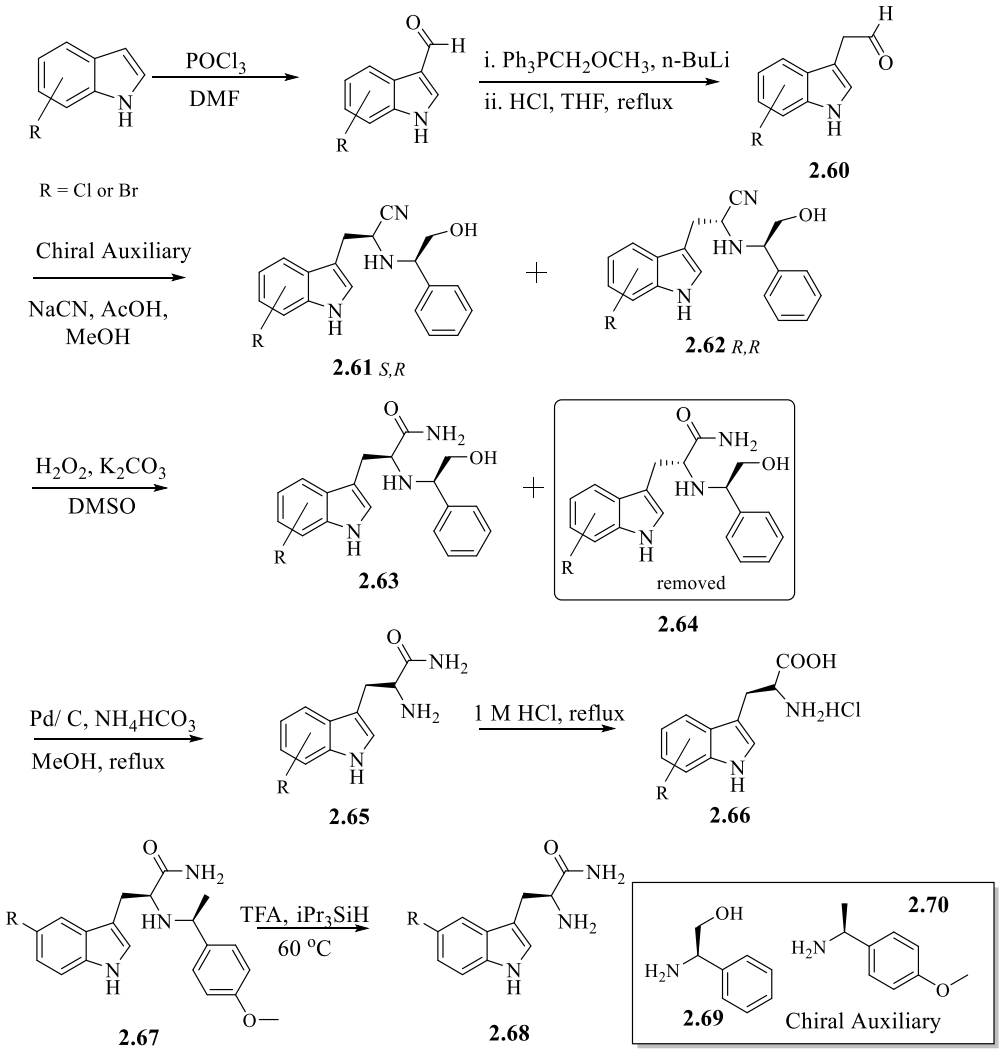
Firstly, an aldehyde intermediate **2.54** was prepared from glutamic acid **2.55** in three steps. The glutamic acid was converted to diester **2.56**, followed by a double *N*-Boc protection of the amine. The desired aldehyde intermediate was obtained from DIBAL reduction of dimethyl *N,N*-di-Boc-glutamate under mild conditions.[225] The aldehyde was annulated to aryl iodide **2.57** using $Pd(OAc)_2$ and DABCO in DMF at 85 ºC, as described by Zhu, to generate the desired tryptophan derivative **2.58**. Finally, hydrolysis of the methyl ester and selective mono-deprotection of one *N*-Boc afforded the *N*-Boc-4-methoxy-L-tryptophan **2.59** with 82% yield. This approach is obviously limited by the interference of aryl halides for the annulation reaction, and hence displays a limited access to substituted tryptophan analogues.



Scheme 2.21: Jiang's approach for the synthesis of (*S*)-4-methyoxy- tryptophan

2.5.4 Chan's Approach for the Synthesis of Substituted Tryptophans

Chan and co-workers investigated Harada's asymmetric Strecker synthesis[207] and developed a flexible and operationally simple synthesis of various substituted L-tryptophan. The Strecker amino acid synthesis is the addition of a nitrile to the prochiral α-carbon of an imine to generate an α-aminonitrile. The hydrolysis of the α-aminonitrile affords the corresponding amino acid.



Scheme 2.22: Chan's approach of asymmetric Strecker (*S*)-tryptophan synthesis

Chan and co-workers[205] discovered the usage of (*R*)-2-phenylglycinol chiral auxiliary **2.69** and the indol-3-acetaldehyde **2.60** to construct the imine intermediate. The imine intermediate was attacked by a cyanide anion to afford the chiral α-aminonitrile. They found that the nucleophilic addition of the nitrile at a more favourable *re*-face resulting in desired (*S,R*)-diastereomer. The *S,R* **2.61** and *R,R* **2.62** diastereoisomers were separated by column chromatography and then converted to the amino amides. After that, a standard catalytic phase transfer hydrogenolysis using 10% Pd/C was applied. In case of 5-Br and 5-Cl substituted analogues, the debenzylation step resulted in dehalogenation. Therefore, (*R*)-2-phenylglycinol chiral auxiliary was replaced with 4-methoxy-α-methylbenzylamine (PMB) **2.70**. The removal of PMB group was accessed by TFA-mediated acidolysis. Finally, acidic hydrolysis of amino amide was carried under mild condition to afford the required amino acid over 80% yield. The full synthetic route is shown in Scheme 2.22.

Chan's method benefits from inexpensive chiral auxiliary reagents and access to a range of substituted tryptophans. However, the use of a hazardous cyanide salt is disadvantage. Further, the poor enantioselectivity of 3:1 diastereoisomeric ration (*dr*) means at least 30% of the amino amides were wasted.

In conclusion, the above previously developed methods for the synthesis of substituted (*S*)-tryptophan analogues for total synthesis of argyrin suffer from either poor versatility or low efficiency. Therefore, a new route was adopted in our research group.

2.6 Asymmetric Synthesis of Substituted (*S*)-Tryptophans Through Alkylation of Belokon's Nucleophilic Glycine

The α-alkylation of nucleophilic equivalents of glycine is considered as a practical and direct way to synthetically access α-amino acid derivatives with varied side-chains. Specially, application of imine derived from a glycine ester has been successfully applied for homologation of glycine to different higher amino acid. The use of chiral imine derivatives of glycine is considered to be a breakthrough for constructing asymmetric amino acids. However, the main disadvantage of these compounds is the low C-H acidity of the glycine methylene moiety, which necessitates the use of strong base and anhydrous condition to produce the reactive enolates. The high cost and multiple steps for large scale manufacture also limited the usage. In contrast, transition metal complexes derived from glycine Schiff base build a convenient template for functionalization of the glycine moiety. For this context, Belokon *et al.* demonstrated the utility of (*S*)-2-[*N*-(*N*'-benzylprolyl)amino]-benzophenone (BPB) as the chiral ligand for Schiff base formation.[226] Further investigation of this approach showed that the Ni(II) complex of the chiral benzophenone-glycine Schiff base has high stability and reactivity.[227]

The Ni-glycine-BPB complex **1.40** is a red crystal and can be purified by crystallization or column chromatography if required. The crystal structure analysis showed the complex is planar. The two positive charges at the central Ni ion are neutralized by two negative charges (CON^- and COO^-) of ligand. The benzyl group is determined to be above the metal in plane assisted by the crystallographic data (Figure 2.4) and theoretical calculations.[228] The possible weak interaction between the Ni atom and the benzyl group contributes to the

stabilization of the complex. In fact, the benzyl group is fixed above the central Ni atom which reduces the distance between the plane of the benzyl group and the Ni atom.[229] The glycine α-protons are acidic due to their coordination to Ni^{2+}. The L-amino acids are synthesised from the L-proline while the D-amino acids are from D-proline. In this thesis, the required (*S*)-tryptophans are synthesised using the (*S*)-isomeric chiral complex **1.40** from (*S*)-proline **2.72**.

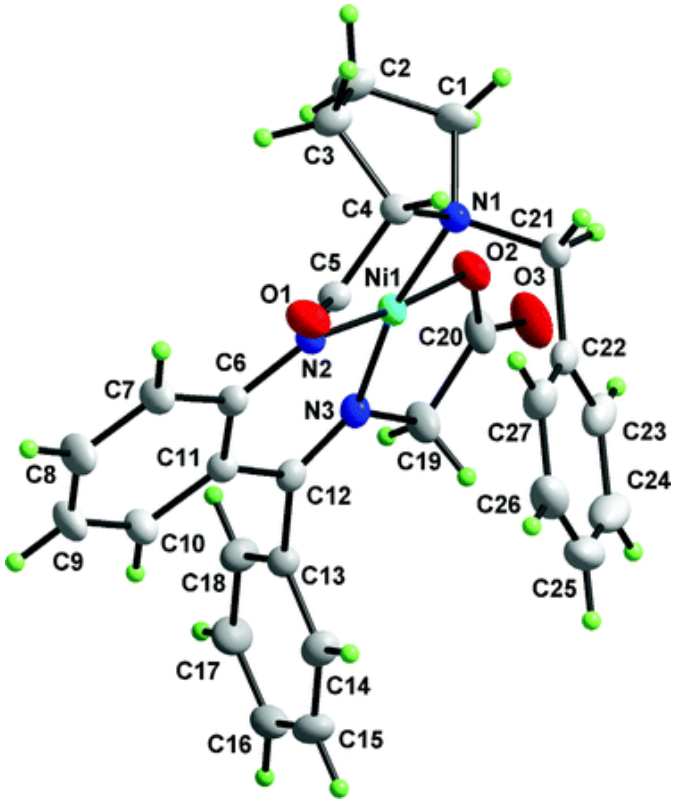


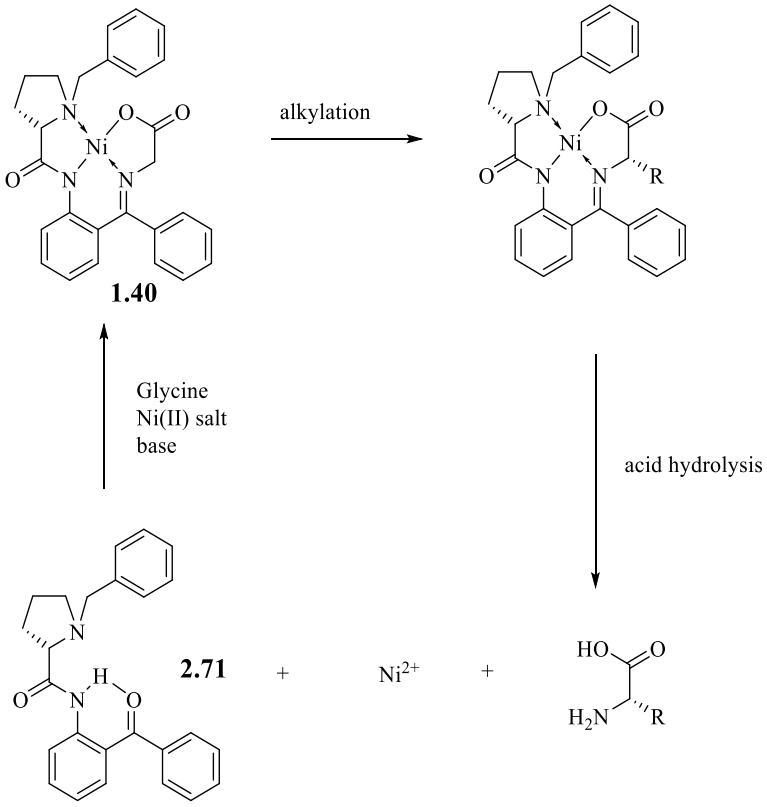
Figure 2.4: The X-ray crystal structure of **1.40.**[230]

2.6.1 Homologation of Chiral Glycine Ni(II) Schiff Base

The homologation of the glycine complex **1.40** can be the result of many kinds of reactions, such as Aldol[231], Michael[232], Mannich[233], and alkyl halide alkylation[234] reactions. All of these reactions can be performed under ambient temperature or moderate heating, open air, and common solvents. The direct

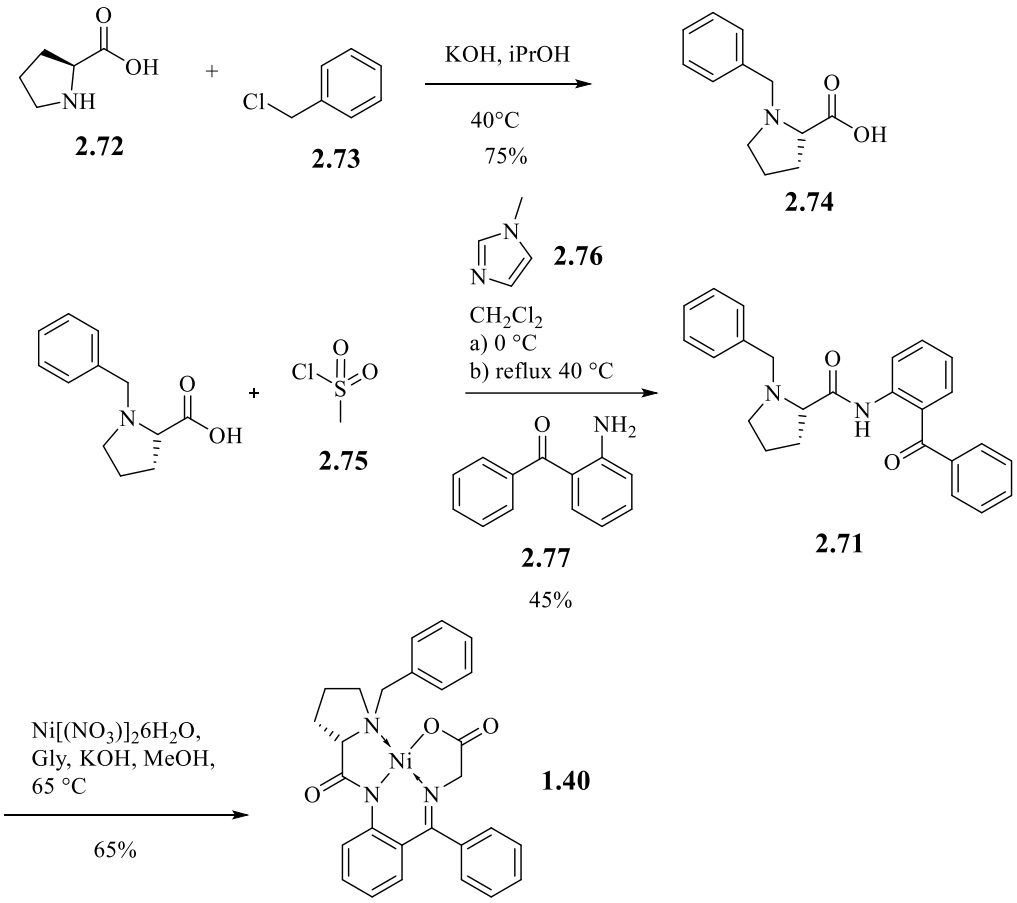
alkylation, which is the most straightforward homologation reaction with **1.40**, is selected in this thesis. The disassembly or decomposition of the homologation products under acidic conditions is operationally convenient, which can be sped up by microwave. Finally, purification of the target amino acids can be obtained through ion-exchange chromatography. Most importantly, the chiral ligand BPB **2.71** can be recovered and reused after purification (Scheme 2.23).

For the synthesis of optically pure L-tryptophan and its derivatives, the glycine Ni(II) Schiff base derived from (*S*)-2-[*N*-(*N*'-benzylprolyl)-amino]-benzophenone (BPB) **2.71**, developed by Soloshonok and co-workers, was chosen. The homologation of **1.40** was achieved through direct alkylation with substituted indole alkyl halides.



Scheme 2.23: Alkylation of glycine Ni(II) Schiff base

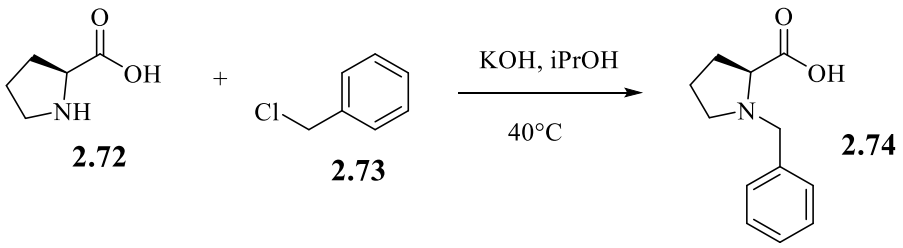
2.6.2 General Preparation of BPB-Glycine Ni(II) Complex



Scheme 2.24: Total synthesis of BPB-glycine Ni(II) complex

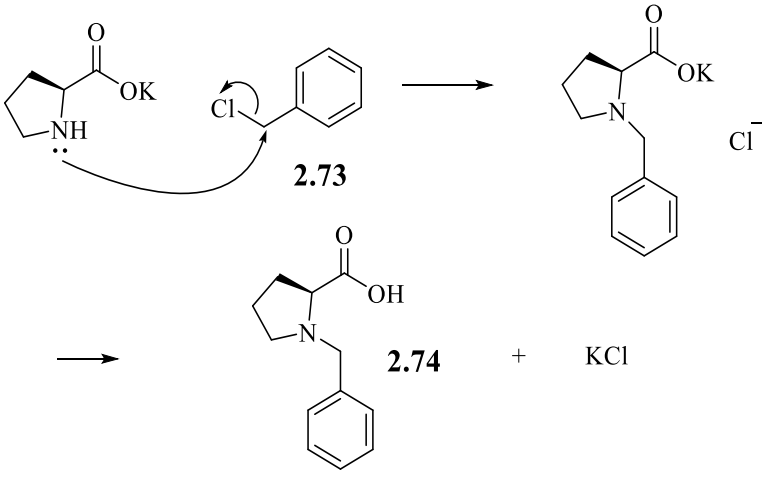
The required Schiff base consists of the following components, benzylprolyl-aminobenzophenone (BPB), glycine and nickel. The BPB was synthetically accessed in three steps from L-proline **2.72**. With BPB ligand **2.71** in hand, the BPB-glycine-Ni(II) complex was assembled following Belokon's method by employing $Ni(NO_3)_2 \cdot 6H_2O$ in anhydrous methanol (Scheme 2.24).

2.6.2.1 *N*-Benzylation of Proline



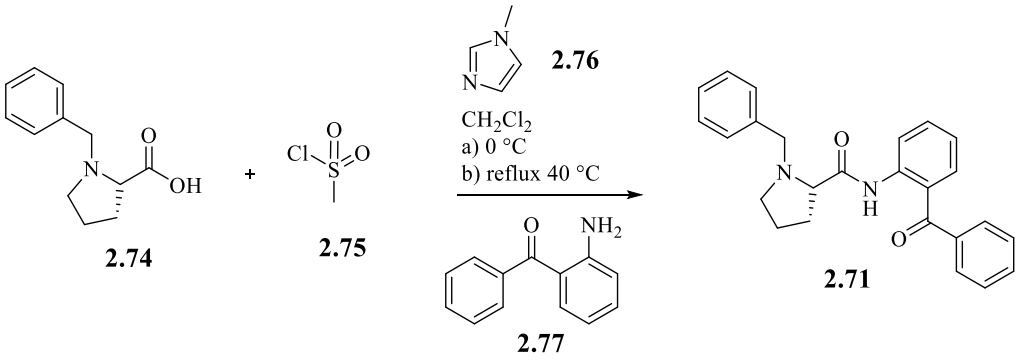
Scheme 2.25: *N*-benzylation of proline

The first step in the synthesis of the glycine-Ni(II) complex **1.40** is the *N*-benzylation of the L-proline **2.72** (Scheme 2.25). The *N*-benzylation was achieved in the presence of the strong base KOH and a polar solvent, isopropanol. The reaction is anticipated to proceed via a S_N2 nucleophilic substitution pathway (Scheme 2.26). Following completion of reaction, the pH of the reaction mixture was adjusted to pH 5–6 with concentrated HCl. If the pH adjustment was not properly applied, the reaction yield was found to be lowered to 10%. In the subsequent reaction work-up, KCl was precipitated with chloroform, and the desired product was triturated from acetone. The general yield of the reaction was typically above 75%.



Scheme 2.26: Anticipated mechanism of *N*-benzylation of proline

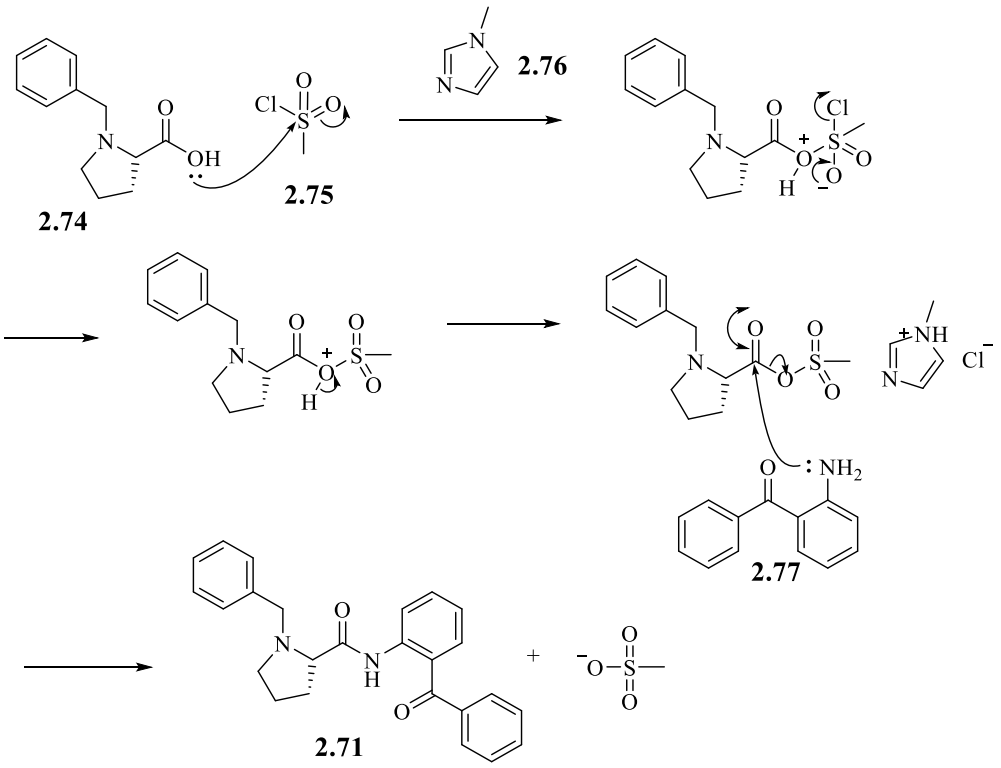
2.6.2.2 Synthesis of (*S*)-2[*N*-*N'*-benzylprolyl)-amino]-benzophenone



Scheme 2.27: Synthesis of chiral ligand BPB

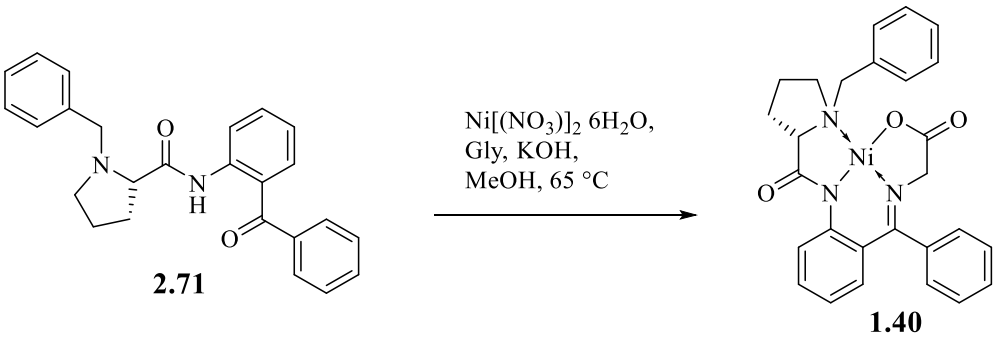
The synthesis of (*S*)-2[*N*-*N'*-benzylprolyl)amino]benzophenone (BPB) **2.71** was achieved through the condensation of *N*-benzylproline with 2-aminobenzophenone (Scheme 2.27). The reaction was facilitated by methane-sulfonyl chloride (MsCl) **2.75** in the presence of a base, *N*-methylimidazole **2.76**, at low temperature. The proposed reaction mechanism is outlined in Scheme 2.28. Following a simple aqueous based work-up, the desired BPB was purified through recrystallization from ethyl acetate to afford the product as white crystal in 45% yield.

In an attempt to improve the reaction yield, an excess of MsCl was added during the reaction. However, the additional MsCl resulted in the formation of an unknown by-product, which was confirmed by an extra spot on TLC. Moreover, the addition of an excess of base did not improve the reaction yield. Around 50% of **2.77** was recovered after purification. Although the reaction condition reported in this thesis did not afford excellent yields, the purification step was easy. The starting material is relatively cheap and the reaction can be scaled up to 8 g.



Scheme 2.28: Proposed amidation reaction mechanism facilitated by MsCl

2.6.2.3 Synthesis of BPB-Glycine-Ni(II) Schiff Base



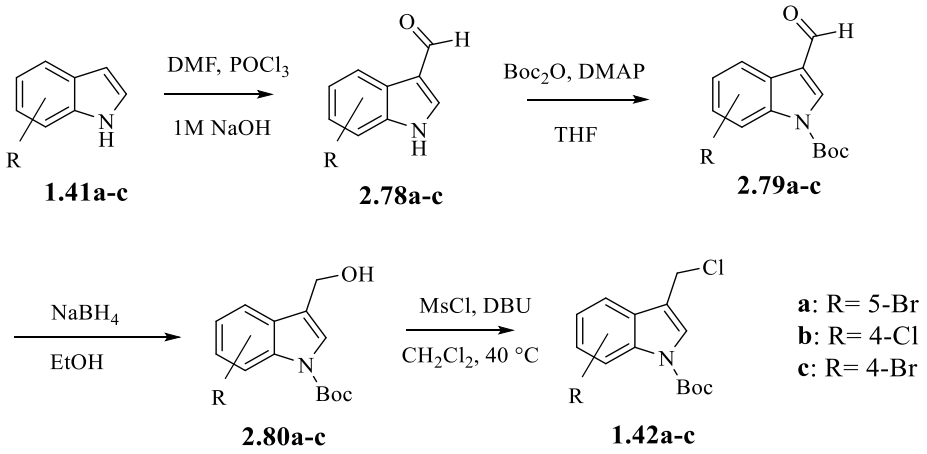
Scheme 2.29: Synthesis of BPB-glycine-Ni(II) Schiff base

With BPB ligand in hand, the BPB-glycine-Ni(II) Schiff base was assembled following Belokon's method by employing $Ni(NO_3)_2 \cdot 6H_2O$ and a strong base in anhydrous methanol (Scheme 2.29). The reaction can be monitored by the

colour change. During synthesis, the green (hydrated Ni^{2+}) $Ni(NO_3)_2 \cdot 6H_2O$ and KOH in MeOH mixture turned blue after the addition of glycine under refluxing. The colour change indicated the formation of coordinated glycine-Ni(II) complex. The blue suspension turned to wine red after the BPB and glycine were added. After completion, the excess Ni^{2+} ion was converted to Ni(II)acetate with acetic acid. The Ni(II)acetate solid was filtered. The residual material was recrystallized from methanol/H_2O to afford the product as red crystal in 70% yield.

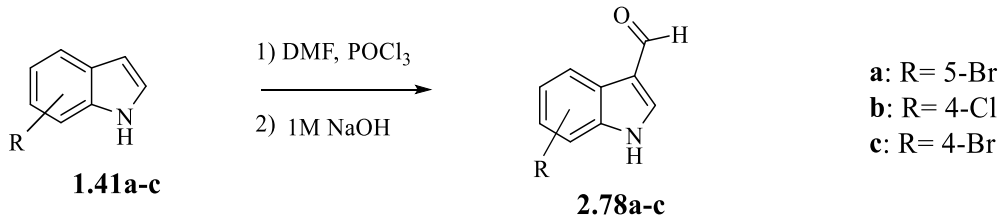
2.6.3 Preparation of Indolemethyl Chloride for Alkylation

The suitable electrophile for the alkylation of BPB-glycine-Ni(II) Schiff base is an indole moiety with an alkyl halide at the C-3 indole carbon. The alkyl halides can be obtained using chlorination reaction from 3-hydroxymethylindole **2.80**, which can be synthesised from indole. The full route to synthesise the indole alkyl halides **1.42** is outlined in Scheme 2.30.



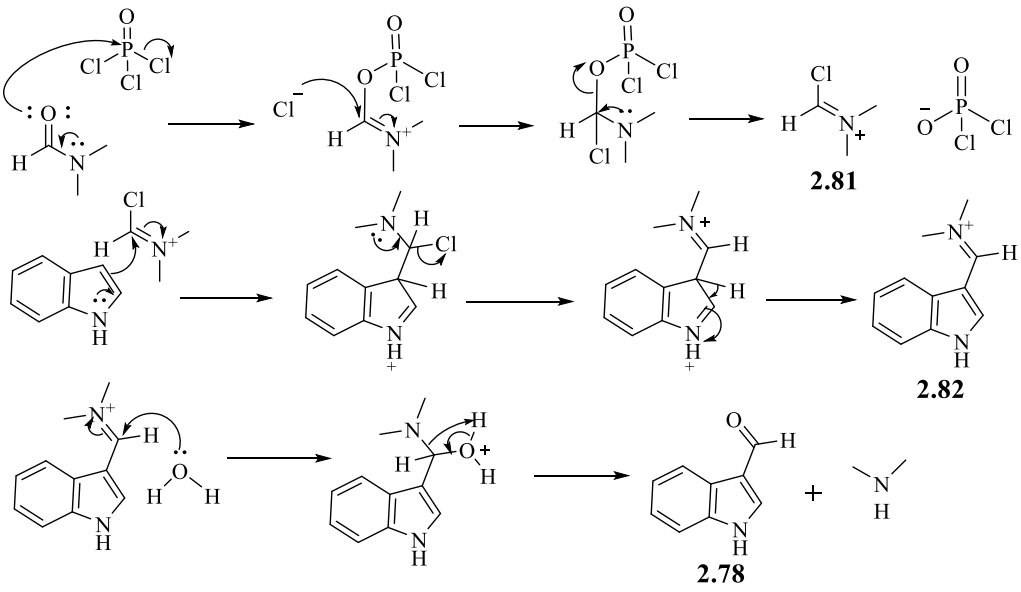
Scheme 2.30: Synthesis of alkyl halide

2.6.3.1 Vilsmeier-Haack Formylation of Indole



Scheme 2.31: Vilsmeier-Haack formylation of indoles

The 4- or 5-halogen substituted indoles were used in this thesis. This is due to a desire to study the effects of 4- or 5-halogen substituted tryptophan on the biological activity of argyrin analogues. Thus, the initial step of the indole C-3 carbon functionalization is C-formylation (Scheme 2.31). The Vilsmeier-Haack formylation[235] of indole is a well-established method, using dimethylformamide (DMF) and phosphorus oxychloride.



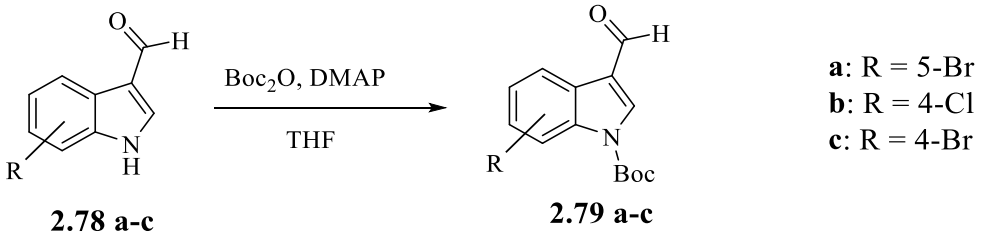
Scheme 2.32: Proposed Vilsmeier-Haack formylation mechanism

The reaction began with the reaction of DMF with the $POCl_3$ to form an iminium salt known as the 'Vilsmeier reagent' **2.81**. DMF was used as the solvent and

reagent. The electron rich aromatic ring of indole then attacks the iminium ion with loss of aromaticity. A deprotonation step restores aromaticity, followed by the release of a chloride ion to form another iminium intermediate **2.82**. The aqueous work up afforded the desired products **2.78**. It was found that Vilsmeier formylation of substituted indoles took place exclusively at C-3 position under the controlled temperature (Scheme 2.32).

After hydrolysis work-up using aqueous NaOH, the precipitated aldehyde was collected by filtration and the yields for the series of indole derivatives were above 80%. The identity of these products was further confirmed by ^{1}H-NMR, with the appearance of aldehyde singlet at around δ 10 ppm.

2.6.3.2 *N*-Boc Protection of Indole-3-carbaldehydes

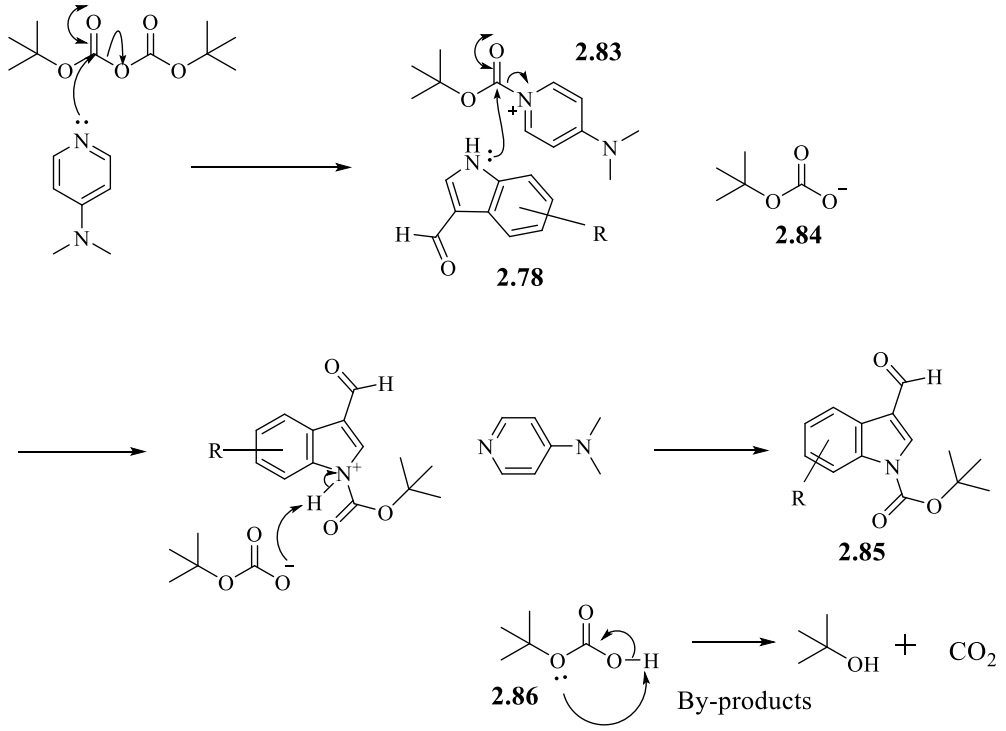


2.78 a-c **2.79 a-c**

Scheme 2.33: *N*-Boc protection of indole-3-carbaldehyde

The indole-3-carboxaldehydes were *N*-Boc-protected employing di-*tert*-butyl dicarbonate (Boc_2O) in the presence of catalytic amount of 4-(dimethylamino)-pyridine (DMAP)[236] in THF (Scheme 2.33). The DMAP accelerates the rate of the reaction, especially in less nucleophilic indole. The straightforward reaction furnished the desired product in near-quantitative yield (99%).

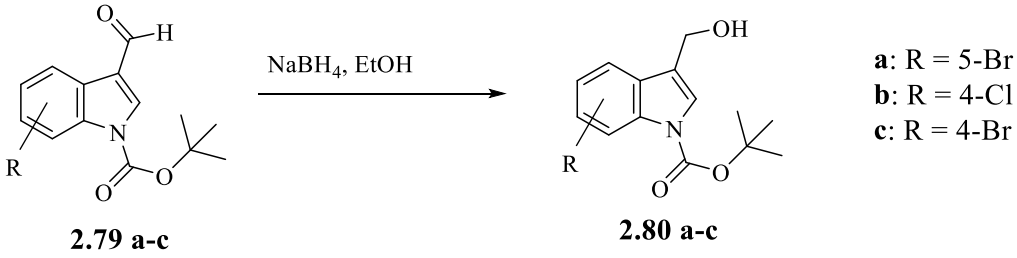
A Boc-pyridinium species formed by nucleophilic attack by DMAP at the carbonyl of Boc_2O. The generated *tert*-butylcarbonate **2.84** is a good leaving group. The indole amine **2.78** then attacks the carbonyl of the Boc-pyridinium species **2.83**, resulting in the regeneration of DMAP. The carbon dioxide and *tert*-butanol are formed from the breakdown of *tert*-butylcabonate **2.86** by-product. Hence, the formation of gas bubble indicated that the reaction was occurring (Scheme 2.34).



Scheme 2.34: DMAP catalysed *N*-Boc protection with proposed reaction mechanism

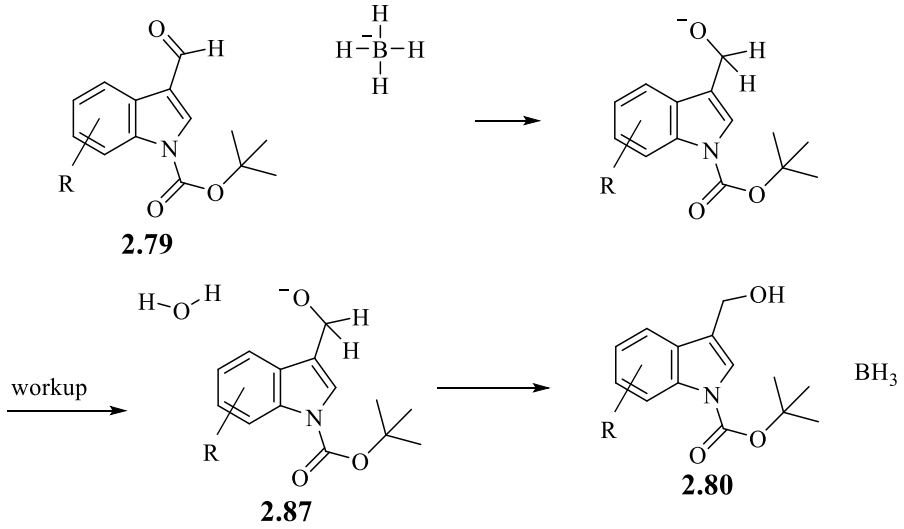
The DMAP-catalysed *N*-Boc protection is fast and efficient, with high yields (>90%). An aqueous based work up removed the DMAP and butanol to afford the desired *N*-Boc-indole-3-carbaldehydes. The singlet between δ 1.6–1.7 in ^{1}H-NMR indicated the presence of the *tert*-butyl moiety. The products **2.79 a–c** were subjected to the next step without further purification.

2.6.3.3 Synthesis of *N*-Boc-3-hydroxymethylindole



Scheme 2.35: Synthesis of N-Boc-3-hydroxymethylindole

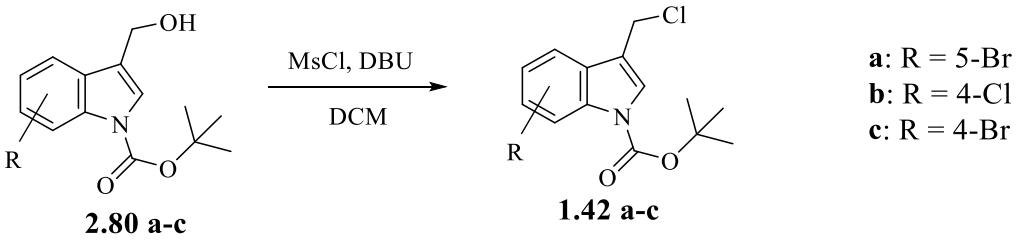
The halogen-substituted *N*-Boc-indole was reduced to the corresponding *N*-Boc-3-hydroxymethylindole using sodium borohydride ($NaBH_4$)[237] in the presence of EtOH (Scheme 2.35). $NaBH_4$ is a good reducing agent, which is not as powerful as lithium aluminium hydride. It can effectively reduce aldehydes and ketones to the corresponding alcohols. The mechanism of reduction is proposed proceed in two steps (Scheme 2.36). Firstly, a H detaches from the BH_4^- and adds to the carbonyl carbon. Secondly, the proton from water is added to the negatively charged oxyanion to form the alcohol. The second step typically occurs at the end of the reaction during an aqueous workup.



Scheme 2.36: $NaBH_4$ reduction of aldehyde

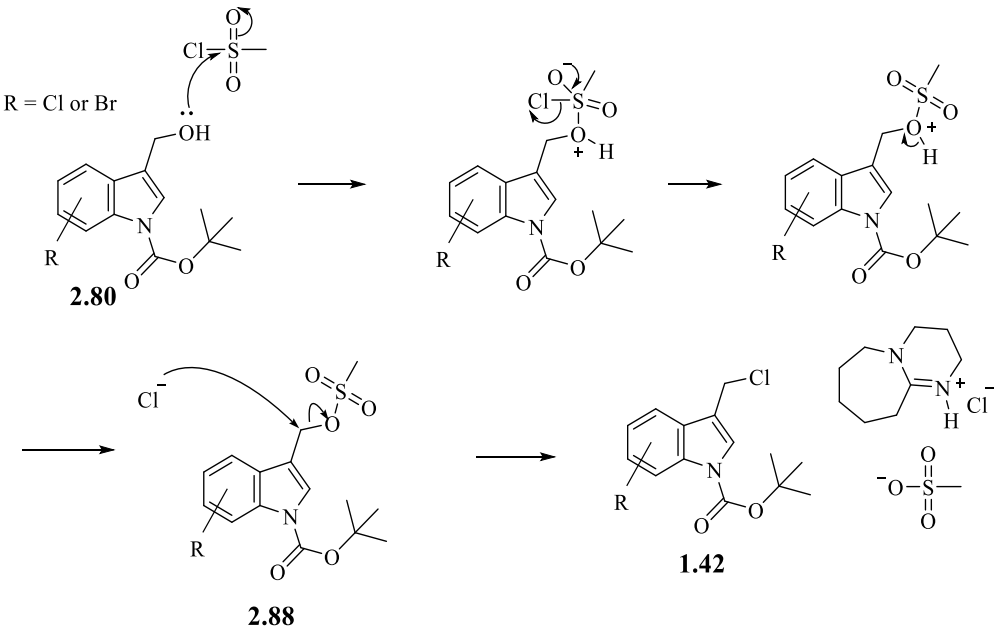
The crude products were purified through column chromatography to afford the pure products **2.80 a–c** in 50–60% yields.

2.6.3.4 Chlorination of the *N*-Boc-3-hydroxymethylindole



Scheme 2.37: Chlorination of *N*-Boc-3-hydroxymethylindole

The electron withdrawing substituents, such as the halogens (as seen in **2.80 a-c**), on the indole in the presence of *N*-Boc-protecting group can deactivate the conjugated π-system. Initially, an Appel bromination reaction was attempted to convert the indolemethyl alcohol to an alkyl halide in the presence of bromine source and triphenylphospine in tetrachloromethane. However, the yield was poor and the products were not stable. To improve the reaction yield, an alternative strategy was evaluated. Chan *et al.* reported the chlorination of *N*-Boc-3-hydroxymethylindole in the presence of MsCl and non-nucleophilic base triethylamine (Et_3N). Later, Kim *et al*. improved the reaction yield by using 1,8-diazabicyclo[5.4.0]undec-7-ene (DBU) in DCM (Scheme 2.37). The proposed reaction mechanism is outlined in Scheme 2.38. In the chemical transformation, the hydroxyl group was converted into a sulfonate ester, via replacing the chloride from methane sulfonyl chloride. The resulting sulfonate **2.88**, which was a good leaving group, was then substituted by a chloride ion to give the desired product.



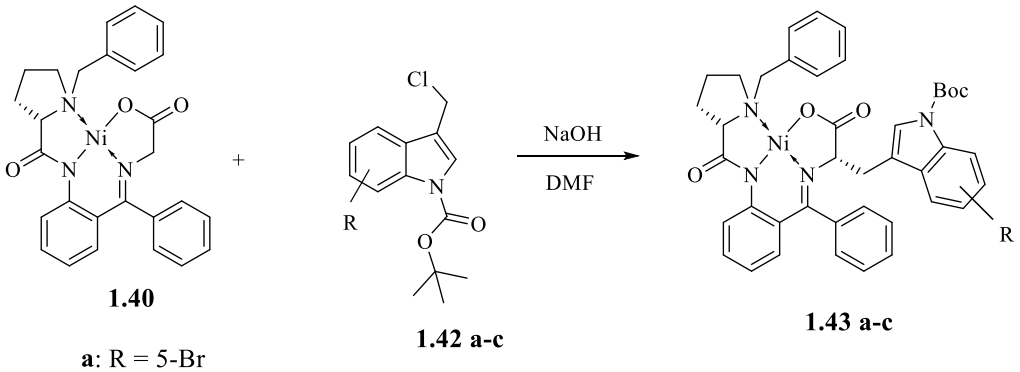
Scheme 2.38: Proposed mechanism of MsCl chlorination

Thus, the MsCl was added dropwise to a solution of the indole and DBU in DCM at 0 ºC. After that, the reaction was refluxed at 40 ºC for 3 hours. The reaction was monitored by TLC. However, complete consumption of the alcoholic starting material did not occur, even with long reaction time. Furthermore, degradation of the product **1.42** was observed during purification by the column purification. Hence, the crude product was taken to next step following a simple aqueous workup. Due to their poor stability, the indole chlorides were always freshly prepared for the subsequent alkylation reaction with BPB-glycine-Ni(II) Schiff base **1.40**.

2.6.3.5 Alkylation of BPB-Glycine-Ni(II) Schiff Base with Alkyl Chloride

A direct alkylation was carried for the homologation of the BPB-glycine-Ni(II) Schiff base (Scheme 2.39). The alkyl halide diastereoselective alkylation of the

chiral complex depends on the high acidity of the glycine α-protons. When a base abstracts the acidic α-proton, the resultant enolate can undergo highly efficient alkylation reaction under operationally simple conditions.



1.40

1.42 a-c

1.43 a-c

a: R = 5-Br
b: R = 4-Cl
c: R = 4-Br

Scheme 2.39: Alkylation of BPB-glycine-Ni(II) Schiff base

The alkylation reaction was performed in the aprotic solvent DMF in the presence of strong base NaOH at 40 ºC. The reaction conditions determine the thermodynamic control which governs the α-epimerisation during the diastereomeric alkylation. In this case, usage of 2 equiv. of NaOH and 40 ºC gave the thermodynamically favoured (*S*,*S*)-isomer in 40-70% yields.

Thus, the freshly prepared crude alkyl chloride (**1.42 a-c**) in DMF was added dropwise to (*S*)-BPB-glycine-Ni(II) Schiff base **1.40** in DMF in the presence of 2 equiv. NaOH at 40 ºC. The reaction was monitored by TLC until all the alkyl chloride was consumed. The reaction is usually finished in 30 minutes. After further analysis using RP-HPLC, one peak corresponding to the desired (*S,S*)-diastereomer was discovered with no appearance of the unfavoured (*S,R*)-diastereomer.

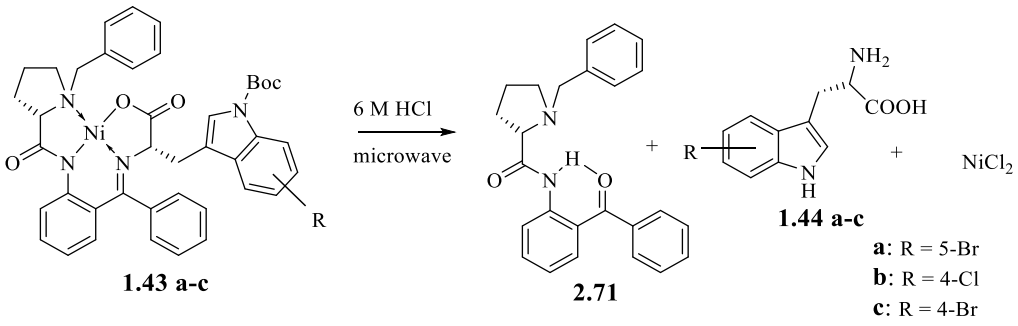
Therefore, such reaction condition was reliable. The crude reaction mixture was purified using column chromatography, after a simple aqueous work-up. All

alkylated complexes (**1.43 a-c**) were isolated as red solids, in 40–70% yields and fully characterised using ^{1}H-NMR, ^{13}C-NMR and melting point analysis (Table 2.1).

Compounds	Yields	Melting point ºC	$[\alpha]_D^{24}$ (MeOH)
1.43 a	40%	98–100	+1231
1.43 b	60%	109–111	+1239.3
1.43 c	70%	99–100	+1100.3

Table 2.1: Characterization of the Glycine-Ni(II) Alkylated Complex

2.6.3.6 Hydrolysis of BPB-Glycine-Ni(II) Alkylated Complexes



Scheme 2.40: Hydrolysis of the BPB-glycine-Ni(II) alkylated complexes

The hydrolysis of the BPB-glycine-Ni(II) alkylated complex was carried out under microwave-assisted conditions, using 6 M HCl/ THF, 2:1 at 50 W and 75 ºC for 20 minutes (Scheme 2.40). The red solution turned into a green/yellow solution, indicating the completion of reaction. In some cases, the reaction was subjected to microwave twice for full disassembly. The completion of the reaction was further determined by RP-PHLC. The volatile THF was evaporated under *vacuo*, and the aqueous layer was extracted with diethyl ether to recover the chiral ligand BPB **2.71**. The green aqueous layer was a mixture containing tryptophan hydrochloric salt, $NiCl_2$, and BPB. Additional organic extraction did

not greatly improve the purity of the aqueous mixture. This was due to tryptophan hydrochloric salt partitioning at the interface between the aqueous and organic phases.

Initially, the aqueous mixture was purified using ion-exchange chromatography. Thus, the aqueous extract was evaporated to dryness. The residual material was dissolved in minimal amount of 0.05% aqueous NH_3 (and pH adjusted to 9–10 with 0.5% aqueous NH_3), and applied to a Dowex 50W x 2 (100-mesh) cation-exchange column. The column was washed with deionised water until the eluent was neutral and then eluted with 0.05% aqueous NH_3 followed by 0.5% aqueous NH_3. The amino acid was eluted when the pH of eluent turned 8–9. However, due to the poor solubility of tryptophan and strong adsorption of the tryptophan to the hydrophobic sulfonic acid functionalised polymeric resin, the yield was low.

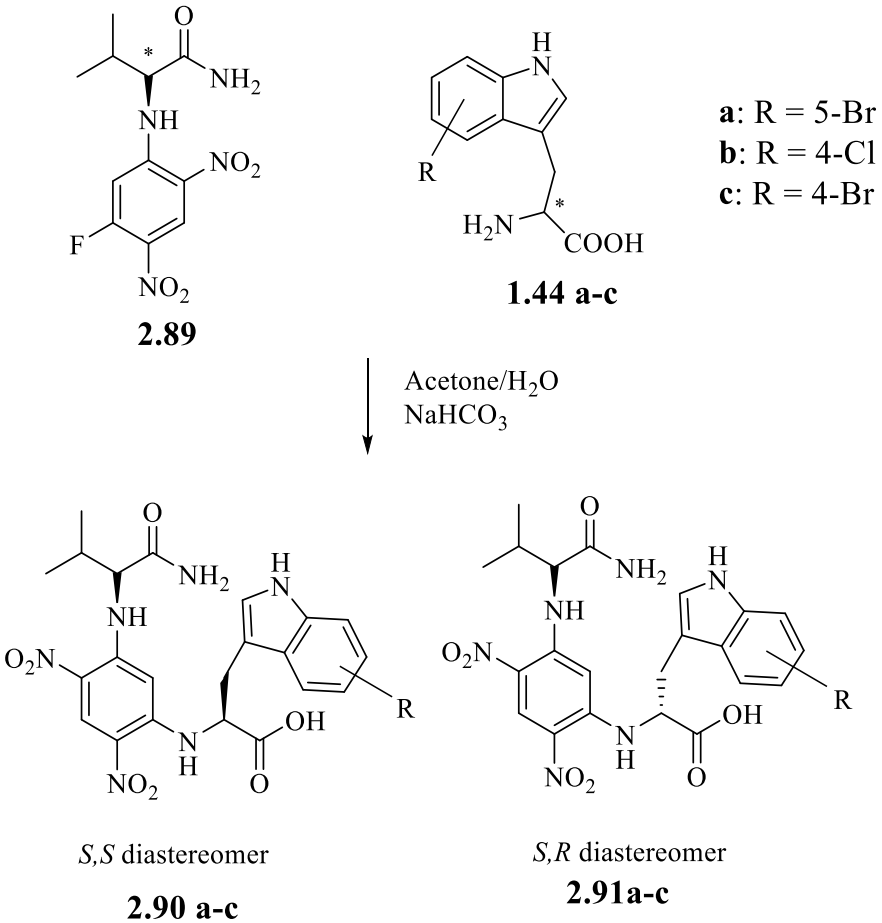
Consequently, the aqueous crude mixtures were subjected to purification by preparative RP-HPLC. The tryptophan containing HPLC eluent was freeze-dried to obtain the optically pure products (Table 2.2).

Compound	Yield	$[\alpha]_D^{24}$ (MeOH)
1.44 a	48%	-27.1 (c=1.0)
1.44 b	40%	-39.2 (c=1.0)
1.44 c	49%	-20.6 (c=1.0)

Table 2.2: Characterization of substituted (*S*)-tryptophan

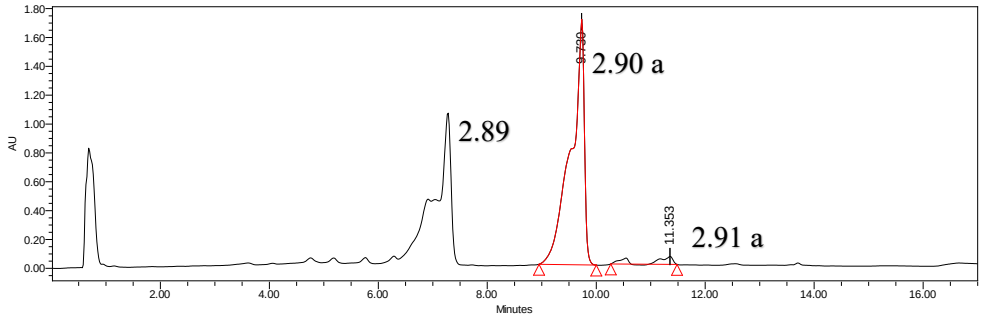
Marfey's reagent [N^{α}-(2,4-dinitro-5-fluorophenyl)-l-valinamide] (FDVA)[238] **2.89**, which belongs to the family of chiral derivatizing agents, was selected to analyse the enantiomers. Recently, the Marfey's reagent has been broadly applied for characterisation of small quantities of amino acids, the reagent with a reactive aromatic fluorine undergoes nucleophilic substitution by the amino group of amino acids.[239] Hence, it reacts stoichiometrically with the α-amino

group of L- and D-amino acids to form diastereomers without racemisation within 1 h under alkaline conditions at 40 ºC (Scheme 2.41). Moreover, the derivatisation installs a highly absorbing chromophore that converts the amino acid into a UV absorbing diastereomer. The diastereomer can be readily separated by standard RP-HPLC. Consequently, the Marfey's reagent enables a quick detection of the resulting derivatives through nonchiral HPLC for analytical application.



Scheme 2.41: FDVA derivatization of substituted tryptophan

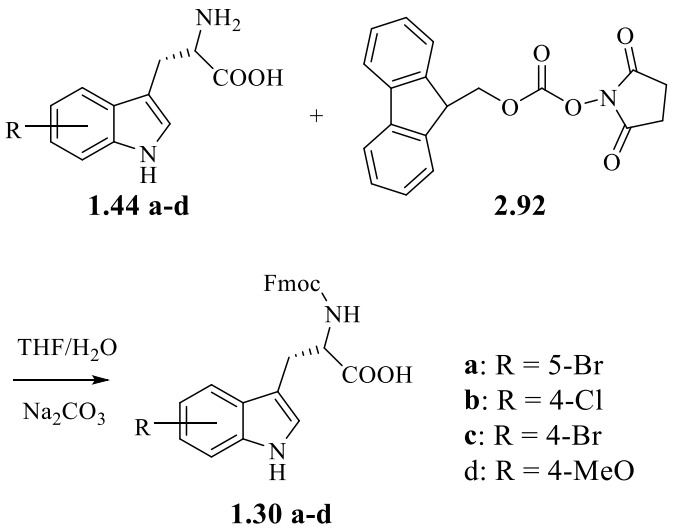
The RP-HPLC analysis of FDVA-derivatized 5-Br-Trp is shown in Figure 2.5. The first peak is the unreacted FDVA reagent, peak 1 and peak 2 are the major and minor diastereomers, respectively. The enantiomeric excess of the tryptophan derivatives was determined to be greater 94%.



	Retention time	Area	% Area
1	9.730	294045231	95.26
2	11.353	144868	4.74

Figure 2.5: HPLC analysis of derivatizing of the tryptophan with FDVA. Solvent system: 10–60% **B** in **A** over 12 min at 3 mL/min. (**A** = 0.06% TFA in water, **B** = 90% acetonitrile in water + 0.06% TFA). Column: Onyx Monolithic C_{18} (100 x 4.6 mm). Eluent was monitored at 216 nm.

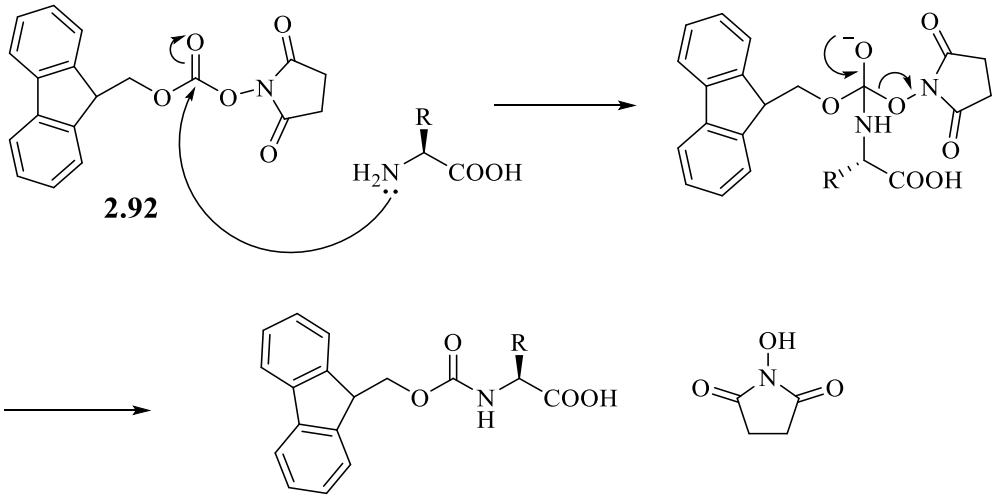
2.6.3.7 Fmoc-Protection of Tryptophan Derivatives



Scheme 2.42: Fmoc-protection of tryptophan

The (*S*)-tryptophan was protected at the α-amino site with a 9-fluorenylmethoxy carbonyl (Fmoc) group, which is appropriate for the Fmoc/*t*Bu solid-phase synthesis of argyrin analogues. The Fmoc-protection was carried by reacting the

amino acid with Fmoc-succinimide (Fmoc-OSu) **2.92** (Scheme 2.42). The usage of Fmoc-chloride has a major drawback since it promotes undesired anhydride formation due to the basic reaction condition described by Schotten-Baumann.[240] However, Fmoc protection using Fmoc-OSu can be achieved through nucleophilic acyl substitution under basic conditions (Scheme 2.43).

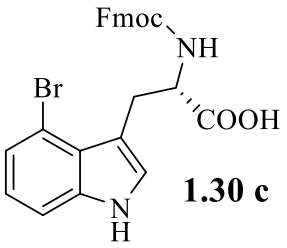


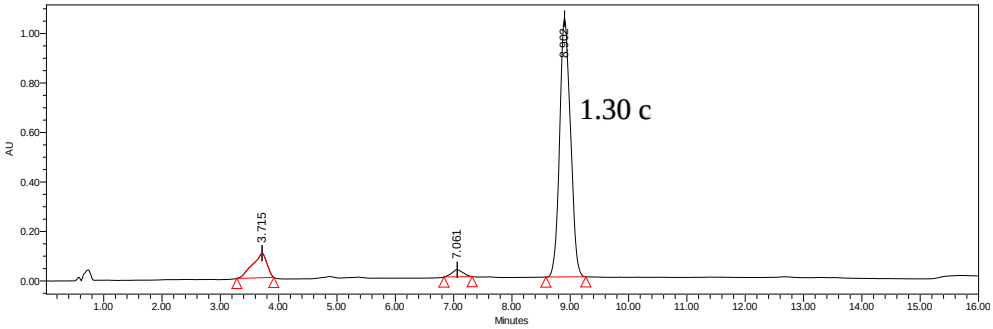
Scheme 2.43: Proposed mechanism of *N*-Fmoc protection using Fmoc-OSu **2.92**

Hence, the tryptophan analogues were dissolved in aqueous sodium carbonate. To this, 1 equivalent of Fmoc-OSu in THF was added and the resultant suspension was stirred for 20 hours. The reaction was monitored by RP-PHLC. Upon completion, the THF was evaporated, and the aqueous mixture was subjected to organic extraction with diethyl ether to remove the unreacted Fmoc-OSu. The aqueous mixture was acidified to pH 2 with 1 M HCl and back-extracted with EtOAc to afford the desired products. The desired product was further triturated with diethyl ether. The yield (45–50 %), melting point and optical rotation of **1.30 a-d** are listed in Table 2.3. An example of RP-HPLC analysis **1.30c** is shown in Figure 2.6. In addition to the synthesised halogenated tryptophan derivatives, a commercially available (*S*)-4-methoxy-tryptophan was also *N*-Fmoc protected.

Compounds	Yield%	Melting point °C	$[\alpha]_D^{24}$ (MeOH)
1.30 a	50	130-131	-28.3 (*c* = 1.0)
1.30 b	45	103-105	-12.3 (*c* = 1.0)
1.30 c	50	92-94	-23.3 (*c* = 1.0)
1.30 d	50	172.9	-24.5 (*c* = 1.0)

Table 2.3. Key characterization of Fmoc-protection of Tryptophan Derivatives





	Retention time	Area	% Area
1	3.715	1686372	10.82
2	7.061	383893	2.46
3	8.902	13515107	86.72

Figure 2.6: RP-HPLC analysis of **1.30 c**. Solvent system: 35–90% **B** in **A** over 12 min at 3 mL/min. (**A** = 0.06% TFA in water, **B** = 90% acetonitrile in water + 0.06% TFA). Column: Onyx Monolithic C_{18} (100 x 4.6 mm). Eluent was monitored at 216 nm.

2.7 Conclusions

In conclusion, this chapter reported the total synthesis of two building blocks, the thiazole dipeptide **1.29** and tryptophan analogues **1.30 a-d** required for the Fmoc/*t*Bu solid-phase peptide synthesis of argyrin analogues.

Two routes for total synthesis of thiazole dipeptides were evaluated. The initial Schmidt's modified Hantzsch thiazole synthesis afforded good yield and good optically purity (Scheme 2.4). However, the usage of unpleasant Lawesson's reagent compelled the consideration of an alternative method, which was successfully achieved (Scheme 2.13).

This chapter also reported the usage of glycine-Ni(II) Schiff base for the synthesis of optically pure tryptophan analogues. The synthesis was based on a direct alkylation of (*S*)-glycine-Ni(II) Schiff base with an appropriate indole alkyl chloride. Compared with synthetic methods reported by other research groups during the total synthesis of argyrin, this method benefited from:

1. The BPB can be easily accessible through a three-step synthetic route from inexpensive starting materials and the process is scalable.
2. The indole alkyl chlorides can be obtained from a four-step synthesis.
3. The alkylation reaction can be operated under mild conditions and short reaction time. The workup is simple and products are optically pure.
4. The tryptophan analogues can be purified through RP-HPLC.

The method described in this thesis can be applied for the synthesis of other optically pure amino acids with simple modification.

Chapter 3
Synthesis of α,β-Dehydroamino Acids

3.1 α,β-Dehydroamino Acids Containing Peptides

α,β-Dehydroamino acids are naturally occurring non-coded amino acids which are mainly produced by bacteria. Fungi are the second primary source. Such peptides containing the α,β-dehydroamino acids display various biological activities, most of which show antibacterial and antifungal activities (Figure 3.1). Therefore, they are considered as important precursors, and important feature of potential new antibiotics.[241] The two classes of natural compounds containing α,β-dehydroamino acids, lantibiotics and thiopeptide antibiotic are under intense study and several members of these classes are already in clinical trials for the treatment of bacterial infections.

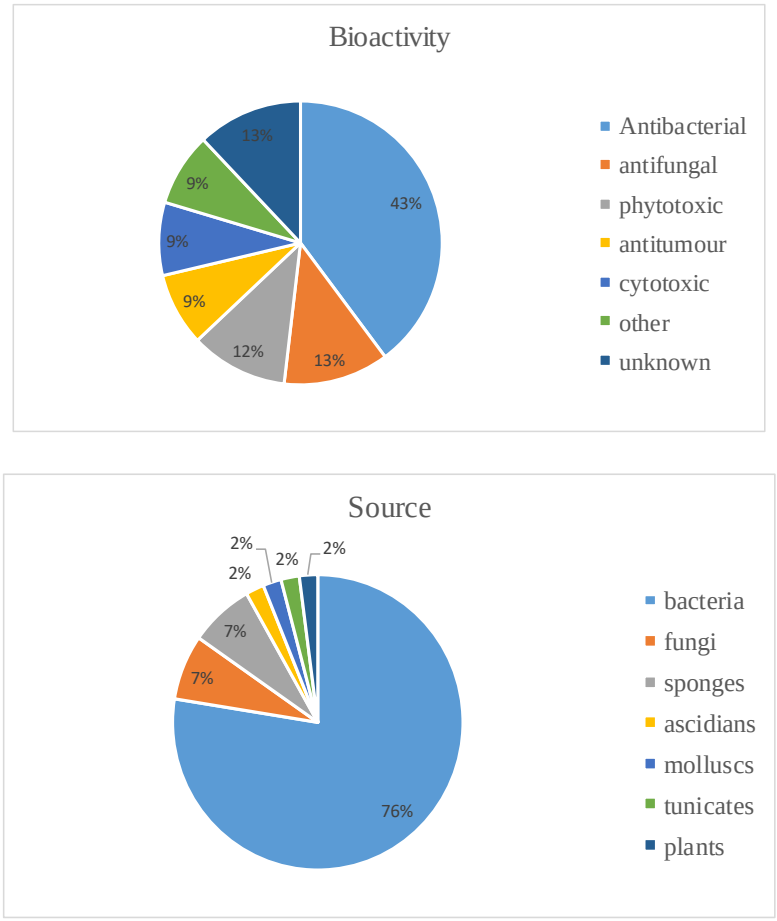


Figure 3.1: Source of origin and bioactivity of α,β-dehydroamino acids containing peptides.[241]

3.1.1 Lantibiotics

The lantibiotics are a family of 80 compounds produced by Gram-positive bacteria. They are ribosomally synthesised, post-translationally modified peptide antibiotics. The most prominent lantibiotic nisin, produced by bacteria *Lactococcus lactis*, has been used in food preservation for more than 60 years.[242] Nisin was first described as a group-N streptococci inhibiting substance in the 1920s and characterised as a lanthionine-containing peptide by Berridge in 1949.[243] A large number of new lantibiotics (Figure 3.2) have been discovered since then.[244] The lantibiotics contain typically the dehydroalanine and/or Z-

dehydrobutyrine residues which are derived from enzymatic dehydration of serine and threonine, respectively. The characteristic structural feature of lanthionine and methyllanthionine is the result of an enzyme-catalysed stereo-specific condensation reaction between the thiol group of a neighbouring cysteine with either a dehydroalanine or dehydrobutyrine. The stable, thioether-based cyclic structure contributing to the three-dimensional structure of the peptides are usually essential for the biological activity.[245]

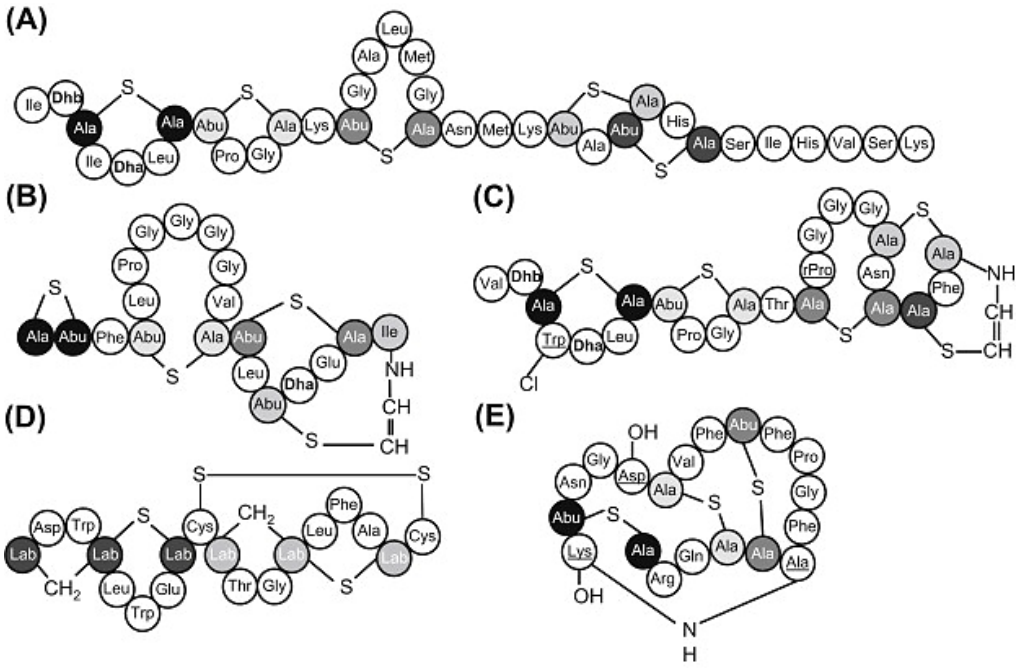


Figure 3.2: Structure of the lantibiotics nisin A **3.1** (**A**), mesacidin **3.2** (**B**), microbisporicin **3.3** (**C**), labyrinthopeptin A2 **3.4** (**D**), and cinnamycin **3.5** (**E**).[245]

Most lantibiotics are active against Gram-positive bacteria while Gram-negative bacteria are resistant to these peptides due to the protective effect of the outer membrane.[244] Nisin **3.1** and other type-A lantibiotics are able to disrupt membranes by forming nonselective, transient pores resulting in the dissipation of the membrane potential, rapid efflux of small metabolites and termination of cellular biosynthetic processes.[243]

The membrane-bound peptidoglycan precursor lipid II was identified as a target for many lantibiotics, such as nisin, epidermin, plantaricin C and mersacidin **3.2**. The binding of these lantibiotics to the lipid II block the precursor from incorporation into the bacterial cell wall, leading to the inhibition of cell wall synthesis.[246] In addition, the pore formation is a second bactericidal mechanism for nisin-type lantibiotics as well as the two-component lantibiotic lacticin 3147. Further investigation of the molecular basis of the interaction between nisin and lipid II revealed that the first two rings in the *N*-terminal part of the peptide are specifically responsible for the interaction with lipid II, while the *C*-terminal and the central flexible hinge region are responsible for the pore formation.[247]

The cinnamycin-like lantibiotics show bactericidal activity against a few bacterial strains, especially *Bacillus* strains. They bind to the phosphoethanolamine resulting in increased membrane permeability, impaired ATP-dependent protein translocation and calcium uptake, and phospholipase inhibition.[248] Such findings make lantibiotics attractive model compounds for the design of new antibiotics.

3.1.2 Thiopeptide Antibiotics

The thiopeptides are highly modified sulfur-rich ribosomal-synthesised peptides with dehydroalanine and dehydrobutyrine. Their most characteristic structural feature is the central nitrogen-containing residues six-membered ring, which is found in many different oxidation states.[249] Such central ring serves as scaffold and can be decorated with various dehydroamino acids and azoles (thiazoles, oxazoles, and thiazolines).

These peptide-based natural products (Figure 3.3) can be either synthesised on the ribosome as product of mRNA translation or assembled by nonribosomal peptide synthases (NRPSs). Recently, the parent pre-peptide of thiopeptide is confirmed by four research group to be ribosomally synthesised and to be genetically encoded.[250–253] The dehydroalanine and dehydrobutyrine residues are the result of elimination reaction of O-phosphorylated serine and threonine, respectively.

The thiopeptides exert their antibacterial activity by inhibiting ribosomal protein synthesis. However, the different mechanisms of action depend on the macrocycle size of the thiopeptides.[254] The thiopeptides of 26-member macrocycles bind the GTPase-associated region of the ribosome/L11 protein complex. Such action results in the blocking of the binding region of EF-G and stopping the translocation of the growing-peptide/tRNA complex in the ribosome to occur.[255] The thiopeptides of 29-membered ring binding to EF-Tu leads to blocking of tRNA/amino acyl complex binding site. Consequently, the complex is not able to bind to ribosome and the peptide elongation is then inhibited.[256] The thiopeptide with 35-membered rings (Figure 3.3) maintain potent antibacterial activity with unknown molecular targets.

Currently, two thiopeptides, thiostrepton[255] and nosiheptide (Figure 3.4), are used in veterinary medicine. Thiostrepton is used as an active ingredient in an ointment for the treatment of cats and dogs skin infections while nosiheptide is used as an animal growth promoter[257]. The low aqueous solubility limits the application of thiopeptide in the treatment of human bacterial infections. Various modifications on the existing thiopeptides have been carried out by many research groups in order to obtain analogues suitable for the treatment of threatening infections. Thus, these vastly unexplored naturally occurring peptides are a source of potentially new classes of antibacterial agents.

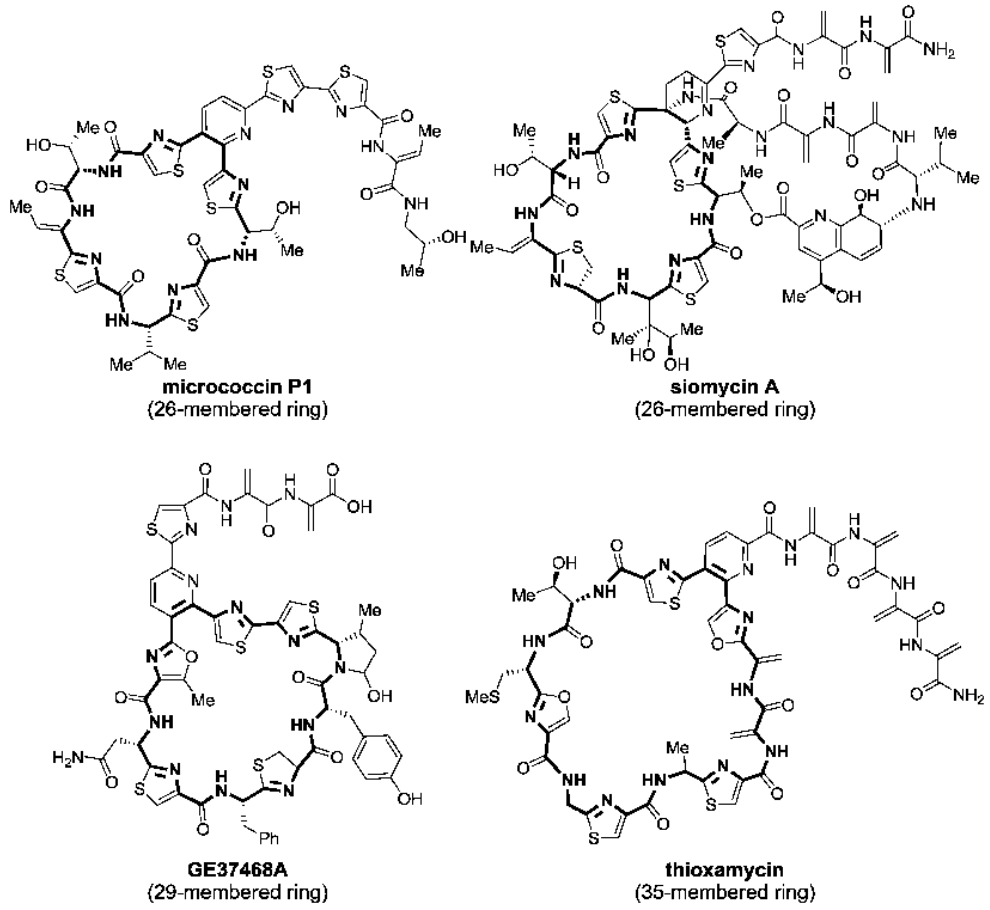


Figure 3.3: Thiopeptides with different macrocycle size[254]

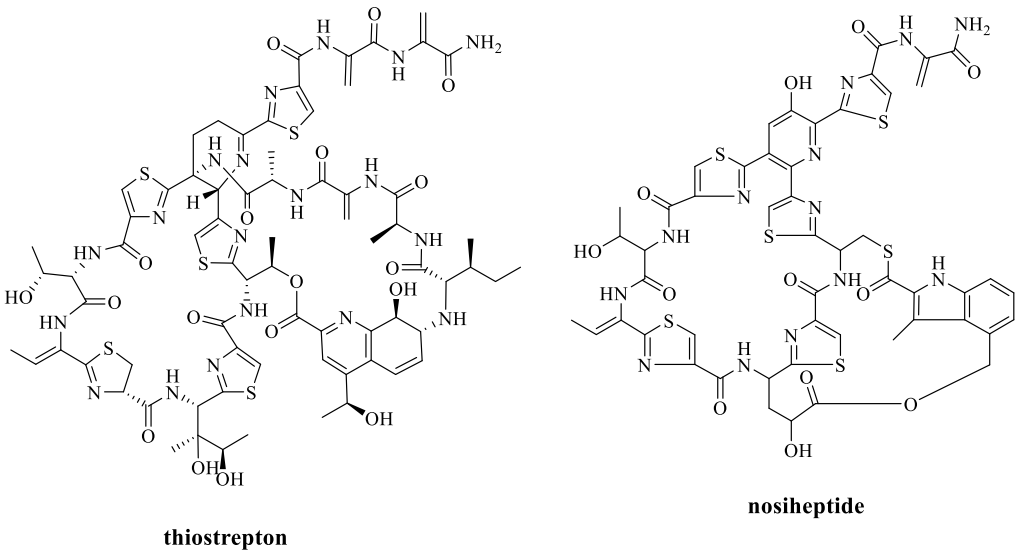


Figure 3.4: Chemical structure of thiostrepton and nosiheptide

3.2 Conformational Property and Chemical Reactivity of the Dehydroamino Acid Residues

The α,β-double bond has a profound effect on the conformational properties of these dehydroamino acid residues. For example, the bond length of sp^2 α-β carbon is shorter. Importantly, the α,β-double bond constricts the topography of the side chain and limits the position of β-substituents, resulting in the geometric isomers *Z* and *E*. The co-planarity of the α,β-double bond and flanking amide groups also enable π-electron conjugation, which are responsible for the stabilisation of conformations.

The α,β-double bond can undergo many reactions, such as halogenation, nucleophilic addition, radical addition reactions, cycloadditions, epoxidation and hydrogenation.[258] Therefore, both conformational properties and chemical reactivity of the α,β-dehydroamino acids can affect the bioactivity of the dehydro amino acid containing peptides.

3.3 Installation of a Dehydroamino Acid into Argyrin

The presence of α,β-dehydroamino acid residues in peptides displays altered bioactivity, as well as increased resistance to enzymatic degradation.[259] The α,β-dehydroamino acid residues have been introduced in several bioactive compounds to afford highly active agonist and antagonist analogues. The dehydroalanine residue of the argyrin is expected to constrain the cyclic conformation of argyrin, thereby governing the rigidity of the structure, which is essential for target binding affinity. Therefore, making modifications at the dehydroalanine residue is a strategy for modulating the bioactivity of argyrin.

Hence, a focused library of α,β-dehydroamino acid analogues will be used to produce novel argyrin analogues.

3.4 Previous Reports for Installing Dehydroamino Acids into Peptides

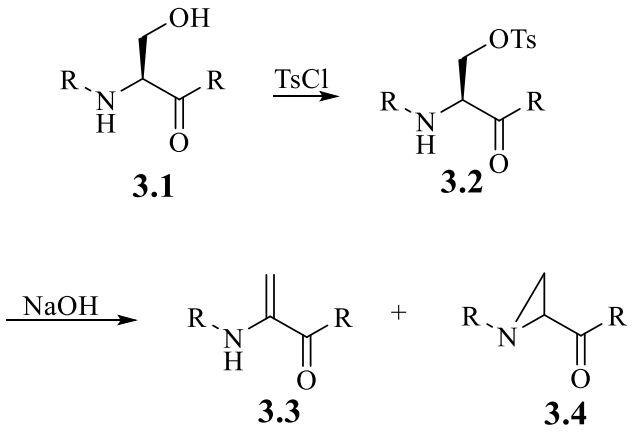
The biosynthetic pathway to dehydroalanine and dehydrobutyrine relies on the dehydration of serine and threonine residues, respectively. Several synthetic routes have been developed to synthesise dehydroamino acids for use as building blocks for direct installation into a peptide chain. However, the reactivity of α,β-unsaturated alkene limits the method of direct introduction of dehydroamino acid to target peptide. The non-*N*-functionalized parent α,β-dehydroamino acids are essentially enamines and are susceptible to hydrolysis.[260] Ammonia is released and α-ketoacids are formed when hydrolysis occurs. Hence, *N*-acylated derivatives of α,β-dehydroamino acids that are incorporated into peptides are more stable than free α,β-dehydroamino acids. Consequently, most reported synthetic methods depend on the incorporation of a masked precursor at an early stage of peptide synthesis, followed by the conversion to the desired α,β-dehydroamino acids after the completion of peptide synthesis. Examples of these synthetic strategies are discussed below.

3.4.1 Elimination Reactions

Elimination of water from β-hydroxy-α-amino acids is a well-developed method to α,β-dehydroamino acids. Such methods have been used for preparation of dehydroalanine and dehydrobutyrine from serine and threonine, respectively.

The hydroxyl group can be activated by various reagents, such as dichloroacetyl chloride/triethylamine[261], tosyl anhydride/1,4-diazabicyclo-[2.2.2]octane (DABCO)[26], triphenylphosphine/diethyl azodicarboxylate (DEAD)[262], tosyl chloride[263] and carbodiimide/copper(I) chloride[264].

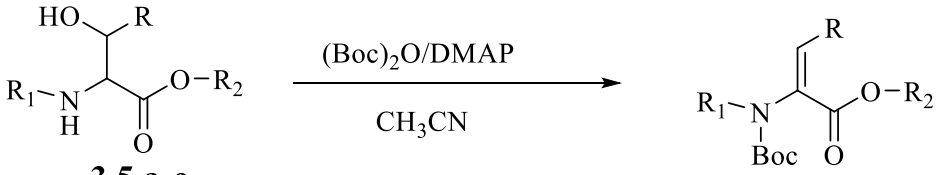
The preparation of dehydroalanine residue was first achieved by Koshland *et al*. (Scheme 3.1).[265] The hydroxyl group of serine residue **3.1** was reacted with *p*-toluenesulfonyl chloride to form the *O*-tosylated serine derivative **3.2**, followed by β-elimination under alkaline conditions to afford dehydroalanine **3.3**. However, Sakai *et al*. reported a high yield of the side-product, an aziridine derivative **3.4** rather than the required dehydroalanine.[266]



Scheme 3.1: Elimination of *O*-tosylated serine[266]

Ferreira *et al*.[267] reported an elimination reaction with Boc-anhydride and DMAP based on the Berkowitz and Pederson's method for simultaneous amine and carboxy protection of amino acids with benzyl chloroformate in the presence of DMAP and triethylamine (Scheme 3.2). They found that under such condition, serine **3.5** underwent an elimination reaction to afford fully protected dehydroalanine derivative **3.6**. They further discovered that *tert*-butoxycarbonyl (Boc) not only fulfilled the requirement of second acyl group but was easier to introduce than reaction of previously protected amino acids with $(Boc)_2O$ and

catalyst DMAP. In the case of threonine and β-hydroxyphenylalanine derivatives, the reaction was stereoselective, which gave exclusively the Z-isomer. This geometric-stereoselectivity is due to the bulkiness of the groups bound to the N-atom, which promotes a *trans* E_2-elimination.

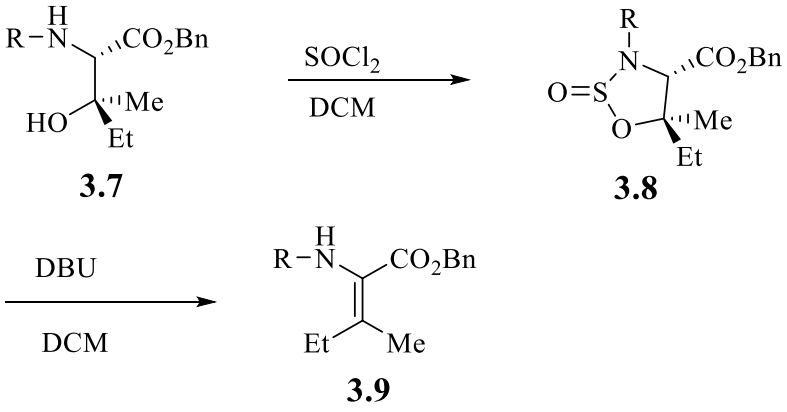


3.5 a-c **3.6 a-c**

a: R = H, Me, Ph
b: R_1 = H, Boc, Z, Z(NO_2), Tos, Bz
c: R_2 = H, Me, Bn

Scheme 3.2: $(Boc)_2O$ and DMAP mediated elimination[267]

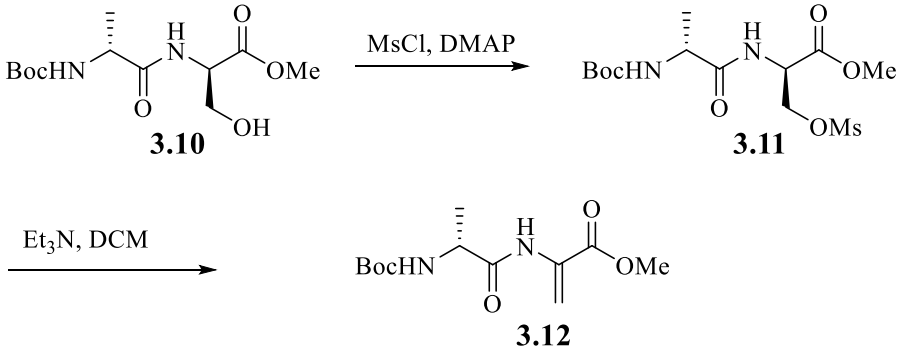
Another geometric-stereoselective elimination method was developed by Wandless *et al*..[268] The β-hydroxyamino acids **3.7** were reacted with thionyl chloride to form the cyclic sufamidites **3.8**, followed by an elimination reaction with DBU to selectively afford (*E*)- or (*Z*)-α,β-dehydroamino acids **3.9** in an *anti*-periplanar fashion, depending crucially on the configuration of the β-hydroxyamino ester. The reaction was carried in a one-pot procedure (Scheme 3.3).



3.7 **3.8** **3.9**

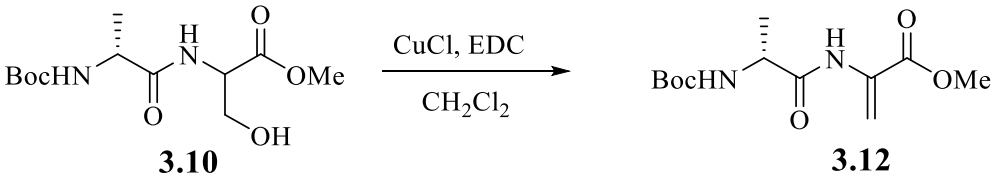
Scheme 3.3: Wandless's method of elimination[268]

In the total synthesis of argyrin A and E, Ley *et al.*[202] subjected the L-serine methyl ester containing dipeptide **3.10** to mesylation product **3.11**, followed by elimination to afford the dehydroalanine moiety **3.12** (Scheme 3.4).



Scheme 3.4: Elimination of Mesylate serine[202]

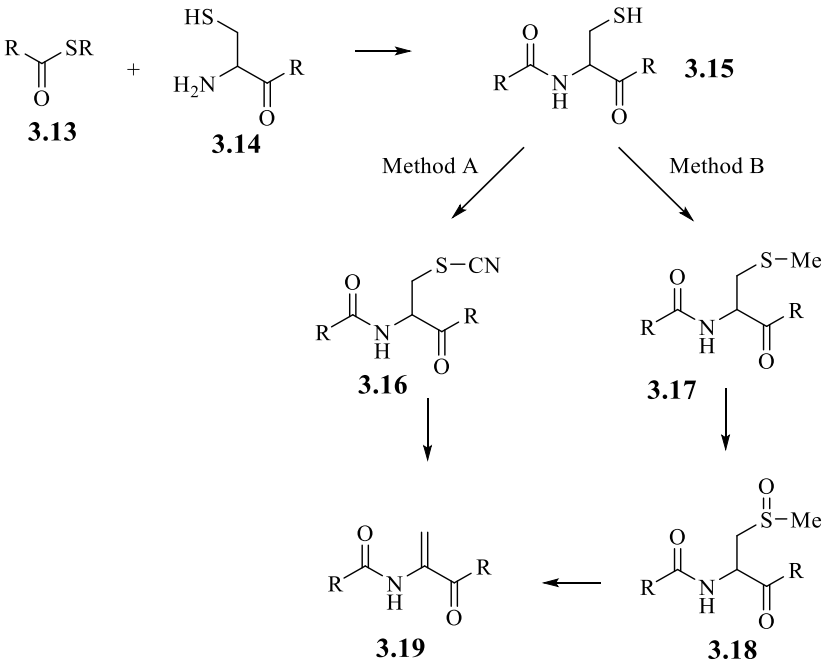
In the total synthesis of argyrin F, Kaless *et al.*[204] used the copper(I)-catalysed elimination of the serine hydroxy group **3.10** to generate the dehydroalanine containing dipeptide **3.12** (Scheme 3.5), which was subsequently used in a fragment condensation reaction to afford the argyrin F.



Scheme 3.5: Copper catalysed elimination of serine[204]

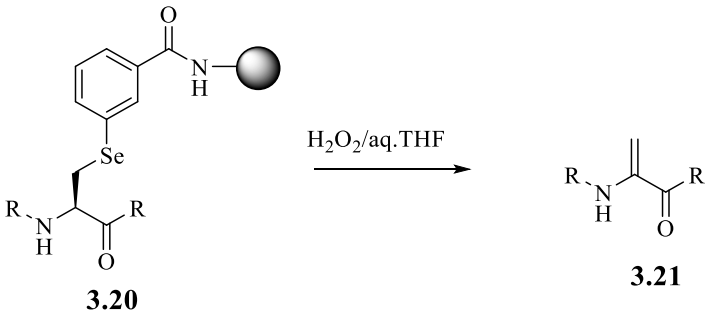
The oxidation of thio[269] and seleno[270] amino acids and subsequent thermolysis is known to afford the corresponding dehydroamino acids in good yields. Miao *et al*.[271] used a cysteine thioester ligation to prepare cysteine containing peptide from unprotected peptide fragments. Such compounds were then converted to cyclic and acyclic peptide α,β-dehydroalanine at the point of ligation. Two methods were used to convert the cysteine residue to dehydroamino acid. Specifically, both methods involved transformation of the thiol functional group into a leaving group followed by a β-elimination reaction. Method A

transformed the thiol into -SCN **3.16** under acidic condition while Method B used a three-step reaction: *S*-methylation, *S*-oxidation, and β-elimination (Scheme 3.6).



Scheme 3.6: Miao and Tam's method for converting cysteine to dehydroalanine[271]

An alternative method introduced by Nakamura *et al*.[272] was the peptide cleavage from the resin and the introduction of the α,β-dehydroalanine in a single step with a seleno-linker **3.20** (Scheme 3.7). The oxidative cleavage from the resin through selenoxide was performed by treatment with hydrogen peroxide in THF.

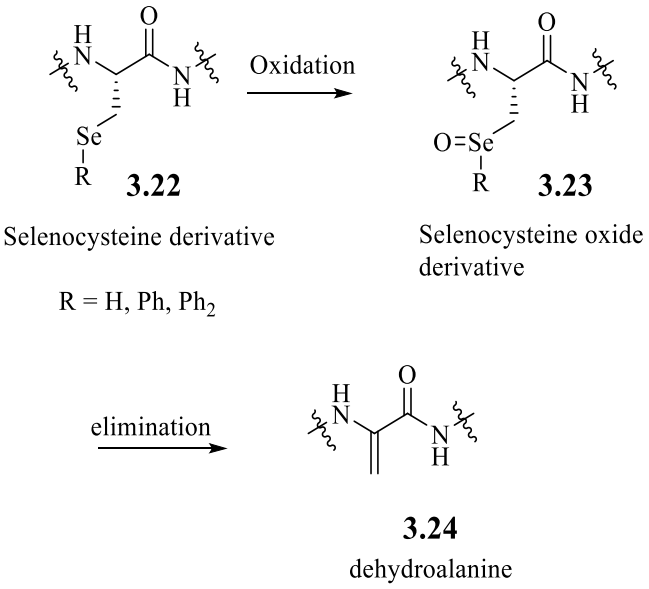


Scheme 3.7: Nakamura's elimination method using seleno-linker.[272]

3.4.2 Preparation of the Dehydroalanine Precursor, Phenylselenocysteine

Walter *et al.*[273] found that selenocysteine derivatives could be selectively converted to dehydroalanine derivatives under mild oxidative elimination conditions (Scheme 3.8). Hence, treatment of diphenylmethylselenocysteine **3.22** with sodium metaperiodate or hydrogen peroxide resulted in corresponding selenoxide derivatives **3.23**, which then underwent elimination to the dehydroalanine derivative **3.24** at room temperature.

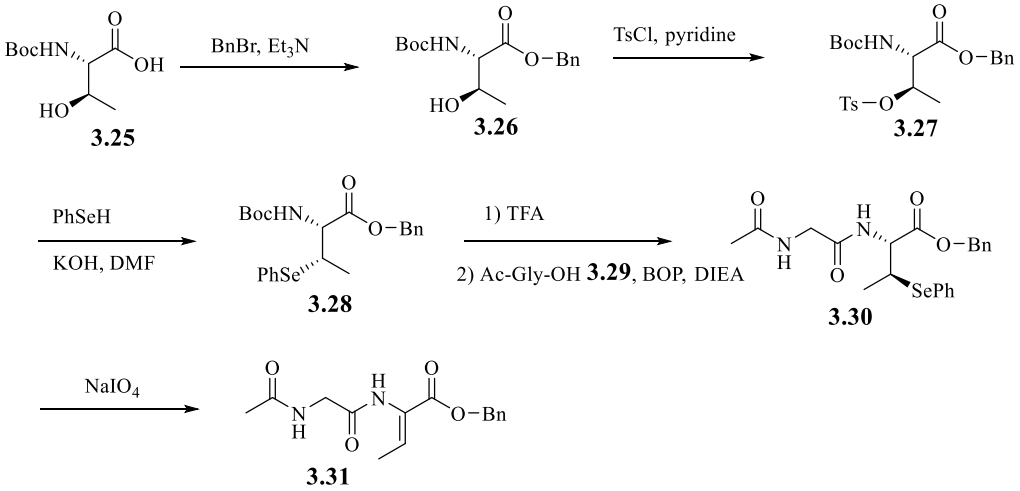
Such method was later adopted by Van der Donk *et al.*[274] for application in the standard Fmoc SPPS. Ley *et al.*[202] first applied this method in the total synthesis of argyrin B. Therefore, this method is utilised in this thesis for the synthesis of dehydroalanine-containing argyrin analogues. The full synthetic procedure is outlined in Section 3.5.



Scheme 3.8: Oxidation elimination of phenylselenocysteine to dehydroalanine[273]

3.4.3 Preparation of Dehydrobutyrine Precursor Methyl-Phenylselenocysteine

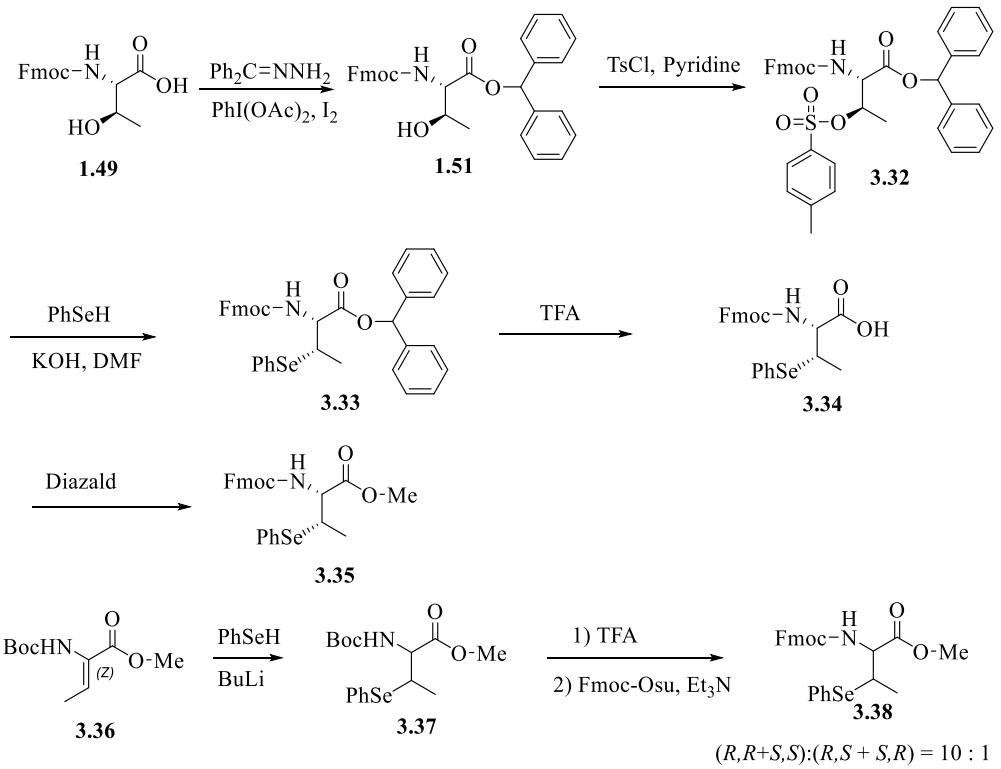
Van der Donk *et al.*[274] extended the above method to the preparation of (*Z*)-dehydrobutyrine from (2*R*,3*S*)-3-methyl-*Se*-phenylselenocysteine (Scheme 3.9). Boc-protected threonine **3.25** was converted to the benzyl ester **3.26**, followed by the activation of hydroxyl group with *p*-toluenesulfonyl chloride. Nucleophilic displacement of the tosyl group **3.27** with phenylselenolate afforded the selenolate derivatives **3.28** in 67% yield. The product was formed through an S_N2 reaction instead of an elimination-addition sequence, which was confirmed by the one diastereomer obtained. Upon oxidation, the (*Z*)-isomer of dehydrobutyrine **3.31** was observed with no γ-elimination product, allylglycine.



Scheme 3.9: Synthesis of dehydrobutyrine containing dipeptide[274]

The above success encouraged the research group to apply the method for the construction of an appropriate building block for Fmoc SPPS. Fmoc-(2*R*,3*S*)-3-methyl-*Se*-phenylselenocysteine was prepared (Scheme 3.10). Fmoc-threonine **1.49** was protected as the diphenylmethyl (Dpm) ester **1.51**, followed by the activation of hydroxy group with *p*-toluenesulfonyl chloride. The tosyl group

was displaced with phenylselenolate. The final deprotection of the Dpm ester **3.33** with TFA afforded the free carboxylic acid **3.34** required for Fmoc SPPS.

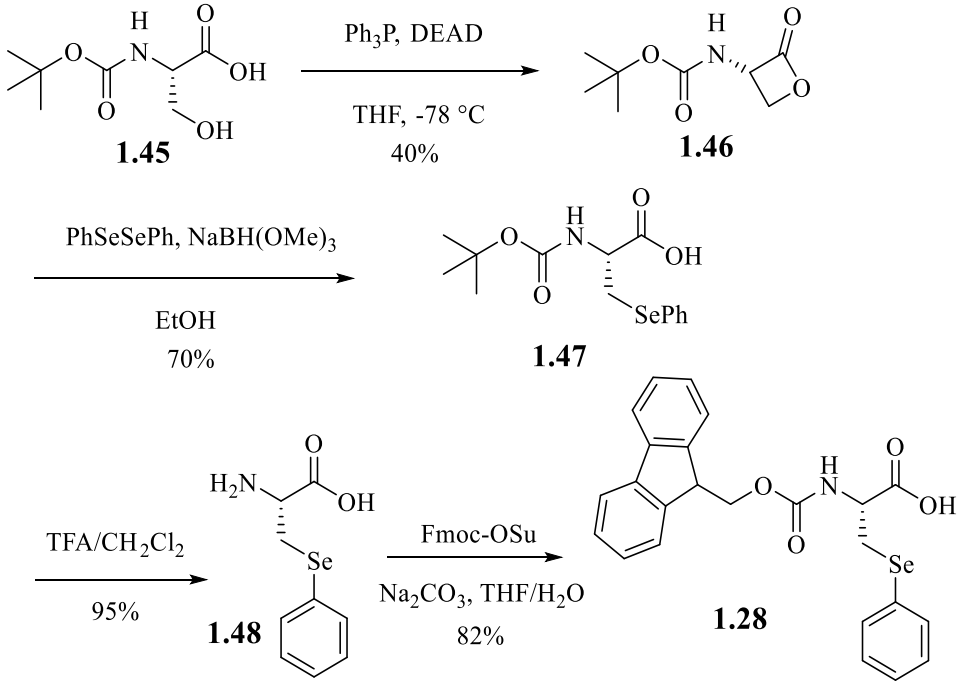


Scheme 3.10: synthesis of Fmoc- (2*R*, 3*S*)-3-methyl-*Se*-phenylselenocysteine[274]

The product was convert to methyl ester **3.35** in order to determine the optical purity. A racemic mixture of diastereomers **3.38** was prepared through Michael addition of phenylselenolate to Fmoc-protected dehydrobutyrine methyl ester **3.36**, resulting in a diastereoselectivity of 10:1. Through HPLC analysis on a Whelk-O1 chiral stationary phase, two sets of enantiomers were observed while a single peak was detected from methyl ester obtained from the displacement of the tosyl group.

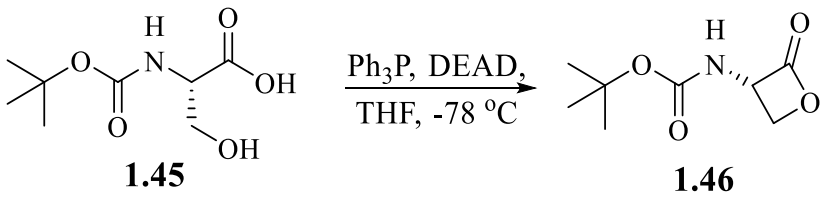
3.5 Synthesis of *N*-Fmoc-Phenylselenocysteine

As mentioned earlier, the Sec(Ph) oxidative elimination strategy was applied to incorporate dehydroalanine into argyrin. The facile approach for synthesis of Sec(Ph) reported by Okeley *et al.*[275] was adopted in this thesis. Thus, Boc-L-serine **1.45** was firstly converted to its β-lactone, followed by ring opening with phenylselenide anion, previously obtained by the reaction of sodium trimethoxyborohydride with diphenyl diselenide. For use in Fmoc SPPS, the *N*-Boc-Sec(Ph)-OH was converted into desired Fmoc-Sec(Ph)-OH through standard methods. The full synthetic route is outlined in Scheme 3.11. The details of each synthetic step are described in the following sections.



Scheme 3.11: Synthetic route to Fmoc-phenylselenocysteine

3.5.1 Synthesis of β-lactone

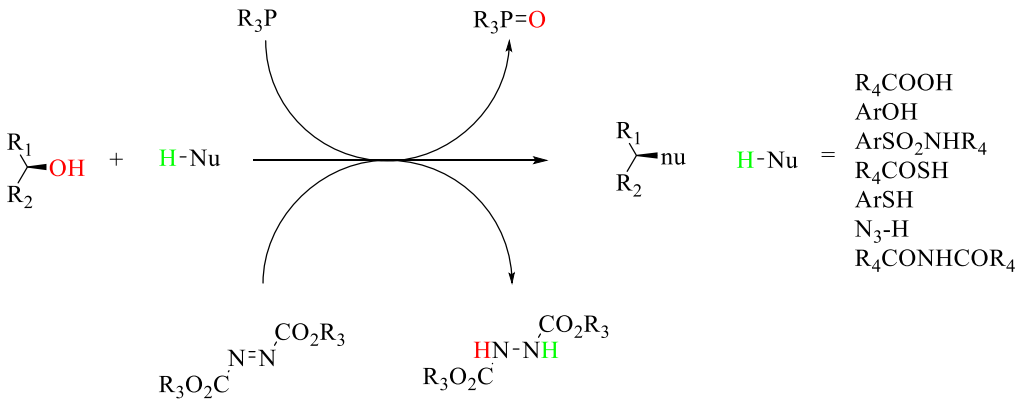


1.45 **1.46**

Scheme 3.12: synthesis of β-lactone

The first step involved the β-lactone ring formation from *N*-Boc-L-serine through an intramolecular Mitsunobu-type reaction (Scheme 3.12). The Mitsunobu reaction, first reported by Oyo Mitsunobu in 1967[276], is the dehydrative coupling of a primary or secondary alcohol to a pro-nucleophile mediated by the reaction of a dialkyl azodicarboxylate with a trialkyl- or triarylphosphine (the Mitsunobu reagents). During the reaction process, the dialkyl azodicarboxylate is reduced to a hydrazine derivative while the phosphine is oxidized to a phosphine oxide. A wide range of pro-nucleophiles, including (thio)carboxylic acids, (thio)phenols, imides and sulfonamides, can participate in this reaction to form corresponding C-O, C-S and C-N bonds.

The pK_a of the pro-nucleophile should be around 11 for a successful reaction. The reason is based on the mechanism of the reaction as the betaine resulting from the reaction of DEAD and PPh_3 has a pK_a of 13 and removes the acidic proton from the pro-nucleophile, otherwise alkylation of DEAD happens. The Mitsunobu reaction can occur under mild conditions, for example at 0 ºC to room temperature. THF, diethyl ether, dichloromethane and toluene can be used as standard solvents (Scheme 3.13).[277]

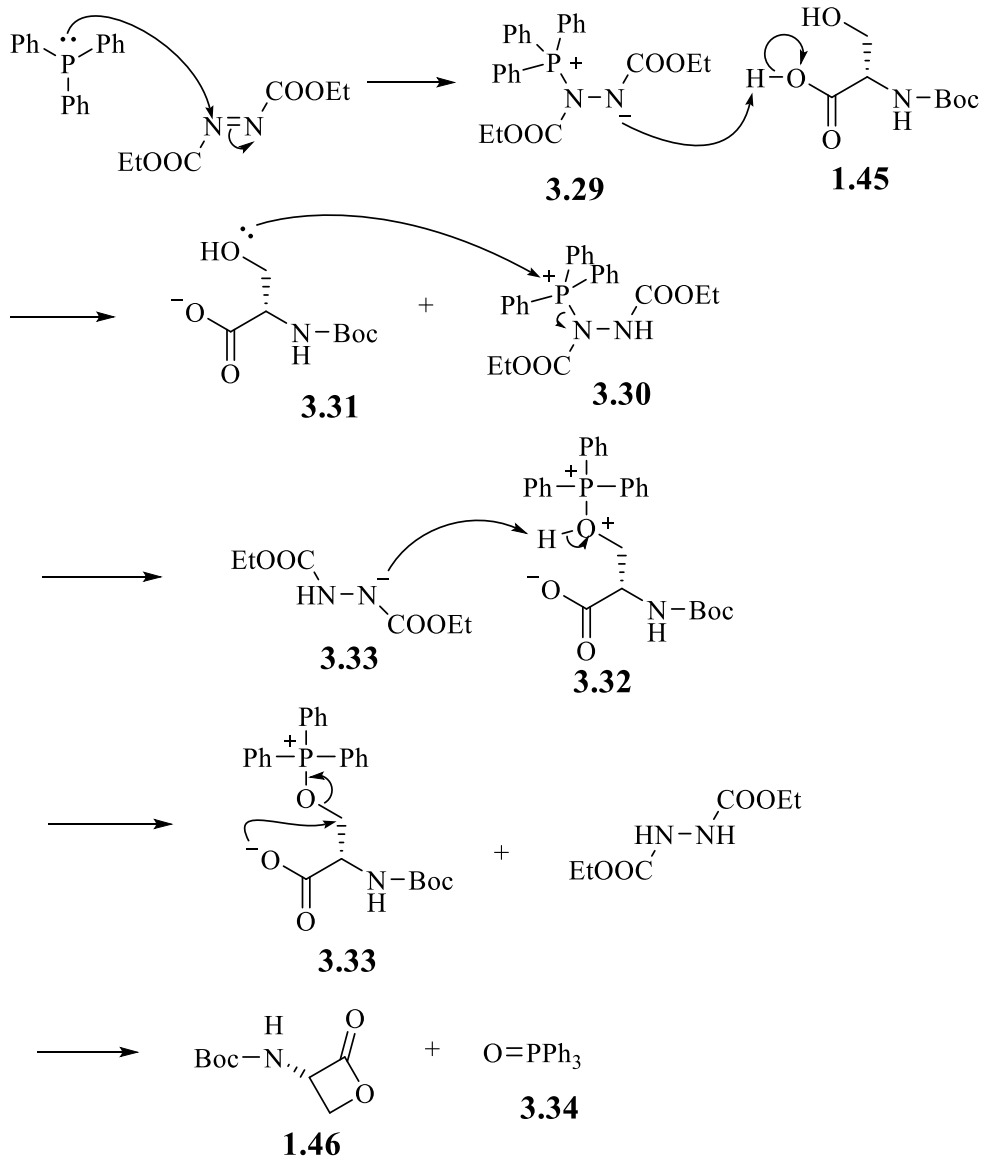


Scheme 3.13: The Mitsunobu reaction[277]

The first step of the reaction was the formation of a reactive betaine intermediate **3.29** from PPh_3 and DEAD. The betaine then deprotonated the carboxylic acid of the serine **1.45** to generate the phosphonium salt **3.30**. The second step was the alcohol activation. The resultant triphenylphosphine group of phosphonium salt was transferred to the hydroxyl group of serine **3.31**. Such step generated the alkoxyphosphonium salt **3.32** and the hydrazine by-product **3.33**. Finally, the formation of β-lactone **1.46** was accomplished through an intramolecular nucleophilic substitution, with triphenylphosphine oxide as by-product **3.34**.[276] The proposed reaction mechanism is illustrated in Scheme 3.14.

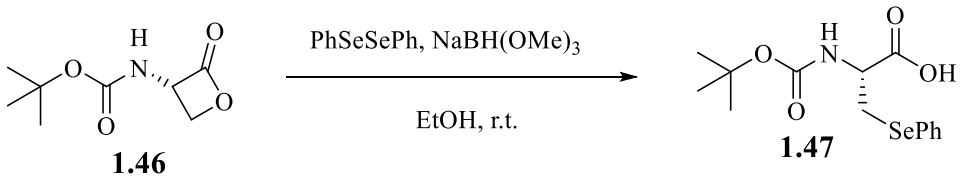
Thus, the above the Mitsunobu intramolecular β-lactone formation was achieved by addition of a stoichiometric amount of DEAD to a stirred solution of PPh_3 in dry THF under nitrogen atmosphere at -78 ºC to form the phosphonium salt. A solution of Boc-L-serine in THF was added dropwise to the reaction mixture over 30 minutes. After completion of addition, the mixture was stirred at -78 ºC for a further 30 minutes before it was warmed up to room temperature. The reaction was stirred at room temperature for 4 hours until completion.

The by-product, triphenylphosphine oxide **3.34**, was partly removed by filtration. The complete removal of by-products, triphenylphosphine oxide and the hydrazine, was achieved by purification through column chromatography. The pure β-lactone was obtained in 40% yield. The high ring-stain four-membered product is unstable, and therefore it should be used immediately in the next step after purification.



Scheme 3.14: Proposed mechanism of Mitsunobu intramolecular β-lactone formation

3.5.2 β-Lactone Ring Opening



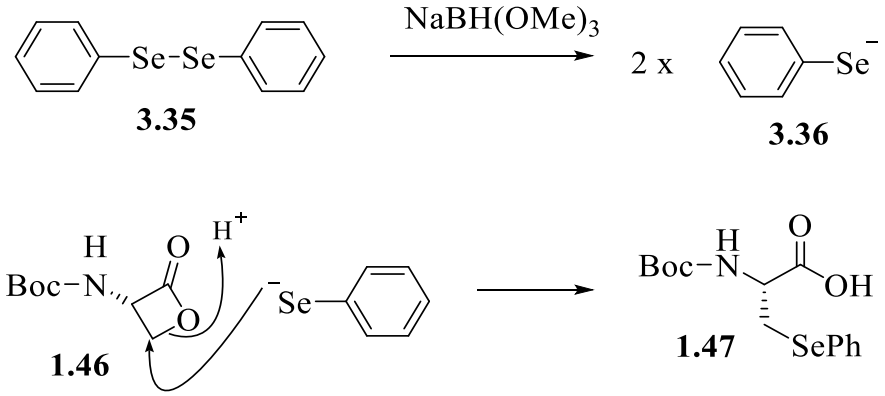
1.46 **1.47**

Scheme 3.15: Ring opening mediated by phenylselenide

The second step was the ring-opening reaction of the β-lactone using a nucleophilic selenide anion to generate the desired selenocysteine derivative (Scheme 3.15). The reaction was achieved through a nucleophilic substitution at the β-carbon using phenylselenide anion. The regioselective ring opening reaction depends on the selection of nucleophile. The small and charged hard nucleophile attacks the carbonyl groups while the large and neutral soft nucleophile attacks the electrophilic β-carbon. The soft nucleophile phenylselenide anion **3.36** is therefore anticipated to undergo an S_N2 reaction at the β-carbon to generate the desired product.[278]

Diphenyl diselenide **3.35** and benzeneselenol are the most common reagents for the generation of nucleophilic phenylselenide. Both Smith *et al*.[279] and Liotta *et al*.[280] reported nucleophilic benzenselenolate anion was capable for lactone ring opening. Smith *et al*. reduced diphenyl diselenide with sodium borohydride in DMF. However, Liotta *et al*.[280] found that the method Smith used generated a sodium benzeneselenolate-diborane complex. Therefore, they reported generation of sodium benzeneselenolate from sodium metal and diphenyl diselenide or from sodium hydride and benzenselenol. Berkowitz and co-workers[281] further investigated both methods and reasoned that the phenylselenide reagent was a potential Lewis acid lacking in reducing ability. Their results suggested that the benzeneselenolate generated from reduction of

diphenyl diselenide with 2 equivalents of sodium trimethoxyborohydride could open the homoserine lactones ring in an S_N2 pathway rather than reduced the lactone (Scheme 3.16).



Scheme 3.16: Proposed mechanism of β-lactone ring opening

Thus, the sodium trimethoxyborohydride was added to a solution of diphenyl diselenide in dry ethanol under nitrogen atmosphere. The resultant yellow solution was stirred for 30 minutes before the β-lactone **1.46** in dry ethanol was added. The reaction mixture was stirred for a further 2 hours until completion. After aqueous work-up, the desired pure product was obtained in quantitative yield.

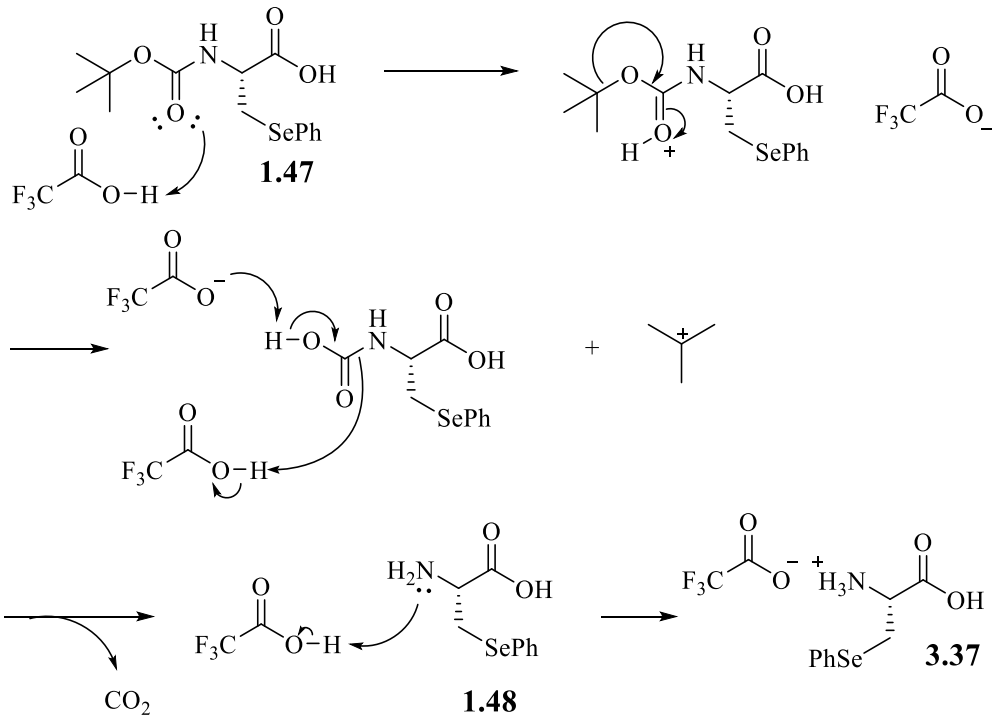
3.5.3 *N*-Boc Deprotection of Phenylselenocysteine



Scheme 3.17: *N*-Boc deprotection

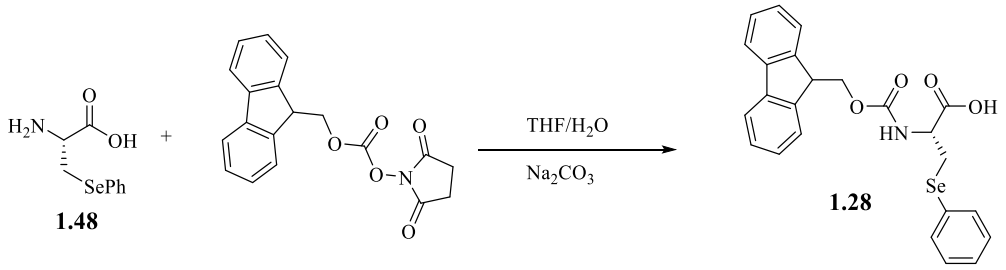
The resulting Boc-phenylselenocysteine is not suitable for Fmoc/*t*Bu SPPS of argyrin. Therefore, in order to obtain the Fmoc-protected phenylselenocysteine, the *N*-*tert*-butyl carbonyl protection group must be removed (Scheme 3.17). The Boc protecting group is stable under basic condition and is not reactive to most nucleophiles, but it can be removed under mild acidic condition. Several methods of selective removal of *N*-Boc protecting group in the presence of other function groups have been reported. The most adopted method is acidolysis using TFA in DCM or HCl in dioxane. The cleavage of *tert*-butyl carbamate under acidic condition generates a *tert*-butyl cation (Scheme 3.18). A butylation of *tert*-butyl cation with the product can occur. Addition of a scavenger, such as anisole, can be added to prevent the butylation.

Hence, the *N*-Boc-phenylselenocysteine was treated with a solution of 50% *v*/*v* TFA in DCM for 1 hours. The solution was evaporated and the resultant solid was triturated with diethyl ether to afford the TFA salt **3.37** of phenylselenocysteine in quantitative yield.



Scheme 3.18: Proposed mechanism of *N*-Boc deprotection

3.5.4 *N*-Fmoc Protection of Phenylselenocysteine



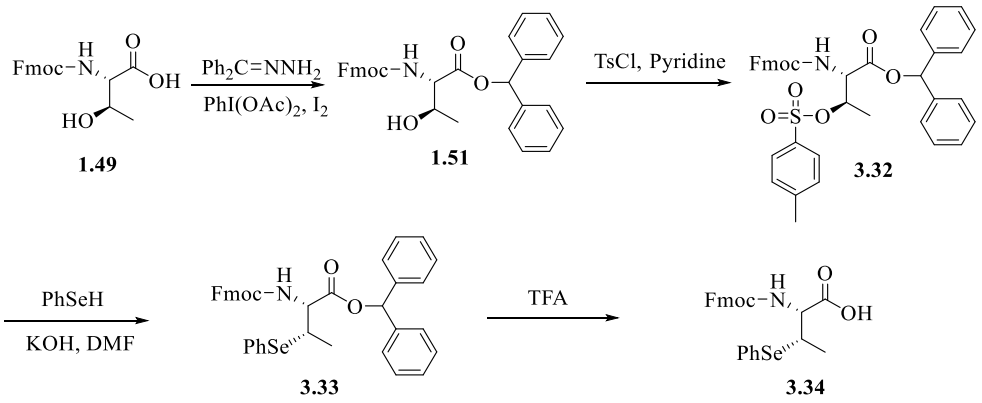
Scheme 3.19: *N*-Fmoc protection

The final step was the *N*-Fmoc protection of the phenylselenocysteine using Fmoc-OSu under basic conditions (Scheme 3.19). The reaction condition and proposed mechanism were discussed in the Chapter 2 (Scheme 2.43). The Fmoc-phenylselenocysteine was afforded in 80% yield. The product was characterised by NMR, HRMS, melting point and optical rotation.

3.6 Synthesis of Dehydrobutyrine and Dehydrophenylalanine

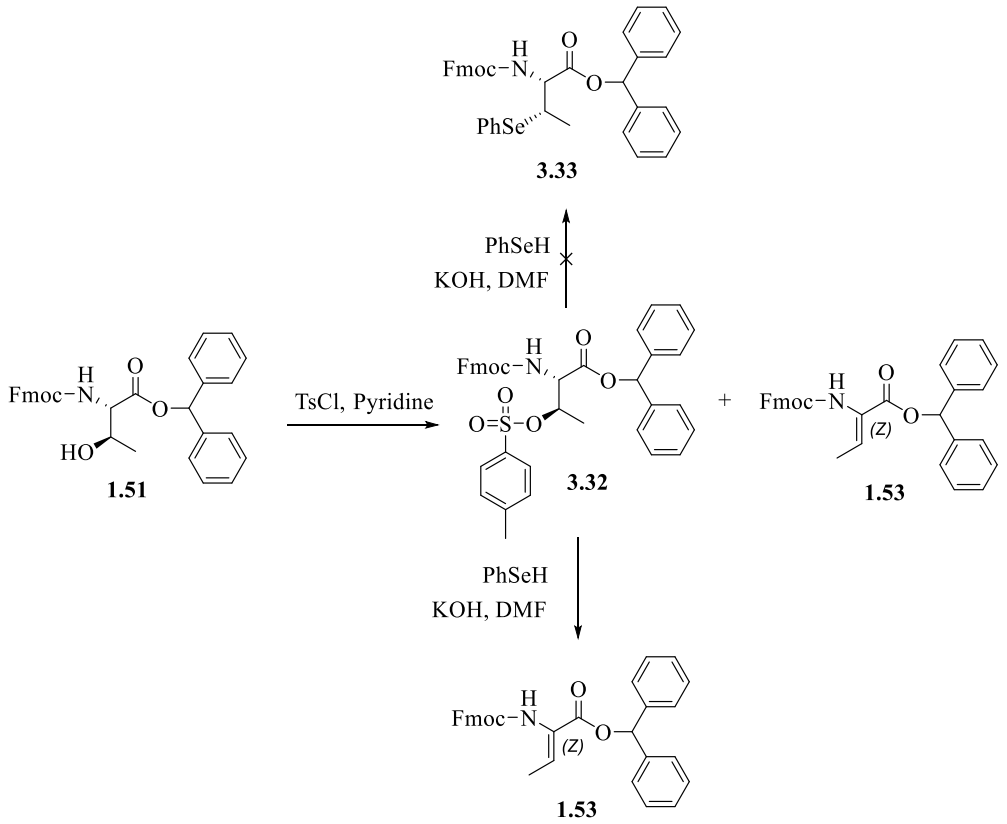
The synthetic route of obtaining Fmoc-(2*R*,3*S*)-3-methyl-*Se*-phenylselenocysteine for the synthesis of dehydrobutyrine-containing peptides reported by Van der Donk *et al*.[274] is adopted in this thesis. Firstly, the Fmoc-threonine **1.49** was protected as the diphenylmethyl (Dpm) ester **1.51**. The hydroxyl group of threonine was then activated with *p*-toluenesulfonyl chloride followed by the nucleophilic displacement of the tosyl group with phenylselenolate to generate the Fmoc-(2*R*,3*S*)-3-methyl-*Se*-phenylselenocysteine Dpm ester **3.33**. The Dpm ester deprotection using TFA afforded the desired free carboxylic acid Fmoc-(2*R*, 3*S*)-3-methyl-*Se*-

phenylselenocysteine **3.34** required for Fmoc/*t*Bu SPPS. The chemoselective conversion of the phenylselenide to (*Z*)-dehydrobutyrine was achieved by oxidation elimination with $NaIO_4$. The full synthetic procedure is outlined in Scheme 3.20.



Scheme 3.20: Van der Donk's approach for Fmoc-3-methyl-*Se*-phenylselenocysteine[274]

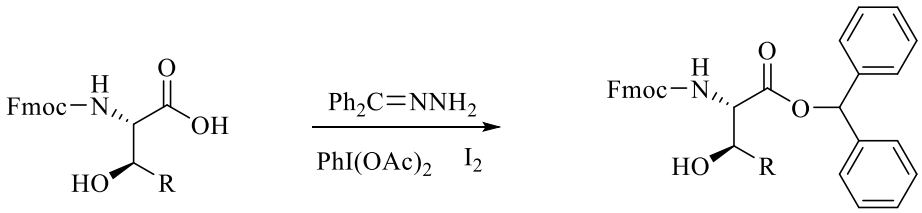
Hence, the method is adopted in this thesis to introduce the masked residue, Fmoc-3-methyl-*Se*-phenylselenocysteine, which will be used for the total synthesis of linear argyrin precursor analogues using Fmoc/*t*Bu SPPS strategy. The on-resin oxidation will be carried as described above followed by final macrocyclisation to afford the argyrin analogue. However, during conversion of the hydroxyl group to a tosyl group, the reaction resulted in the mixture of *O*-tosylate **3.32** and a by-product **1.53** in a ratio of 4:1 (Scheme 3.21). The by-product was predicted to be Fmoc-dehydrobutyrine Dpm ester **1.53** based on the β-elimination mechanism (described in the section 3.6.2). The ^{1}H-NMR and HR-MS confirmed the prediction. The *O*-tosylate product was applied for next step. A modified condition, which used diphenyl diselenide and sodium trimethoxyborohydride as reagent, was used for the phenylselenolate substitution reaction (Scheme 3.21). However, the final product was identified to be Fmoc-dehydrobutyrine Dpm ester. Such results might due to the usage of reducing agent sodium trimethoxyborohydride, which could cause a β-elimination reaction.



Scheme 3.21: Tosylation and phenylselenolate substitution reaction afforded **1.53**

Nevertheless, since a good amount of Fmoc-dehydrobutyrine Dpm ester was obtained, the Dpm ester deprotection was carried using TFA to afford the Fmoc-dehydrobutyrine **1.55**. The resulting Fmoc-dehydrobutyrine was applied directly to the Fmoc/*t*Bu SPPS. No degradation was found while analysing the resulting linear precursor. The Fmoc-dehydrobutyrine was found to be stable through the SPPS procedure. The details and results are discussed in Chapter 4. In conclusion, the synthetic route for masked residue, Fmoc-(2*R*,3*S*)-3-methyl-*Se*-phenylselenocysteine, can be modified for a direct synthesis of Fmoc-dehydrobutyrine. The reaction conditions are described in the section 3.6.1. Additionally, the Fmoc-dehydrophenylalanine was synthesised successfully using the same approach.

3.6.1 Carboxyl Group Protection by Diphenylmethyl Ester



1.49 R = Me
1.50 R= Ph

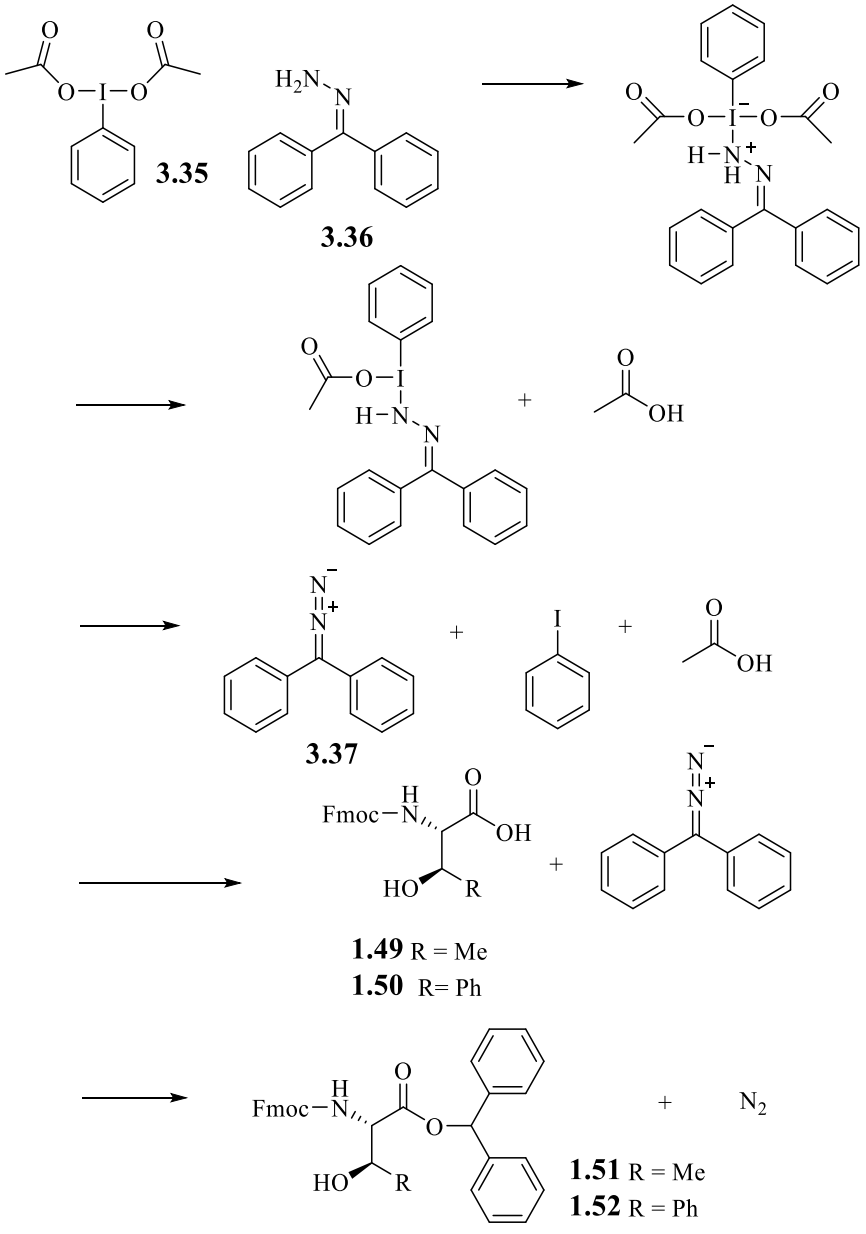
1.51 R = Me
1.52 R = Ph

Scheme 3.22: Carboxyl group protection by diphenylmethyl ester

The diphenylmethyl (Dpm) ester have been used as an alternative to *t*-butyl esters, methyl ester and benzyl ester in synthetic organic chemistry as protecting groups of carboxylic acids. The Dpm ester can be easily removed by acidolysis and hydrogenolysis. The use of Dpm esters of *N*-protected amino acids, especially of serine and threonine are widely used in peptide synthesis. In addition, the use of Dpm derivatives is well reported in the synthesis of sensitive compounds, such as penicillin and cephalosporins.

The introduction of such protecting group can be achieved through the reaction of carboxylic acids with diphenylmethyl phosphates, diphenyldiazomethane generated by oxidation of benzophenone hydrazine, or by the reaction of diphenylmethyl chloride with silver carboxylates. Among them, the alkylation properties of diphenyldiazomethane in aprotic solvents are well studied and have been used for the preparation of the diphenylmethyl esters of *N*-protected serine and threonine. Lapatsanis *et al*. reported that the *N*-protected serine and threonine could be alkylated by diphenyldiazomethane in ethyl acetate with hydroxy group not being affected (Scheme 3.22). The oxidation reagents they used were mercury(II) oxide, ozone or peracetic acid in the presence of a base. However, the commercial peracetic acid used during synthesis contains 39%

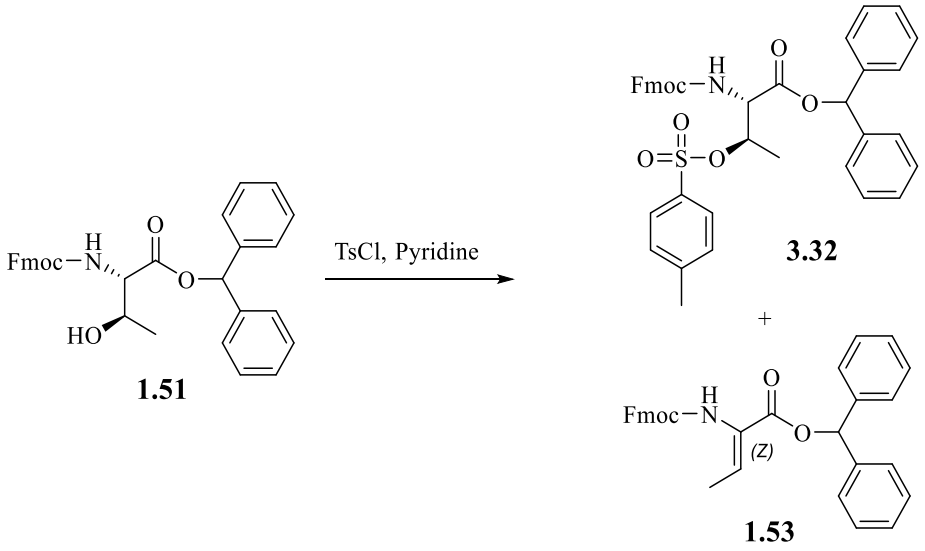
(*w*/*w*) acetic acid, which would participate in a competing reaction. Hence, they described a one-pot reaction by phenyliodine(III) diacetate **3.35** as an oxidizing agent. The phenyliodine(III) diacetate is a very efficient oxidizing agent, commercially available, stable and easy to handle. In a one-pot reaction, the benzophenone hydrazine **3.36** was oxidized by the iodobenzene diacetate to generate in situ the diphenyldiazomethane **3.37**. The carboxyl-group of, for example Fmoc-threonine, was proposed to be alkylated by the diphenyldiazomethane to yield the desired ester (Scheme 3.23).



Scheme 3.23: Proposed Dpm ester protection route

Hence, the Fmoc-protected amino acids (**1.49** and **1.50** as shown in Scheme 3.22) and benzophenone hydrazine were suspended in DCM. After addition of 1% (*w*/*v*) iodine in DCM, the suspension (purple in colour) was then cooled to -10 ºC. The crystalline phenyliodine(III) diacetate was then added over 45 minutes. The colour changed from purple to orange. The reaction was monitored by TLC. After completion, an aqueous based workup was applied to remove acetic acid and iodobenzene generated from the reaction. The Fmoc-threonine Dpm ester **1.51** was afforded by crystallization from petroleum ether (40–60 ºC) as a white solid in 80% yield. In contrast, the Fmoc-phenylserine Dpm ester **1.52** was not pure after crystallization, and hence it was purified through column chromatography to afford the desired product in 50% yield.

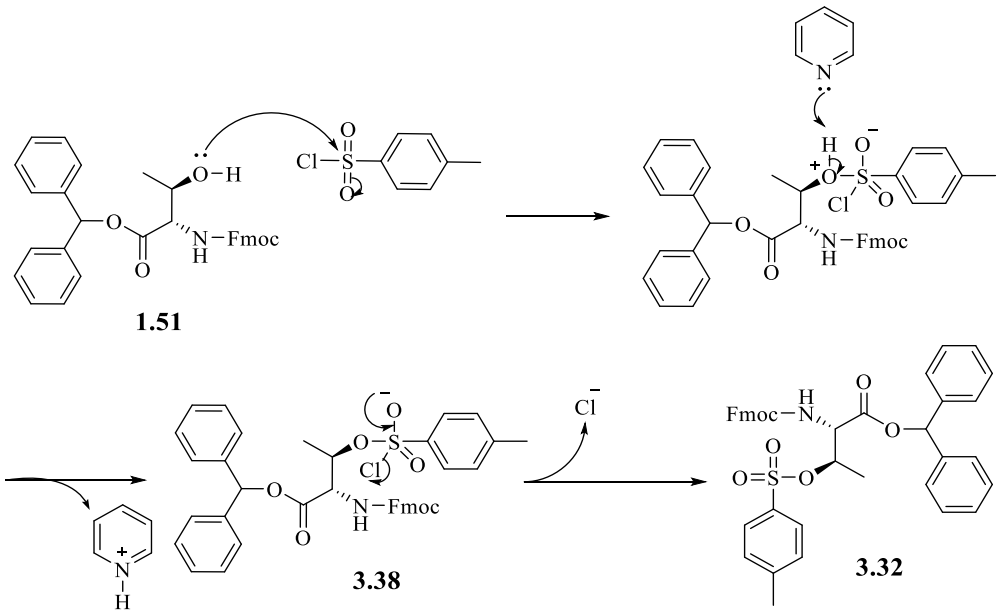
3.6.2 Conversion of Hydroxyl Group into a Tosylate Using Tosyl Chloride



Scheme 3.24: TsCl mediated tosylation leading to tosylate and dehydro by-product

The second step was the conversion of hydroxyl group into a tosylate using tosyl chloride and pyridine (Scheme 3.24). The resulting tosylate, which is a good leaving group, can be substituted by phenylselenolate in the next step. The most common sulfonates leaving groups are *p*-toluenesulfonyl (Ts) and methanesulfonyl (Ms). To be specific, the methanesulfonate is the conjugate base of methanesulfonic acid with pK_a of -2, and the *p*-toluenesulfonate is the conjugate base of *p*-toluenesulfonic acid with pK_a of -3, and therefore are excellent leaving group. The mechanism of such tosylation is illustrated in Scheme 3.25.

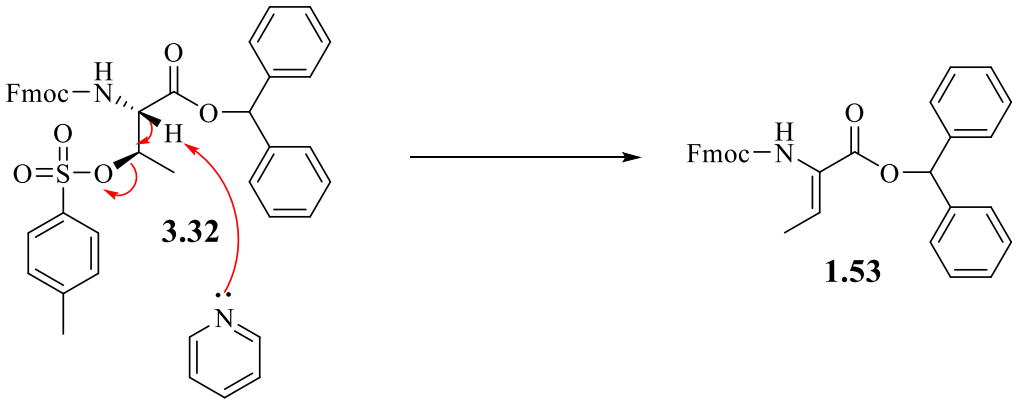
The reaction is usually carried out in the presence of a non-nucleophilic base, such as DIPEA, DBU or pyridine. Such weak non-nucleophilic base neutralizes the HCl generated by the reaction.



Scheme 3.25: Proposed mechanism of *O*-tosylation mediated by TsCl and pyridine

As mentioned above, the first attempt led to a mixture of *O*-tosylate and the dehydro derivative in a ratio 4:1. It was postulated that the *O*-tosylate might undergo an instant β-elimination under basic condition to form the dehydro derivative. The promotion of such elimination is anticipated to take place in the

presence of non-nucleophilic base and at high temperature. The more stable *Z*-isomer formed (Scheme 3.26).

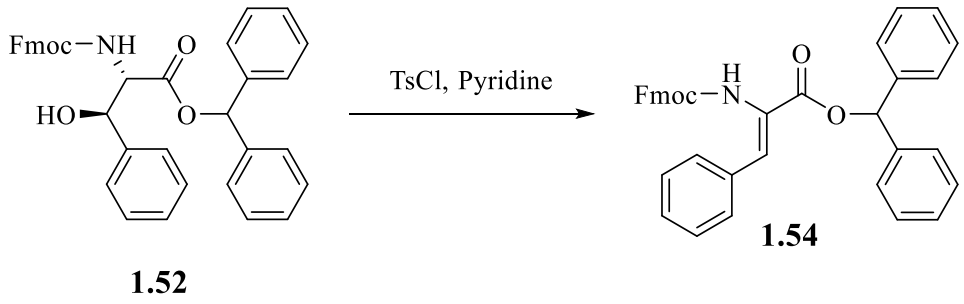


Scheme 3.26: Anticipated mechanism of pyridine mediated elimination

Therefore, the reaction condition was further investigated. The initial attempt was carried out at 5 ºC, which led to the formation of a by-product. Hence, the reaction temperature was maintained at -15 ºC, which afforded 10:1 ration of tosylate product and dehydro product, the yield of the tosylate product was 70%, while stirring at 23 ºC afforded a 1:1 ratio of tosylate product and dehydro product. The low temperature is considered to be important for the generation of tosylate product.

Nevertheless, the generation of the dehydro product **1.53** using such a method could be an alternative for the synthesis of Fmoc-dehydro amino acid building blocks. The generation of tosylate product is crucial for a successful dehydration based on the mechanism illustrated above.

Therefore, the TsCl was added to the starting material and pyridine mixture at -15 °C. After the starting material was fully converted to the tosylate (usually 2 days), the reaction was heated to 50 ºC to promote the dehydration step. The synthesis of **1.54** was carried out using the same condition (Scheme 3.27).

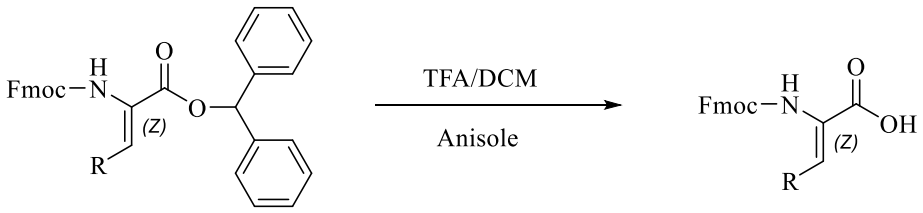


1.52 **1.54**

Scheme 3.27: Synthesis of **1.54**

After completion, an aqueous based workup was applied. The crude product was purified through column chromatography to afford the desired product. The yield of **1.53** and **1.54** were 50 %.

3.6.3 Dpm Ester Deprotection by TFA

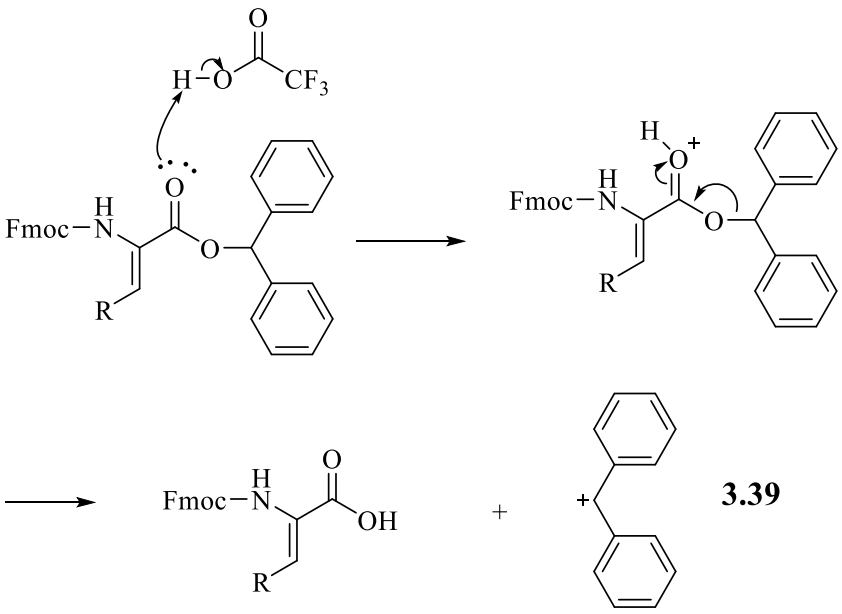


1.53 R = Me
1.54 R = Ph

1.55 R = Me
1.56 R = Ph

Scheme 3.28: Dpm ester deprotection by TFA

As mentioned above, the Dpm ester protecting group can be easily removed using acidolysis and hydrogenolysis without affecting the *N*-Fmoc protecting group. Various conditions, including refluxing in acetic acid, hydrogenolysis using H_2/Pd, stirring in HCl and refluxing in HCOOH have been developed. In this thesis, the deprotection of Dpm ester was carried out by acidolysis using TFA in DCM (Scheme 3.28). The mechanism is similar to the deprotection of *N*-Boc protecting group, which is illustrated in Scheme 3.29.



Scheme 3.29: Proposed mechanism of TFA mediate Dpm ester deprotection

However, the product generated was not pure, which was determined by TLC with 5% MeOH in DCM as eluent. The impurity might result from the formation of diphenyl methyl cation **3.39**. Hence, a scavenger, anisole, was added to the reaction. The addition of anisole to the TFA/DCM mixture afforded pure product.

Therefore, the Fmoc-dehydro amino acid Dpm ester was dissolved in DCM/TFA/anisole (20/16/4) and stirred at room temperature for 2 hours. After completion, the reaction solution was evaporated under *vacuo* and then triturated with diethyl ether to afford the desired product as a white solid. The products were identified using NMR, HRMS, RP-HPLC, and melting point. The quartet peak at 6.78 ppm in ^{1}H-NMR, assigned to the Fmoc-dehydrobutyrine indicated β-proton (Figure 3.5 in red). The doublet peak at 1.75 ppm in ^{1}H-NMR, assigned to the Fmoc-dehydrobutyrine indicated -CH_3 (Figure 3.5 in blue). The purity of both dehydroamino acids **1.55** and **1.56** (Figure 3.6) were determined using RP-HPLC for greater than 90 % pure. The RP-HPLC trace of Fmoc-dehydrobutyrine **1.55** is listed in the Figure 3.7 while the trace of Fmoc-dehydrophenylalanine **1.56** is listed in the Figure 3.8.

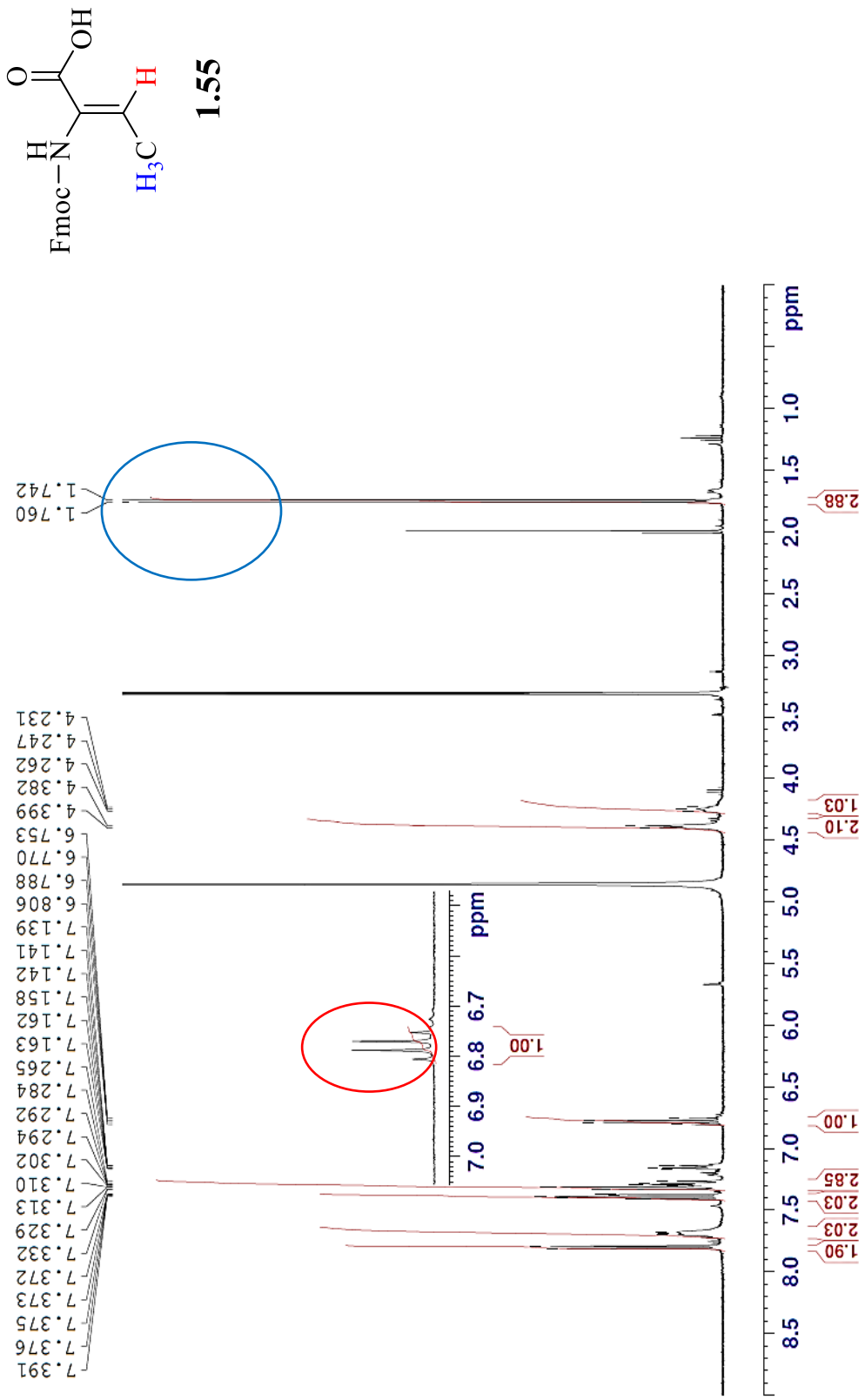
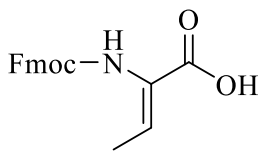
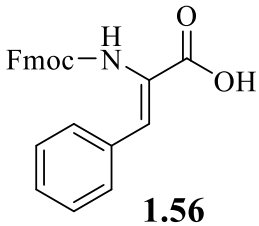


Figure 3.5: [1]H-NMR for Fmoc-dehydrobutyrine **1.55**

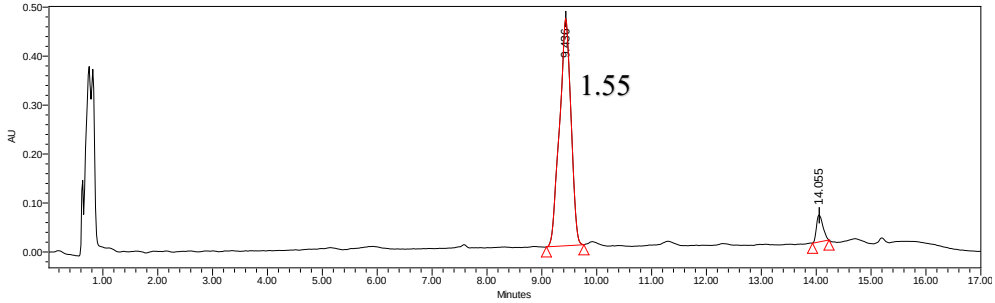


1.55



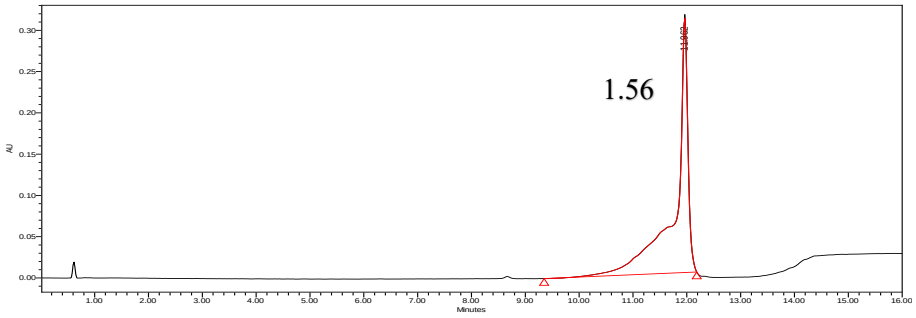
1.56

Figure 3.6. Fmoc-dehydrobutyrine **1.55** and Fmoc-dehydrophenylalanine **1.56**



	Retention time	Area	% Area
1	9.436	6719307	93.71
2	14.055	450770	6.29

Figure 3.7: RP-HPLC analysis of Fmoc-dehydrobutyrine **1.55**. Solvent system: 10–60% **B** in **A** over 12 min at 3 mL/min. (**A** = 0.06% TFA in water, **B** = 90% acetonitrile in water + 0.06% TFA). Column: Onyx Monolithic C_{18} (100 x 4.6 mm). Eluent was monitored at 216 nm.



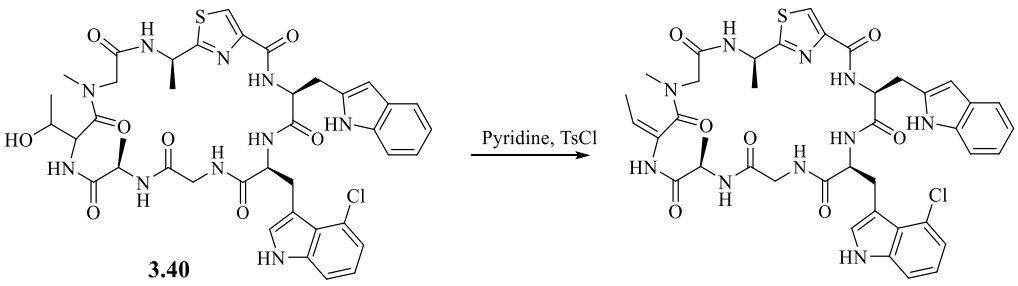
	Retention time	Area	% Area
1	11.962	5063610	100

Figure 3.8: RP-HPLC analysis of Fmoc-dehydrophenylalanine **1.56**. Solvent system: 10–60% **B** in **A** over 12 min at 3 mL/min. (**A** = 0.06% TFA in water, **B** = 90% acetonitrile in water + 0.06% TFA). Column: Onyx Monolithic C_{18} (100 x 4.6 mm). Eluent was monitored at 216 nm.

3.7 Applying an *O*-Tosylation Followed by Elimination for a Threonine-Containing Cyclic Peptide

The successful synthesis of dehydroamino acid using TsCl and pyridine mediated β-elimination encourages the application of such a method using a preformed cyclic peptide. The Fmoc-dehydro amino acids used are stable through Fmoc/*t*Bu SPPS procedure which will be discussed in the Chapter 4. However, the direct application of such method at a cyclic peptide level would avoid multiple-step synthetic procedures. In order to evaluate such a reaction, an argyrin analogue **3.40** containing threonine at the dehydroalanine position was obtained from Sivaneswary Genapathy. Such attempt has the advantage of using commercially available Fmoc-threonine rather than the synthesis of a masked residue.

The reaction (scheme 3.30) was stirred at -15 ºC and monitored by RP-HPLC. After two days, no conversion was observed. Different reaction conditions described in Table 3.1 were attempted with no observable chemical transformation.



3.40

Scheme 3.30: Application of pyridine and TsCl mediated elimination to a cyclic peptide

In summary, different bases and different temperatures were attempted. An alternative elimination method using MsCl in the presence of the triethylamine

and DMAP was tested. No tosylate intermediate was found. The starting material was recovered under all the above reaction conditions. The possible reasons are: (i) the argyrin macrocyclic structure shields the key hydroxyl-group of threonine, (ii) the polar side group of the cyclic peptide folds away from the organic solvent, and is therefore inaccessible to the reactants. In order to explore the effect of the solvent on the reaction outcome, water and DMF mixture was used. The addition of water may expose parts of the molecule to the reagent and solvent. However, no conversion was observed. The results indicated that under the condition outlined in Table 3.1, the synthesis of dehydrobutyrine containing cyclic peptide from the threonine containing cyclic peptide could not be achieved.

Temperature (ºC)	Solvent	Reagents	Sulfonate agent	Time (hours)	Conversion
-15	Pyridine	Pyridine	TsCl	48	0
R.T.	Pyridine	Pyridine	TsCl	48	0
55	Pyridine	Pyridine	TsCl	24	0
-15	DCM	Pyridine	TsCl	24	0
0	DCM	DBU (1 equiv.)	TsCl	24	0
0	DCM	DBU (5 equiv.)	TsCl	24	0
0	DCM	Triethylamine (2 equiv.)	TsCl	24	0
0-40	DCM	Triethylamine, DMAP (0.1 equiv.)	MsCl	24	0
0	DMF with 10% H_2O	Pyridine	TsCl	24	0

Table 3.1. Reaction conditions for the elimination

3.8 Conclusions

In conclusion, this chapter reviewed current synthetic methods, especially elimination reactions, for the synthesis of dehydroamino acids. Additionally, two classes of dehydroamino acids-containing antibiotics peptides, lantibiotics and thiopeptide, were reviewed. The conformational properties and chemical reactivity of dehydroamino acids make them attractive in terms of installing into argyrin. The dehydroalanine moiety of the argyrin could be replaced with various dehydroamino acid to enhance its antibacterial activity which will be discussed in Chapter 5.

This chapter also outlined the synthetic route to key building block, dehydrobutyrine, dehydrophenylalanine, and phenylselenocysteine required for the Fmoc/*t*Bu SPPS of argyrin analogues.

The preparation of *N*-Fmoc-phenylselenocysteine was accessed through a reported synthesis route from Okeley *et al* (Scheme 3.11). Commercially available *N*-Boc-L-serine was converted to a β-lactone ring through intramolecular Mitsunobu-type cyclisation. The ring opening was performed in the presence of diphenyl diselenide to afford the *N*-Boc-Sec(Ph), which was then converted to the *N*-Fmoc-Sec(Ph) required for the Fmoc SPPS.

The initial attempt for the synthesis of Fmoc-(2*R*,3*S*)-3-methyl-*Se*-phenylselenocysteine led to a direct β-elimination in the tosylation step to afford Fmoc-(*Z*)-dehydrobutyrine. Therefore, such method was modified and used directly for the successful synthesis of Fmoc-(*Z*)-dehydrobutyrine and Fmoc-(*Z*)-dehydrophenylalanine. Thus, the Fmoc-threonine and Fmoc-hydroxyphenylalanine were converted to the corresponding Dpm esters. The Fmoc-threonine and Fmoc-hydroxyphenylalanine Dpm esters then underwent a

β-elimination reaction mediated by TsCl and pyridine. In both cases, a tosylation intermediate was initially formed under low temperature, followed by a temperature-promoted β-elimination. The Fmoc-dehydroamino acid Dpm esters were then subjected to acidolysis using TFA/DCM/anisole to afford pure Fmoc-dehydroamino acids in good yields. The success application of Fmoc-dehydrobutyrine and Fmoc-dehydrophenylalanine for Fmoc SPPS will be described in Chapter 5.

Encouraged by the results of the TsCl and pyridine mediated Fmoc-dehydroamino acids synthesis, the method was applied to the threonine-containing argyrin analogue (Scheme 3.30). Various reaction conditions (Table 3.1) were attempted with failure. Moreover, no tosylation intermediate was discovered.

Chapter 4
Fmoc Solid-Phase Peptide Synthesis of Argyrin Analogues

In the previous two chapters, the synthesis of three key building blocks of argyrin, namely *N*-Boc-thiazole dipeptides, the Fmoc-L-tryptophans, and the dehydroalanine precursor Fmoc-phenylselenocysteine and Fmoc-dehydroamino acids were reported (Figure 4.1). With all these building blocks in hand, this chapter outlines the assembly of the required argyrin analogues. These argyrin analogues were selected in order to establish the effects of installed halogenated tryptophan and β-substituted α,β-dehydroamino acid residues on the antimicrobial activity.

As described in Chapter 1, Ley *et al*. first reported the total synthesis of argyrin B using the solution-phase fragments condensation strategy.[202] Two tripeptides and a dipeptide were synthesised, followed by removal of protection groups and coupling of three fragments to afford the linear heptapeptide. The macrocyclisation was achieved by deprotection of the two termini, followed by intramolecular cyclisation. The final unmasking of phenylselenocysteine gave a dehydroalanine residue to yield the argyrin B. This approach was adopted by

Nickeleit *et al.*[204] and Jiang *et al.*[203] for the total synthesis of other argyrin analogues. However, the overall method suffered from the following limitations: (1) not suitable for synthesis of multiple analogues; (2) time-consuming process; (3) purification required after each fragment coupling step.

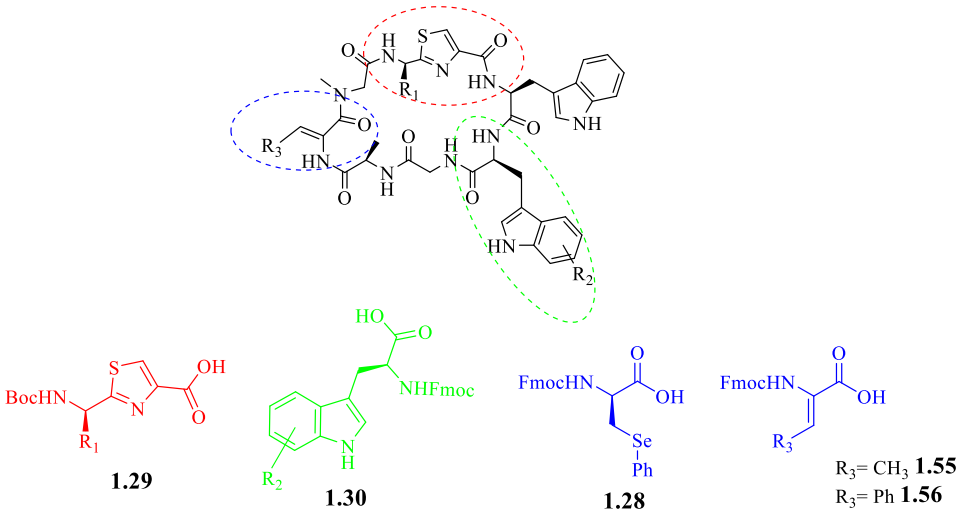


Figure 4.1. Key building blocks of argyrin

In order to enhance the synthesis efficiency and avoid laborious purification procedures after each condensation step, Chan and co-workers reported the first Fmoc/*t*Bu solid phase peptide synthesis (SPPS) of argyrins (Scheme 1.10).[205] This chapter starts with a brief introduction of Fmoc-SPPS. Next, the usage of Chan's method for the total synthesis of argyrin analogues is described. As mentioned in Chapter 3, the direct application of Fmoc-dehydroamino acids to the Fmoc-SPPS is discussed in this chapter.

4.1 Solid-Phase Peptide Synthesis

The past four decades saw the fast development of the chemical assembly of amino acids to form peptides. Two principle methods, solution and solid-phase,

are routine practice for chemists in the field of peptide chemistry. The classic synthesis in solution suffers from the disadvantages of time consuming, skill-intensive and unpredictable solubility of intermediates. Hence, Merrifield in 1963 developed an alternative approach, known as the solid phase peptide synthesis.[282] Comparing to the solution-phase peptide synthesis, the solid-phase peptide synthesis is of high efficiency at each coupling step. The excess reagents and by-products formed could be easily removed by washing and filtration. In recognition of the advantages and impact of this development, Merrifield was honoured with the Nobel Prize in Chemistry in 1984[283]. Table 4.1 gives an overview of important developments during the history of SPPS.

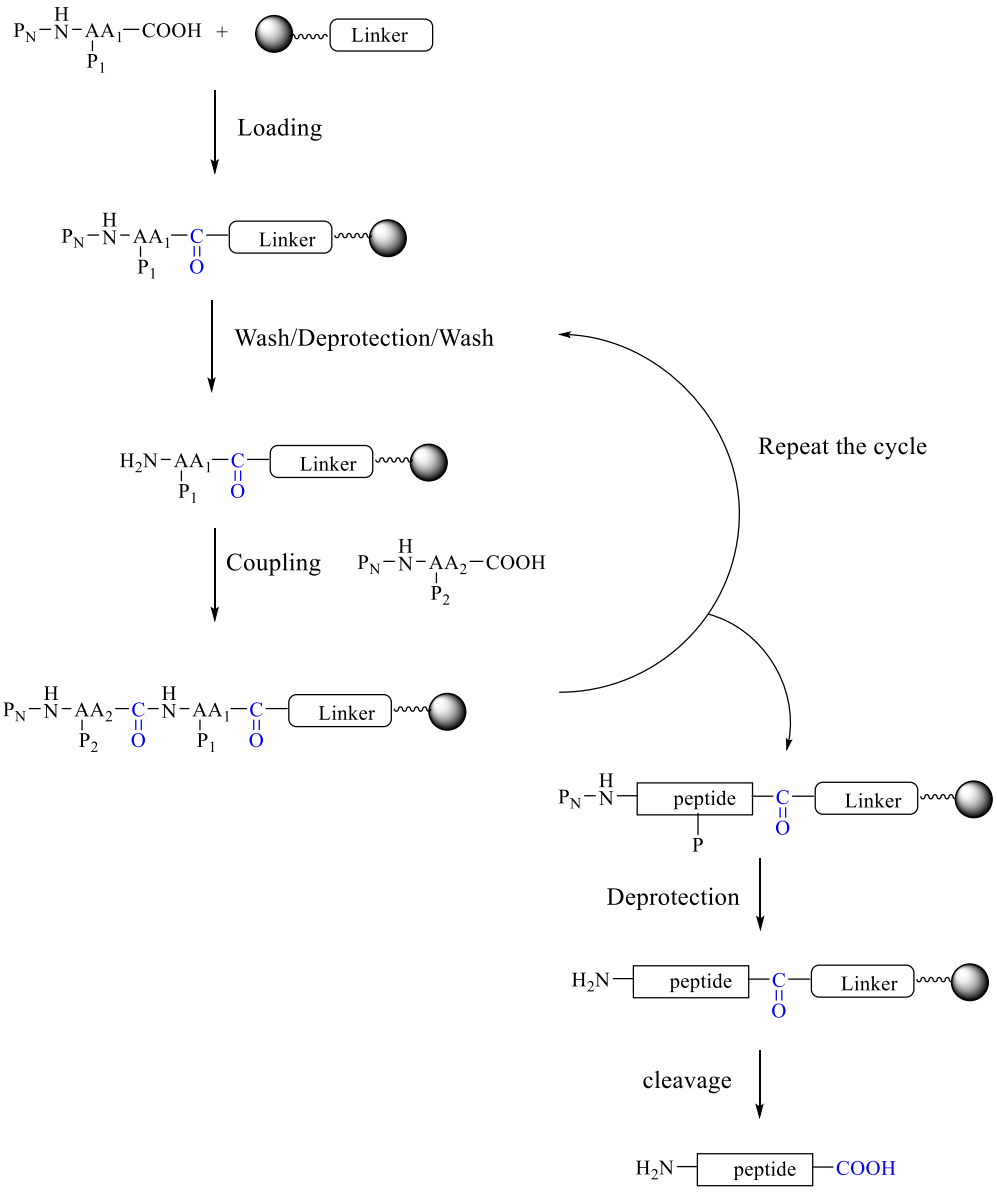
Year	Authors	Developments
1963	Merrifield	Development of SPPS on crosslinked polystyrene beads[282]
1964	Merrifield	*N*-protecting group: Boc[284]
1967	Sakakibara	HF cleavage[285]
1968		Automatic synthesiser
1970	Carpino & Han	*N*-protecting group: Fmoc[286]
1970	Pietta & Marshall	BHA-resin for peptide amides[287]
1973	Wang	Development of *p*-alkoxybenzyl alcohol resin (Wang resin); TFA Cleavage; *N*-protecting group: Bpoc[288]
1976	Burgus & Rivier	Preparative RP-HPLC for the purification of peptides prepared by Boc SPPS[289]
1977	Barany *et al.*	Development of the concept of 'orthogonal' protection scheme[290]
1978	Meienhofer *et al*	Fmoc/*t*Bu strategy using Wang resin[291]
1985	Houghten	Simultaneous parallel peptide synthesis;

	and others	synthesis of peptide libraries[292,293]
1987	Mergler *et al*.	Development of 2-methoxy-4-alkoxybenzyl alcohol resin SASRIN for Fmoc/*t*Bu SPPS[294]
1987	Rink	Introduction of various TFA-labile linkers for Fmoc/*t*Bu SPPS of peptide amide[295]
1987	Sieber	'Xanthenyl linker' for Fmoc/*t*Bu SPPS of peptide amide[296]
1988	Barlos *et al.*	2-chlorotritylchloride resin for Fmoc/*t*Bu SPPS of peptide amide[297]
1988		First commercial large-scale synthesiser
1992	Kent and Alewood	Fast Boc protocol[298]
1993	Hobbs de Witt, Ellman and others	Combinatorial Chemistry and solid phase organic synthesis for rapid synthesis of libraries of small peptide molecules[299]
1995	Mutter *et al*.	Pseudoproline dipeptides[300]
2002	Gogoll and others	Microwave-assisted SPPS[301]
2003	White and others	Long peptides (100 amino acids) by Fmoc protocols[302]

Table 4.1. Important developments during the history of SPPS

The general process for SPPS on a resin or solid support begins with the attachment of the first amino acid, the *C*-terminal residue (carboxyl group), to the resin. The α-amino acid *N*-terminus and reactive side-chain are protected with a temporary and semi-permanent protecting group to prevent polymerization. The carboxyl group of the first amino acid must be activated for its coupling to the resin. Once the first amino acid is attached to the resin, the resin is filtered and washed to remove the excess reagents and by-products. After that, the N^{α}-protecting group is removed and the resin is washed again to remove the excess reagents and by-products. The next amino acid is coupled to

the attached amino acid, followed by another washing process. Then, the resin with peptide is ready for the next coupling cycle. The cycle repeats from *C*-terminal residue (carboxyl group), then proceeding with the peptide sequence construction to the *N*-terminal end. Typically, the protecting groups are removed before the resin is washed and the peptide is cleaved from the resin. Scheme 4.1 demonstrates the process.



Scheme 4.1. General process of SPPS

The side chains of many amino acids are reactive and may form side-products during synthesis. Hence, these side chains must remain protected despite repeated exposure to N^{α}-deprotection conditions. Consequently, the N^{α}-protecting groups and the side-chain protecting groups should be deprotected under completely different conditions. Such a protection scheme is named 'orthogonal' protection. There are two principle protecting strategies in SPPS, Merrifield's Boc/Benzyl (Boc/Bzl) approach[282] and Sheppard's fluorenylmethyloxycarbonyl/*tert*-Butyl (Fmoc/*t*Bu) approach[303].

For the first 25 years, the majority of SPPS efforts employed the Boc/Bzl approach, which is based on a system of graduated acid lability. In Boc/Bzl approach, TFA is used for iterative deprotection of the Boc protecting group from N^{α} functionality, while the side-chain benzyl-based protecting group and final cleavage from resin is achieved simultaneously by a much stronger acid, anhydrous hydrogen fluoride (HF).[285] The HF is highly toxic and requires extensive safety protection, i.e. full-face shield in conjunction with goggles. The repeated treatment with TFA may also degrade sensitive peptide sequences. In order to prevent the usage of HF for the final deprotection, the Fmoc/*t*Bu approach was developed. This approach differs from the Boc/Bzl approach in that N^{α} protections and side-chain protections are based on the orthogonality described above. In Fmoc/*t*Bu approach, 20% *v/v* piperidine in DMF is applied to remove N^{α}-Fmoc protecting groups while the side-chain *t*Bu or the *trityl* (triphenylmethyl) protecting groups and peptidyl cleavage from resin are achieved simultaneously using TFA. The Fmoc/*t*Bu approach is generally preferred over the Boc/Bzl approach for routine synthesis because of the mild deprotection and cleavage conditions.[304] The progress of each coupling and deprotection can be monitored with the help of real time spectrophotometry which detects excess reagents and the dibenzofulvene-piperidine adduct. The main characteristics of the two approaches are summarised in Table 4.2.

	Fmoc/*t*Bu	**Boc/Bzl**
Application	Routine synthesis	Special equipment required
***N*$^{\alpha}$/side chain protection**	Orthogonal	Acid labile
Final cleavage	TFA treatment in SPPS vessel	HF treatment in special equipment
Automation	Yes	Yes
Scale	Any scale	Limited scale of HF cleavage
Monitoring	UV-absorption, chromophores: Fmoc, dibenzofulvene-piperidine adduct	Ninhydrin test
Synthetic steps	Deprotection, wash, couple, wash	Additional neutralization step
Diketopiperazine formation avoiding	Synthesis on 2-chlorotrity resin,	Neutralization or concomitant coupling
Special application	Acid sensitive peptide, such as sulfated peptides or O-glycosylated peptides	Aggregation impeded by repetitive TFA treatment, base sensitive peptides

Table 4.2: Main characteristics of Fmoc/*t*Bu and Boc/Bzl approaches

4.1.1 Resins and Linkers

The resin, also known as solid support, is an insoluble polymeric material that swells in organic solvents. The resin is usually functionalised with a linker (handle), which is a chemical moiety used to attach an amino acid to a resin

bead. The nature of the linker determines the chemistry to be used, and the conditions for the products to be cleaved or released from the resin. The overall physical properties and peptidic utility of the solid support are determined by the polymeric material and the type of linker. The success of SPPS is highly dependent on the selective of resin and linker, which is based on the desired peptide sequence and Fmoc/*t*Bu or Boc/Bzl strategy employed.

The ideal characteristic of the resin for efficient SPPS includes, chemical inertness to reaction solvents, ability to swell in the reaction solvents, and highly efficient attachment of the first amino acid. The swelling factor is important in SPPS, since reaction kinetics are diffusion controlled. Consequently, resins that swells more will have a higher diffusion rate of reagents into the core of the matrix leading to shorter reaction times and higher synthetic efficiency. The most commonly used polymeric solid supports are core matrices comprised of polystyrene, polyacrylate, polyacrylamide, and polyethylene glycol (PEG).[305] The majority of polystyrene resins contain 1% to 2% divinylbenzene (DVB)[282] as a cross linking agent, which is insoluble in most commonly used solvents. Typically, these resins are prepared and used as small, spherical beads of two different sizes: 100-200 mesh (75-150 μm) and 200-400 mesh (35-75 μm). The first polystyrene solid support developed by Merrifield is a polystyrene resin cross-linker with 2% divinylbenzene (PS-DVB).[282] The hydrophobic resin is free-flowing, powder-like consistency when dry, and facile swelling in most organic solvents. However, the efficiency of PS-DVB is affected by the length of peptide and particular amino acids used. Additionally, Merrifield discovered that the swelling of the unloaded resin was higher in DCM than in DMF. Hence, frequently DMF-DCM mixture solvent system is used for SPPS with PS resin in the first coupling while DMF is used in the rest coupling.[306]

Later, continuous-flow synthesiser assisted SPPS method was developed. In this method, the resin swelling should remain constant. Therefore, a hydrophilic

resin, polyethylene glycol-polyacrylamide (PEGA) resin[307] was developed, the swelling of which changes negligibly over synthesis due to it high initial polarity. PEGA resin is a cross-linked, amine functionalized ternary copolymer containing only secondary amide and ether bonds, resulting in high hydrophilicity and is inert to most peptide synthesis conditions.

An alternative strategy for enhancing resin swelling in polar solvents, as well as for maintaining consistent swelling during peptide synthesis, is the attachment of polyethylene glycol (PEG) chains onto a PS-DVB resin. Such hydrophilic chains are typically terminated with pendant amino groups that can be functionalized with a linker. This modification results in an increased swelling compared to PS-DVB in most organic solvents, and particularly in the polar aprotic solvents (such as DMF and acetonitrile) used for SPPS.[308] The length and the sterically unhindered nature of the PEG chain, which links the peptide chain and the polystyrene resin backbone, results in a more 'solvent-like' environment for resin-bound peptide.

A wide variety of linkers for polystyrene core resin have been developed. The linkers in SPPS provide a reversible connection between the peptide chain and the resin, as well as protect the *C*-terminal carboxyl group. The linkers are designed to be stable through the SPPS process, and under appropriate chemical conditions would result in the release of the peptidic product from the solid support. Different linkers are applied for Fmoc/*t*Bu and Boc/Bzl SPPS strategy because of the different chemical conditions used for the N^{α}-deprotection. Most commercially available resins for Fmoc/*t*Bu strategy come with linker pre-loaded.[309] Table 4.3 below listed some of the most popular resin with different linkers with the particular cleavage conditions and the final *C*-terminal functionalization.

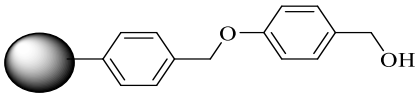
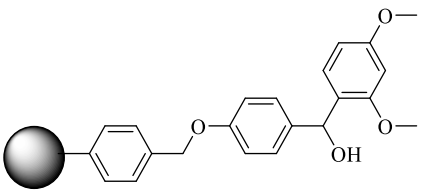
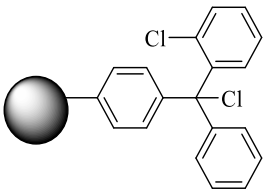
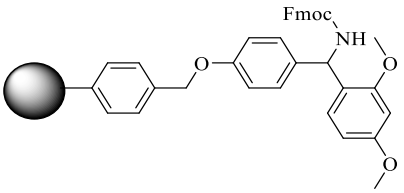
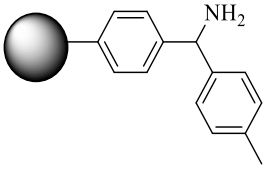
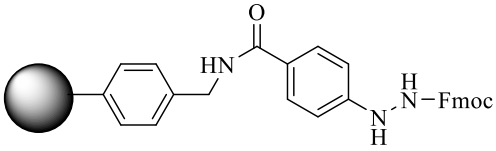
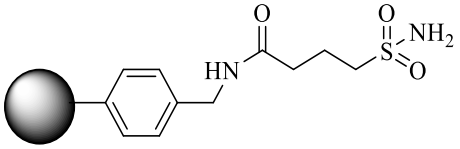
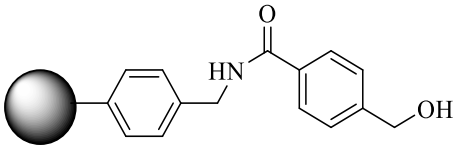
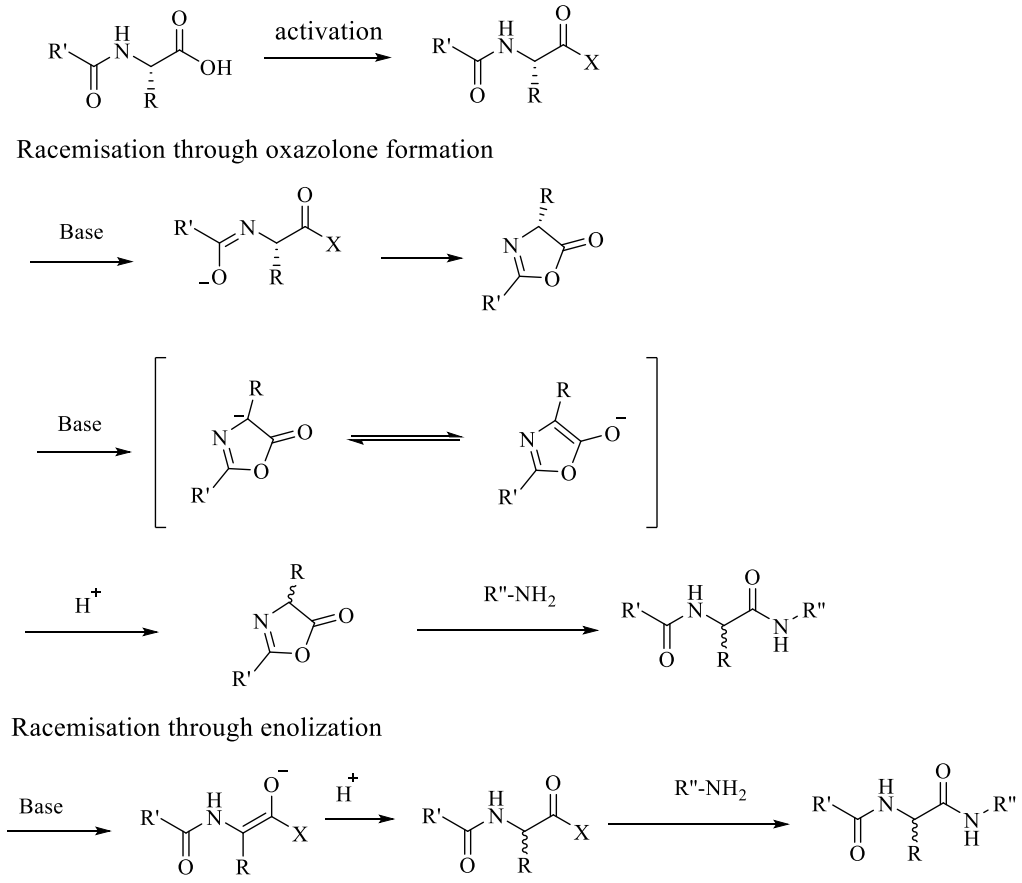
Resin name	Resin structure	Peptide product
Wang resin		Acid
Rink acid resin		Acid
2-chlorotrityl chloride resin		Acid
Rink amide resin		Amide
MBHA resin		Amide
Hydrazine resin		Acid, ester, amide
Sulfonamide resin		Acid, ester, thioester, amide
HMBA resin		Acid, hydrazide, amide, ester, alcohol

Table 4.3: Different resins for SPPS

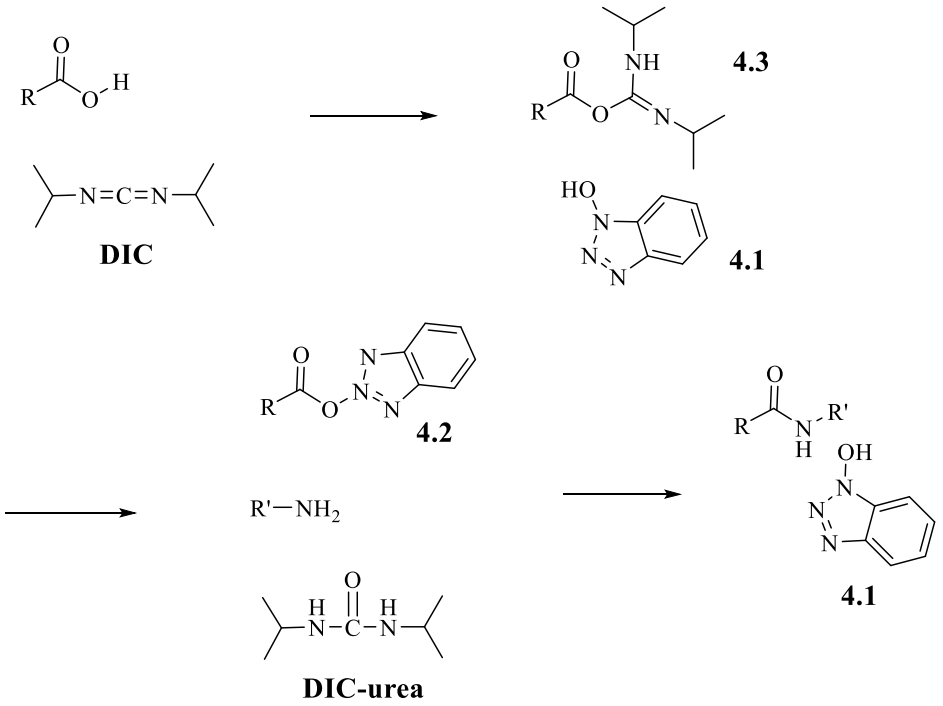
4.1.2 Activation of the Carboxyl Group of the Amino Acid

The coupling of an amino acid to the N-terminal of the proceeding amino acid residue of the resin-bound peptide chain is important part of the SPPS cycle. The rate and yield of the reaction are influenced by the choice of solvents, the steric hindrance of amino acids, and the reactivity of the activated carboxylic acids. The activation of carboxyl group of the amino acid is usually achieved through increasing electrophilicity of the carbonyl group by replacement of the hydroxyl with electron withdrawing group. The ideal carboxyl-activating reagents should have good solubility in common organic solvents at a high concentration, and suppress racemisation caused by oxazolone formation or direct enolization of the resultant activated amino acids (Scheme 4.2).[309]



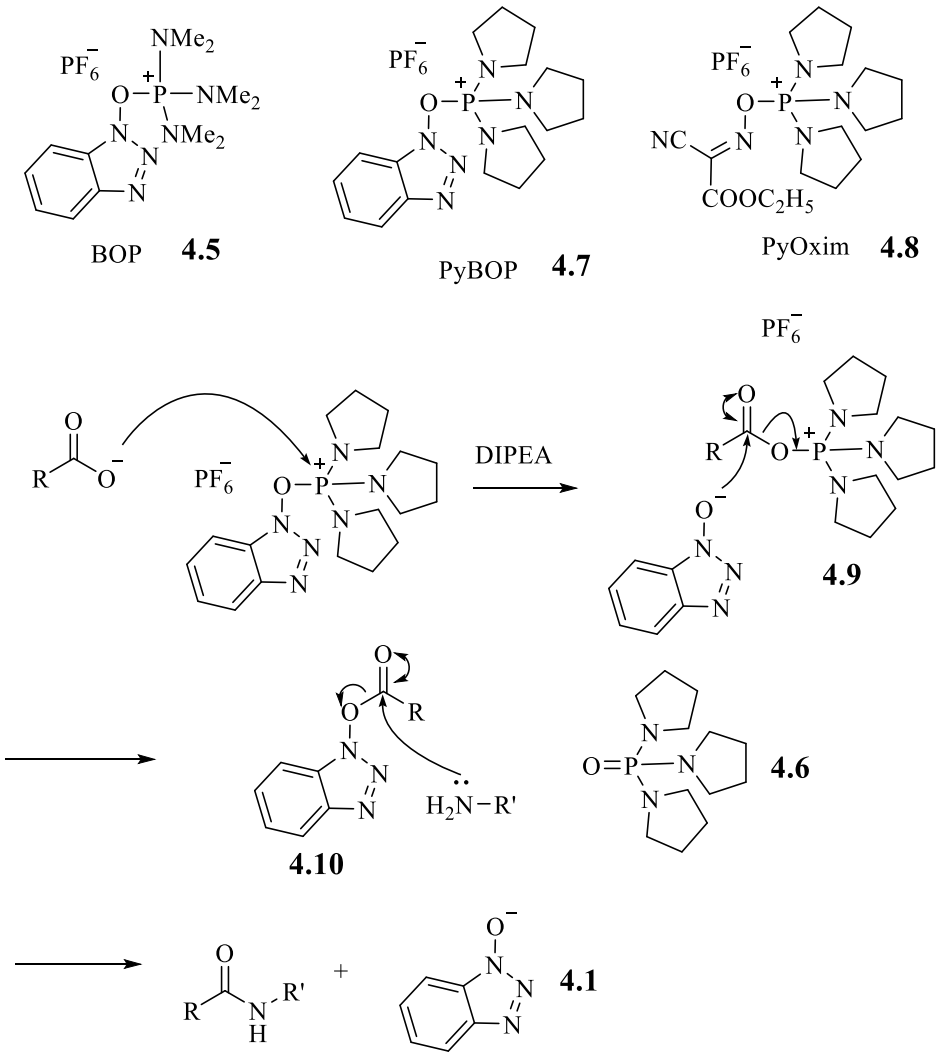
Scheme 4.2: Racemisation through oxazolone formation and enolization

The *N,N*'-dicyclohexylcarbodiimide, DCC **2.20**, was first used by Sheehan *et al.* as the carboxyl activation for the formation of peptide bonds.[310] The reaction was performed in DCM[311], and the by-product dicyclohexylurea **2.23** formed from DCC was nearly insoluble in most organic solvents. Therefore, DCC is suitable for solution phase reaction, but not for solid phase. Instead, *N,N*'-diisopropylcarbodiimide (DIC) is used in solid phase synthesis as the urea by-product is generally more soluble in some organic solvents. However, the racemisation process described above was observed, because the *O*-acylisourea formed is very reactive causing loss of chiral integrity of the amino acid. Later, the addition of 1-hydroxybenzotriazole (HOBt) **4.1** minimised the problem, because the corresponding benzotriazolyl ester **4.2** was less reactive, more stable and less prone to racemisation than the *O*-acylisourea **4.3** (Scheme 4.3).[311]



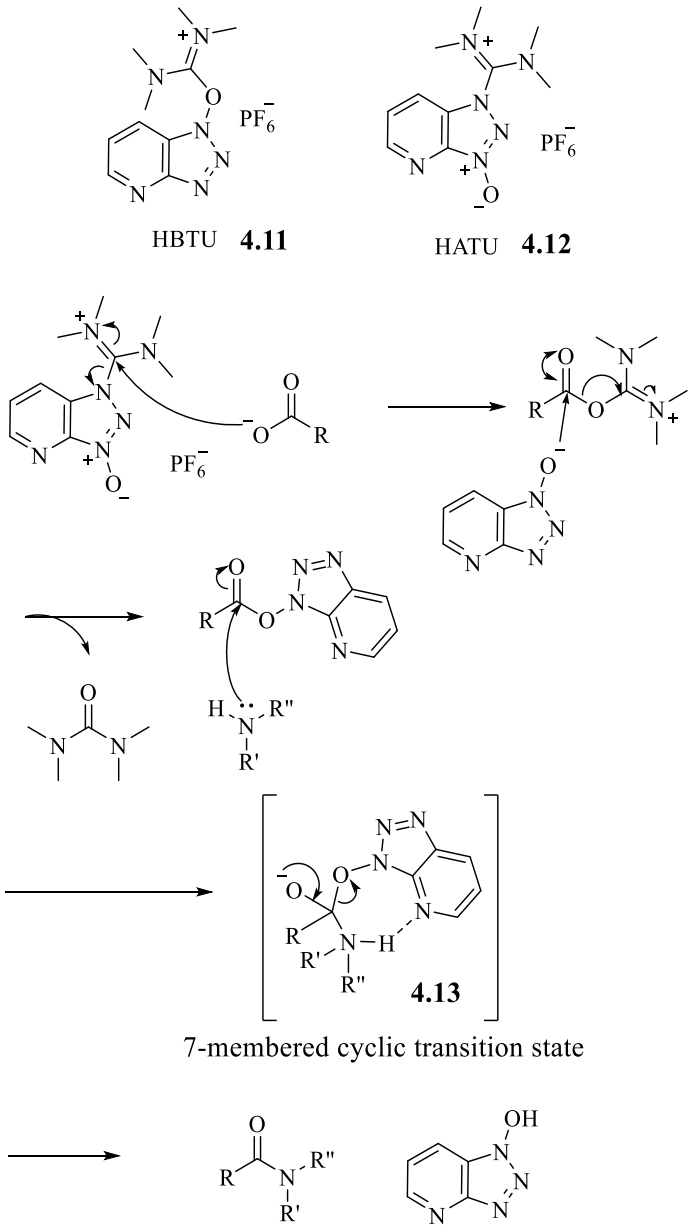
Scheme 4.3: Proposed DIC and HOBt **4.1** mediated peptide bond formation reaction

In 1975, based on HOAt **4.4** and HOBt **4.1**, Castro *et al*. developed the phosphonium-based coupling reagent, benzotriazol-1-yloxy-tris(dimethyl-amino)phosphonium hexafluorophosphate (BOP) **4.5**.[312] Although the BOP is proved to be an excellent coupling reagent, causing minimal racemisation, its by-product, hexamethylphosphoramide (HMPA) **4.6** is highly toxic.[313] In order to overcome this hazard, benzotriazole-1-yl-oxytripyrrolidinophosphonium hexafluorophosphate (PyBOP) **4.7** and (ethylcyano(hydroxyamino)acetate)-tri-(1-pyrrolidinyl)phosphonium hexafluorophosphate (PyOxim) **4.8** were developed.[314] The PyBOP and PyOxim are easy to handle and display high efficiency for the coupling of sterically hindered amino acids. (Scheme 4.4)



Scheme 4.4: The three phosphonium reagents and proposed mechanism of PyBOP mediated carboxyl-activation

The carboxylate anion attacks the phosphonium cation yielding a highly reactive acyloxyphosphonium intermediate **4.9**, which undergoes a nucleophilic attack by the hydroxybenzotriazole anion to generate the activated benzotriazolyl ester **4.10**. After that, a peptide bond is formed by a nucleophilic acyl substitution with an amine. The use of phosphonium reagent avoids the guanidation occurring from unreacted reagents with free amino acids, resulting in the termination of peptide chain assembly (Scheme 4.4).[312]



Scheme 4.5. Structure of HBTU and HATU; proposed mechanism of HATU mediated carboxyl activation

In 1978, Gross *et al*. developed the first aminium reagent, *N*-[(1*H*-benzotriazol-1-yl)(dimethylamino)methylene]-*N*-methylmethanaminium hexafluorophosphate *N*-oxide (HBTU) **4.11**.[315] After that, *N*-[(dimethylamino)-1*H*-1,2,3-triazolo[4,5-*b*]pyridine-1-ylmethylene]-*N*-methylmethanaminium hexafluorophosphate *N*-oxide (HATU) **4.12**, which shows high reaction rate with less epimerization during coupling, was developed. HATU is preferred over HBTU in most protocols due to the anchimeric assistance of the 7-pyridine nitrogen atom in the azabenzotriazole moiety, which stabilises the amino acid through a proton bound 7-membered cyclic transition state **4.13** (Scheme 4.5).[316,317]

4.2 Total Synthesis of Argyrin Analogues Using Fmoc/*t*Bu SPPS

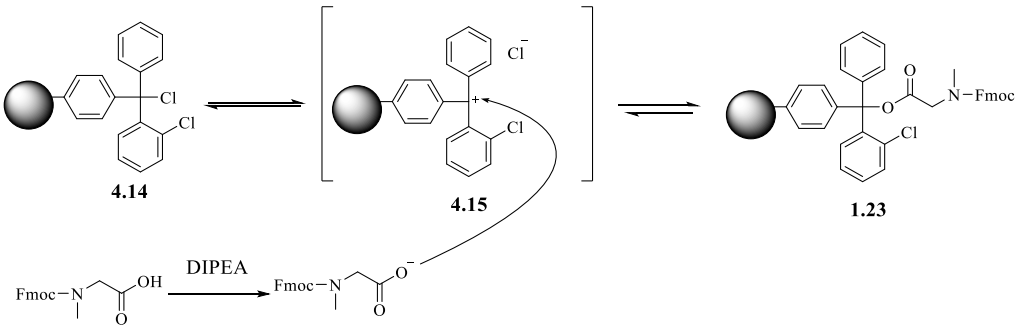
A linear argyrin precursor was synthesised through Fmoc/*t*Bu SPPS followed by solution-phase macrocyclisation to afford the argyrin analogues. A head-to-tail (*C*- to *N*-terminus) cyclisation is required for the synthesis of argyrin. The sarcosine was selected as the *C*-terminal end. This is based on: (1) sarcosine is an achiral amino acid, hence epimerisation during backbone macrocyclisation is avoided; (2) sarcosine is a non-sterically hindered residue that could facilitate cyclisation; (3) the N^{α}-Boc-protected thiazole dipeptide building block could be used without the need to replace with. N^{α}-Fmoc-protected thiazole dipeptide. The N^{α}-Boc can be simultaneously removed during the acidolytic cleavage of the fully assembled peptide from the resin.

Together with all the necessary amino acid building blocks, including the three building blocks described in Chapter 2 and 3, the linear argyrin precursors were assembled through Fmoc/*t*Bu SPPS. The unmasking of the phenylselenyl group

to afford dehydroalanine residue was discussed, as well as the direct application Fmoc-dehydroamino acids in peptide assembly.

4.2.1 Resin Loading: Attachment of Fmoc-Sarcosine

The hyper acid-labile 2-chlorotrity chloride polystyrene **4.13**, was selected as the solid support for the synthesis of linear argyrin precursors. The choice of such resin is based on the peptide acid released on acidolysis. The acidolysis of 2-chlorotrityl resin could be carried out under very mild conditions (1–5% TFA in DCM) because of the high stability of resultant trityl cation.[318] In addition, the weak electrophile trityl cation does not undergo alkylation side reaction.[319]

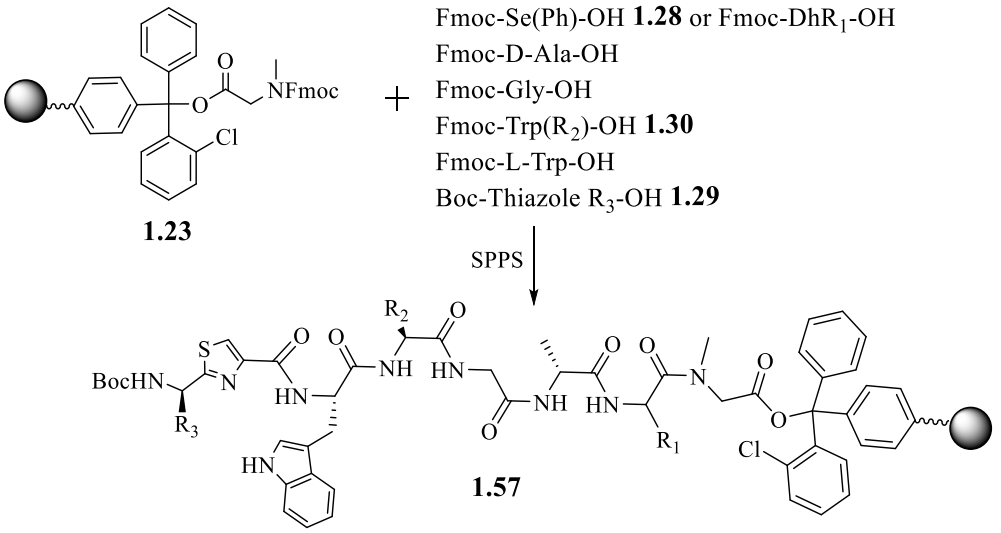


Scheme 4.6: Esterification of 2-chlorotrity chloride resin with Fmoc-Sar-OH

The loading of the *C*-terminal amino acid, Fmoc-sarcosine-OH, to the resin **4.14** was performed in the presence of DIPEA in DCM at room temperature. The coupling undergoes an S_N1 mechanism. In DCM, 2-chlorotrity chloride undergoes heterolysis to afford an equilibrium mixture of the chloride anion and the 2-chlorotrity cation **4.15**. The carboxylate of sarcosine attaches the stabilised tertiary carbocation to form the ester bond. Thus, the 2-chlorotrity chloride resin was swollen in DCM for 2 hours before the addition of stoichiometric amount of Fmoc-Sar-OH and 2 equivalents DIPEA. The reaction mixture was stirred at room temperature for 3 hours, after which the reaction mixture was quenched

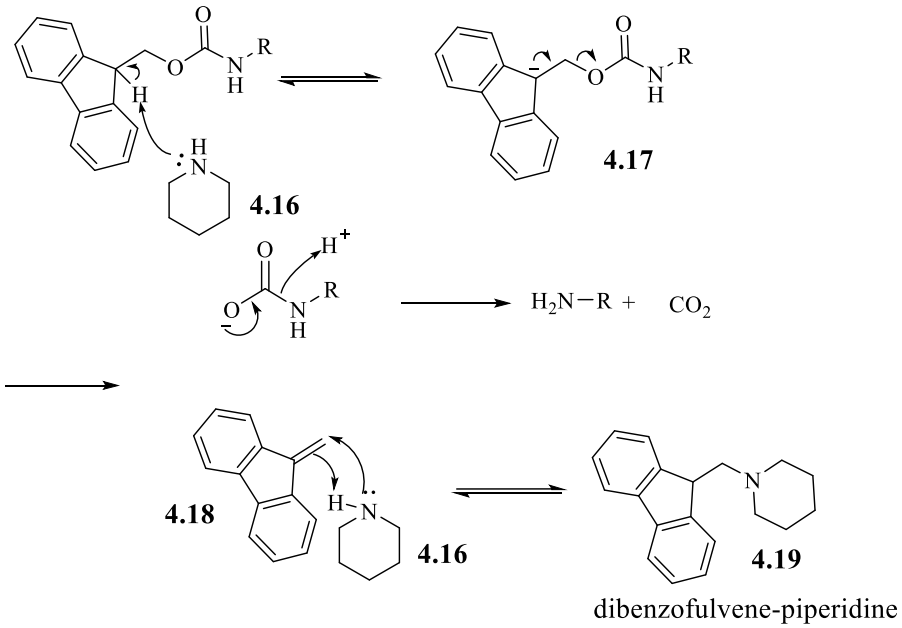
by a small amount of MeOH. The resin was collected, dried and the loading was determined before storage. The efficiency of loading was greater than 65%, based on the theoretical loading as described in Chapter 7. The dried loaded resin is re-swollen in a suitable solvent before usage.

4.2.2 Peptide Assembly



Scheme 4.7: Argyrin linear peptide precursors assembly

The assembly of linear argyrin precursors started from the resin-bound Fmoc-sarcosine (Scheme 4.7). The resin was swollen in DMF/DCM 1:1 overnight before the Fmoc-deprotection of Fmoc-sarcosine was carried out under 20% *v/v* piperidine **4.16** in DMF in a semi-automated peptide synthesiser. The mechanism of Fmoc deprotection using piperidine is antipicated to be an E1cB reaction, and is illustrated in Scheme 4.8. The base removes the acidic fluorenyl proton to form the stable dibenzocyclopentadienyl anion **4.17**. Dibenzofulven by-product **4.18** was then generated through the elimination of the carbamic acid. The dibenzofulvene then reacts with piperidine to form a strong UV-absorbing dibenzofulvene-piperidine **4.19** adduct, which allows the monitoring of the Fmoc-deprotection with a spectrophotometer at 290 nm.

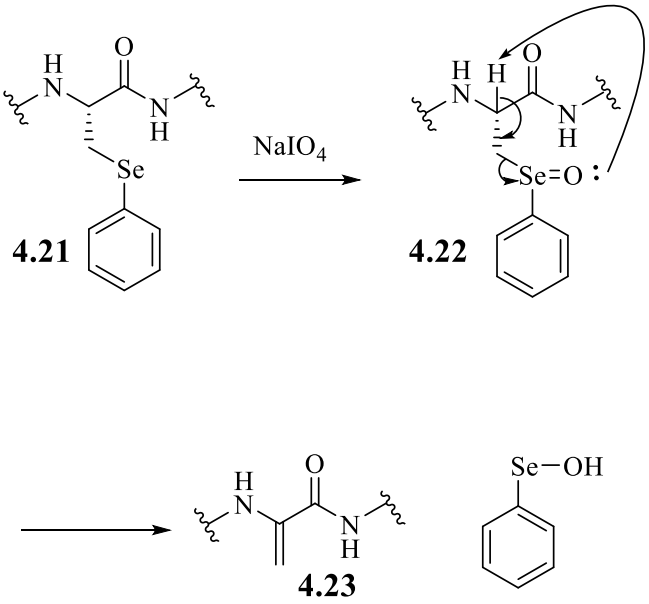


Scheme 4.8: Proposed mechanism of *N*-Fmoc deprotection with piperidine and formation of dibenzofulvene-piperidine **4.19**

After the Fmoc-deprotection of *C*-terminal sarcosine, the stepwise coupling of the N^{α}-Fmoc protected amino acids in the sequence was achieved in the same manner as shown in Scheme 4.7. For the commercially available *N*-Fmoc amino acids, such as Fmoc-(*R*)-Ala-OH, Fmoc-Gly-OH and Fmoc-Trp-OH, each coupling reaction was carried out using the mixture of *N*-Fmoc amino acid (4 equiv.), activating reagent HATU (3.9 equiv.) and DIPEA (8 equiv.), while the synthesised building blocks was carried out using the mixture of *N*-Fmoc amino acid (2 equiv.), activating reagent HATU (1.9 equiv.) and DIPEA (4 equiv.). The N^{α}-Fmoc amino acid were pre-activated in the presence of HATU and DIPEA in DMF, in order to avoid the reaction of HATU with free amino group of the growing peptide to form the substituted guanidines. After the final coupling, the peptidyl-resin with Sec(Ph) residue was subjected to on-resin oxidative elimination to afford the DhA residue while the peptidyl-resin with dehydroamino acids was cleaved from resin for cyclisation.

4.2.3 Oxidative Elimination

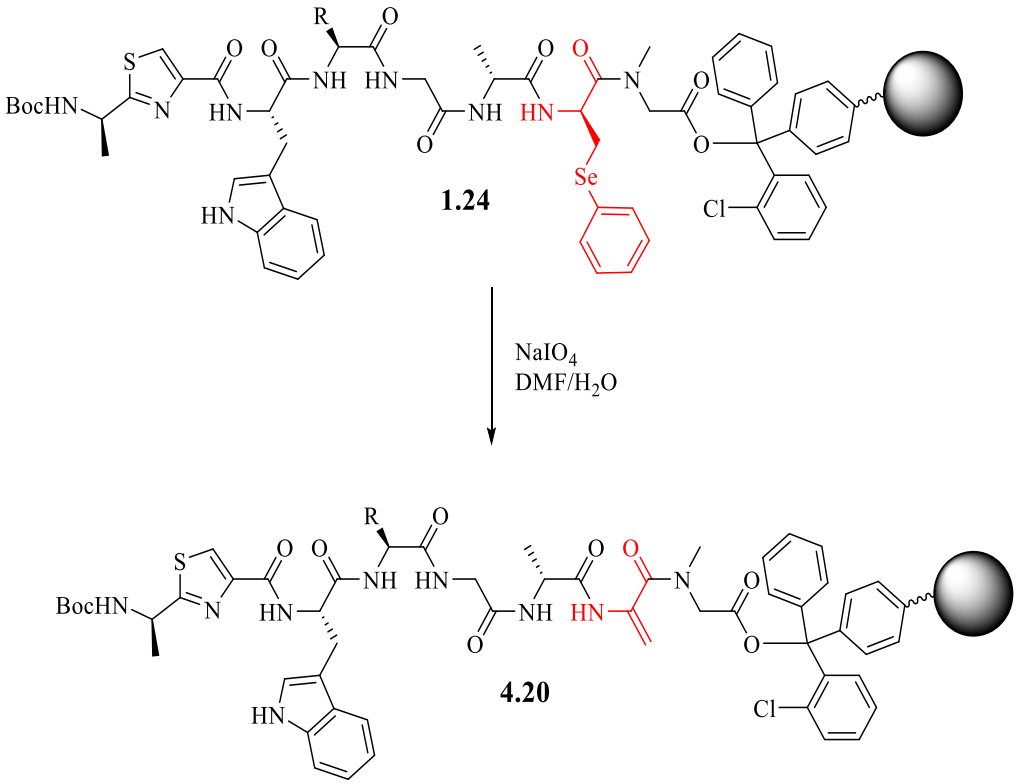
The dehydroalanine residue was revealed by chemoselective oxidative elimination of the Sec(Ph) residue using $NaIO_4$ as reported by Okeley *et al*..[275] The $NaIO_4$ oxidized the Sec(Ph) **4.21** residue to generate the phenylselenoxide **4.22**, which undergoes *syn*-elimination to afford the *exo*-methylene moiety of DhA **4.23** (Scheme 4.9). Ley *et al.* employed the oxidative elimination of Sec(Ph) after cyclisation of the peptide from resin.[202] However, such approach suffers from low overall yield and time consuming due to the two purification steps required (one after cyclization and the other after oxidative elimination).



Scheme 4.9. $NaIO_4$ mediated oxidative elimination of Sec(Ph)

In order to reduce the number of purification steps, Chan *et al*. established an on-resin oxidative elimination (Scheme 4.10), which was utilised the peptidyl resin suspended in a solution of $NaIO_4$ (2 equiv.) in DMF/H_2O 1:1. The reaction mixture was intermittently agitated at room temperature.[205] The reaction was monitored by reacting a small amount of resin product, which in turn is treated with 50% *v*/*v* TFA/DCM over 1 hour.

The resultant crude peptidic material was analysed by RP-HPLC. Up to 90% reaction completion was observed within 24 hours. Figure 4.2 shows the RP-HPLC trace of one analogue **4.25**. The successful oxidative elimination was confirmed by HR-MS. The elution peak at 8.2 minute is assigned to the starting material **4.24**, while the peak at 6.0 minute accounts for the dehydro product **4.25**.



Scheme 4.10. On-resin oxidative elimination of phenylselenocysteine

After completion, the resin product was washed with DMF, H_2O and DMF until no white fibrous phenylselenoxide precipitate was observed. The resin was collected in Buchner funnel, washed with DCM and hexane, and dried under *vacuo* overnight before acidolytic cleavage.

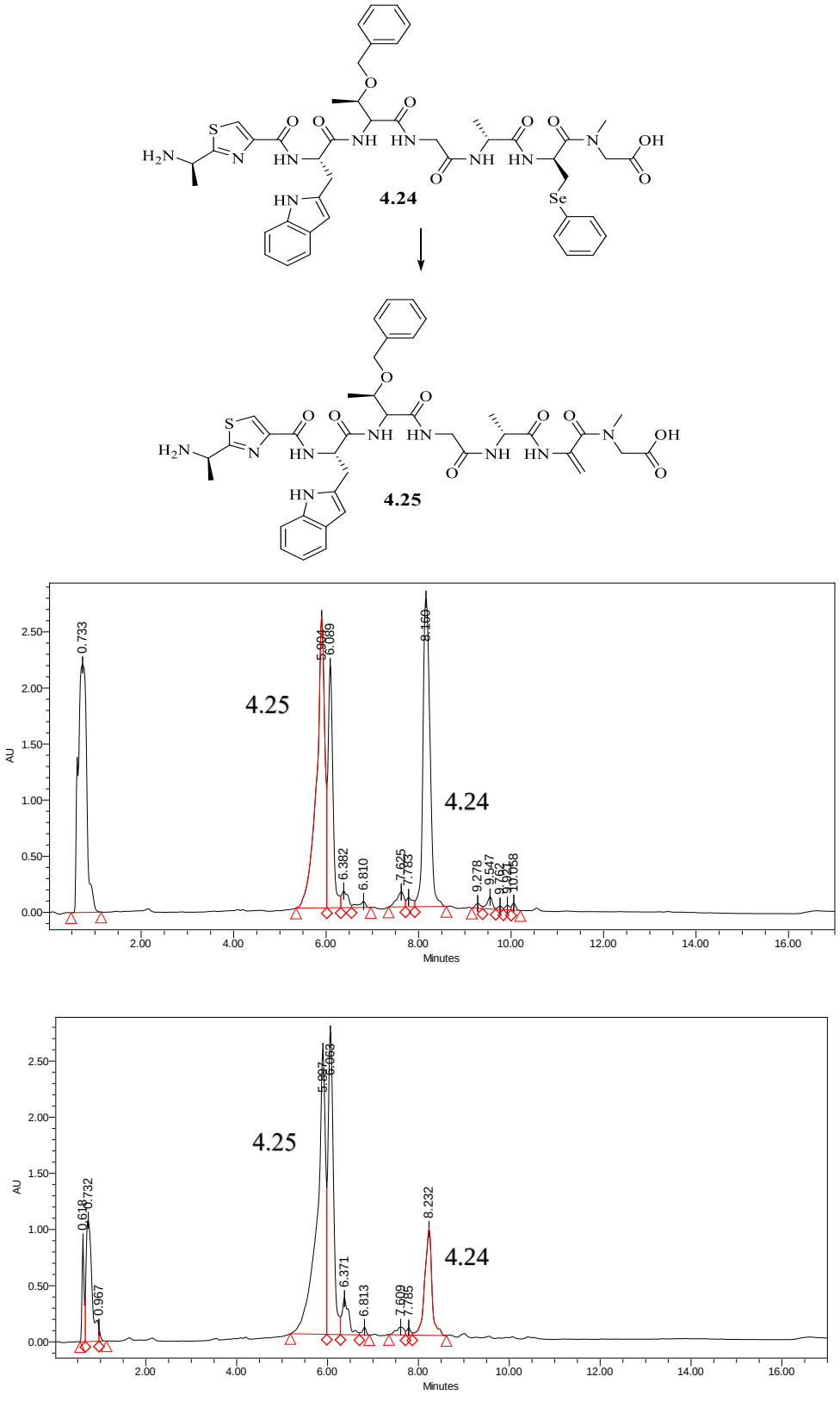
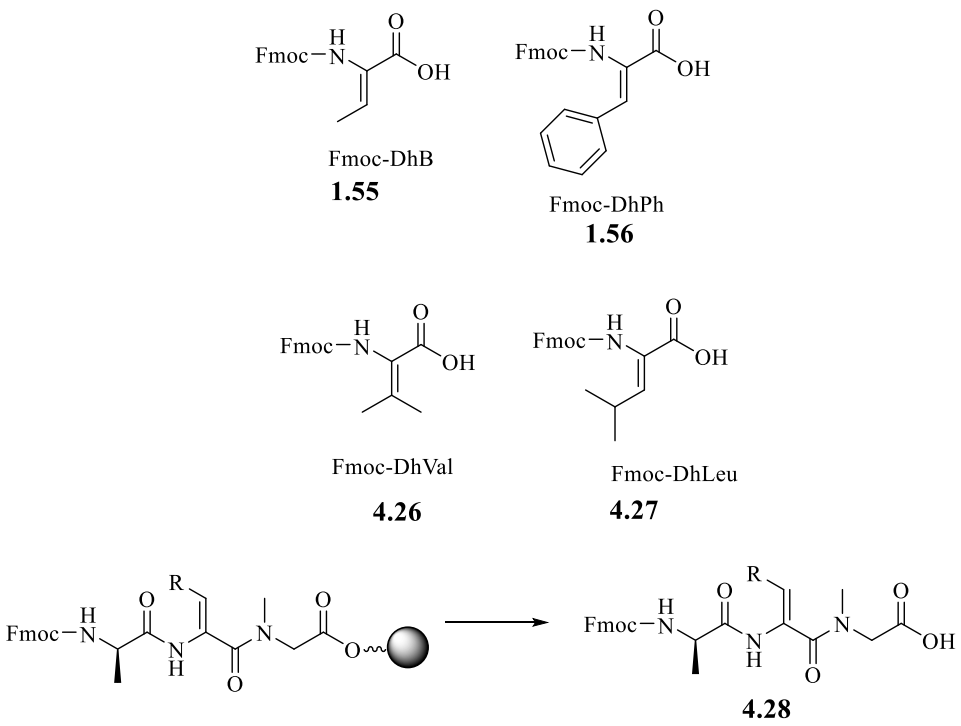


Figure 4.2. RP-HPLC analysis of $NaIO_4$ treatment after of **4.24** 9 h (top) and after 16 h (bottom). Solvent system: 10-60% **B** in **A** over 10 min at 3 mL/min. (**A** = 0.06% TFA in water, **B** = 90% acetonitrile in water + 0.06% TFA). Column: Onyx Monolithic C_{18} (100 x 4.6 mm). Eluent was monitored at 216 nm.

4.2.4 Direct Application of Fmoc-Dehydroamino Acid



Scheme 4.11. Fmoc-dehydroamino acids and tripeptide **4.28** for analysis

As mentioned in Chapter 3, two β-substituted Fmoc-dehydroamino acids (**1.55** and **1.56**) synthesised and two β-substituted Fmoc-dehydroamino acids (**4.26** and **4.27**) purchased were directly used in Fmoc/*t*Bu SPPS. Thus, Fmoc-DhB was coupled directly to sarcosine followed the procedure described above. The reaction was monitored through the spectrophotometer. Furthermore, after coupling of Fmoc-glycine-OH to DhB, a small amount of resin product was collected and cleaved for HR-MS analysis (Scheme 4.11). A correct mass of the tripeptide **4.28** was observed. Hence, the assembly was carried on until the full sequence was obtained. The fully assembled linear peptide was cleaved from resin and analysed by HR-MS. The desired linear product was obtained. In subsequent assembly of other argyrin analogues, Fmoc-DhB, Fmoc-DhPh, Fmoc-DhVal **4.26** and Fmoc-DhLeu **4.27** were stable throughout Fmoc/*t*Bu SPPS. The Figure 4.3 is the RP-HPLC trace of **4.29**.

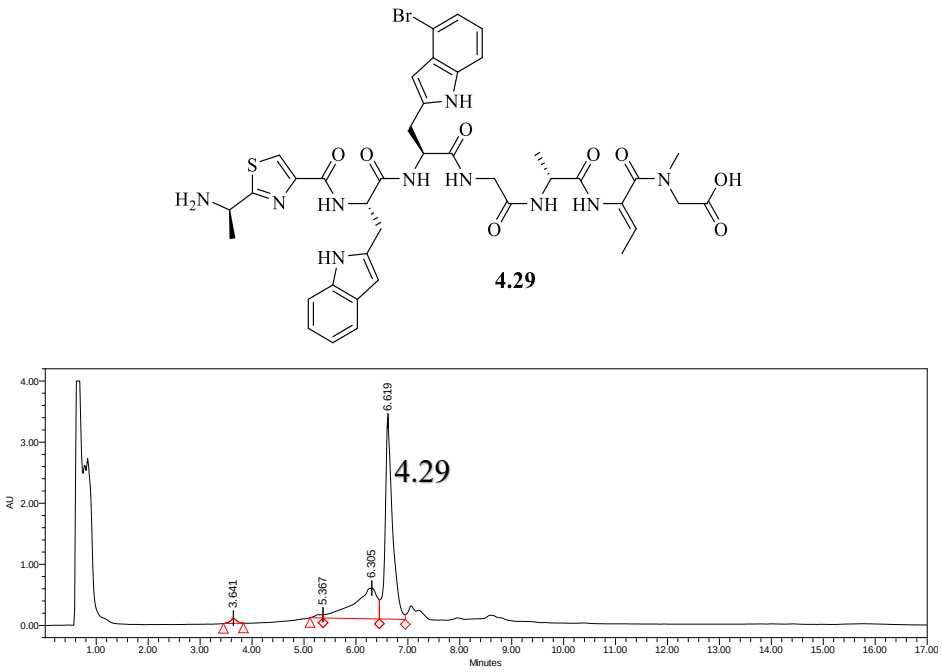
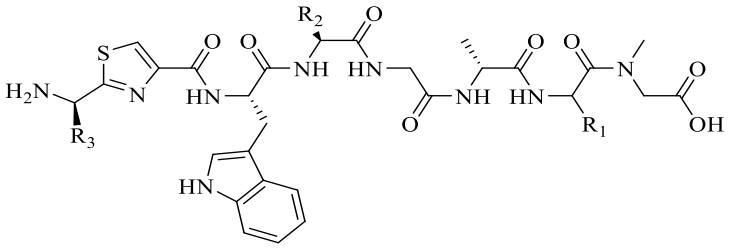


Figure 4.3. The crude HPLC trace of Fmoc-DhB analogue **4.29**. Solvent system: 10–60% **B** in **A** over 10 min at 3 mL/min. (**A** = 0.06% TFA in water, **B** = 90% acetonitrile in water + 0.06% TFA). Column: Onyx Monolithic C_{18} (100 x 4.6 mm). Eluent was monitored at 216 nm.

4.2.5 Deprotection and Cleavage of Peptide from Solid Support

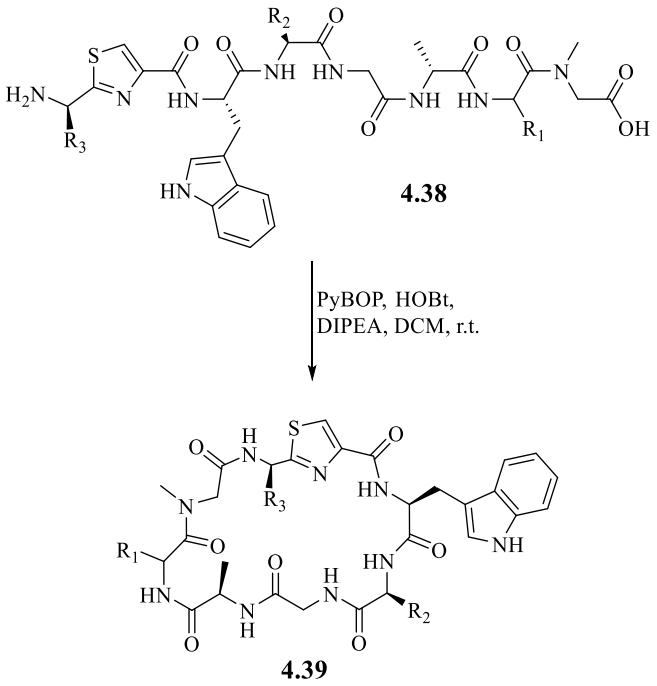
The simultaneous *N*-terminal Boc-deprotection and release of linear peptide precursor from 2-chlorotrityl chloride resin was achieved using 50% *v*/*v* TFA in DCM over 3 hours. The acidolytic cleavage solution and resin mixture were filtered, and the filtrate was evaporated under *vacuo*. The resultant peptidic product was precipitated from diethyl ether, to afford the crude argyrin linear precursor as off-white solids. Without further purification, the crude product was subjected to macrocyclisation conditions. The analytical data of all the linear precursors synthesised are listed in Table 4.4. The methoxy-thiazole used for the synthesis of **4.33** and Fmoc-allygly-OH were obtained for Sivaneswary Genapathy.



Sequence	T_R (min)	HR-MS calculated	HR-MS found
H-D-Ala-Thz-Trp-Thr(Bzl)-Gly-D-Ala-DhA-Sar-OH **4.25**	6.72	818.3290	818.0645
H-D-Ala-Thz-Trp-Trp(5-Br)-Gly-D-Ala-DhA-Sar-OH **4.30**	6.58	891.2242	891.2200
H-D-Ala-Thz-Trp-Trp(4-Cl)-D-Allygly-D-Ala-DhA-Sar-OH **4.31**	6.72	873.2904	872.9678
H-D-Ala-Thz-Trp-Trp(4-Br)-Gly-D-Ala-DhB-Sar-OH **4.29**	6.58	927.2218	927.2190
H-D-Ala-Thz-Trp-Trp(4-Cl)-Gly-D-Ala-DhB-Sar-OH **4.32**	6.50	861.2904	861.2911
H-D-Ser(OMe)-Thz-Trp-Trp(4-Br)-Gly-D-Ala-DhB-Sar-OH **4.33**	6.60	957.2324	957.2304
H-D-Ala-Thz-Trp-Trp(4-MeO)-Gly-D-Ala-DhB-Sar-OH **4.34**	6.58	857.3399	857.3439
H-D-Ala-Thz-Trp-Trp(4-Br)-Gly-D-Ala-DhPh-Sar-OH **4.35**	7.59	967.2555	967.2553
H-D-Ala-Thz-Trp-Trp(4-Br)-Gly-D-Ala-DhVal-Sar-OH **4.36**	6.93	919.2555	919.2546
H-D-Ala-Thz-Trp-Trp(4-Br)-Gly-D-Ala-DhLeu-Sar-OH **4.37**	7.58	933.2712	933.2725

Table 4.4: Summary of the RP-HPLC retention times and MS for the linear precursors. Solvent system: 10–60% **B** in **A** over 10 min at 3 mL/min. (**A** = 0.06% TFA in water, **B** = 90% acetonitrile in water + 0.06% TFA). Column: Onyx Monolithic C_{18} (100 x 4.6 mm). Eluent was monitored at 216 nm

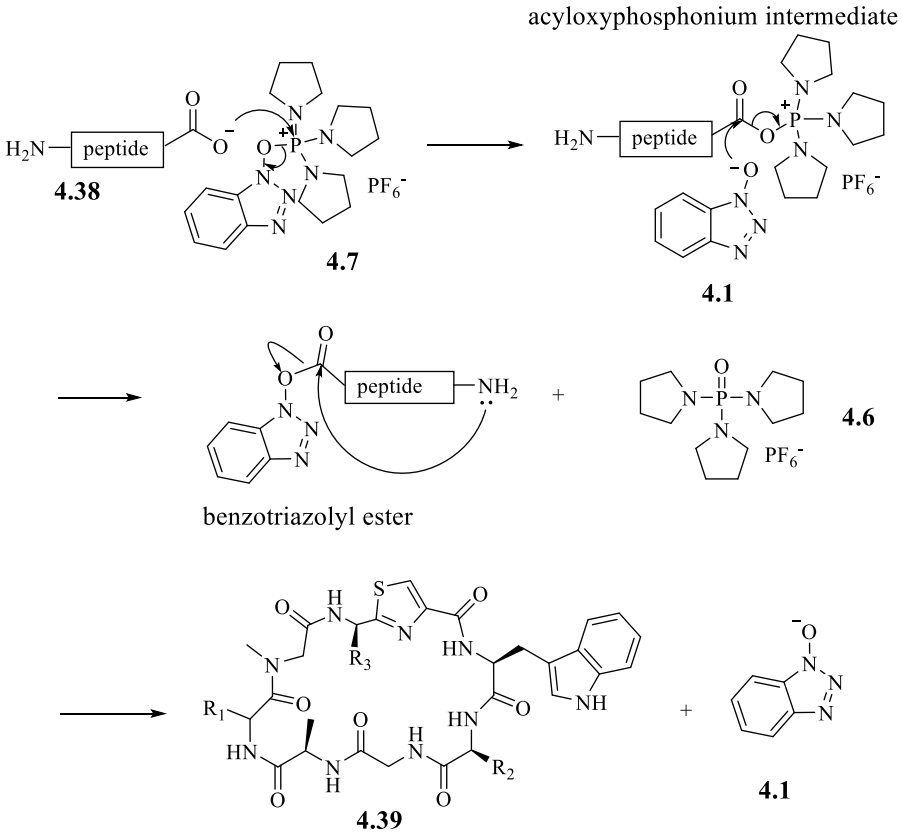
4.2.6 Macrocyclisation of Argyrin Linear Precursors



Scheme 4.12. Macrocyclisation of argyrin linear precursors

The final step was the solution-phase head-to-tail macrocyclisation of crude argyrin linear precursors to afford the cyclic argyrin analogues Scheme 4.12. In order to avoid cyclodimerization or oligomerisation side-reactions during the macrocyclisation, the reaction was carried out in high dilution conditions, typically 0.1 to 1 mM solution.[320] The choice of coupling reagents also contributes to the success of macrocyclisation. In the total synthesis of argyrin B and argyrin F reported by Ley *et al*.[202] and Bickeleit *et al*.[204], respectively, TBTU and HOBt were selected. In contrast, Jiang *et al*.[203] selected the activating agents, HATU and HOAt. However, the usage of aminium based reagents, e.g. HATU and TBTU, potentially suffers from the *N*-guanidylation of the amino terminus.[321] In order to avoid this potential side-reaction, Chan *et al*. used PyBOP in combination with HOBt as coupling reagents.[205]

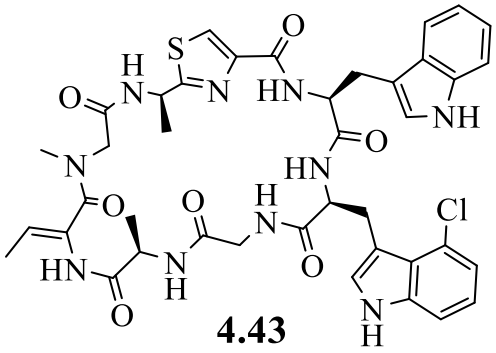
Therefore, the cyclisation of linear peptide was performed in DCM/DMF (1:50) at 0.5 nM in the presence of DIPEA, HOBt, and PyBOP; the mechanism of cyclisation is outlined in Scheme 4.13. The reaction results in the initial formation of a highly reactive acyloxyphosphonium intermediate. The intermediate is then attacked by the nucleophilic HOBt anion to generate the activated benzotriazolyl ester. The *N*-terminal amine then attacks the carbonyl of the benzotriazolyl ester, resulting in intramolecular macrocyclisation and regeneration of HOBt.



Scheme 4.13: Proposed mechanism of PyBOP and HOBt mediated cyclization

The reaction was found to be completed by 12-72 hours, depending on the analogue. The cyclisation of oxidative elimination generated DhA required 72 hours due to the low purity of linear precursors. The cyclisation of linear precursors from direct coupling of β-substituted Fmoc-dehydroamino acids was completed within 15 hours. Only one linear peptide **4.31** failed to cyclise. As an

example, the RP-HPLC trace of purified cyclic argyrin **4.43** was shown in Figure 4.4 below. The product was confirmed by HR-MS analysis. The crude reaction mixture was dried under *vacuo* and then subjected to preparative RP-HPLC purification to afford the desired product in >95% purity.



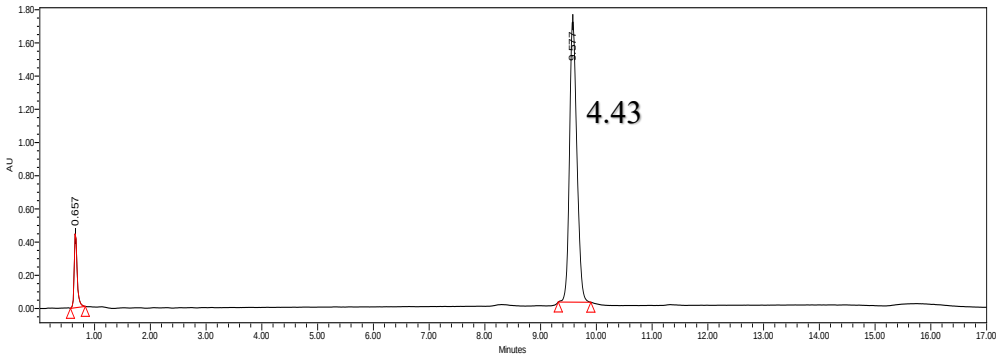


Figure 4.4. The HPLC trace of purified **4.43**. Solvent system: 10–60% **B** in **A** over 10 min at 3 mL/min. (**A** = 0.06% TFA in water, **B** = 90% acetonitrile in water + 0.06% TFA). Column: Onyx Monolithic C_{18} (100 x 4.6 mm). Eluent was monitored at 216 nm.

All the cyclic peptides **4.40-4.48** were characterised using ^{1}H-NMR and 2D-^{1}H-^{1}H correlation NMR (COSY). Six secondary amide proton signals are readily identified and are located at the down-field region in the ^{1}H-NMR of all the cyclic peptides. The cyclic structure of the peptide can be confirmed by the correlation between the amide protons with the α-proton. The sharp singlet at aromatic region of ^{1}H-NMR indicated the existence of the thiazole proton. Additionally, the characteristic quartet located around 5.6 ppm indicated the β-proton of the dehydrobutyrine. An example of ^{1}H-NMR spectrum of **4.42** is

shown in Figure 4.5. Figure 4.6 shows the ^{1}H-NMR spectrum of **4.42** at the region 3.0-5.6 ppm, and Figure 4.7 shows the region 6.0-8.8 ppm. The characteristic quartet, which is highlighted in red circle, indicates the presence of β-proton of the dehydrobutyrine residue. As all the compounds are newly synthesised, all the optical rotation values are also reported.

Sequence	T_R (min)	HR-MS calculated	HR-MS found
Cyclo[D-Ala-Thz-Trp-Thr(Bzl)-Gly-D-Ala-DhA-Sar] **4.40**	9.42	799.3112	800.0704
Cyclo[D-Ala-Thz-Trp-Trp(5-Br)-Gly-D-Ala-DhA-Sar] **4.41**	9.34	873.2137	873.2130
Cyclo[Ala-Thz-Trp-Trp(4-Br)-Gly-D-Ala-DhB-Sar] **4.42**	9.87	887.2293	887.2287
Cyclo[Ala-Thz-Trp-Trp(4-Cl)-Gly-D-Ala-DhB-Sar] **4.43**	9.55	865.2623	865.2650
Cyclo[D-Ser(OMe)-Thz-Trp-Trp(4-Br)-Gly-D-Ala-DhB-Sar] **4.44**	9.50	917.2399	917.2375
Cyclo[D-Ala-Thz-Trp-Trp(4-MeO)-Gly-D-Ala-DhB-Sar] **4.45**	9.46	839.3294	839.3309
Cyclo[D-Ala-Thz-Trp-Trp(4-Br)-Gly-D-Ala-DhPh-Sar] **4.46**	10.91	949.2450	949.2402
Cyclo[D-Ala-Thz-Trp-Trp(4-Br)-Gly-D-Ala-DhVal-Sar] **4.47**	10.09	901.2450	901.2435
Cyclo[D-Ala-Thz-Trp-Trp(4-Br)-Gly-D-Ala-DhLeu-Sar] **4.48**	11.30	915.2606	915.2622

Table 4.5: Summary of the RP-HPLC retention times and MS for the cyclic peptides **4.40-4.48**. Solvent system: 10–60% **B** in **A** over 10 min at 3 mL/min. (**A** = 0.06% TFA in water, **B** = 90% acetonitrile in water + 0.06% TFA). Column: Onyx Monolithic C_{18} (100 x 4.6 mm). Eluent was monitored at 216 nm.

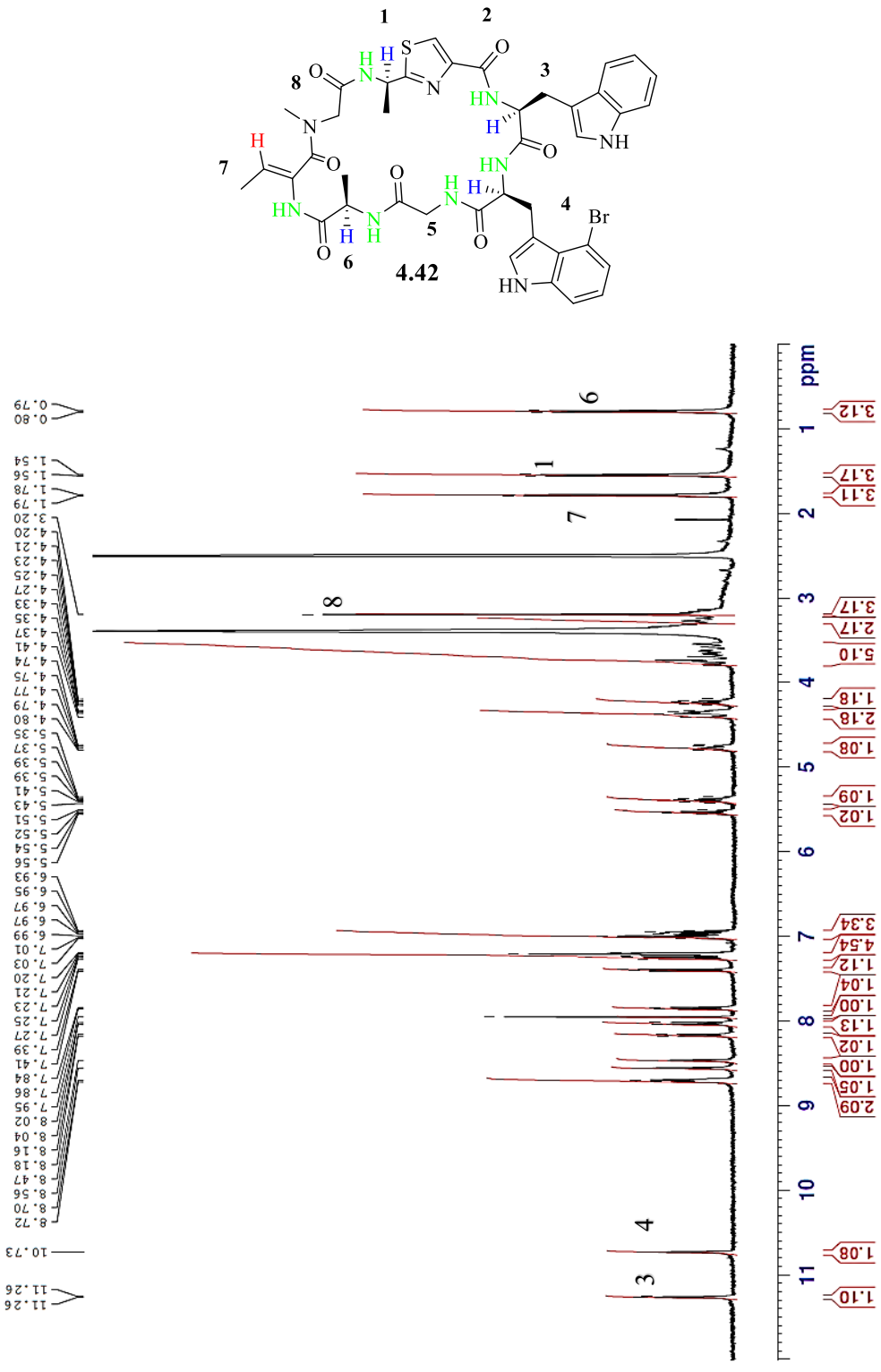


Figure 4.5. ^{1}H-NMR spectrum of **4.42**

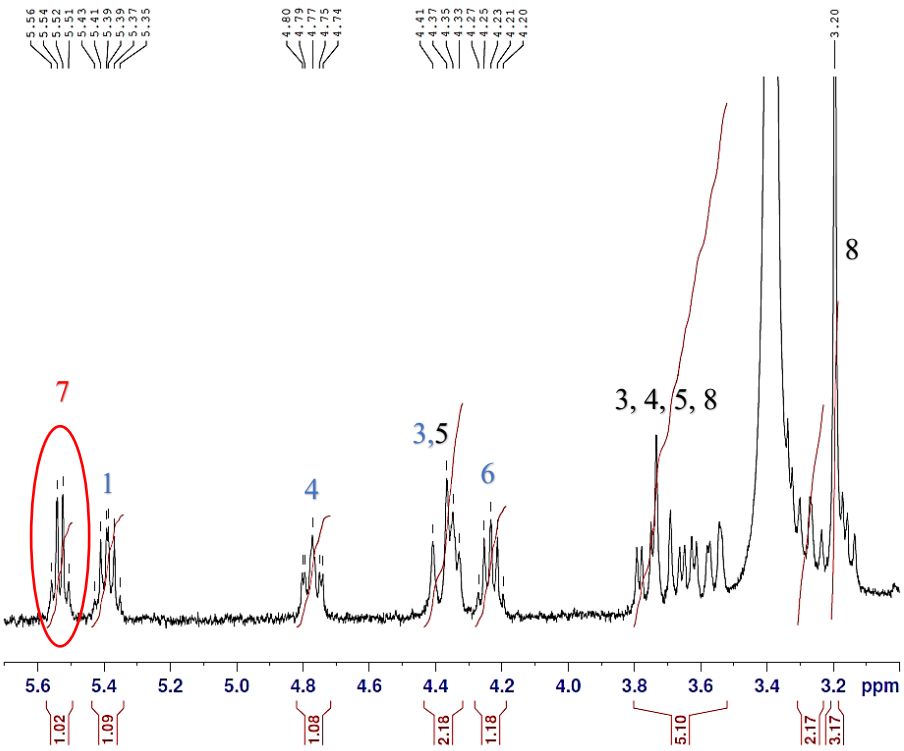


Figure 4.6. ^{1}H-NMR spectrum of **4.42** at region 3.0-5.6 ppm

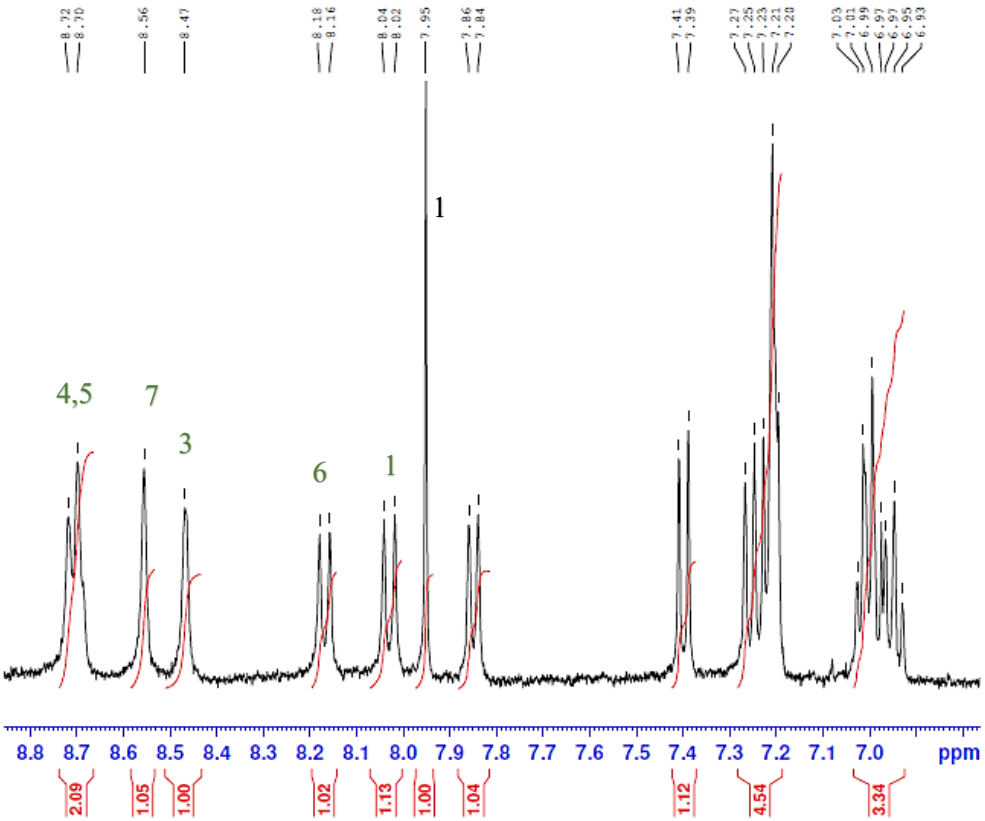


Figure 4.7. ^{1}H-NMR spectrum of **4.42** at region 6.0-8.8 ppm

4.2.7 Chemical Stability of Argyrins

The chemical stability of the synthesised argyrin analogues were determined in a chemical stability assay as described in the Chapter 7. The macrocyclic peptide argyrins are anticipated to be chemically stable at various gastrointestinal pH. Hence, the argyrin analogues were tested at pH 1.0 and 7.4 and kept at 37 ºC for 24 h. The chemical stability was monitored at 0, 1, 2, 6 and 24 h using RP-HPLC.

All the argyrin analogues synthesised were found to be chemically stable for up to 24 h at 37 ºC at pH 1.0 and 7.4. Therefore, the argyrin analogues should be gastrointestinal chemically stable.

4.3 Conclusions

In conclusion, this chapter described the application of Fmoc/*t*Bu SPPS and solution-phase head-to-tail macrocyclisation to afford the desired argyrin analogues. Firstly, a brief view of the development of Fmoc/*t*Bu SPPS strategy was outlined. Secondly, a variety of linker-resins and coupling reagents were reviewed. For a successful Fmoc/*t*Bu SPPS of argyrin, the 2-chlorotrityl chloride resin was selected as the solid support. The N^{α}-Fmoc-sarcosine was selected as the *C*-terminal amino acid, which was pre-loaded on the resin. All the couplings were carried out using HATU and DIPEA in DMF. The N^{α}-Fmoc-deprotection was performed using a continuous flow of 20% piperidine in DMF via a semi-automated peptide synthesiser.

In terms of obtaining the dehydroalanine residue of the target argyrin analogue, an on-resin oxidative elimination of the Sec(Ph) residue was achieved using $NaIO_4$ (Scheme 4.9). Most importantly, this Chapter reported the successful direct application of β-substituted Fmoc-dehydroamino acids in Fmoc/*t*Bu SPPS. Four β-substituted Fmoc-dehydroamino acids applied were proved to be stable during the repeating coupling and deprotection process of the Fmoc/*t*Bu SPPS. Such a discovery may aid further production of more dehydro amino acid-containing argyrin analogues.

After the full assembly of the required peptide sequence, a simultaneous deprotection of N^{α}-Boc and cleavage from resin was achieved using the acidolytic mixture, 50% TFA in DCM. Although the cleavage of peptide from resin can performed under 1% TFA in DCM, the usage of 50% in this case resulted in the simultaneous deprotection of the N^{α}-Boc group. The crude linear precursors after cleavage were subjected to a solution-phase macrocyclisation using PyBOP and HOBt in the presence of DIPEA (Scheme 4.12). The choice of PyBOP in combination with HOBt prevented side-reaction. The 0.5 mM reaction concentration facilitated an intramolecular cyclisation. The cyclic peptides were purified through preparative RP-HPLC to achieve >95% purity. Previously, an Onyx monolithic-C_{18} semi-preparative column (100 x 10 mm) with flow rate 9 mL min^{-1} was used for purification. In this study, a Phenomenex Luna® 5 µm C18(2) 100 Å, AXIA™ Packed LC column (250 x 21.20 mm) with flow rate 20 mL min^{-1} was used. The purification efficiency has been greatly enhanced since the sample loading of the new column is much higher.

Chapter 5
Antibacterial Activity of the Argyrin Analogues

In 1996, Selva *et al.* reported that argyrin A **1.1** and B **1.2** had selective antimicrobial activity against Gram-negative bacteria, including *P. aeruginosa* and *Pr. mirabilis*, by inhibiting bacterial protein synthesis. In addition, the argyrin A and B were reported to be bacteriostatic against *P. aeruginosa*, which was judged by the four-fold difference in the MICs and MBCs (minimum bactericidal concentrations) against *P. aeruginosa*.[166] Later in 2002, Sasse *et al.* reported that argyrin A-H had slight antibacterial activity against the intrinsically drug-resistant bacteria *P. aeruginosa*. They then compared the IC_{50} of argyrin A-H against *P. aeruginosa* to gain SAR information. Consequently, they confirmed that 4-methoxy group of the tryptophan and the methyl group in the thiazole dipeptide domain were essential for good activity.[167]

In 2012, Nyfeler *et al* identified that EF-G was the conserved cellular target of argyrin B in *P. aeruginosa*.[170] In the same year, Bielecki *et al*. reported that argyrin A targeted EF-G in *P. aeruginosa*.[199] Notably, Nyfeler *et al*. reported a co-crystal structure of argyrin B bound to *P. aeruginosa* EF-G (Figure 1.17).

They then identified the key interactions between argyrin B and domain III and domain V of EF-G. Hydrogen bonding interactions were found between the backbone amide of Ala489 and the sarcosine of argyrin B, the hydroxyl group of Ser417 to the oxygen on the 4-methoxy-tryptophan and side chain of Lys448 to the glycine of argyrin B. The thiazole of argyrin B was observed to participate in Van der Waals interactions with the backbone of Gln 487 and Val488. Similarly, Van der Waals interaction was also observed between the indole ring of the tryptophan of argyrin B and Met620 and Met685, as well as between argyrin B to Leu663 and Phe687 (Figure 5.1).[170]

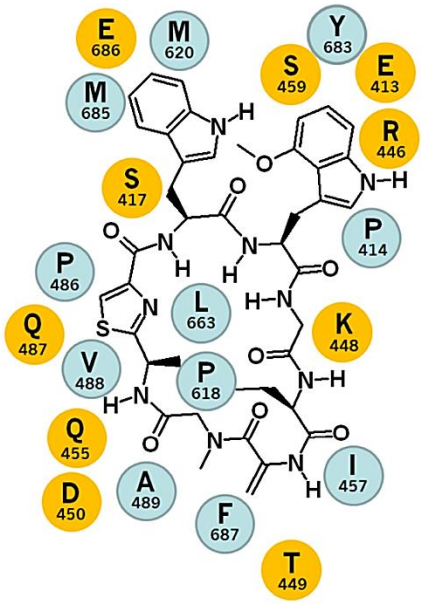


Figure 5.1: 2D protein-ligand interaction plot of argyrin B and the hydrophobic (cyan) and hydrophilic (yellow) amino acid residues in EF-G.[170]

In 2014, Chan and co-workers in their preliminary investigation into the structure-activity relationships (SARs) of argyrin that govern their antibacterial activity explored the role of (*S*)-4-methoxytryptophan.[205] They found that the 4-methoxy functionality was crucial to maintain antibacterial activity, since shifting the methoxy functionality from the 4-position to 5-position weakened its activity. This finding indicated the importance of H-bond interaction between the oxygen of the 4-methoxytryptophan and Ser417 of EF-G. Later,

Sivaneswary Genapathy of the Chan's research group discovered the crucial H-bond interaction can be replaced with a halogen-bond, in order to maintain or, in some cases, increase antibacterial activity.[322] She then carried out further modification of other parts of argyrin framework. Thus, inspired by her findings, modifications of different parts of argyrin framework, especially on the three unusual building blocks, were performed to gain investigation into the SAR that governs the antibacterial property of argyrins against *P. aeruginosa*.

The first part of this chapter is the description of argyrin susceptibility assay procedure. The second part of this chapter focused on the SAR of argyrin analogues against *P. aeruginosa* and *B. multivorans*:

- Activity of argyrin analogues with modification in the substituted tryptophan residue
- Activity of argyrin analogues with modification at the side chain of thiazole dipeptide
- Activity of argyrin analogues with β-substituted dehydroamino acid residue

The argyrin analogues with most potent antibacterial activity towards *P. aeruginosa* and *B. multivorans* was then tested with other bacterial organisms, *Pr. mirabilis, Streptococcus pyogene* and *Streptococcus agalactiae*.

5.1 The Argyrin Susceptibility Assay Procedure

Bielecki *et al*.[199] and Nyfeler *et al*.[170] reported the MIC values of argyrin A **1.1** and B **1.2** using either the broth microdilution or 96 well-plate microdilution methods. Both methods identify the MIC value as the lowest concentration for argyrin to inhibit the growth of the organism in the tube or the microdilution

well completely, which was determined by visual inspection after 18 hours of incubation. Although both methods are easy and quick to carry out, the use of such methods for the MIC determination of argyrin in *P. aeruginosa* are not straight forward. Nyfeler *et al.* reported the antibacterial effect of argyrin B **1.2** as susceptibility rather than MIC value due to the precipitation of **1.2** at concentrations greater than 16–32 μg/ml. Therefore, the bacterial susceptibility of argyrin is reported as IC_{50} (concentration for 50% growth inhibition) or percentage growth inhibition at highest tested concentration. The turbidimetric measurement method using a spectrophotometer was applied in this thesis to generate the overnight growth curve for the determination of IC_{50} or percentage growth inhibition values.

The bacterial susceptibility assay was carried out using periodic turbidimetric measurements over a period of bacteria growth. The measurement therefore depends on the increasing turbidity of bacterial culture resulting from the increasing bacterial cell number in the solution. In this thesis, a Tecan microplate reader, which measures the turbidity at 610 nm was employed with controlled temperature.

Typically, a colony of *P. aeruginosa* or *Pr. mirabilis* was grown aerobically overnight in Mueller-Hinton media (MH media) in a shaking incubator (200 rpm) at 37 ºC. *B. multivorans* was grown aerobically overnight in MH media in a shaking incubator at 30 ºC. *Streptococcus pyogene* and *Streptococcus agalactiae* were grown aerobically overnight in Brain Heart Infusion media (BHI media) in a static incubator at 37 ºC. The overnight culture was then diluted with the same growth media in order to achieve an optical density (OD) at 600 nm of 0.05 for (*P. aeruginosa, Pr. mirabilis, Streptococcus pyogene* and *Streptococcus agalactiae*) and 0.005 for *B. multivorans*. The freshly diluted bacterial broth was used to prepare aliquots containing test compounds at desired concentrations. The test compounds were prepared as 10 mM stock

solutions in DMSO. The aliquots were dispensed into a 96-well microtiter plate and incubated at the desired temperature, *P. aeruginosa, Pr. mirabilis, Streptococcus pyogene* and *Streptococcus agalactiae* at 37 ºC and *B. multivorans* at 30 ºC, for an overnight kinetic growth study in the Tecan plate reader. The experimental detail was described in the Chapter 7. The example of the overnight growth curve generated for *P. aeruginosa* by using the Tecan plate reader is displayed in Figure 5.2. The growth curve generated for *P. aeruginosa* PAO1 in the presence of **4.42** at concentration range of 0.78-100 µM is shown in Figure 5.3.

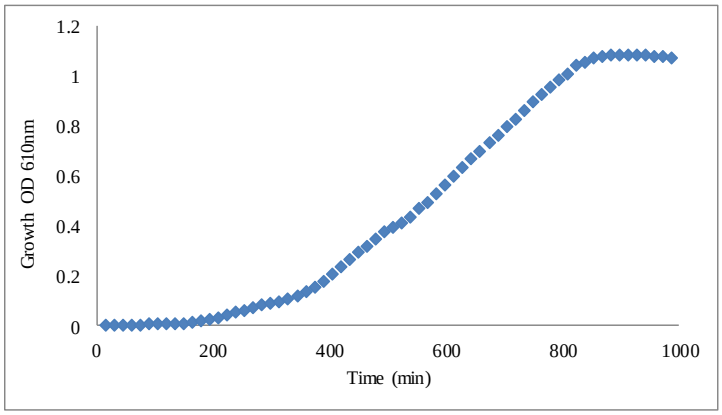


Figure 5.2: An overnight growth curve of *P. aeruginosa* PAO1 in MH media

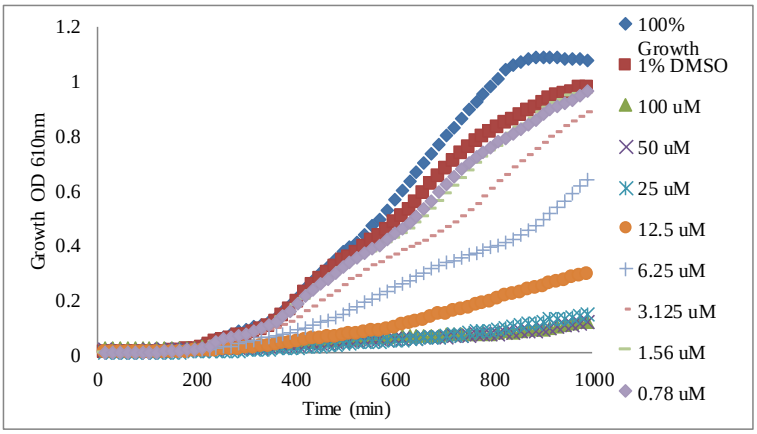


Figure 5.3: Growth curve of *P. aeruginosa* PAO1 in MH media. The growth of bacteria was measured in the absence and presence of **4.42** at concentration range of 0.78-100 µM. MH media with bacteria, without bacterial and with 1% DMSO are used as controls.

5.2 Activity of Argyrin Against *P. aeruginosa*

This section outlines the activity of argyrin analogues, which are either synthesised in this thesis or obtained from Sivaneswary Genapathy, against *P. aeruginosa*. The argyrin analogues obtained from Sivaneswary Genapathy are listed in the Figure 5.4.

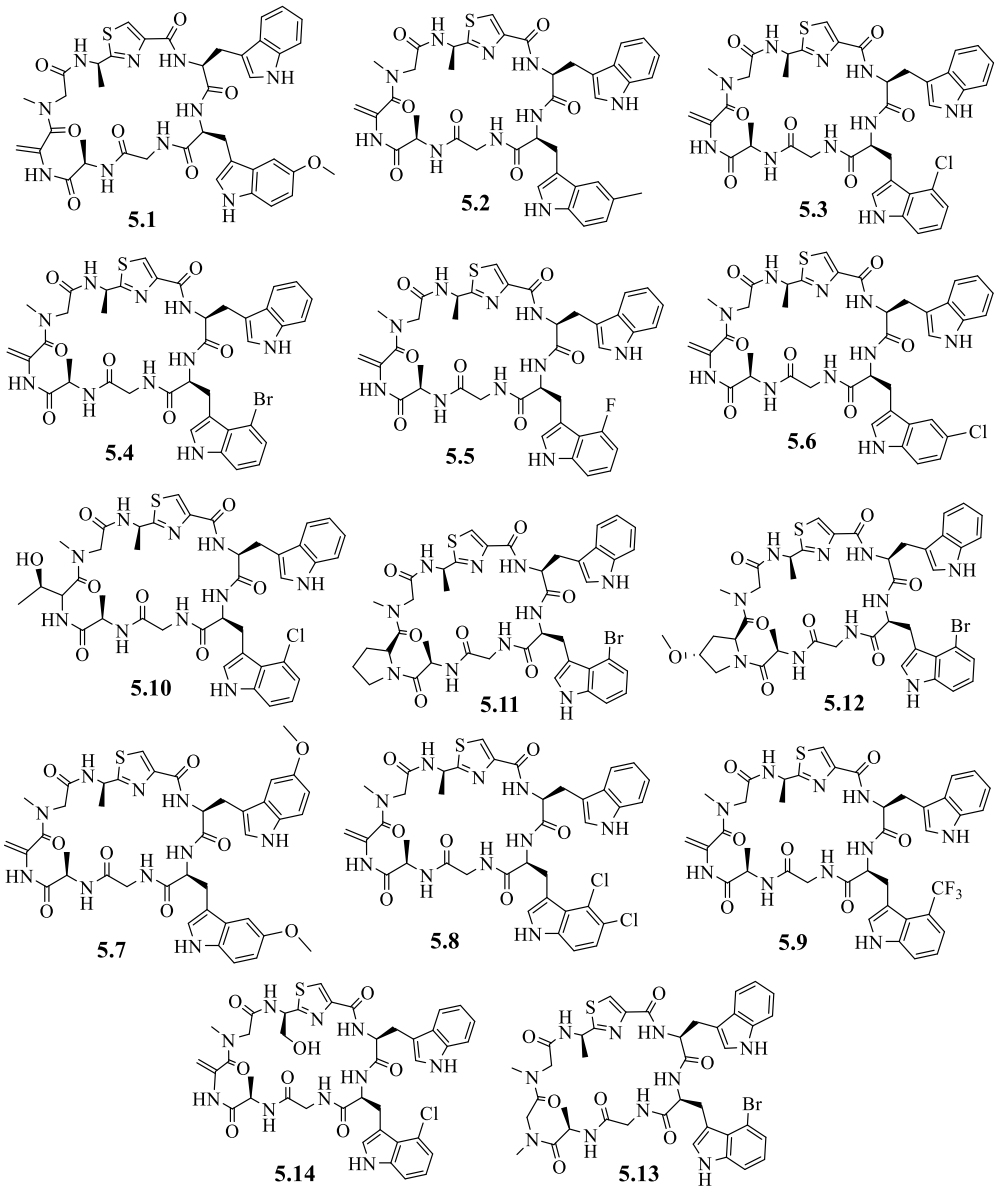


Figure 5.4: Argyrin analogues obtained from Sivaneswary Genapathy

5.2.1 Activity of Substituted-L-Tryptophan Argyrins Against *P. aeruginosa*

The preliminary investigation into the SAR of argyrin analogues in *P. aeruginosa*, reported by Chan's research group, revealed that the 4-MeO-L-Trp residue was crucial for the antibacterial activity. By replacing the 4-MeO-L-Trp (argyrin A **1.1**) with 5-MeO-L-Trp **5.1**, the IC_{50} dropped dramatically from 19.8 ± 1.6 μM to 90–100 μM against *P. aeruginosa* wild-type strain PAO1. Furthermore, **1.1** at 100 μM displayed a 93% growth inhibition at 13-hour time point while Argyrin E **1.5** and **5.2** displayed 33% and 23%, respectively. The IC_{50} and percentage growth inhibition values of **1.1**, **1.5**, **5.1** and **5.2** (Figure 5.5) are listed in Table 5.1.

Based on the co-crystal structure of argyrin bound to *P. aeruginosa* EF-G^{170}, an H-bond interaction between Ser417 and the oxygen of the 4-MeO-group on tryptophan was observed (Figure 1.17). The IC_{50} and % growth inhibition values above supported this observation, as **1.5** and **5.2** displayed high IC_{50} value and lower % growth inhibition than **1.1**. Furthermore, shifting the methoxy from 4-position to 5-position dramatically reduced the antibacterial activity. This might due to an increased distance of Ser417 to oxygen of MeO-group, which results in a weakened H-bond interaction. In addition, the 5-MeO-L-Trp might interact with Tyr683 (Figure 1.17 and Figure 5.1).

In summary, the above finding indicated that 4-MeO-group in Trp residue is essential for antibacterial activity. Moreover, the argyrin analogue lacking an H-bond acceptor in 4-position of tryptophan (such as **1.5**) display relatively low antibacterial activity.

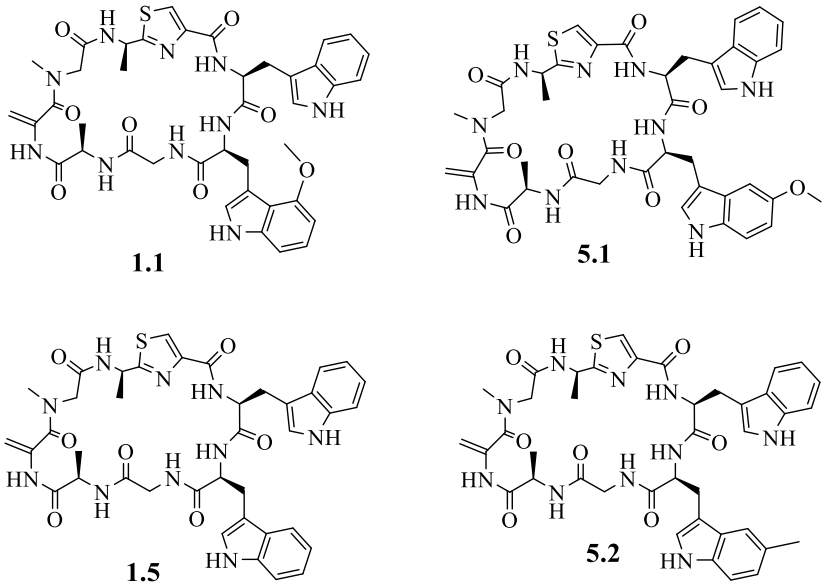


Figure 5.5: Four argyrin analogues to probe the necessity of 4-MeO-L-Trp residue for antibacterial activity

Compound	IC_{50} (μM)	% Growth inhibition at 100 μM
1.1	19.8 ± 1.6	93
1.5	90–100	33
5.1	90.7 ± 3.7	61
5.2	>100	23

Table 5.1: The IC_{50} and % growth inhibition values of *P. aeruginosa* PAO1 in MH media at 13h

Later, Sivaneswary Genapathy discovered the H-bond could be replaced with a halogen-bond interaction.[322] Therefore, a library of argyrin analogues containing halogen (Cl, Br and F) substitution at 4- and 5-position of tryptophan were investigated (Figure 5.6). The IC_{50} and the percentage growth inhibition at 100 μM are listed in Table 5.2.

The antibacterial assay indicated a small increase in activity with the 4-Cl and 4-Br substituted analogues, **5.3** and **5.4**, and in contrast, a two-fold decrease in activity with 4-F substituted analogue **5.5**. This finding indicated an interesting trend in the activity profile of the halogenated compounds. The halogen-bond (XB) has been introduced for describing the non-covalent interaction involving

halogens as acceptors of electron density. The general scheme D···X-Y applies to halogen bonding, where X is the halogen (Lewis acid, XB-donor), D is any electron-donor (Lewis base, XB-acceptor), and Y is carbon, halogen, nitrogen. The term halogen bonding sheds light on the nature of XB, which possesses similarily as hydrogen bonding, wherein hydrogen functions as the acceptor of electron density. The XB strength scales with the polarizability of the XB donor atom, that is (F<Cl<Br<I). The organic fluorine (C-F) is the least prone to be involved in XB, and can act as an XB donor only when attached to particularly strong electron-withdrawing groups. This supports the finding that 4-F substituted analogue **5.5** has a two-fold decreased in activity.

In addition, the difference in the carbon-halogen bond length may also affect the trend in activity. The C-Br bond length is 194 pm while C-Cl and C-F are 177 and 135 pm, respectively. The increase in activity is likely to be related to the increase in the carbon-halogen bond length at the 4-position of tryptophan. Therefore, the short C-F bond and weak electron directionality of fluorine might be the reason of low activity of **5.5**.

To explore the potential halogen-bond interaction between the phenolic hydrogen of Tyr683 and the 5-halogen substituted of tryptophan, **5.6**, **5.7** and **4.41** was tested against *P. aeruginosa* PAO1. Compared to **5.3** and **5.4**, **5.6** and **4.41** displayed dramatically decreased activity. Such loss of activity is similar when shifting the methoxy from 4-position to 5-position. The double Cl substituted analogue **5.7** was completely inactive. The two Cl substituent might change the electronic property of the indole, which makes it a poor halogen-bond donor.

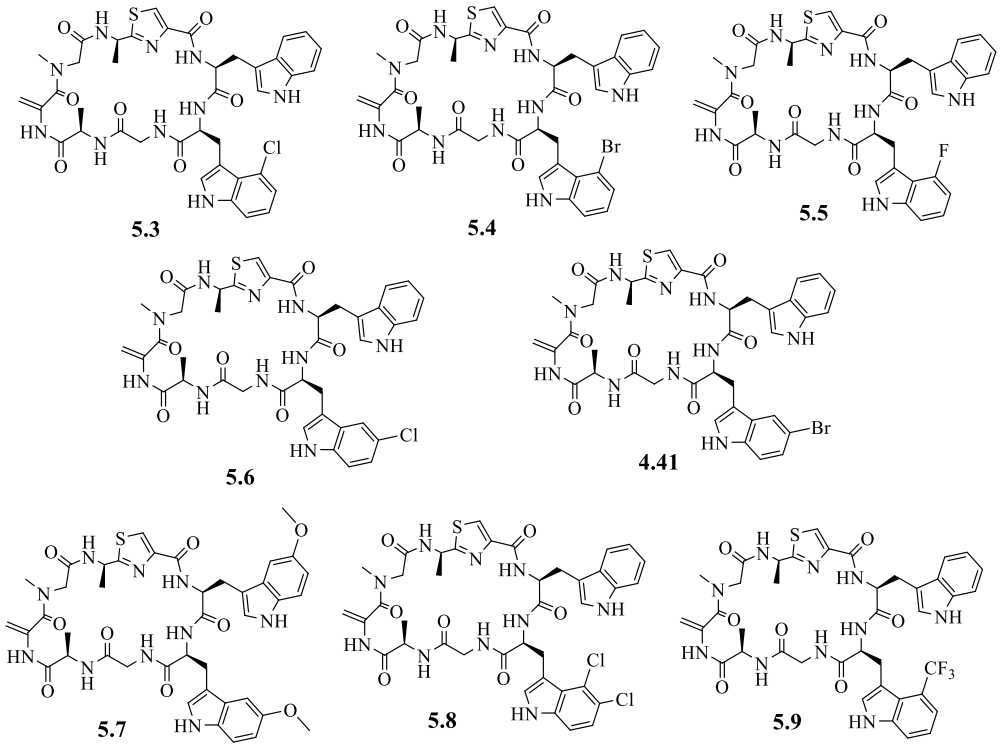


Figure 5.6: Argyrin analogues with modification on tryptophan

Compound	IC_{50} (μM)	% Growth inhibition at 100 μM
1.1	19.8 ± 1.6	82.6 ± 7.4
5.3	16.8 ± 2.9	87 ± 1.0
5.4	13.2 ± 3.2	85.7 ± 0.6
5.5	46.9 ± 2.7	73.3 ± 6.3
4.41	68.9 ± 4.6	65.1 ± 5.6
5.6	>100	45
5.7	>100	n.d.
5.8	>100	n.d.
5.9	>100	4.1 ± 1.9

Table 5.2: IC_{50} and the % growth inhibition of argyrin analogues, with modification on tryptophan, against *P. aeruginosa* PAO1 in MH media at 13 h

Based on the results of the halogen-substituted argyrin analogues, the 4-Cl substituted argyrin **5.3** and the 4-Br substituted argyrin **5.4** were selected as lead analogues. Thus, further modifications were introduced to the other parts of **5.3**.

5.2.2 Activity of Argyrins with Different Dehydroamino Acid Residues Against *P. aeruginosa*

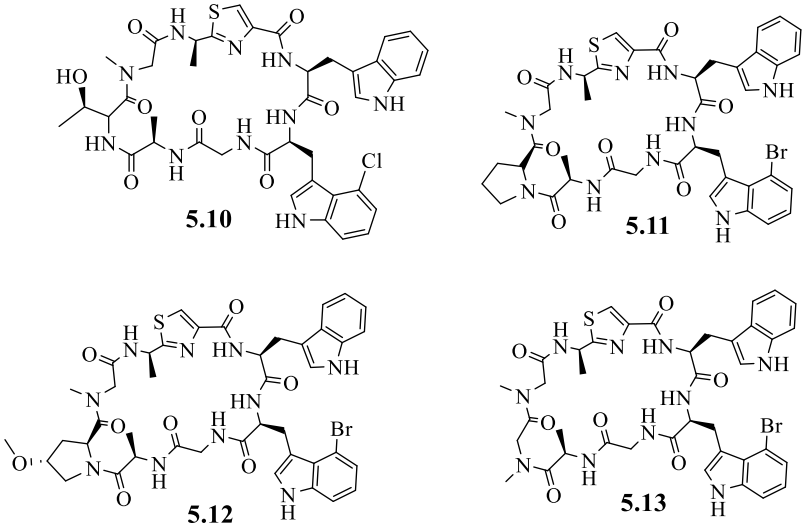


Figure 5.7: Replacement of dehydroalanine functionality

The *exo*-methylene moiety of the dehydroalanine is important for maintaining the planarity of argyrin and restriction the flexibility of the cyclic structure. Hence, replacing the DhA with a threonine residue in **5.10**, a proline **5.11**, a methoxy-proline **5.12** and a sarcosine **5.13** (Figure 5.7) resulted in loss of activity. These results indicated that the *exo*-methylene moiety of the dehydroalanine, which restricts the conformation of argyrin, is absolutely crucial for antibacterial activity. Therefore, a library of argyrin analogues with different β-substituted dehydroamino acid residues are synthesised to shed more light into the SAR.

The success of direct application of dehydrobutyrine during the Fmoc/*t*Bu SPPS allowed access to various dehydrobutyrine containing argyrins. As mentioned in the Section 5.2.1, the 4-substitution on tryptophan is crucial for the antibacterial activity of argyrins. Therefore, 4-Cl, 4-Br and 4-methoxy substituted L-tryptophan argyrin analogues with dehydrobutyrine (Figure 5.8)

were synthesised and tested against *P. aeruginosa* PAO1. The IC_{50} and the % growth inhibition at 100 μM of these three compounds are listed in Table 5.3. Not significantly, by comparing with related dehydroalanine analogues, a 3- to 4-fold increase in activity was discovered. In addition, a similar trend of activity, the 4-Cl and 4-Br tryptophan-containing analogues are more active than the 4-methoxy (Figure 5.9).

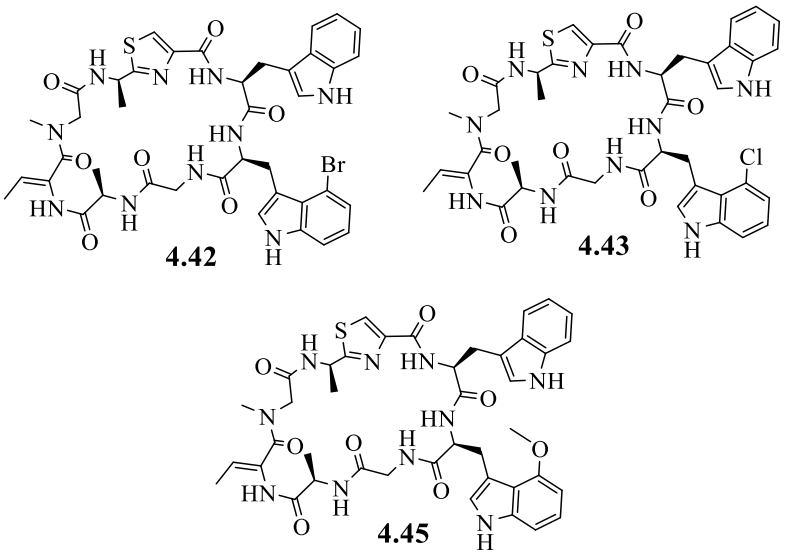


Figure 5.8: DhB containing argyrin analogues with different 4-substituted tryptophans

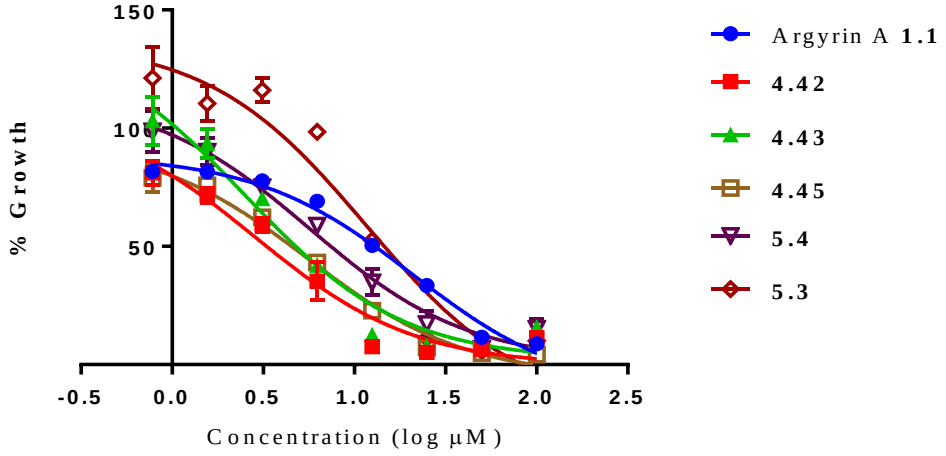


Figure 5.9: The effect of argyrin analogues on the growth of *P. aeruginosa* PAO1 in MH media at 13h

This finding indicates that replacing the dehydroalanine with dehydrobutyrine can improve antibacterial activity. The amide N of F687 might form a potential H-bond interaction with the donor at DhA. An extra methyl group on the dehydrobutyrine might increase the bonding interaction with F687 of EF-G by shortening the bonding distance (Figure 5.10). The β-substitution at the α,β-dehydroamino acids could also contribute to a previously unknown hydrophobic-hydrophobic interaction. In order to investigate such bonding interaction, different β-substituted dehydroamino acids were installed into the argyrin.

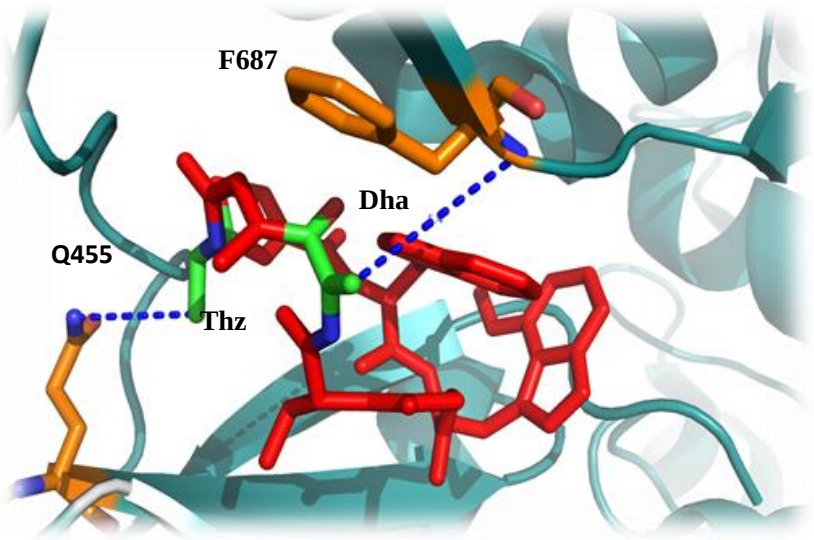


Figure 5.10. Insert view of argyrin B bound to *P. aeruginosa* EF-G with highlighted interaction of F687 with DhA and Q455 and thiazole[322]

Hence, a series of β-substituted dehydroamino acid containing argyrin analogues (Figure 5.11) were synthesised and tested against *P. aeruginosa* PAO1. The IC_{50} and percentage growth inhibition is listed in Table 5.3. The hydrophobicity side chain of these analogues (**4.46**>**4.48**>**4.47**>**4.42**) are anticipated to affect the bonding interaction with EF-G. As observed in Figure 5.12, the increased hydrophobicity of β-side-chain at the dehydroamino acid site of argyrin displays a decrease in the antibacterial activity. In conclusion, the dehydrobutyrine containing argyrin analogue remains the most active against *P.*

aeruginosa PAO1, followed by dehydrovaline and dehydroleucine. The dehydrovaline **4.47** is 3-fold less active as **4.42** (Table 5.3). Crucially, the extra methyl group on the side-chain caused a reduction in antibacterial activity. The dehydroleucine **4.48**, with further extend side-chain, displayed a dramatic reduction in activity. Expectedly, replacing the methyl side-chain with an aromatic group displayed a complete loss of activity, as the dehydrophenylalanine **4.46** is inactive (Table 5.3). The aromatic ring of dehydrophenylalanine was expected to form π-π interaction with the aromatic ring of Phe687 on EF-G. The loss of activity might indicate the distance for the two aromatic is not close in proximity for interaction.

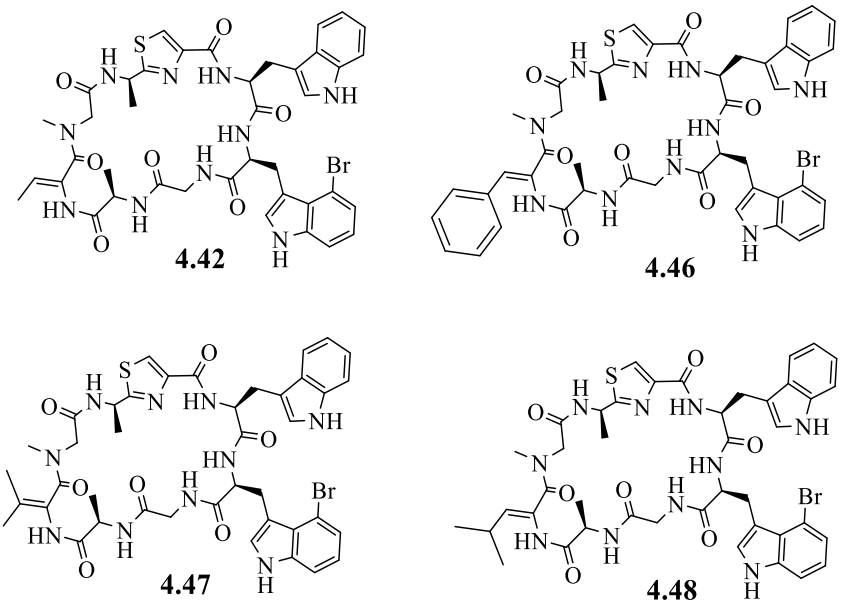


Figure 5.11: 4-Br-L-tryptophan containing argyrins with different dehydroamino acids

In summary, the extended methyl side-chain and the aromatic side-chain cannot improve the bonding affinity of argyrin with EF-G. Therefore, with the promising results seen with dehydrobutyrine halogen-substituted argyrin analogues, the 4-Br substituted dehydrobutyrine argyrin **4.42** was selected as a new lead analogue.

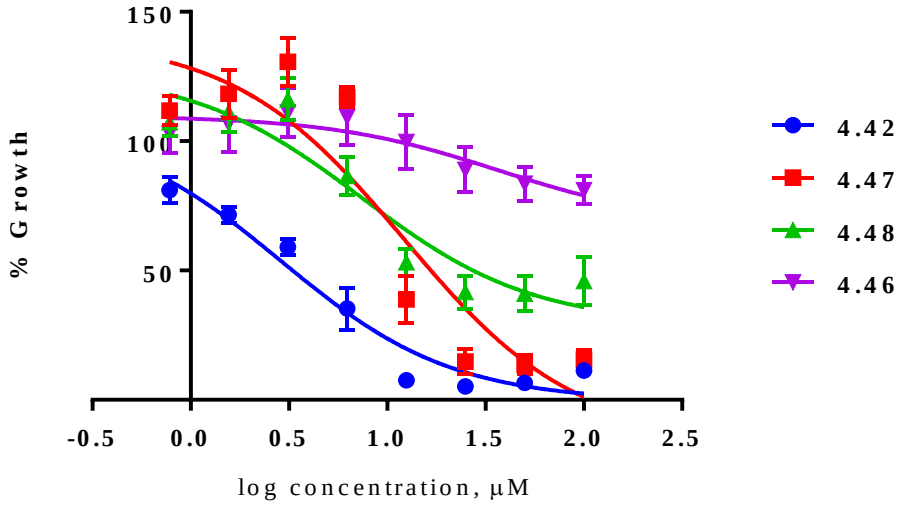


Figure 5.12: The effect of argyrin analogues on the growth of *P. aeruginosa* PAO1 in MH media at 13h

Compound	IC_{50} (µM)	% Growth inhibition at 100 µM
Argyrin A	19.8 ± 1.6	82.6 ± 7.4
4.42	3.7 ± 0.1	91.1 ± 1.1
4.43	3.0 ± 0.4	89.2 ± 2.9
4.45	5.8 ± 0.5	90.2 ± 0.8
4.46	>100	20.1 ± 5.4
4.47	12.19 ± 0.2	85.1 ± 3.4
4.48	>100	40.1 ± 6.8

Table 5.3: IC_{50} and the % growth inhibition of argyrin analogues with modification on tryptophan against *P. aeruginosa* PAO1 in MH media at 13h.

5.2.3 Activity of Thiazole Side-Chain Modified Argyrins Against *P. aeruginosa*

As described early in this chapter, Van der Waals interaction was observed between the thiazole in argyrin B and backbone of Q487 and V488. In addition, as show in Figure 5.10, the methyl-functionality of the thiazole moiety in argyrin is at a desirable distance from the amino group of Q487, which forms a

potential H-bond interaction in the presence of a suitable H-bond donor. However, neither **5.14** or **4.44** (Figure 5.13) showed activity against *P. aeruginosa* PAO1. It is notable that **5.14** is closely related to argyrin F **1.6**. Argyrin F was reported to had a IC_{50} of 5 μg/ml, though less active than argyrin A at 0.12 μg/ml. However, the methylhydroxyl-functionality at the thiazole caused complete loss of antibacterial activity. Replacing the methyl-functionality with methoxy-functionality on thiazole also caused complete loss of antibacterial activity. The methoxy-thiazole used for the synthesis of **4.44** was obtained for Sivaneswary Genapathy.

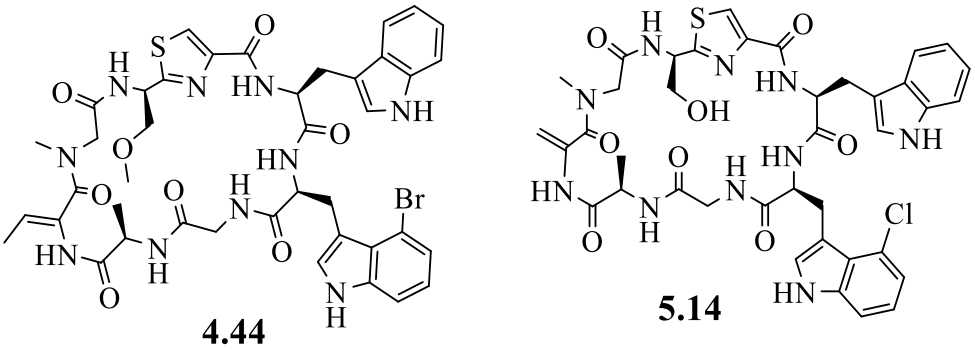


Figure 5.13: Argyrins with modified thiazole side-chain

5.3 Activity of Argyrins Against *B. multivorans*

Apart from *P. aeruginosa*, Nyfeler *et al*. reported the potent antibacterial activity of argyrin B against another multi-drug resistant Gram-negative human pathogen *B. multivorans*. However, no follow-up investigations have been reported. Therefore, the antibacterial activity of the argyrin analogues was tested against *B. multivorans* (Figure 5.14). The pathogenesis and clinical importance of this bacteria was discussed in Chapter 1.

Previously, Chan's research group reported that **5.3** and **5.4** are more potent than argyrin A against *B. multivorans*. In addition, **5.3** and **5.4** are five-fold more potent against *B. multivorans* than against *P. aeruginosa*. The leading compound **4.42** is 2-fold more potent than **5.3** and **5.4** against *B. multivorans*. The IC_{50} of these compounds against *B. multivorans* and *P. aeruginosa* are listed in the Table 5.4.

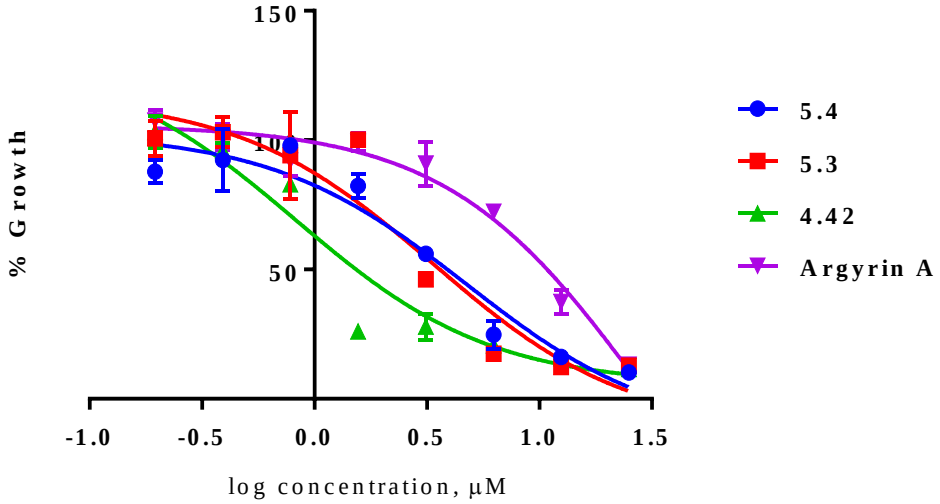
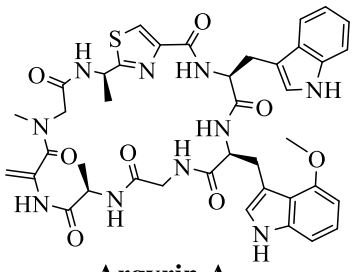
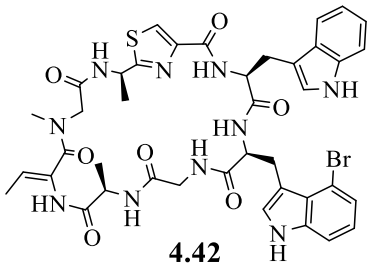


Figure 5.14: The effect of argyrin A and three analogues on the growth of *B. multivorans* at 25 h.

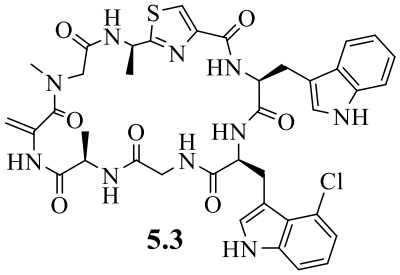
Moreover, **4.43** and **4.45** were also more active against *B. multivorans* than their related dehydroalanine analogues (Figure 5.15 and Table 5.5). This finding indicated that dehydrobutyrine could also improve the antibacterial activity of argyrin against *B. multivorans*. Unexpectedly, the previously observed inactive **4.46** and less active **4.47** and **4.48** against *P. aeruginosa* all displayed excellent activity against *B. multivorans*, at a potency comparable to **4.42**. In contrast, the inactive methoxy thiazole analogue, **4.44** was also inactive against *B. multivorans*.



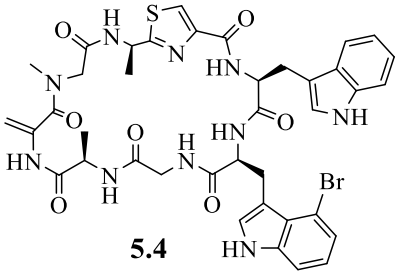
Argyrin A



4.42



5.3



5.4

Organisms	IC_{50} (μM)			
	5.3	**5.4**	**4.42**	Argyrin A
P. aeruginosa PAO1	16.8 ± 2.9	13.2 ± 3.2	3.7 ± 1.0	19.8 ± 1.6
B. multivorans ATCC17616	2.9 ± 2.5	1.6 ± 1.4	0.84 ± 0.1	3.1 ± 1.7

Table 5.4: IC_{50} values for argyrins measured against *P. aeruginosa* at 13 h and *B. multivorans* at 25 h

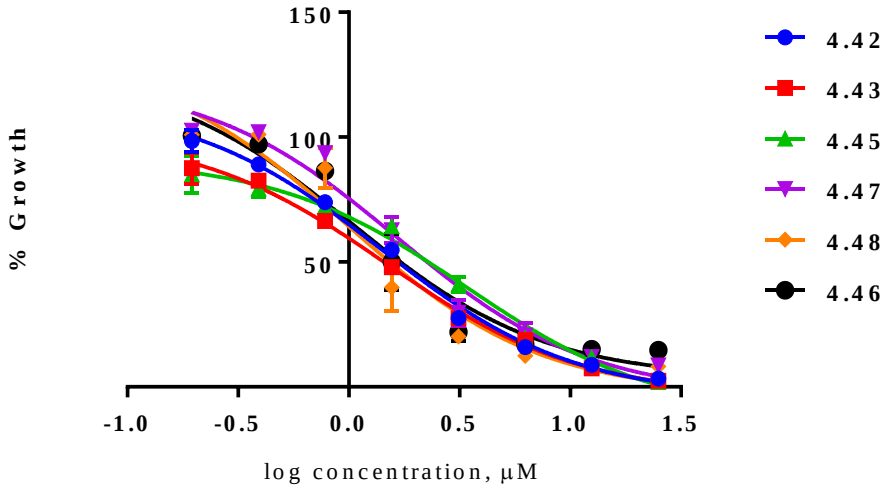
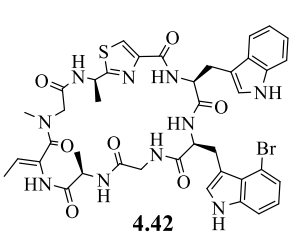
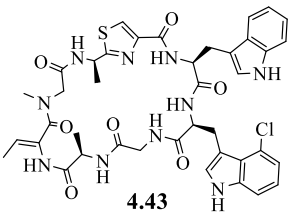


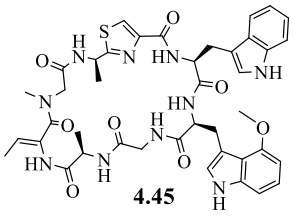
Figure 5.15: The effect of argyrins on the growth of *B. multivorans* at 25 h.



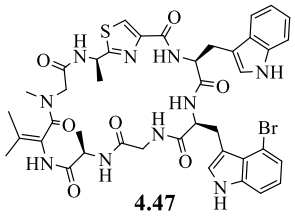
4.42



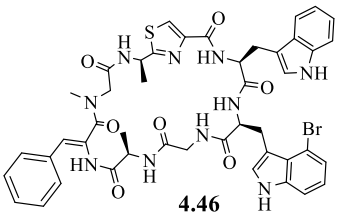
4.43



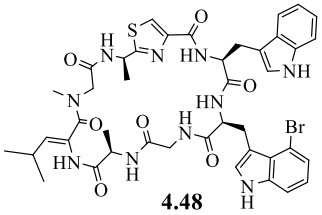
4.45



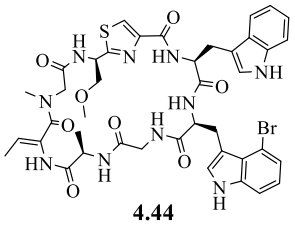
4.47



4.46



4.48



4.44

Compounds	IC_{50} μM
4.42	0.84 ± 0.1
4.43	1.1 ± 0.1
4.44	>100
4.45	3.0 ± 0.2
4.46	1.1 ± 0.2
4.47	1.54 ± 0.2
4.48	0.98 ± 0.1

Table 5.5: IC_{50} values for argyrins measured against *B. multivorans* at 25 h

5.4 The Activity of Argyrins Against Other Organisms

Having identified compound **4.42** as the lead analogue that displayed most potent activity against *P. aeruginosa* and *B. multivorans* so far, the next focus was to test its activity against different microorganisms. The unusual antibacterial activity spectrum of argyrins was first reported by Selva *et al.*, as

shown in Table 1.3. Accordingly, argyrin A, **5.4** and **4.42** were then screened for activity against *Pr. mirabilis*, *Strep. pyogenes* and *Strep. agalactiae* (Figure 5.16 and Table 5.6). As expected, they were inactive against the Gram-positive *Strep. pyogenes* and *Strep. agalactiae*. Previously, the antibacterial activity of **5.3** and **5.4** against *Pr. mirabilis* were reported to be comparable to that against *P. aeruginosa*. Interestingly, the dehydrobutyrine analogues-containing **4.42**, **4.43** and **4.45** displayed a dramatic increase in activity against *Pr. mirabilis* compared with their corresponding dehydroalanine analogues (Table 5.7). Therefore, apart from *P. aeruginosa* and *B. multivorans*, *Pr. mirabilis* can also be a target for dehydrobutyrine containing argyrin analogues.

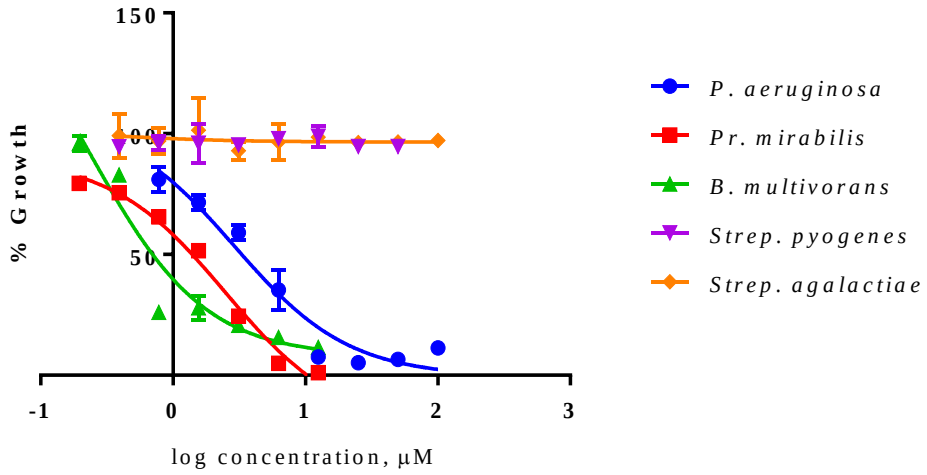
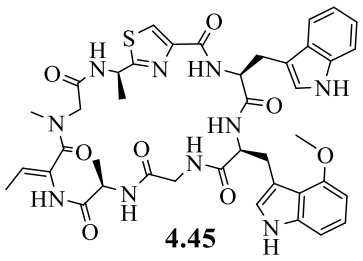


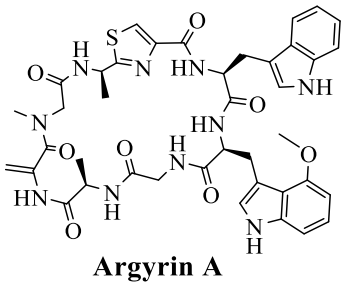
Figure 5.16: The effect of **4.42** on the growth of various organisms at 13 h (*B. multivorans* at 25 h).

Organism	IC_{50} (µM)		
	4.42	**5.4**	Argyrin A
P. aeruginosa PAO1	3.7 ± 1.0	13.2 ± 3.2	19.8 ± 1.6
Pr. mirabilis Hauser 1885	3.5 ± 1.6	15.6 ± 5.6	19.2 ± 1.7
B. multivorans ATCC17616	0.84 ± 0.1	1.6 ± 1.4	3.1 ± 1.7
Strep. pyogenes	>100	>100	>100
Strep. agalactiae	>100	>100	>100

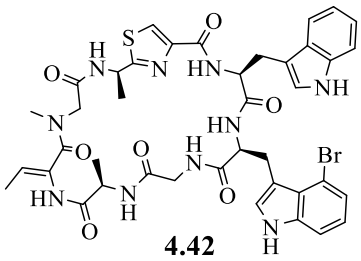
Table 5.6: IC_{50} values for argyrins measured at 13 h (*B. multivorans* at 25 h)



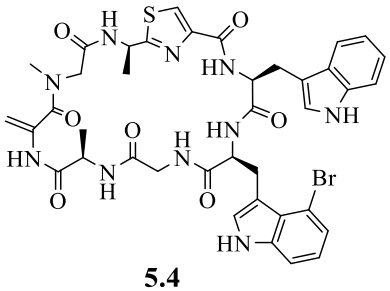
4.45



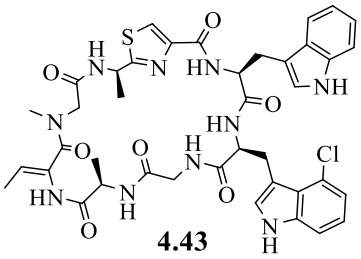
Argyrin A



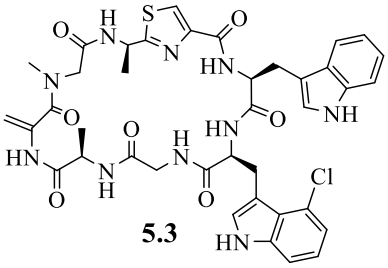
4.42



5.4



4.43



5.3

Compounds	IC_{50} μM
4.42	2.5 ± 1.6
4.43	2.4 ± 1.4
4.45	3.9 ± 1.2
5.3	16.7 ± 4.2
5.4	15.6 ± 5.6
Argyrin A	19.2 ± 1.7

Table 5.7: IC_{50} values for argyrins against *Pr. mirabilis* measured at 13 h

5.5 Molecular Target of Argyrins

The section above discussed the activity of argyrins against different bacteria. The molecular target of argyrin A and B in *P. aeruginosa* was identified as the conserved bacterial protein EF-G.[170,199] With the help of NCBI protein-protein basic local alignment search tool (BLAST) analysis, Sivaneswary Genapathy

confirmed the EF-G in all the organism tested (Table 5.6) has high degree of homology (>59%) to EF-G of *P. aeruginosa*. [322]

Nyfeler *et al*. and Bielecki *et al.* used the whole genome sequencing of *P. aeruginosa* mutants with reduced susceptibility to argyrin A and B and identified seven point mutations, which are P414S, S417L, S459F, P486S, L663Q, T671A, and Y683C, in the *fusA1* gene that encodes EF-G. Sivaneswary Genapthy adopted this method. She aligned the amino acid sequence of EF-G of these organisms against that of *P. aeruginosa* PAO1 using ClustalX sequence alignment methodology[323].[322] The results displayed a striking conservation in all the corresponding EF-G amino acids in *P. aeruginosa, B. multivorans,* and *Pr. mirabilis*. However, the two *Streptococci sp*. seems to have a Glu in place of Ser417, Ala in place of Ser459, and Phe in place of Y683. Nevertheless, the amino acid substitutions in the *Streptococci sp.* are different to those substitutions in *P. aeruginosa* mutants with reduced susceptibility to argyrins. It can then be concluded that the EF-G is the molecular target of argyrin in *B. multivorans,* and *Pr. mirabilis*. Moreover, the organism specific activity of argyrin may not due to the variation in the molecular target. However, other factors such as the difference in cell wall penetration and outer membrane permeability may also be considered. The finding may also partly explain the trend of activity of analogues are similar among different organisms. For example, the 4-Cl and 4-Br substituted analogue are more active than the 4-Me substituted. However, the different dehydroamino acids analogues (**4.42**, **4.46**, **4.47** and **4.48**) are all active against *B. multivorans* while only two of them (**4.42** and **4.47**) are active against *P. aeruginosa*.

5.6 Conclusions

In conclusion, this chapter outlined the investigation into the SAR that governs the antibacterial activity of argyrin against *P. aeruginosa*. The most potent *in vitro* activity was observed with 4-Br-L-tryptophan dehydrobutyrine containing argyrin analogue **4.42**.

It was first concluded that the crucial H-bond interaction between the oxygen atom of 4-MeO-tryptophan and S417 of EF-G could be replaced with a halogen-bond. The 4-halogenated tryptophan is important for antibacterial activity. Further, modification on the thiazole side chain of the argyrin resulted in complete loss of activity.

Previously, it was established that substitution of DhA with threonine, proline, sarcosine and methoxy proline resulted in loss of activity. However, replacing the dehydroalanine with dehydrobutyrine resulted in a dramatic 4-fold increase in activity. In contrast, the dehydrovaline analogue displayed a small increase in activity, while the dehydrophenylalanine was inactive and dehydroleucine displayed a dramatic decrease in activity. The result suggests that the dehydroamino acid residue not only restrict the planarity of the cyclic structure but also plays a crucial role in the antibacterial activity of argyrin. However, the potential pocket of EF-G around the dehydroalanine is apparently unable to allow large hydrophobic moieties, such as the side-chain of dehydroleucine and aromatic ring of dehydrophenylalanine.

Moreover, analogue **4.42** was found to be 4-fold more potency against *B. multivorans* compared to *P. aeruginosa*. It displayed similar potency against *Pr. mirabilis* compared to *P. aeruginosa*. Such results are supported by the fact that argyrins targets the EF-G of these organisms. Unexpectedly, the β-substituted

dehydrobutyrine-containing analogues **4.42**, **4.43** and **4.45** are 6-fold more potent against *Pr. mirabilis* than their corresponding dehydroalanine analogues.

Overall, the SAR findings reported in this Chapter encouraged further investigation of argyrin antibacterial activity against the multi-drug resistant bacteria, particularly *P. aeruginosa* and *B. multivorans*.

Chapter 6
General Conclusion and Future Work

6.1 General Conclusion

The argyrins (Figure 1.9), a family of eight cyclic peptides, were isolated from the *Archangium gephyra* strain during the screening of myxobacteria as a potential source of novel antibiotics. The argyrins displayed an unusual spectrum of antibacterial activity against certain Gram-positive and Gram-negative bacteria. Most notably, they displayed potent activity against the multi-drug resistant human pathogens, *P. aeruginosa* and *B. multivorans*, which encouraged the research work carried out in this thesis.

The primary aim of this thesis was to synthesise argyrin analogues with improved antibacterial activity by evaluation of the SAR of argyrin towards *P. aeruginosa*. In 2012, the EF-G was identified as the conserved cellular target of argyrin A and B in *P. aeruginosa*. The key interaction of argyrin with EF-G was established by the co-crystal complex of argyrin bound *P. aeruginosa* EF-G.

The total synthesis of argyrin analogues was achieved through Fmoc/*t*Bu solid-phase peptide synthesis followed by a solution-phase head-to-tail macrocyclisation (Figure 6.1). Three unusual building blocks, *N*-Boc-thiazole dipeptide **1.29**, substituted L-tryptophan analogues **1.30** and Fmoc-dehydroamino acid (masked precursor *N*-Fmoc-Sec(Ph) **1.28** for dehydroalanine) (Figure 4.1), for the assembly of the linear argyrin using Fmoc/*t*Bu SPPS strategy were synthesised. The synthetic routines and the outcomes are summarised in the sections below.

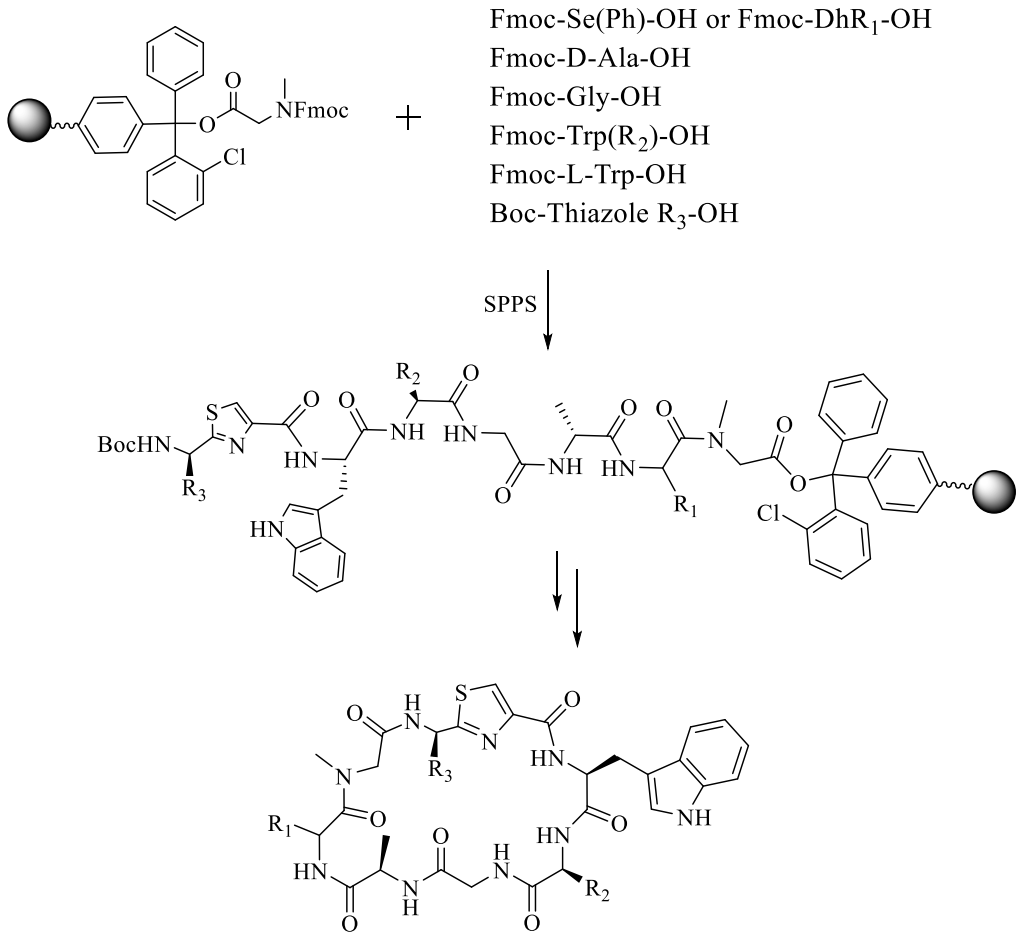
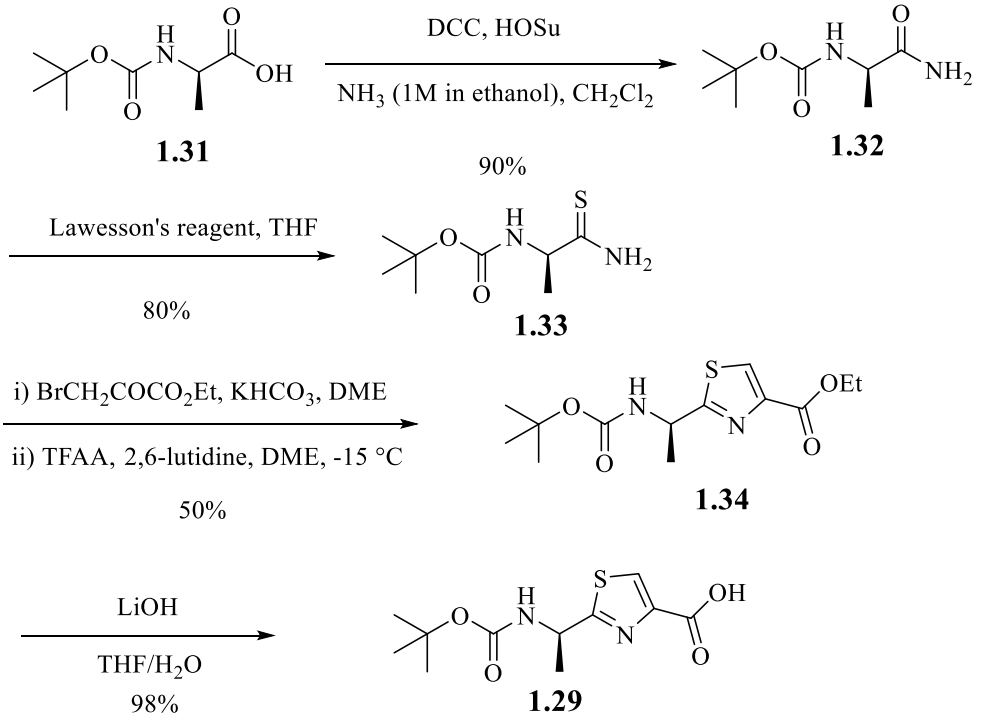


Figure 6.1: Combination of Fmoc/*t*Bu SPPS strategy and macrocyclisation for the synthesis of argyrin analogues

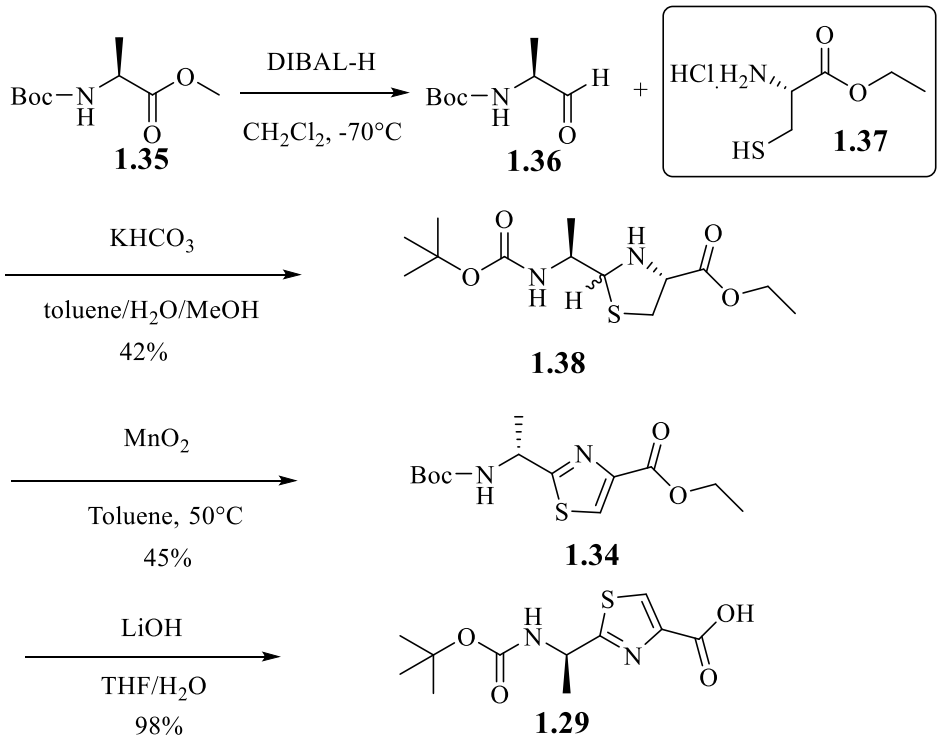
6.1.1 Synthesis of Thiazole Dipeptide

The *N*-Boc-thiazole dipeptide was synthesised using Schmidt's modified Hantzsch thiazole synthesis method (Scheme 6.1). The *N*-Boc protect D-alanine **1.31** was converted to the corresponding thioamide **1.33** through an intermediate amide **1.32**. The resultant thioamide was condensed with ethyl bromopyruvate to generate an intermediate which was then reacted with trifluoroacetic anhydride (TFAA) and 2,6-lutidine to afford the *N*-Boc protected thiazole dipeptide ethyl ester **1.34**. The ethyl ester was hydrolysed with lithium hydroxide to give the *N*-Boc protected thiazole amino acid **1.29** in an overall yield of 30-40%.



Scheme 6.1: Total synthesis of thiazole dipeptide using Schmidt's modified Hantzsch method

However, owing to the use of unpleasant Lawesson's reagent, an alternative method was evaluated. The alternative method (Scheme 6.2) was achieved by the condensation of L-cysteine **1.37** with pyruvaldehyde **1.36** to form a thiazolidine **1.38**, which was then oxidized to thiazole **1.34** using MnO_2. The ethyl ester was hydrolysed with lithium hydroxide to give the *N*-Boc protected thiazole amino acid **1.29** in an overall yield of 30%. Although these two approaches resulted in similar yields, the thiazolidine method avoided the usage of unpleasant Lawesson's reagent and all the reagents are commercially available and cheap. In addition, this later method is scalable.

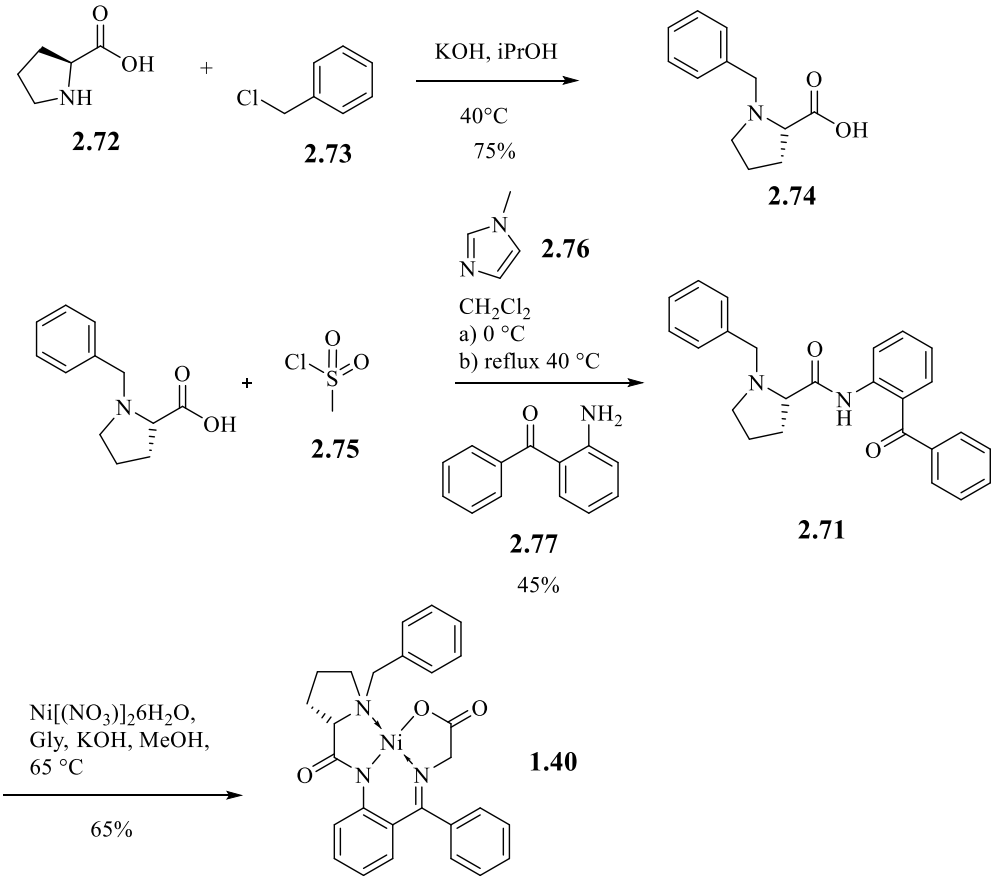


Scheme 6.2: Alternative total synthesis of thiazole dipeptide

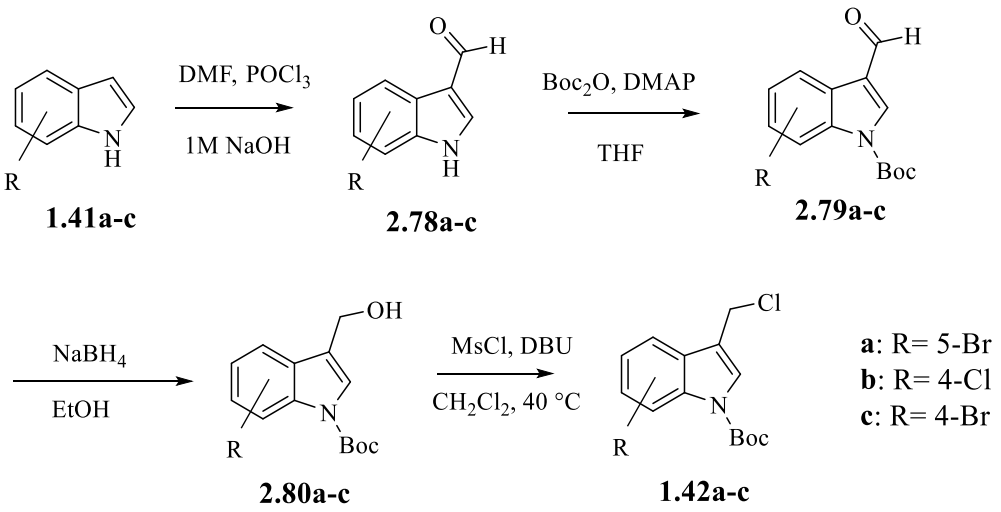
6.1.2 Asymmetric Synthesis of Substituted Tryptophans

Chapter 2 also reported the synthesis of various substituted Fmoc-(*S*)-tryptophans to investigate the role of tryptophan in the antibacterial activity of

argyrin. An operationally convenient asymmetric synthesis of substituted (*S*)-tryptophan analogues was established using the BPB-glycine-Ni(II) Schiff base **1.40**. The substituted indole methyl chloride **1.42** was alkylated with **1.40** to afford the intermediate **1.43**. The intermediate **1.43** was then hydrolysed with 6M HCl in a microwave-assisted reaction condition to yield the optically pure (>90% *ee*) substituted tryptophan, which was then Fmoc-protected to afford the desired substituted Fmoc-(*S*)-tryptophan for Fmoc/*t*Bu SPPS (Scheme 6.3, 6.4 and 6.5). The key characterisation data and overall yields are listed in Table 6.1.

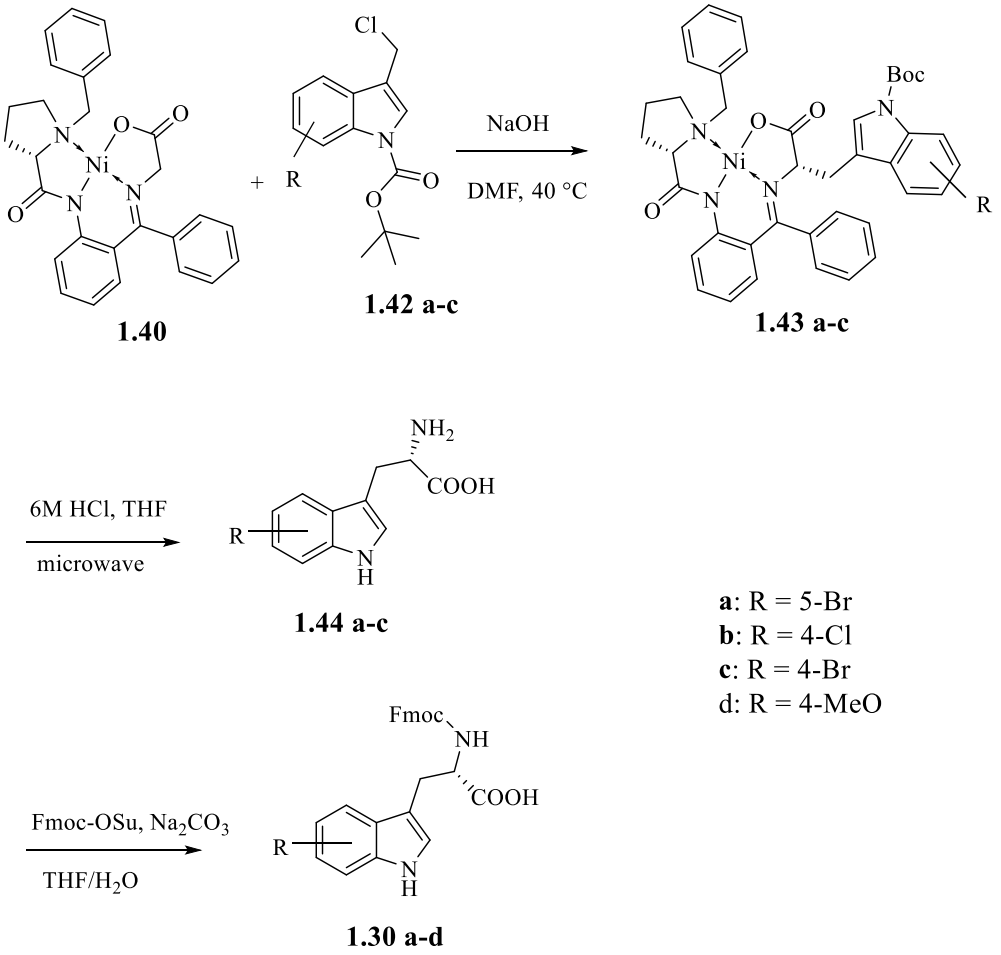


Scheme 6.3: Total synthesis of BPB-glycine Ni(II) complex



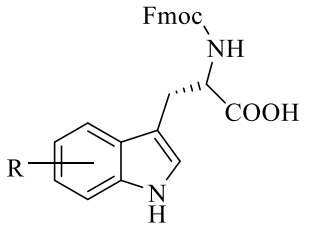
1.41a-c 2.78a-c 2.79a-c 2.80a-c 1.42a-c

Scheme 6.4: Total synthesis of alkyl chloride



1.40 1.42 a-c 1.43 a-c 1.44 a-c 1.30 a-d

Scheme 6.5, Alkylation, hydrolysis and Fmoc-protection



a: R = 5-Br
b: R = 4-Cl
c: R = 4-Br
d: R = 4-MeO

1.30 a-d

Compounds	Yield%	Melting point °C	$[\alpha]_D^{24}$ (MeOH)
5-Br **1.30 a**	15	130–131	-28.3 (*c* = 1.0)
4-Cl **1.30 b**	15	103–105	-12.3 (*c* = 1.0)
4-Br **1.30 c**	20	92–94	-23.3 (*c* = 1.0)
4-MeO **1.30 d**	50	172–173	-24.5 (*c* = 1.0)

Table 6.1. Key characterization of Fmoc-(*S*)-tryptophan Derivatives

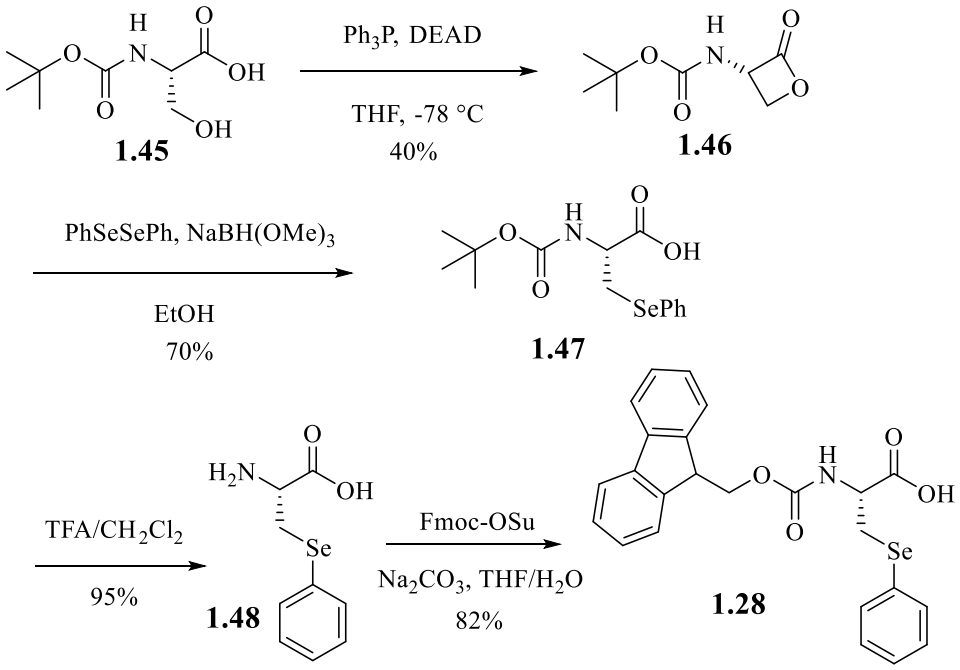
6.1.3 Synthesis of *N*-Fmoc-phenylselenocysteine

The synthesis of *N*-Fmoc-phenylselenocysteine **1.28** was achieved using the procedure reported by Okeley *et al.* (Scheme 6.6). The commercially available Boc-L-serine was **1.45** firstly converted to its β-lactone **1.46**, followed by ring opening with phenylselenide anion obtained by reaction of sodium trimethoxyborohydride with diphenyl diselenide. For usage in Fmoc SPPS, the *N*-Boc-Sec(Ph)-OH **1.47** was converted into desired Fmoc-Sec(Ph)-OH **1.28** through standard methods. The overall yield of the reaction was around 30%.

6.1.4 Synthesis of Dehydrobutyrine and Dehydrophenylalanine

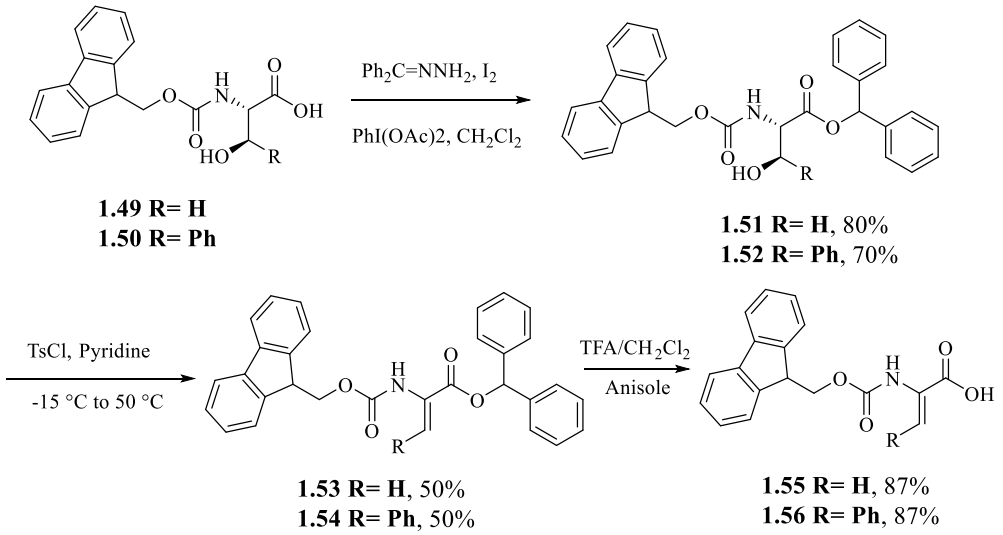
Fmoc-(2*R*,3*S*)-3-methyl-*Se*-phenylselenocysteine for the synthesis of dehydrobutyrine-containing peptides reported by Van der Donk *et al*. was

adopted in this thesis for the synthesis of dehydrobutyrine-containing argyrin analogues. However, during conversion of hydroxyl group to tosyl group, the reaction resulted in the mixture of *O*-tosylate and a by-product in a ratio of 4:1. The by-product was predicted to be Fmoc-dehydrobutyrine Dpm ester **1.53**. Taking the advantage of the β-elimination reaction occurring during the *O*-tosylation reaction, a modified reaction procedure was established to synthesise dehydrobutyrine and dehydrophenylalanine from threonine and hydroxyphenylalanine (Scheme 6.7).



Scheme 6.6: Total synthesis of masked precursor Fmoc-Sec(Ph)

Thus, the Fmoc-threonine and Fmoc-hydroxyphenylalanine were converted to the corresponding Dpm esters. The corresponding Dpm ester then underwent a β-elimination mediated by TsCl and pyridine. In both cases, a tosylation intermediate was initially formed under low temperature, followed by the high temperature promoted elimination. The resulting Dpm ester protected Fmoc-dehydroamino acids were deprotected by acidolysis using TFA/DCM/anisole to afford pure Fmoc-dehydroamino acids in good yields.

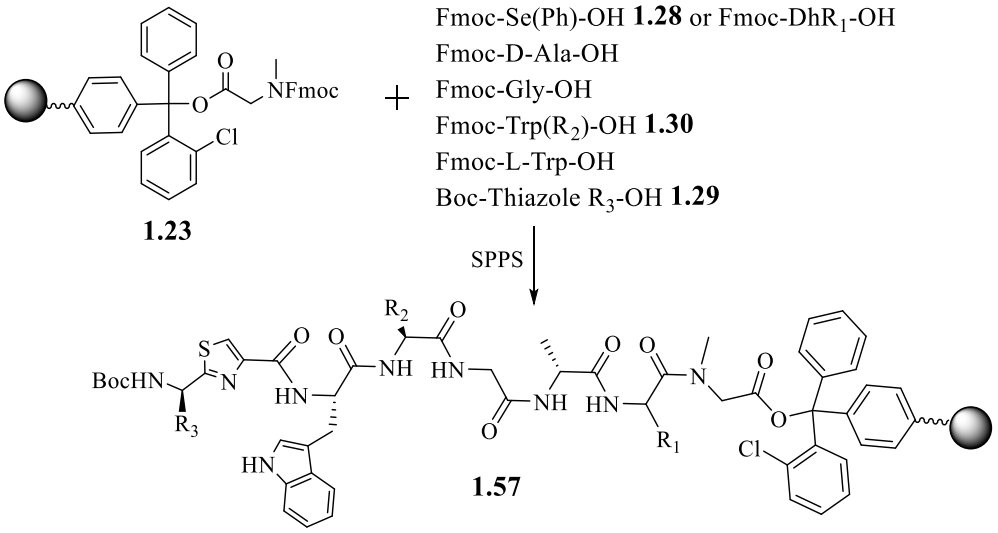


Scheme 6.7: Synthesis route for Fmoc-dehydroamino acids using β-elimination

6.1.5 Fmoc/*t*Bu Solid-Phase Peptide Synthesis of Argyrin Analogues

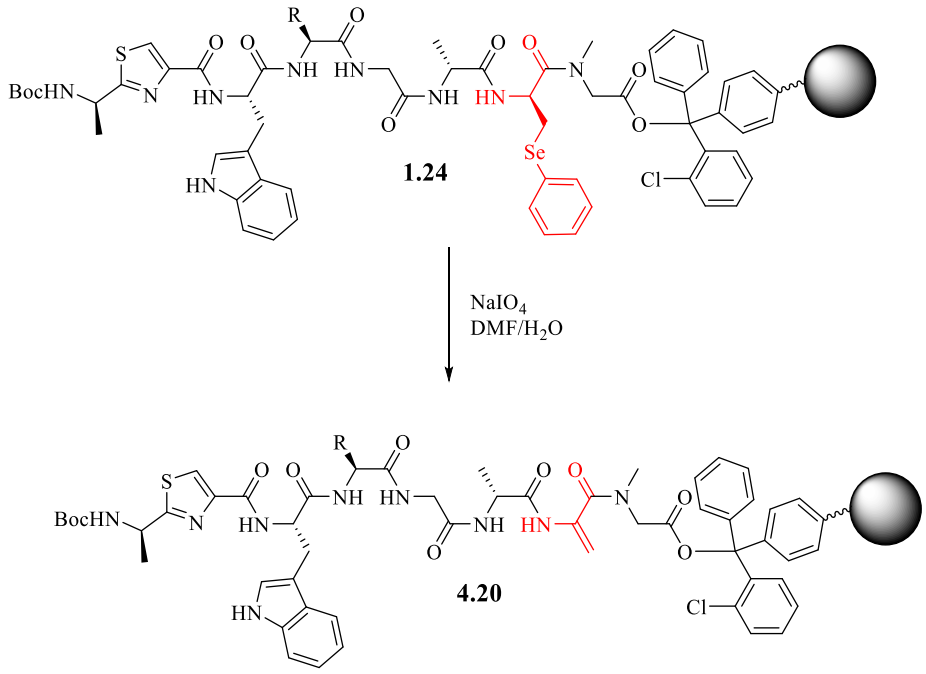
Chapter 4 described the application of Fmoc/*t*Bu SPPS and solution-phase head-to-tail macrocyclisation to afford argyrin analogues. For a successful Fmoc/*t*Bu SPPS of argyrin, 2-chlorotrityl chloride resin was selected as the solid support. The N^{α}-Fmoc-sarcosine was selected as the *C*-terminal amino acid, which was "loaded" on the resin. All the couplings were carried out using HATU and DIPEA in DMF as the carboxyl-activating mixture. The N^{α}-Fmoc-deprotection was performed using a continuous flow of 20% piperidine in DMF by a semi-automated peptide synthesiser (Scheme 6.8).

In addition, Chapter 4 reported the successful direct application of β-substituted Fmoc-dehydroamino acid to the Fmoc/*t*Bu SPPS. The four Fmoc-dehydroamino acids (**1.55**, **1.56**, **4.24** and **4.25**) were proved to be stable during the repeated coupling and deprotection process of the Fmoc/*t*Bu SPPS.



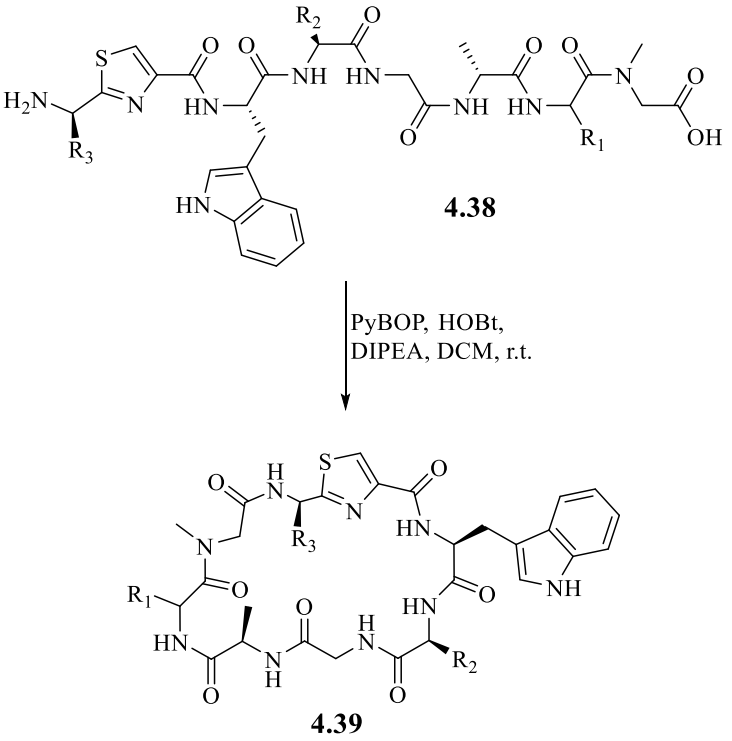
Scheme 6.8: Argyrin linear peptide precursor assembly

In terms of obtaining the dehydroalanine moiety of the target argyrin, an on-resin oxidative elimination of the Sec(Ph) residue was achieved using $NaIO_4$ (Scheme 6.9).



Scheme 6.9: On-resin oxidative elimination of phenylselenocysteine

After the full assembly of linear peptide sequence, a simultaneous deprotection of N^{α}-Boc-deprotection and cleavage from resin was achieved using 50% TFA in DCM. The crude linear precursors after cleavage were subjected to a solution-phase macrocyclisation using PyBOP and HOBt in the presence of DIPEA. A 0.5 mM reaction concentration ensured an intramolecular cyclisation (Scheme 6.10). The resultant cyclic peptides were purified using preparative RP-HPLC to achieve >95% purity. a Phenomenex Luna® 5 µm C18(2) 100 Å, AXIA™ Packed LC column (250 x 21.20 mm) with flow rate 20 mL min^{-1} was used for large scale purification. The key characterisation data and yields are listed in Table 6.2. The yields listed in the table are based on original resin loading (0.1 mmol).



Scheme 6.10. Macrocyclisation of argyrin linear precursors

Sequence	T_R (min)	HR-MS calculated	HR-MS found	Yield%
Cyclo[D-Ala-Thz-Trp-Thr(Bzl)-Gly-D-Ala-DhA-Sar] **4.40**	9.42	799.3112	800.0704	15
Cyclo[D-Ala-Thz-Trp-Trp(5-Br)-Gly-D-Ala-DhA-Sar] **4.41**	9.34	873.2137	873.2130	20
Cyclo[Ala-Thz-Trp-Trp(4-Br)-Gly-D-Ala-DhB-Sar] **4.42**	9.87	887.2293	887.2287	25
Cyclo[Ala-Thz-Trp-Trp(4-Cl)-Gly-D-Ala-DhB-Sar] **4.43**	9.55	865.2623	865.2650	15
Cyclo[D-Ser(OMe)-Thz-Trp-Trp(4-Br)-Gly-D-Ala-DhB-Sar] **4.44**	9.50	917.2399	917.2375	19
Cyclo[D-Ala-Thz-Trp-Trp(4-MeO)-Gly-D-Ala-DhB-Sar] **4.45**	9.46	839.3294	839.3309	25
Cyclo[D-Ala-Thz-Trp-Trp(4-Br)-Gly-D-Ala-DhPh-Sar] **4.46**	10.90	949.2450	949.2402	15
Cyclo[D-Ala-Thz-Trp-Trp(4-Br)-Gly-D-Ala-DhVal-Sar] **4.47**	10.09	901.2450	901.2435	24
Cyclo[D-Ala-Thz-Trp-Trp(4-Br)-Gly-D-Ala-DhLeu-Sar] **4.48**	11.30	915.2606	915.2622	22

Table 6.2: The key characterisation data and yields of argyrins

6.1.6 SAR studies of Argyrins

Chapter 5 described the investigation into the SAR that governs the antibacterial activity of argyrins against *P. aeruginosa*. This chapter confirmed that the crucial H-bond interaction between the oxygen atom of 4-MeO-tryptophan and S417 of EF-G can be replaced with a halogen-bond. The 4-halogenated

tryptophans, especially the 4-Cl and 4-Br derivatives, were found to be important for antibacterial activity. The 4-Cl and 4-Br analogues **5.3** and **5.4** (Figure 6.2) were concluded as lead analogues in our research group. Further modifications were made based on these two analogues. However, modification on the thiazole side chain **4.44** (Figure 6.2) resulted in complete loss of activity.

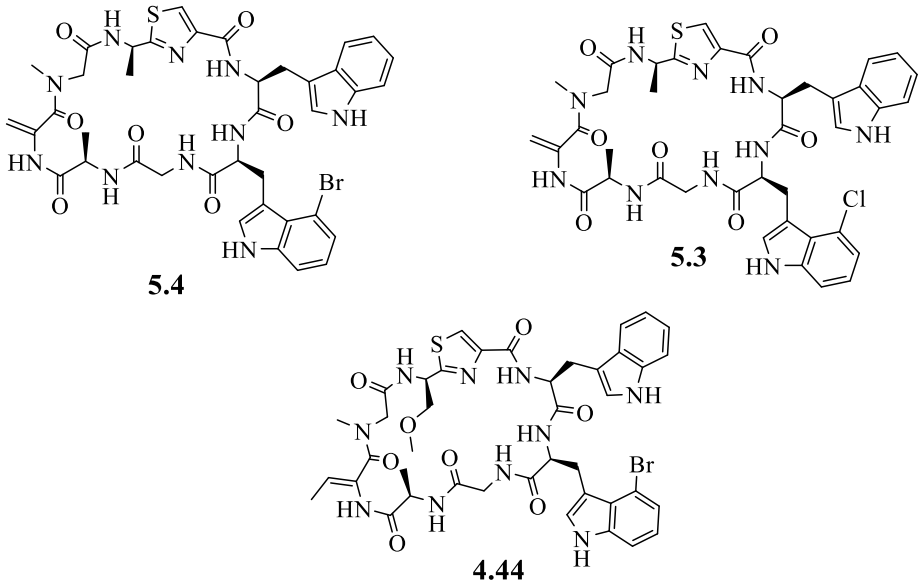
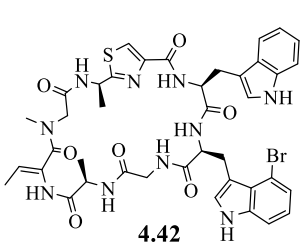


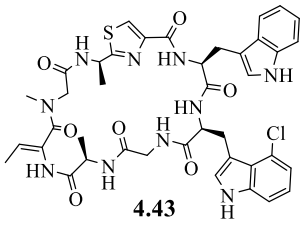
Figure 6.2: Compounds **5.3**, **5.4** and **4.44**.

Most importantly, this chapter established the importance of α,β-dehydroamino acid residue in the argyrin in two aspects. Firstly, after replacing the DhA with threonine, proline, sarcosine and methoxy proline (tertiary amides), the resulting argyrin analogues were found to be inactive. This result indicated the *exo*-methylene moiety of the dehydroalanine was crucial for maintaining the planarity of argyrin and in restricting the flexibility of the cyclic structure. Secondly, replacing the dehydroalanine with β-substituted dehydroamino acids (dehydrobutyrine, dehydrovaline, dehydrophenylalanine and dehydroleucine), an interesting trend of activity was observed. Replacing the dehydroalanine with dehydrobutyrine resulted in a 4-fold increase in activity when tested against *P. aeruginosa*. The dehydrovaline-containing analogue displayed a small increase in activity while dehydroleucine displayed a dramatic decrease in activity and

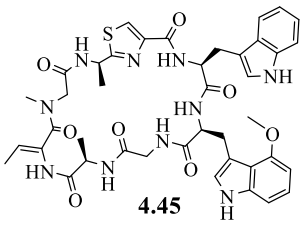
dehydrophenylalanine was inactive against *P. aeruginosa*. The 4-Br-L-tryptophan dehydrobutyrine containing analogue **4.42** displayed most potent antibacterial activity against *P. aeruginosa*, *Pr. mirabilis* and *B. multivorans* (Table 6.3).



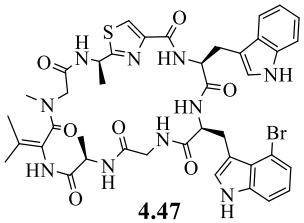
4.42



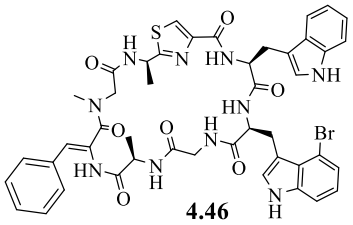
4.43



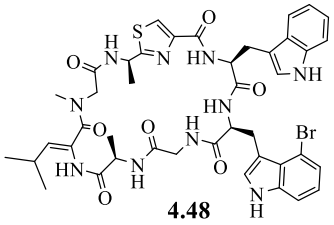
4.45



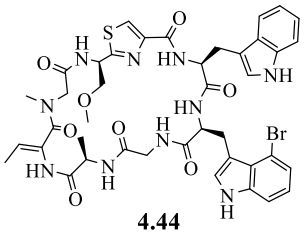
4.47



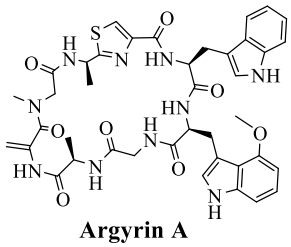
4.46



4.48



4.44



Argyrin A

Compound	IC_{50} (μM)		
	P. aeruginosa PAO1	*Pr. mirabilis* Hauser 1885	*B. multivorans* ATCC17616
4.42	3.7 ± 1.0	2.5 ± 1.6	0.84 ± 0.1
4.43	3.0 ± 0.4	2.4 ± 1.4	1.1 ± 0.1
4.44	>100	>100	>100
4.45	5.8 ± 0.5	3.9 ± 1.2	3.0 ± 0.2
4.46	>100	n.d	1.1 ± 0.2
4.47	12.19 ± 0.2	n.d	1.54 ± 0.2
4.48	>100	n.d	0.98 ± 0.1
Argyrin A	19.8 ± 1.6	19.2 ± 1.7	3.1 ± 1.7

Table 6.3: IC_{50} of argyrins at 13 h (*B. multivorans* at 25h)

Moreover, **4.42** was found to be most potent compound against *B. multivorans* and *Pr. mirabilis* among all the analogues tested so far. It was found to be 4-fold more potent against *B. multivorans* compared to *P. aeruginosa*. It displayed similar potency against *Pr. mirabilis* compared to *P. aeruginosa* (Table 6.3). Nevertheless, the 4-Br tryptophan β-substituted dehydroamino acid-containing analogues (apart from **4.44**) were found to be broadly equally potent against *B. multivorans*. Significantly, these analogues are more potent against *B. multivorans* than the parent compound, argyrin A. Previously, with the help of BLAST analysis and ClustalX alignment, Sivaneswary Genapthy suggested that EF-G might be molecular target of argyrins in *B. multivorans* and *Pr. mirabilis*. The results obtained in this thesis might encourage further investigating in this aspect.

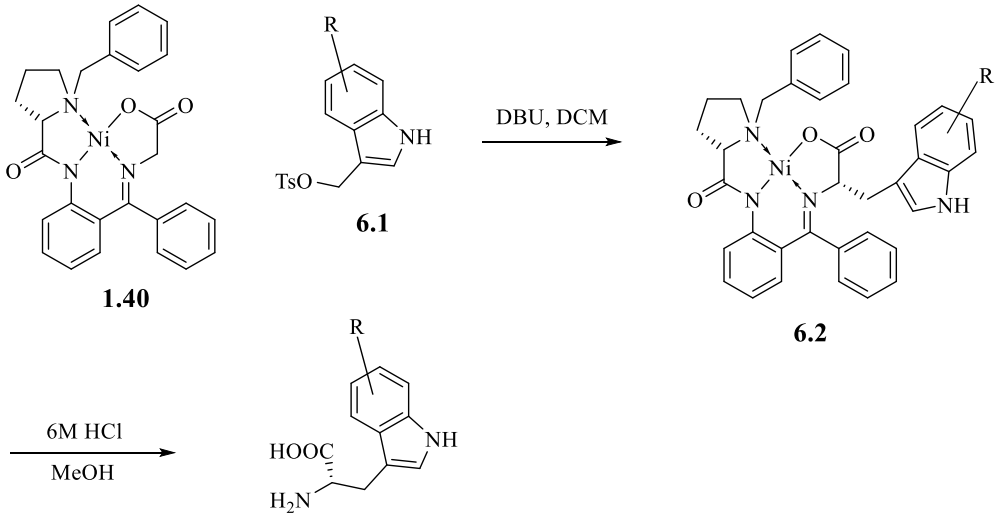
6.2 Future Work

The primary aim of this thesis was to synthesise an argyrin analogue with most potent antibacterial activity. The **4.42**, which contains dehydrobutyrine and 4-Br-L-tryptophan residues compound was identified as the most potent analogue tested so far. It displayed potent antibacterial activity against *P. aeruginosa, B. multivorans* and *Pr. mirabilis*. Therefore, it was regarded as the lead analogue.

6.2.1 Optimisation of the Synthetic Procedure and Purification

The future work will include the development of synthetic route for manufacturing the lead analogue in medium to large scale. Initially,

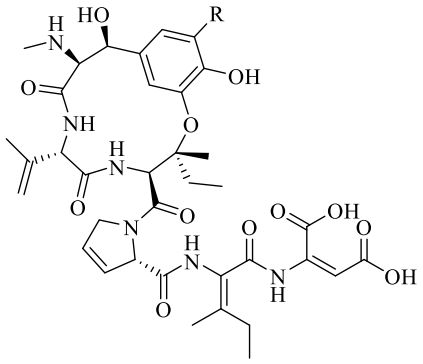
optimisation will be applied to the synthesis of the three unnatural building blocks. As mentioned in Chapter 2, both the *N*-Boc-thiazole dipeptide and *N*-Fmoc-4-Br-L-tyrptophan can be synthesised in relative large scale. It is reported by Belokon *et al*. that BPB-glycine-Ni(II) Schiff base **1.40** can be synthesised in 70 g scale. The major shortage of the asymmetric tryptophan adopted in this thesis is the unstable indole alkyl chloride **1.42**. Wang *et al*. reported the Michael additions of glycine-Ni(II) Schiff base **1.40** to sulfonylindoles, e.g. the tosylates, for the synthesis of tryptophan. Hence, it is proposed that the sulfonylindoles **6.1** will be used instead of the highly unstable indole methyl chloride (Scheme 6.11). The BPB-glycine-Ni(II) Schiff base was previously reacted with various substituted sulfonylindoles in the presence of DBU to afford **6.2** with excellent diastereoselectivity at the α-carbon. The desired (*S*)-tryptophan analogue is then easily obtained after the disassembly of the corresponding Ni(II) complex.



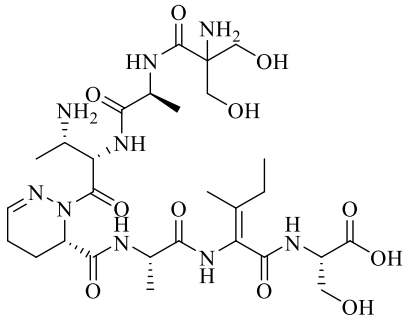
Scheme 6.11: Michael additions of BPB-glycine-Ni(II) Schiff base **1.40** to sulfonylindoles

In this thesis, all the argyrin analogues were synthesised using *Z*-dehydroamino acids. The *Z*- or *E*-isomerism of dehydroamino acid could be critical for biological activity of argyrin. The *Z*-isomers are much more common than the *E*-isomers that are found in natural occurring bioactive compounds. However,

in the case of antimitotic peptides phomopsins A and B (Figure 6.3), the dehydroisoleucine is *E*-isomer.[324] In addition, the antibiotic heptapeptide antrimycin A[325] (Figure 6.3) are also characterised to contain *E*-dehydroisoleucine. Therefore, the *E*-isomer of all the three analogues (**4.42**, **4.46** and **4.48**) reported in this thesis will be synthesised. In addition, the dehydroisoleucine containing argyrin analogues will also be synthesised in both *Z*- and *E*-isomer. These analogues all contain hydrophobic side chain on the dehydroamino acid moiety. More importantly, these *E*-dehydroamino acid containing analogues offer opportunities for the comparative biological and chemical studies. Figure 6.4 lists the analogues to be synthesised in future.



Phomopsin A: R = Cl
Phomopsin B: R = H



Antrimycin A

Figure 6.3: Chemical structure of Antrimycin A and Phomopsin A and B

In terms of synthesising these (*E*)-α,β-dehydroamino acids, Ohfune *et al.*[326] reported the a stereoselective synthetic method using acids esters by olefination of phosphonates (**6.3**, **6.4** and **6.5**) with commercially available and easily prepared aldehydes with three reaction conditions (Scheme 6.12). The three reaction conditions are: (1) NaH/NaI and DBU/NAI systems are effective for aromatic aldehydes and aldehydes derived from amino acids; (2) $MgBr_2 \cdot OEt_2$/DBU is used for aldehydes bearing an alky side chain; (3) $ZnCl_2$/DBU is used from the olefination of the aldehydes bearing an oxygen functionality.

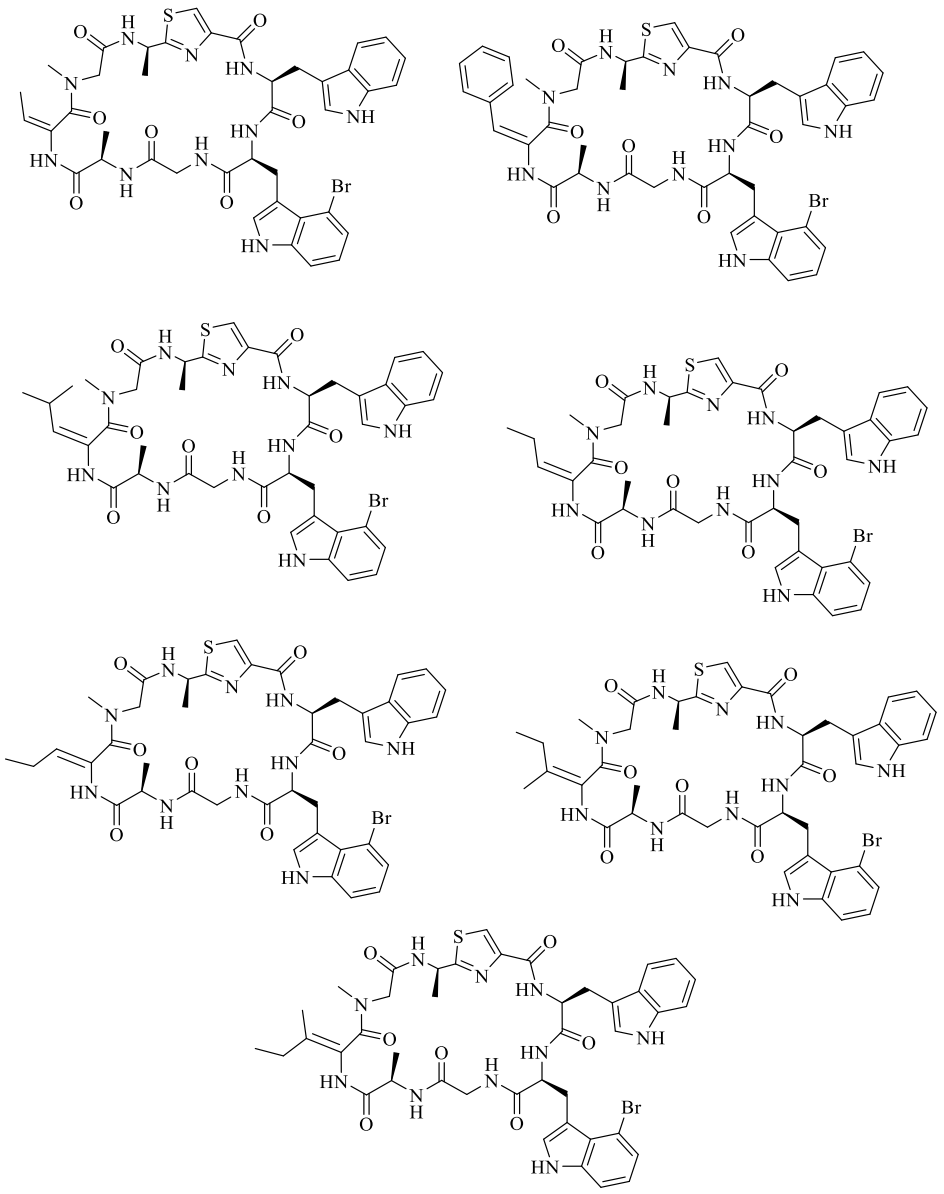
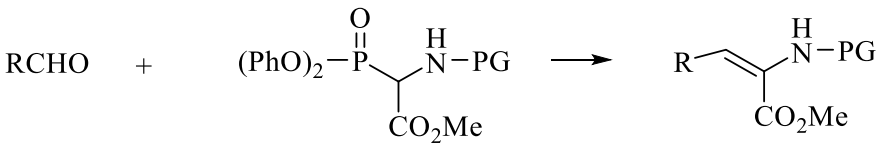


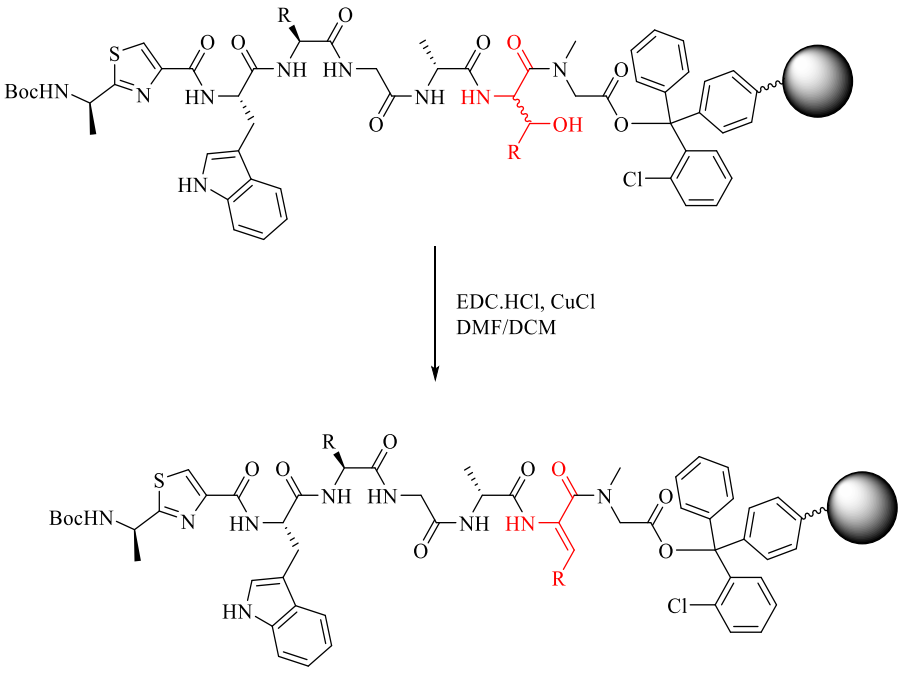
Figure 6.4: Dehydroamino acids containing argyrins to be synthesised in the future



6.3: PG = Cbz
6.4: PG = Ac
6.5: PG = Boc

Scheme 6.12: Ohfune *et al.*' method for the synthesis of (*E*)-α,β-dehydroamino acid esters[326]

In this thesis, *O*-tosylation followed by elimination for a threonine-containing cyclic peptide to afford the dehydrobutyrine containing cyclic peptide was evaluated. Due to the macrocyclic structure of argyrin, the reaction was not achieved. Therefore, the *O*-tosylation followed by elimination for a linear threonine-containing cyclic peptide will be evaluated. Inspired by the previously discussed on-resin oxidation elimination of phenylselenocysteine to afford dehydroalanine, an on-resin β-elimination for a threonine-containing linear peptide to afford the dehydrobutyrine will be evaluated. Albericio and co-workers[327] reported a copper-carbodiimide mediated elimination performed on a resin-bound peptide during the total synthesis of Tentoxin. In their case, the thermodynamically more stable *Z*-isomer was obtained. A library of tentoxin analogues was then generated via this SPPS-based route. Therefore, this method will be evaluated for the synthesis of dehydroamino acid containing argyrin analogues (Scheme 6.13).



Scheme 6.13: An on-resin copper-carbodiimide mediated elimination

6.2.2 Computational Studies

The co-crystal structure of argyrin B bound to *P. aeruginosa* EF-G can be adopted to virtually dock the argyrin analogues in order to gain further understanding of the binding interaction. The information generated could be used to understand the interaction of current analogues with the EF-G, and hence help the design of a new focused library of argyrin analogues.

6.2.3 Cytotoxicity of Argyrin Analogues

It is important that argyrin analogues applied for antibacterial activity have low or no cytotoxic effects. In order to establish the cytotoxicity of argyrin analogues synthesised, the most potent analogue **4.42** will be evaluated in MTT cell viability assay using the HCT1-116 (colon cancer cell line) and MCF-7 (breast adenocarcinoma) cell lines.

6.2.4 MIC_{50} of Argyrin Analogues

The most potent analogue **4.42** displayed a significant low IC_{50} against *B. multivorans* and *P. aeruginosa* than the parent compound, Argyrin A. Selva *et al*. reported that the Argyrin A, with a MIC_{50} 4–32 μg/ml, was bacteriostatic against *P. aeruginosa*.[166] Hence, it is crucial to determine whether the lead analogue **4.42** is a bacteriostatic or bactericidal agent. The agar and broth dilution methods[328] will be used to determine the MIC_{50} of **4.42**. The MBC is the lowest concentration of an antibacterial agent that either totally prevents growth or results in a >99.9% decrease in the initial inoculum.[329] The

bacteriostatic activity is defined as the ratio of MBC to MIC of >4.[330]

Chapter 7
Experimental

7.1 Material

All commercially available reagents and solvents were purchased from Sigma Aldrich, Acros Organic or Fisher Scientific and used without further purification. Deuterated chloroform ($CDCl_3$), deuterated methanol (CD_3OD), deuterated acetone (CD_3COCD_3), deuterated dimethyl sulfoxide (DMSO-d_6) and deuterated water (D_2O) were purchased from Cambridge Isotope Laboratories Inc. Methoxy-thiazole, Fmoc-allygly-OH, **5.1-5.14**, and **3.4** were obtain from Sivaneswary Genapathy. **4.26** was purchased from Fluorochem Ltd. **4.27** was purchased from Iris Biotech GmbH. All solvents used were either high performance liquid chromatography (HPLC) or reagent grade and were purchased from Fisher Scientific and Sigma Aldrich. Anhydrous tetrahydrofuran (THF), anhydrous 1,2-dimethylethane (DME), anhydrous ethanol (EtOH) and anhydrous dichloromethane (DCM) were purchased from Sigma Aldrich. Milli-Q water was used for chemical reactions and purifications. Reaction progress and product mixtures were monitored by TLC on silica gel (Merck 60 F254) and visualized by UV lamp at 254 nm or by staining with

ninhydrin solution. Column chromatography was performed on Acros Organic Kieselgel (0.035 – 0.070 mm).

7.2 General methods

Reactions were carried out at ambient temperature and moisture sensitive reactions were carried out under nitrogen atmosphere using oven-dried or heating gun dried glassware. Reactions were monitored using the techniques described below.

- Analytical TLC on pre-coated aluminium backed plates (Merck 60 F254) and visualized by UV lamp at 254 nm.
- Analytical TLC staining with ninhydrin solution
- Analytical reverse-phase high performance liquid chromatography (RP-HPLC) as mentioned in the instrumentation
- Liquid chromatography-mass spectrometry (LC-MS)

Organic solvents were evaporated under *vacuo* at temperature at 40 °C. Following work-up, all organic extracts were dried over anhydrous sodium sulphate, filtered under gravity and evaporated to dryness under *vacuo*.

7.3 Instrumentation

^{1}H-Nuclear magnetic resonance (NMR) spectra were acquired at room temperature using a Bruker 400 Ultrashield operating at 400 MHz. Chemical shifts given in δ values are reported in parts per million (ppm), referenced to $CHCl_3$ (δ_H = 7.26 ppm), DMSO (δ_H = 2.50 ppm), H_2O (δ_H = 4.79 ppm), $(CH_3)_2CO$ (δ_H = 2.05 ppm) and CH_3OH (δ_H = 3.31 ppm). The multiplicity of a

signal is displayed by one of the following abbreviation. s, singlet; d, doublet; t, triplet; q, quartet; br, broad; m, multiplet; dd, doublet of doublet. ^{1}H assignments were acquired using correlation spectroscopy (COSY). All coupling constants are given in Hz. Similarly, ^{13}C-NMR spectra were acquired at same condition a Bruker 400 Ultrashield operating at 100 MHz. Chemical shifts (δ) are reported in parts per million (ppm), referenced to $CDCl_3$ (δ_H = 77.166 ppm), DMSO-d_6 (δ_H = 39.52 ppm), $(CD_3)_2CO$ (δ_H = 29.84 ppm) and CD_3OD (δ_H = 49.00 ppm).

Mass spectra were obtained using Waters 2759 spectrometer by positive or negative electrospray ionization. Infrared spectra were obtained using Nicole Fourier-transform infra-red (FTIR) spectrometer. Lyophilisation from water was achieved from using Edwards modulyo FD freeze drier. Melting points (m.p.) were obtained in a glass capillary using a Gallenkamp 3A 3790 melting point apparatus. $[\alpha]_D$ values are reported in 10^{-1} deg cm^{-2} g^{-1} with the concentration, concentration in gram per 100 mL.

Analytical reverse-phase high performance liquid chromatography (RP-HPLC) was carried out with a Waters 510 twin-pump using an Onyx Monolithic C18 column (100 x 3 mm) at a flow rate of 4 mL min^{-1} or Onyx Monolithic C18 column (100 x 4.6 mm) at a flow rate of 3.0 mL min^{-1}. Eluent detection was recorded by UV absorbance at 214 and 254 nm using a Waters 486 Tunable Absorbance Detector. The two solvents are A = 0.06% aqueous trifluoroacetic acid (TFA) and B = 0.06% aqueous TFA in 90% aqueous acetonitrile. The linear elution gradient was either:

- **Method 1**: 10-60% **B** over 12 min at 3.0 mL min^{-1};
- **Method 2**: 1-30% **B** over 12 min at 3.0 mL min^{-1};

Purification by preparative RP-HPLC was performed using a Waters 2525 twin-pumps and a Waters 2487 Detector using Phenomenex Luna® 5 μm C18(2) 100 Å, AXIA™ Packed LC column (250 x 21.20 mm) at 20 mL min^{-1}. The detector

recorded the absorbance of the effluent at 214 nm. Standard solvents used were: 100% H_2O, 0.06% TFA (solvent **A**) and 90% acetonitrile, 10% H_2O and 0.06% TFA (solvent **B**). The linear elution gradient was either:

- **Method 1**: 50 to 90% **B** over 12 min at 20 mL min^{-1}
- **Method 2**: 20 to 60% **B** over 12 min at 20 mL min^{-1}

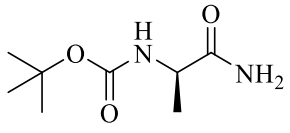
Solid-phase peptides synthesis was operated in an Omnifit™ continuous flow glass column (150 x 10 mm) and all wash and deprotection steps were performed using a Novasyn Gem® manual peptide synthesiser. UV absorbance was measured at 344 nm using a Gilson 115 UV detector. *N*-Fmoc deprotection profiles were recorded by a LKB Bromma 2210 recorder.

Microwave reactions were carried out in the CEM Discover microwave reactor. All the microwave reactions were conducted in a sealed glass tube.

7.4 Experimental for Chapter 2

7.4.1 Preparation of Thiazole Dipeptide

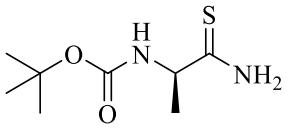
(*R*)-*tert*-butyl (1-amino-1-oxopropan-2-yl)carbamate (1.32).



N-hydroxysuccinimide (1.52 g, 13.2 mmol) was added to a stirring solution of Boc-D-Alanine-OH **1.31** (2.50 g, 13.2 mmmol) in DCM (15 mL) at 0 °C. DCC (2.73, 13.2 mmol) was then assed at 0 °C. The resultant mixture was brought to room temperature and stirred for 1 hour. The solution was cooled to 0 °C and

ammonia in ethanol 2 M (6.6 mL, 13.2 mmol) was added and stirred for another 1 hour. The suspension was filtered and the filtrate was concentrated under *vacuo*. The residue was then dissolved in dry acetone. The resulting suspension was filtered and the filtrate was concentrated under *vacuo* and purified by column chromatography (hexane/ethyl acetate, 1:1) to yield the amide **1.32** as white solid (2.25 g, 90%). m.p. 128–130 °C (Lit[219] m.p. 132 °C); R_f = 0.3 (hexane/EtOAc 1:1); MS: *m/z* (+ESI) calcd for $C_8H_{16}N_2O_3^+$ is 188.1161, found 378.2842 [MH^+]. ^{1}H-NMR (400 MHz, $CDCl_3$): δ= 1.36 (d,3H, *J*= 7.00 Hz, CH_3), 1.44 (s, 9H, C (CH_3)$_3$), 4.19 (br, 1H, α-CH), 5.00 (br, 1H, NH), 6.49 (br, 1H, N*HA*HB), 6.17 (br, 1H, NHA*HB*) ppm. ^{13}C-NMR (100 MHz, $CDCl_3$): δ= 18.1, 28.2, 61.0, 81.1, 155.8, 164.1; $[\alpha]_D^{23}$ = -24.2º (c=1.0, Methanol)

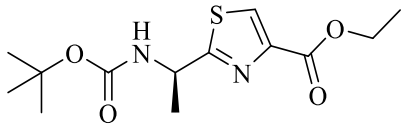
(*R*)-*tert*-butyl (1-amino-1-thioxopropan-2-yl)carbamate (1.33)



To a solution of Boc-D-alanine-NH_2 **1.32** (2.5g, 13.4 mmol) in THF (15 mL) stirring at 0 °C, Lawesson's reagent (3.25 g, 8.04 mmol) was added. The resulting mixture was brought to room temperature and stirred for 1 hour. The reaction mixture was then poured into a separating funnel containing ice (50 mL) and saturated aqueous $NaHCO_3$ (50 mL) and extracted with diethyl ether (2 x 50 ml). The organic layers were pooled, dried with sodium sulphate and concentrated under *vacuo*. The residue was purified through column chromatography (hexane/ethyl acetate, 3:1) to yield the thioamide **1.33** as white solid (2.6 g, 85%). m.p. 100–102 °C (Lit[219] m.p. 104–105 °C); R_f = 0.3 (hexane/EtOAc 3:2);^{1}H-NMR (400 MHz, $CDCl_3$): δ = 1.42 (s, 9H, C(CH_3)$_3$), 1.45 (d, 3H, *J*= 6.88 Hz, CH_3), 4.53 (br, 1H, α-CH), 5.37 (br, 1H, α-NH), 7.72 (br,1H, N*HA*HB), 8.13 (br, 1H, NHA*HB*) ppm. ^{13}C-NMR (100 MHz, CDCl3):

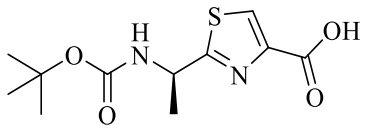
δ= 18.9, 28.4, 60.6, 80.9, 155.9, 164.5; $[\alpha]_D^{23}$ = -30.1º (c=1.0, methanol); MS: *m/z* (+ESI) $C_8H_{17}N_2O_2S^+$ calcd. 205.1005, found 205.0951 [MH^+].

(*R*)-ethyl 2-(1-((*tert*-butoxycarbonyl)amino)ethyl)thiazole-4-carboxylate (1.34)



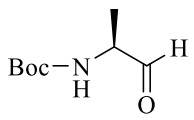
To a solution of Boc-D-alanine-thioamide **1.33** (1g, 4.9 mmol) in dry DME (10 mL) stirring at -15 °C under nitrogen, finely ground $KHCO_3$ (1.9 g, 19.6 mmol) was added. The resultant suspension was stirred for a further 30 minutes then ethyl bromopyruvate (1.85 mL, 14.7 mmol) was added. After 5 minutes of stirring, 2, 6-lutidine (4.8 mL, 41.7 mmol) and trifluoroacetic anhydride (2.77 mL, 19.6 mmol) in dry DME (5 mL) were added to the mixture at -15 °C. After stirring for 2 hours, the mixture was poured into a separating funnel containing water (100 mL) and extracted with diethyl ether (3 x 30 mL). The organic layers were pooled, dried over sodium sulphate and concentrated under *vacuo*. The resultant residue was purified through column chromatography (hexane/ethyl acetate, 3:1) to yield the thiazole **1.34** as yellow solid (0.74g, 50%). m.p 82–84 °C (Lit[219] m.p. 85–86 °C); R_f = 0.4 (hexane/EtOAc, 3:2); MS: *m/z* (+ESI) calcd for $C_{13}H_{20}N_2O_4SNa^+$ 323.1036, found 323.1944 [MNa^+]. ^{1}H-NMR (400 MHz, $CDCl_3$): δ= 1.39 (t, 3H, *J*= 7.18 Hz, CH_2CH_3), 1.44 (s, 9H, C (CH_3)$_3$), 4.40 (q, 2H, *J*= 7.08 Hz, CH_2CH_3), 5.10 (br, 1H, α-CH), 5.47 (br, 1H, α-NH), 8.07 (s, 1H, C_5-H) ppm.^{13}C-NMR (100 MHz, $CDCl_3$): δ= 14.5, 22.0, 29.0, 48.6, 61.5, 80.3, 127.6, 147.5, 154.6, 161.2, 178.6 ppm. $[\alpha]_D^{23}$ = +38.3º (c=1.0, $CHCl_3$) (Lit[219] $[\alpha]_D^{23}$ = +40.8º (c=1.0, $CHCl_3$))

(*R*)-2-(1-((*tert*-butoxycarbonyl)amino)ethyl)thiazole-4-carboxylic acid (1.29)



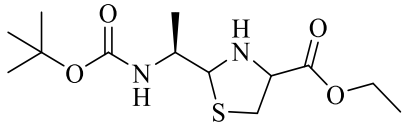
Boc-thiazole-OEt **1.34** (0.3 g, 1 mmol) was dissolved in a solution of THF/H_2O 1:1 (5 mL) and stirred at 0 °C. To this, lithium hydroxide (0.03 g, 1.3 mmol) dissolved in 1 mL of H_2O was added. The reaction mixture was brought to room temperature and stirred for 15 h. The reaction was concentrated under *vacuo*. The resultant residue was dissolved in H_2O (20 mL) and extracted with EtOAc (2 x 20 mL). The aqueous layer was acidified with $KHSO_4$ to pH = 2 and extracted with DCM (3 x 15 mL). The organic layers were pooled, dried over sodium sulphate, and concentrated under *vacuo* to give as light brown solid **1.29** (270.0 mg, .98%). m.p. 59–61 ºC (Lit[205] m.p. 58-61 °C) MS: *m/z* (+ESI) calcd for $C_{11}H_{16}N_2O_4S$ Na^+ 295.073, found 295.0679 [MNa^+]. 1H-NMR (400 MHz, $CDCl_3$): δ= 1.44 (s, 9H, C (CH_3)$_3$), 1.62 (d, 3H, *J*= 7.44 Hz, CH_3), 5.12 (br, 1H, α-CH), 5.20 (br, 1H, α-NH), 8.20 (s, 1H, C_5-H) ppm.^{13}C-NMR (100 MHz, $CDCl_3$): δ= 22.3, 29.6, 61.5, 82.0, 129.1, 146.7, 155.9, 164.3, 171.6 ppm; $[\alpha]_D^{23}$ = +29.1º (c=1.0, $CHCl_3$) (Lit[205] $[\alpha]_D^{23}$ = +40.8º (c=1.0, $CHCl_3$))

Ethyl 2-((S)-1-((tert-butoxycarbonyl)amino)ethyl)thiazolidine-4-carboxylate (1.38)



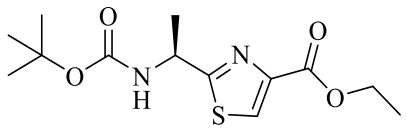
A solution of Boc-D-alanine methyl ester **1.35** (2.272 g, 11.2 mmol) in dichloromethane (20 mL) was cooled at -78°C and diisobutylaluminium

hydride (1 M in DCM) (22.4 mL, 22.4 mmol) was added and the reaction mixture stirred at this temperature for 3 h, before a saturated aqueous solution of sodium potassium tartrate (10 mL) was added and the reaction mixture stirred vigorously at room temperature for a further 1 h. The reaction mixture was extracted with dichloromethane (3 x 100 mL) and the combined organic extracts were extracted with a saturated solution of sodium chloride (2 x 80 mL) and dried over magnesium sulfate before the solvent was removed under *vacuo* to afford the aldehyde **1.36** (1.824 g, 10.5 mmol), which was used immediately for the next chemical transformation step.



The above crude **1.36** (1.824 g, 10.5 mmol) was added to toluene (10 mL) and methanol (10 mL). A solution of cysteine ethyl ester hydrochloride **1.37** (1.958 g, 10.5 mmol) and potassium bicarbonate (0.945 g, 9.45 mmol) in water (10 mL) was then added. The resulting mixture was stirred vigorously for 10 h before the solvent was removed under *vacuo*. Water (80 mL) was added, the reaction mixture extracted with ethyl acetate (3 x 100 mL) and the combined organic extracts washed with brine (100 mL) before the solvent was removed under *vacuo*. The crude product was purified through column using hexane: EtOAc = 1:2 as eluent, to afford the title product **1.38** as oil (1.268 g, 42%). ^{1}H-NMR (400 MHz, $CDCl_3$):δ 1.17 (3H, t, J = 7.1 Hz, CH_3), 1.39 (9H, s, Boc), 1.48 (3H, d, J = 7.00 Hz, CH_3), 3.32 (dd, J = 13.70, 6.70 Hz, CH_AH_B), 3.42 (dd, J= 13.70, 8.10 Hz, CH_AH_B), 3.91 (1H, dd, J= 8.10, 6.70 Hz), 4.17 (3H, m) , 4.57 (1H, d, J = 4.20 Hz, CH); ^{13}C-NMR (100 MHz, $CDCl_3$): δ= 14.5, 22.0, 29.0, 48.6, 61.5, 80.3, 127.6, 147.5, 154.6, 161.2, 178.6 ppm; MS: m/z (+ESI) calcd. for $C_{13}H_{26}N_2O_4S^+$ 305.1530, found 305.1557 [MH^+].

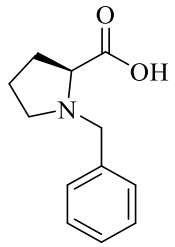
Ethyl (S)-2-(1-((tert-butoxycarbonyl)amino)ethyl)thiazole-4-carboxylate (1.34)



A solution of activated manganese dioxide (6.46 g, 63.2 mmol) and the thiazolidine intermediate (0.96 g, 3.16 mmol) in acetonitrile (25 mL) were heated to 65 °C for 1 h before cooling to room temperature and filtering through a pad of silica, eluting with ethyl acetate (200 ml). The filtrate was evaporated under *vacuo* to afford crude product, which was then purified by flash chromatography using EtOAc: Hexane, 1:3 as eluent to afford the title product **1.34** as yellow solid (416 mg, 42%); $[\alpha]_D^{23}$ = +39.0º (c = 1.0, $CHCl_3$) (Lit[219] $[\alpha]_D^{23}$ = +40.8º (c=1.0, $CHCl_3$)); ^{1}H-NMR (400 MHz, $CDCl_3$): δ = 1.39 (t, 3H, J= 7.18 Hz, CH_2CH_3), 1.44 (s, 9H, C $(CH_3)_3$), 4.40 (q, 2H, J= 7.08 Hz, CH_2CH_3), 5.10 (br, 1H, α-CH), 5.47 (br, 1H, α-NH), 8.07 (s, 1H, CH); ^{13}C-NMR (100 MHz, $CDCl_3$): δ= 14.5, 22.0, 29.0, 48.6, 61.5, 80.3, 127.6, 147.5, 154.6, 161.2, 178.6 ppm; MS: m/z (+ESI) calcd. for $C_{13}H_{20}N_2O_4SNa^+$ 323.1036, found 323.1944 [MNa^+].

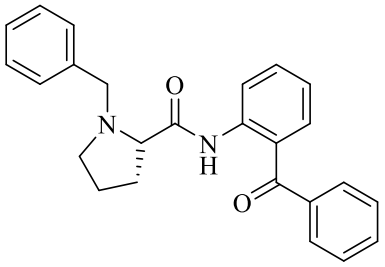
7.4.2 Preparation of BPB-Glycine-Ni(II) Schiff Base

Benzyl-L-proline (2.74)



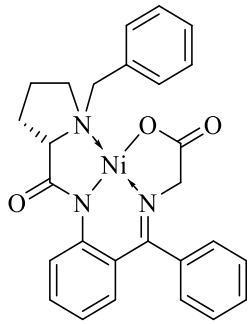
Proline **2.72** (3.45 g, 30 mmol) was added to a solution of KOH (5.89 g, 105 mmol) in isopropanol (40 mL) stirred at 40-45 °C. The flask was connected to a dropping funnel equipped with a drying tube containing a solution of benzyl chloride (4.49 g, 36 mmol) and isopropanol (20 mL). This was added drop wise over 1 hour, and the mixture was stirred overnight at the same temperature. After neutralization with concentrated HCl (6 ml) until pH 5-6, the reaction mixture was diluted with ½ volume of $CHCl_3$ (30 mL) and decanted overnight. The mixture was filtered and the solid washed with $CHCl_3$. After evaporation of the solvent the residue was triturated with acetone and a white/slight yellow precipitate of crude product **2.74** was obtained (4.92 g, 80%). m.p. 169–171 °C (Lit[331] m.p. 174–175 ºC); ^{1}H NMR (400 MHz, $CDCl_3$): δ 7.40-7.28 (m, 5H), 4.34 (d, *J* = 13.22 Hz, 1H), 4.17 (d, *J* = 12.81, 1H), 3.8 (q, *J* = 15.65, 2.81 Hz, 1H), 3.66(m, 1H), 3.28 (m, 1H), 2.30 (m, 2H), 1.95 (m, 2H); ^{13}C NMR (100 MHz, $CDCl_3$): δ 175.2, 137.7, 129.4, 128.4, 127.9, 73.4, 63.5, 58.8, 29.2, 20.0; m.p. 174-176 °C, $[\alpha]_D^{23}$ = -24º (c=1.0, Methanol) (Lit[332] $[\alpha]_D^{20}$ = –29.1º (*c* = 1.0, EtOH))

(*S*)-*N*-(2-benzoylphenyl)-1-benzylpyrrolidine-2-carboxamide (BPB) (2.71)



A solution of methyl sulfonyl chloride (4.13 g, 36 mmol) in dichloromethane (20 ml) was added drop wise to a solution of **2.74** (6.16 g, 30 mmol) and dichloromethane (20 ml) and 1-methylimidazole (5.41 g, 66 mmol) stirred at 0 °C in a round bottom flask equipped with a reflux condenser and a drying tube. After 15 min, a solution of 2-aminobenzophenone (5.33 g, 27 mmol) in 20 ml dichloromethane was added and the solution was refluxed at 40 °C overnight. The dark red solution was washed with saturated NH_4Cl (3 x 20 mL), saturated $NaHCO_3$ (pH = 8) (3 x 20 ml) and brine (3 x 30 mL); the pooled organic phases were dried and concentrated. The dark red residue was filtered through a silica pad and eluted with ethyl acetate to give a solution containing mainly BPB and APB. This was recrystallized from (ethyl acetate/hexane, 1:1) (10 mL) to give BPB **2.71** as white/yellow crystal (2.34 g, 45%). Recrystallization from methanol (10 mL) was used for further purification. m.p. 99–100°C (Lit[226] m.p. 101–102 °C) ^{1}H NMR (400 MHz, $CDCl_3$): δ 8.5 (d, *J* = 8.01 Hz, 1H), 7.8 (d, *J* = 8.42 Hz, 2H), 7.63 (m, 1H), 7.5 (m, 4H), 7.4 (m, 2H), 7.17 (m, 3H), 7.1 (m, 1H), 3.9 (d, *J* = 13.26 Hz, 1H), 3.60 (d, *J* = 13.21 Hz, 1H), 3.35 (q, *J* = 14.85 Hz, 4.4 Hz, 1H), 3.25 (m, 1H), 2.45 (m, 1H), 2.3 (m, 1H), 2.0 (m, 1H), 1.8 (m, 2H); ^{13}C NMR (100 MHz, $CDCl_3$): δ 24.1, 31.0, 53.9, 68.3, 121.5, 122.2, 125.3, 127.1, 128.1, 128.3, 129.1, 130.1, 132.5, 132.6, 133.3, 138.1, 138.5, 139.2, 174.7, 198.0; m.p. 101.2-102.1°C, $[\alpha]_D^{23}$ = -130.0º (c=1.0, Methanol) (Lit[331] $[\alpha]_D^{20}$ = –133.0º (*c* = 0.3, MeOH)); MS: *m/z* (+ESI) calcd. for $C_{25}H_{25}N_2O_2^+$ is 385.1911, found 385.1213 [MH^+].

Glycine-Ni(II)-BPB complex (1.40)



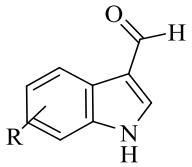
A suspension of Nickel (II) nitrate hexahydrate (11.632 g, 40 mmol) and KOH (10.1 g, 160 mmol) (pellets grinded before addition) in 5 ml of molecular sieve dried methanol (10 mL) was stirred under inert atmosphere. After addition of glycine (9.01 g, 120 mmol) and heating at reflux the colour changed from green to light blue. After that, solid **2.71** (7.69 g, 20 mmol) was added and the vessel of 23 rinsed with 5 mL methanol. The solution was stirred under reflux at 65 °C (temperature of water bath) with 100 mg of molecular sieves for 90 minutes. After cooling down to room temperature, concentrated acetic acid was added and the suspension was decanted and then filtered. Recrystallization from 50 ml of hot (methanol/H_2O, 1:1) gave white crystals, which were filtered. The dark red filtrate was concentrated under reduced pressure and recrystallized from (methanol/H_2O, 1:5) at 4 °C. The red crystals **1.40** were filtered, washed with water and dried in desiccator (65%). m.p. 222.5 ^oC; ^1H NMR (400 MHz, $CDCl_3$): δ 8.3 (d, *J* = 8.03 Hz, 1H), 8.1 (d, *J* = 8.42 Hz, 2H), 7.5-7.6 (m, 3H), 7.45 (t, *J* = 7.41 Hz, 2H), 7.35 (t, *J* = 7.26 Hz, 1H), 7.25 (t, *J* = 7.0 8Hz, 1H), 7.13 (d, *J* = 8.69 Hz, 1H), 6.98-7.04 (m, 1H), 6.83 (dd, *J* = 8.10 Hz, 1H), 6.72 (t, *J* = 8.10 Hz, 1H), 4.5 (d, *J* = 12.06 Hz, 1H), 3.65-6.85 (m, 4H), 3.5 (q, *J* = 11.05 Hz, 5.51 Hz, 1H), 3.3-3.4 (m, 1H), 2.55-2.65(m, 1H), 2.4-2.5 (m, 1H), 2.05-2.2 (m,2H); ^{13}C NMR (100 MHz, $CDCl_3$): δ 22.0, 30.5, 62.5, 67.9, 122.0, 122.8, 124.1, 125.1, 125.9, 128.6, 128.8, 129.2, 129.4, 131.7, 132.9, 134.1, 141.9, 143.2, 171.1, 177.2, 180.9; m.p. 222.5 °C, $[\alpha]_D^{23}$ = +2131^o (c=1.0, Methanol) (Lit[331]

$[\alpha]_D^{20}$ = +2117º (*c* = 0.0015, $CHCl_3$)); MS: *m/z* (+ESI) calcd. for $C_{27}H_{26}N_3NiO_3^+$ is 498.1322, found 498.1317 [MH^+].

7.4.3 Preparation of 3-hydroxyethylindole

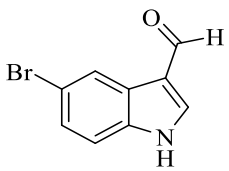
7.4.3.1 Preparation of Indole-3-carbaldehydes

General procedure



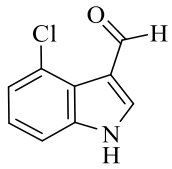
Phosphoryl chloride (1.5 equiv.) was added dropwise to anhydrous DMF (10 mL) at 0 ℃ and left to stir for 10 min. To this, a solution of **1.41** (1 equiv.) in anhydrous DMF (5 mL) was added dropwise and the resultant mixture was heated to 45 ° C and left to stir for 2 h. The reaction mixture was cooled to room temperature and pH was adjusted to 9–10 with 1 M NaOH. The resultant suspension was then heated to 60 °C and left to cool to room temperature. Deionized water was added to the cooled mixture and the resultant precipitate was filtered and washed with excess deionized water. The precipitate was air dried overnight to yield the title compound.

5-Bromo-1*H*-indole-3-carbaldehyde (2.78 a)



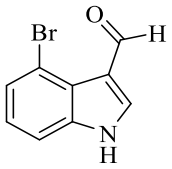
Synthesis was carried out using the general procedure, using phosphoryl chloride (0.7 mL, 7.65 mmol), 5-bromoindole (1 g, 5.1 mmol) and DMF (5 mL) to yield the title compound as white solid **2.78 a** (0.97 g, 89% yield); m.p. 203–205 °C (Lit.[205] m.p. 204–207 °C); R_f = 0.2 (hexane/EtOAc 2:1); 1H-NMR (400 MHz, CDCl3): δ = 7.21 (t, J = 8.03 Hz, 1H, H-6), 7.28 (dd, J = 8.01, 1 Hz, H-5), 7.76 (dd, J = 8.03, 1.10 Hz, 1H, H-7), 7.83 (d, J = 3.03 Hz, 1H, H-2), 9.16 (br, 1H, NH), 10.05 (s, 1H, CHO) ppm; 13C-NMR (100 MHz, CDCl3): δ = 113.1, 113.8, 118.2, 121.6, 123.7, 126.3, 135.5, 139.9, 185.1 ppm; MS: m/z (+ESI) calcd. for $C_9H_7BrNO^+$ 223.9633, found 225.0570 [MH^+].

4-chloro-1*H*-indole-3-carbaldehyde (2.78 b)



Synthesis was carried out using the general procedure, using phosphoryl chloride (1.5 mL, 9.93 mmol), 4-chloroindole (1.0 g, 6.62 mmol) and DMF (5 mL) to yield the title compound as white solid **2.78 c** (1.005 g, 85%); m.p. 145–147 °C (Lit.[205] m.p. 147–148 °C); R_f = 0.2 (hexane/EtOAc 2:1); ^{1}H NMR (400 MHz, acetone-d_6): δ = 7.20 (td, *J* = 9.53, 3.12 Hz, 1H, H-6), 7.27 (td, *J* = 8.52, 5.63 Hz, H-7), 7.46 (d, *J* = 8.13 Hz, 1H, H-5), 8.17 (s, 1H, H-2), 10.57 (d, *J* = 2 Hz, 1H, CHO) ppm. ^{13}C NMR (100 MHz, acetone-d_6): δ = 107.7 (d, *J* = 20 Hz), 113.6 (d, *J* = 20 Hz), 119.2 (d, *J* = 5 Hz), 126.5 (d, *J* = 8 Hz), 135.9, 142.4, 155.2, 158.5, 182.2 ppm; MS: m/z (+ESI) calcd for $C_9H_7ClNO^+$ 179.0106, found 179.0360 [MH^+].

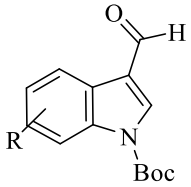
4-Bromo-1*H*-indole-3-carbaldehyde (2.78 c)



Synthesis was carried out using the general procedure, using phosphoryl chloride (2.8 mL, 30.6 mmol), 4-bromoindole (4.0 g, 20.4 mmol) and DMF (20 mL) to yield the title compound **2.78 b** as white solid (3.94 g, 90% yield); m.p. 163–165 °C (Lit.[205] m.p. 168–170 °C); R_f = 0.2 (hexane/EtOAc 2:1); 1H-NMR (400 MHz, CDCl3): δ = 7.16 (t, J = 8.03 Hz, 1H, H-6), 7.44 (dd, J = 8.03, 1.63 Hz, H-5), 7.50 (dd, J = 8.93, 1.56 Hz, 1H, H-7), 8.12 (d, J = 3.56 Hz, 1H, H-2), 9.16 (br, 1H, NH), 10.94 (s, 1H, CHO) ppm; 13C-NMR (100 MHz, CDCl3): δ = 111.7, 114.1, 119.9, 124.6, 125.7, 127.3, 131.5, 137.9, 187.1 ppm; MS: m/z (+ESI) calcd. for C9H7BrNO+ 223.9706, found 223.9734 [MH+].

7.4.3.2 Preparation of *N*-Boc-indole-3-carbaldehydes

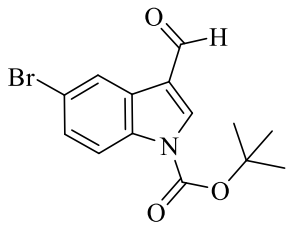
General procedure



Boc_2O (1.5 equiv.) followed by DMAP (0.5 equiv.) was added to a solution of intermediate **2.78** (1 equiv.) in anhydrous THF. The reaction mixture was stirred at room temperature under nitrogen atmosphere. When no starting material was detected by TLC, H_2O was added to the reaction mixture and the volatiles were

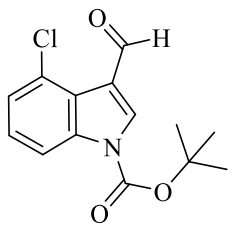
evaporated under *vacuo*. The residual water phase was extracted with EtOAc. The pooled organic phase was washed with brine, dried over Na_2SO_4, filtered and concentrated under *vacuo* to yield the **2.79**.

tert-Butyl 5-bromo-3-formyl-1*H*-indole-1-carboxylate (2.79 a)



Synthesis was carried out using the general procedure, using a solution of intermediate (2.22 g, 10 mmol), Boc_2O (3.27 g, 15 mmol) and DMAP (0.70 g, 0.5 mmol) in anhydrous THF (10 mL) to yield the title compound as white powder (3.20 g, 90%); m.p. 109–111 °C; R_f = 0.3 (hexane/EtOAc 1:1); ^{1}H-NMR (400 MHz, $CDCl_3$): δ = 1.70 (s, 9H, Boc), 7.49 (dd, J = 8.23, 1.32 Hz, 1H, H-6), 8.01 (d, J = 8.32 Hz, 1H, H-6), 8.21 (s, 1H, H-2), 8.45 (d, J = 8.01 Hz, 1H, H-5), 10.06 (s, 1H, CHO) ppm; ^{13}C-NMR (100 MHz, $CDCl_3$): δ = 28.3, 86.4, 110.3, 112.1, 115.9, 120.1, 126.7, 132.1, 138.3, 148.9, 156.8, 186.3 ppm; MS: m/z (+ESI) calcd. for $C_{14}H_{15}BrNO_3^+$ 323.0157, found 323.0196 [MH^+].

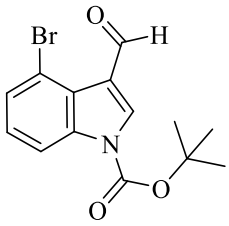
tert-Butyl 4-chloro-3-formyl-1*H*-indole-1-carboxylate (2.79 b)



Synthesis was carried out using the general procedure, using a solution of intermediate (0.895 g, 5 mmol), Boc_2O (1.635 g, 7.5 mmol) and DMAP (183 g,

1.5 mmol) in anhydrous THF (20 mL) to yield the title compound as white powder (1.30 g, 90%); m.p. 109–111 °C (Lit.[205] m.p. 110–112 °C); R_f = 0.3 (hexane/EtOAc 1:1); ^{1}H NMR (400 MHz, $CDCl_3$): δ = 1.70 (s, 9H, Boc), 7.20 (td, *J* = 9.51, 3.23 Hz, 1H, H-6), 7.27 (td, *J* = 8.32, 5.19 Hz, H-7), 7.46 (d, *J* = 8.56 Hz, 1H, H-5), 8.17 (s, 1H, H-2), 10.57 (d, *J* = 2.91 Hz, 1H, CHO). ^{13}C NMR (100 MHz, $CDCl_3$): δ = 28.4, 87.4, 110.4, 113.9, 116.9, 120.2, 127.9, 132.1, 138.3, 148.9, 156.75, 185.3 ppm; MS: m/z (+ESI) calcd for $C_{14}H_{15}ClNO_3^+$ 279.0712, found 279.6321 [MH^+].

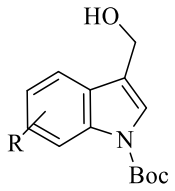
tert-Butyl 4-bromo-3-formyl-1*H*-indole-1-carboxylate (2.79 c)



Synthesis was carried out using the general procedure, using a solution of intermediate (3.6 g, 16 mmol), Boc_2O (5.2 g, 24.2 mmol) and DMAP (1 g, 8 mmol) in anhydrous THF to yield the title compound as white powder (4.7 g, 94%); m.p. 106–107 °C (Lit.[205] m.p. 117–119 °C); R_f = 0.3 (hexane/EtOAc 1:1); ^{1}H-NMR (400 MHz, $CDCl_3$): δ = 1.67 (s, 9H, Boc), 7.30 (t, J = 8.32 Hz, 1H, H-6), 7.355 (dd, J = 8.67, 1.82 Hz, 1H, H-6), 8.24 (dd, J = 8.12, 1.36 Hz, 1H, H-5), 8.35 (s, 1H, H-2), 10.95 (s, 1H, CHO) ppm; ^{13}C-NMR (100 MHz, $CDCl_3$): δ = 28.2, 86.3, 106.7, 113.6, 115.0, 121.2, 126.1, 127.0, 128.6, 132.1, 137.4, 148.5, 149.8, 187.1 ppm; MS: m/z (+ESI) calcd. for $C_{14}H_{15}BrNO_3^+$ 325.1572, found 325.1615 [MH^+].

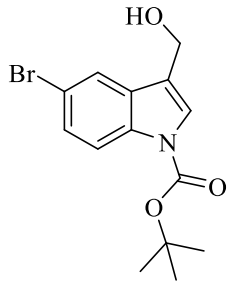
7.4.3.3 Preparation of *N*-Boc-3-hydroxymethylindole

General procedure



$NaBH_4$ (2 equiv.) was added to a stirring suspension of **2.79** (1 equiv.) in EtOH and the resultant mixture was stirred overnight. The volatile was evaporated under *vacuo* and the resultant oil was shaken with 1 M NaOH. The alkaline solution was extracted with Et_2O. The organic layers were combined, dried over Na_2SO_4, filtered and concentrated under *vacuo*. The crude was purified using column chromatography to yield the **2.80**.

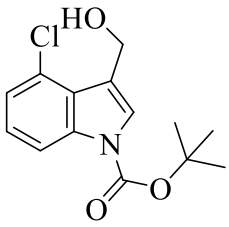
***tert*-Butyl 5-bromo-3-(hydroxymethyl)-1*H*-indole-1-carboxylate (2.80a)**



Synthesis was carried out using the general procedure, using $NaBH_4$ (0.582 g, 15.4 mmol) and **2.79a** (2.49 g, 7.71 mmol) to yield the title compound as off-white solid (1.85 g, 75%); m.p. 98–99 °C; R_f = 0.3 (hexane/EtOAc 3:1); ^{1}H-NMR (400 MHz, $CDCl_3$): δ = 1.61 (s, 9H, Boc), 2.99 (br, 1H, OH), 4.79 (s, 2H, CH2), 7.26 (dd, J = 9.23, 1.35 Hz, 1H, H-4), 7.42 (d, J =7.16 Hz, 1H, H-6), 7.776 (s, H-7), 8.00 (d, J = 8.25 Hz, 1H, H-2) ppm. ^{13}C NMR (100 MHz, $CDCl_3$):

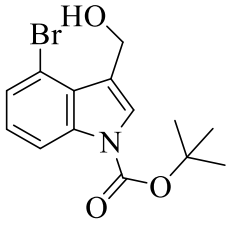
δ = 28.5, 59.4, 89.3, 109.6, 112. 6, 118.6, 119.4, 125.3, 126.7, 139.3, 149.6, 157.8, ppm; MS: m/z (+ESI) calcd for $C_{14}H_{17}BrNO_3^+$ 325.0310, found 325.0680 [MH^+].

***tert*-Butyl 4-chloro-3-(hydroxymethyl)-1*H*-indole-1-carboxylate (2.80 b)**



Synthesis was carried out using the general procedure, using $NaBH_4$ (0.541 g, 14.3 mmol) and **2.79b** (2.0 g, 7.17 mmol) to yield the title compound as off-white solid (1.51 g, 75%); m.p. 97–99 °C (Lit.[205] m.p. 98–112 °C); R_f = 0.4 (hexane/EtOAc 2:1); ^{1}H-NMR (400 MHz, $CDCl_3$): δ = 1.66 (s, 9H, Boc), 4.96 (s, 2H, CH2), 7.23 (m, 2H, H-7), 7.62 (s, 1H, H-6), 8.13 (m, 1H, H-7), 10.06 (s, 1H, CHO) ppm. ^{13}C NMR (100 MHz, $CDCl_3$): δ = 28.6, 59.6, 86.4, 108.6, 119.6, 117.7, 120.3, 126.3, 139.6, 158.6, ppm; MS: m/z (+ESI) calcd for $C_{14}H_{17}ClNO_3^+$ 268.1187, found 268.1235 [MH^+]

***tert*-Butyl 4-bromo-3-(hydroxymethyl)-1*H*-indole-1-carboxylate (2.80 c)**

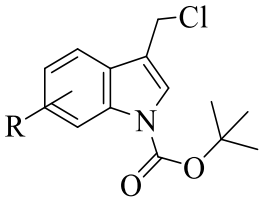


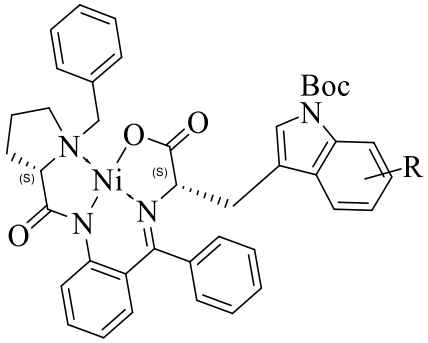
Synthesis was carried out using the general procedure, using $NaBH_4$ (1.12 g, 29.6 mmol) and **2.79 c** (4.8 g, 14.8 mmol) to yield the title compound as off-white solid (2.9 g, 65%); m.p. 97–98 °C (Lit.[205] m.p. 97–99 °C); R_f = 0.3

(hexane/EtOAc 3:1); ^{1}H-NMR (400 MHz, $CDCl_3$): δ = 1.66 (s, 9H, Boc), 4.97 (s, 2H, CH2), 7.16 (t, *J* = 8.27 Hz, 1H, H-7), 7.40 (dd, *J* = 8.12, 1.36 Hz, H-6), 7.65 (s, 1H, H-2), 8.19 (d, *J* = 9.34 Hz, 1H, H-5) ppm; ^{13}C-NMR (100 MHz, $CDCl_3$): δ = 27.3, 56.3, 84.9, 113.1, 114.5, 120.1, 125.2, 126.7, 127.9, 129.0, 137.5, 149.2 ppm; MS: *m/z* (+ESI) calcd. for $C_{14}H_{16}BrKNO_3^+$ 365.9925, found 365.9937 [MK^+].

7.4.3.4 Preparation of Alkylated Chiral BPB-Gly-Ni(II) Schiff Base

General procedures



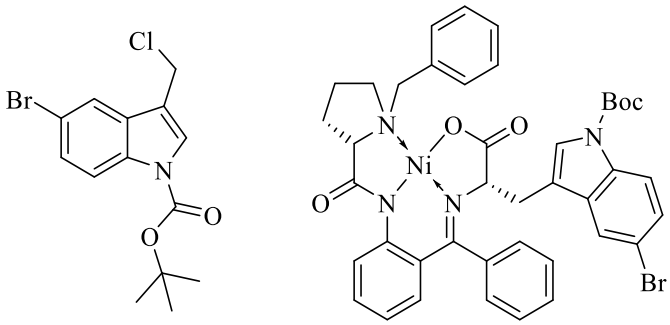


To a solution of **2.80** (1 equiv.) in CH_2Cl_2 stirred at 0 ºC, DBU (2 equiv.) followed by methane sulfonyl chloride (1.5 equiv.) were added. The reaction mixture was brought to room temperature and refluxed for 2 h before quenching with saturated $NaHCO_3$. The aqueous layer was separated and back extracted with CH_2Cl_2. The organic layers were combined, dried over Na_2SO_4, filtered and concentrated under *vacuo* to afford **1.42** as unstable crude mixture which was taken to the next step without purification.

Freshly ground NaOH (2 equiv.) was added to a stirred solution of **1.40** (1 equiv.)

in anhydrous DMF at 40 °C. To this, a solution of the crude **1.42** dissolved in DMF was added dropwise over 15 min and the resultant reaction mixture was left to stir for a further 30 min. Upon completion, the reaction mixture was quenched by pouring the crude reaction mixture over aqueous sat. NH_4Cl. The suspension was extracted with ethyl acetate. The organic layer was dried over Na_2SO_4, filtered and concentrated under *vacuo*. The crude was purified using column chromatography (EtOAc/hexane/acetone 3:1:1) to yield the **1.43** as dark red solid.

Nickel(II)-(*S*)-BPB/(*S*)-2-Amino-3-(1-(*tert*-butoxycarbonyl)-5-bromo-1*H*-indol-3-yl)propanoic acid Schiff base complex (1.43a)

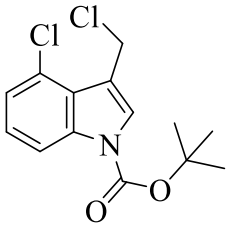


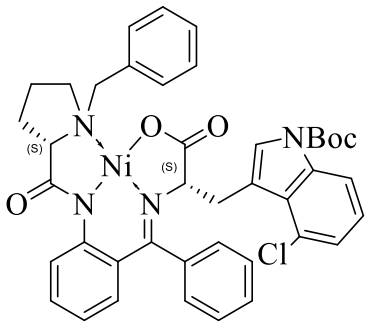
Synthesis was carried out using the general procedure, using **2.80a** (0.885 g, 3.15 mmol), DBU (0.988 mL, 6.3 mmol) and methane sulfonyl chloride (0.58 mL, 4.73 mmol) to yield the unstable crude **1.42a** which was taken to the next step without purification.

The crude mixture from above reaction was subjected to the synthetic procedure described under general procedure using DMF (18 mL), **1.43a** (1.42 g, 2.86 mmol) and NaOH (0.286 g, 7.15 mmol) to yield the title compound as dark red solid (0.948 g, 40%); m.p. 98–100 °C; R_f = 0.3 (EtOAc/hexane/acetone, 3:1:1); $[\alpha]_D^{24}$ = +1231 (*c* = 1.0, MeOH); ^{1}H-NMR (400 MHz, $CDCl_3$): δ = 1.76 (s, 2H, Bn-CH_2), 2.16 (s, 9H, Boc), 2.58 (m, 2H, pro-CH_2), 3.44 (m, 2H, pro-CH_2), 3.52

(m, 2H, pro-CH_2), 3.84 (dd, J = 15.12, 8.53 Hz, 1H, CH_AH$_B$), 4.11 (dd, J = 14.17, 7.32 Hz, 1H, CH$_A$$H_B$), 4.40 (m, 1H, Trp α-H), 4.44 (m, 1H, pro α-H), 6.13 (d, J = 7.11 Hz, Ar H), 6.53 (dd, J = 8.33, 2.34 Hz, 1H, Ar H), 6.61 (m, 1H, Ar H), 7.86 (d, J = 7 Hz, 1H, Ar H), 7.05-7.16 (m, 3H, Ar Hs), 7.20-7.24 (m, 2H, Ar Hs), 7.36 (s, 1H, Ar H), 7.42 (m, 1H, Ar H), 8.06 (m, 2H, Ar Hs), 8.21 (d, J = 8.31 Hz, 1H, Ar H), 8.21 (dd, J = 8.78, 1.91 Hz, 1H, Ar H) ppm; ^{13}C-NMR (100 MHz, $CDCl_3$): δ = 24.1, 28.1, 31.0, 33.4, 57.3, 60.5, 63.2, 70.6, 72.0, 84.4, 114.3, 114.5, 115.4, 120.7, 123.5, 125.3, 126.4, 127.0, 127.4, 127.7, 127.8, 128.4, 128.5, 128.7, 129.0, 129.5, 131.6, 132.3, 133.4, 133.41, 133.7, 137.0, 142.7, 148.8, 170.7, 178.4, 180.3, 207.1 ppm; MS: *m/z* (+ESI) calcd. for $C_{41}H_{41}BrN_4NiO_5^+$ 804.1569, found 804.1690 [MH^+]; RP-HPLC **Method 3**, t_R 8.13 min, de 96%

Nickel(II)-(*S*)-BPB/(*S*)-2-Amino-3-(1-(*tert*-butoxycarbonyl)-4-bromo-1*H*-indol-3-yl)propanoic acid Schiff base complex (1.43b)



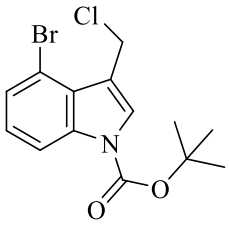


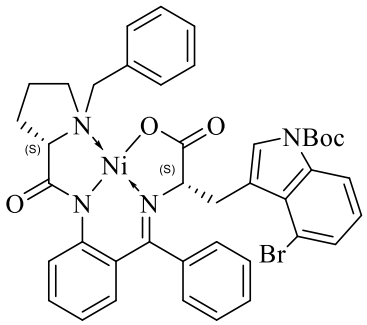
Synthesis was carried out using the general procedure, using **2.80b** (2.5 g, 8.9 mmol), DBU (2.52 mL, 18 mmol) and methane sulfonyl chloride (1.08 mL, 13.5 mmol) to yield the unstable crude **1.42b** which was taken to the next step without purification.

The crude mixture from above reaction was subjected to the synthetic procedure described under general procedure using DMF (20 mL), **1.43b** (4.47 g, 9 mmol)

and NaOH (0.72 g, 18 mmol) to yield the title compound as dark red solid (3.8 g, 60%); m.p. 109–111 °C; R_f = 0.3 (EtOAc/hexane/acetone, 3:1:1); $[\alpha]_D^{24}$ = +1239.3 (c = 0.15, MeOH); ^{1}H-NMR (400 MHz, $CDCl_3$): δ = 1.74 (s, 2H, Bn-CH_2), 2.14 (s, 9H, Boc), 2.56 (m, 2H, pro-CH_2), 3.47 (m, 2H, pro-CH_2), 3.55 (m, 2H, pro-CH_2), 3.86 (dd, J = 15.23, 8.41 Hz, 1H, CH_AH$_B$), 4.11 (dd, J = 14.22, 7.31 Hz, 1H, CH$_A$$H_B$), 4.40 (m, 1H, trp α-H), 4.44 (m, 1H, pro α-H), 6.15 (d, J = 7.13 Hz, Ar H), 6.55 (dd, J = 8.34, 2.91 Hz, 1H, Ar H), 6.63 (m, 1H, Ar H), 7.05-7.16 (m, 3H, Ar Hs), 7.20-7.24 (m, 2H, Ar Hs), 7.36 (s, 1H, Ar H), 7.52 (m, 1H, Ar H), 7.66 (d, J = 7.10 Hz, 1H, Ar H), 8.06 (m, 2H, Ar Hs), 8.21 (d, J = 8.30 Hz, 1H, Ar H), 8.21 (dd, J = 8.12, 1.61 Hz, 1H, Ar H) ppm; ^{13}C-NMR (100 MHz, $CDCl_3$): δ = 24.1, 28.1, 31.0, 33.4, 57.3, 60.5, 63.2, 70.6, 72.0, 84.4, 114.3, 114.5, 115.4, 120.7, 123.5, 125.3, 126.4, 127.0, 127.4, 127.7, 127.8, 128.4, 128.5, 128.7, 129.0, 129.5, 131.6, 132.3, 133.4, 133.41, 133.7, 137.0, 142.7, 148.8, 170.7, 178.4, 180.3, 207.1 ppm; MS: *m/z* (+ESI) calcd. for $C_{41}H_{40}ClN_4NiO_5^+$ 761.2035, found 761.1999 [MH^+]; RP-HPLC **Method 3**, t_R 8.29 min, de 85%

Nickel(II)-(*S*)-BPB/(*S*)-2-Amino-3-(1-(*tert*-butoxycarbonyl)-4-bromo-1*H*-indol-3-yl)propanoic acid Schiff base complex (1.43c)





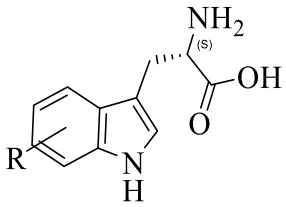
Synthesis was carried out using the general procedure, using **2.80c** (3.0 g, 9.3 mmol), DBU (2.61 mL, 18.45mmol) and methane sulfonyl chloride (1.08 mL, 13.95 mmol) to yield the unstable crude **1.42c** which was taken to the next step

without purification.

The crude mixture from above reaction was subjected to the synthetic procedure described under general procedure using DMF (25 mL), **1.43c** (2.5 g, 5 mmol) and NaOH (0.4 g, 10 mmol) to yield the title compound as dark red solid (2.8 g, 70%); m.p. 99-100 °C; R_f = 0.3 (EtOAc/hexane/acetone, 3:1:1); $[\alpha]_D^{24}$ = +1100.3 (c = 0.1, MeOH); ^{1}H-NMR (400 MHz, $CDCl_3$): δ = 1.75 (s, 2H, Bn-CH_2), 2.18 (s, 9H, Boc), 2.68 (m, 2H, pro-CH_2), 3.64 (m, 2H, pro-CH_2), 3.55 (m, 2H, pro-CH_2), 3.94 (dd, J = 15.30, 8.40 Hz, 1H, CH_AH$_B$), 4.16 (m, 7.37 Hz, 1H, CH$_A$$H_B$), 4.40 (m, 1H, trp α-H), 4.46 (m, 1H, pro α-H), 6.19 (d, J = 7.10 Hz, Ar H), 6.53 (dd, J = 8.02, 2.08 Hz, 1H, Ar H), 6.66 (m, 1H, Ar H), 7.05-7.15 (m, 3H, Ar Hs), 7.20-7.25 (m, 2H, Ar Hs), 7.37 (s, 1H, Ar H), 7.45 (dt, J = 7.00, 1.87 Hz, 1H, Ar H), 7.88 (t, J = 7.12 Hz, 1H, Ar H),8.16 (m, 2H, Ar Hs), 8.31 (d, J = 8.37 Hz, 1H, Ar H), 8.42 (dd, J = 8.13, 1.37 Hz, 1H, Ar H) ppm; ^{13}C-NMR (100 MHz, $CDCl_3$): δ = 17.4, 23.0, 27.2, 33.0, 33.1, 58.3, 65.2, 68.0, 71.6, 72.6, 88.4, 114.0, 114.8, 120.7, 123.5, 125.0, 125.6, 126.5, 126.8, 127.2, 127.7, 127.8, 128.5, 128.6, 129.0, 129.5, 131.7, 132.2, 133.4, 133.8, 133.9, 138.1, 142.8, 149.0, 172.9, 173.1, 178.4, 182.3 ppm; MS: *m/z* (+ESI) calcd. for $C_{41}H_{40}BrN_4NiO_5^+$ 805.1530, found 805.1501 [MH^+]; RP-HPLC **Method 3**, t_R = 8.15 min, dr 95%

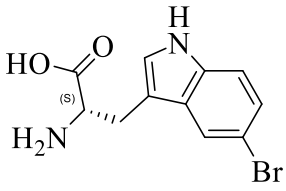
7.4.3.4 Preparation of L-Tryptophan Derivatives

General Procedure



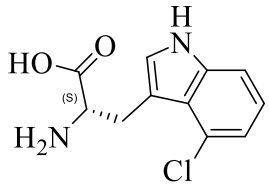
A solution of **1.43** in 2:1 mixture of THF/ 6 M HCl (12mL) was subjected to disassembly under microwave reaction condition. The disassembly was carried out in a sealed glass tube in a CEM microwave reactor at 50 W and 75 ℃ for 20 min until the red colour of the solution disappeared. The pressure was monitored and did not exceed 40 psi. The reaction mixture was cooled to room temperature and extracted with Et_2O and the aqueous layer was evaporated to dryness. The crude product was purified using preparative RP-HPLC.

(*S*)-2-amino-3-(5-bromo-1*H*-indol-3-yl)propanoic acid (1.44a)



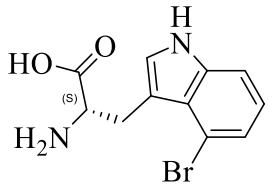
The disassembly of **1.43a** (1 g, 1.28 mmol) was carried out using the general procedure to yield the title compound as a crude mixture. The crude was purified using preparative RP-HPLC **Method 2** and freeze dried to afford the product as white powder (134 mg, 48%).; m.p. 215.8 °C; $[\alpha]_D^{23}$ = -27.1º (c=1.0, Methanol); ^{1}H-NMR (400 MHz, CD_3OD): δ = 3.26 (d, *J* = 6.13 Hz, 2H, CH_2), 4.13 (t, *J* = 6.12, 2.01 Hz, 1H, CH), 7.19 (t, J = 9.12, 1.31 Hz, 1H, H-4), 7.32 (t, J = 9.12, 1.39 Hz, H-7), 7.79 (s, 1H, H-6), 8.36 (br, 1H, H-2), 11.34 (s, 1 H, OH) ppm, ^{13}C NMR 100 MHz, CD_3OD): δ = 27.50, 57.86, 109.30, 113.60, 116.30, 123.65, 124.80, 127.30, 139.63, 176.91 ppm; MS: m/z (+ESI) calcd for $C_{11}H_{11}BrN_2O_2^+$ 282.0011, found 282.9366 [MH^+]; RP-HPLC **Method 2**, t_R = 7.47 min.

(*S*)-2-amino-3-(4-chloro-1*H*-indol-3-yl)propanoic acid (1.44 b)



The disassembly of **1.43b** (1.2 g, 1.6 mmol) was carried out using the general procedure to yield the title compound as a crude mixture. The crude was purified using preparative RP-HPLC **Method 2** and freeze dried to afford the product as white powder (152 mg, 40%).; m.p. 222.8 °C (Lit.[205] m.p. 224–226 °C); $[\alpha]_D^{24}$ = –39.2º (*c* = 0.10, MeOH) (Lit.[205] $[\alpha]_D^{24}$ = –40.2º (*c* = 0.15, MeOH)); ^{1}H-NMR (400 MHz, acetone-d_6): δ = 3.23 (dd, *J* = 10.10, 15.13 Hz, 1H, CH_ACH$_B$), 3.98 (dd, *J* = 16.97, 4.03 Hz, 1H, CH$_A$CH_B), 4.22 (dd, *J* = 16.13, 4.36 Hz, 1H, α-H), 7.12 (dd, *J* = 8.34, 1.97 Hz, 1H, Ar H), 7.16 (t, *J* = 8.17, 1.39 Hz, 1H, Ar H), 7.34 (s, 1H, Ar H), 7.39 (dd, *J* = 8.38, 1.34 Hz, 1H, Ar), 10.92 (br, 1H, COO*H*) ppm; ^{13}C-NMR (100 MHz, acetone-d_6): δ = 28.2, 55.6, 108.4, 110.8, 118.9, 122.9, 123.7, 124.8, 128.3, 139.3 ppm; MS: *m/z* (+ESI) calcd. for $C_{11}H_{12}ClN_2O_2^+$ 239.0582, found 239.0544 [MH^+]; RP-HPLC **Method 2**, t_R = 5.72 min.

(*S*)-2-Amino-3-(4-bromo-1*H*-indol-3-yl)propanoic acid (1.44c)



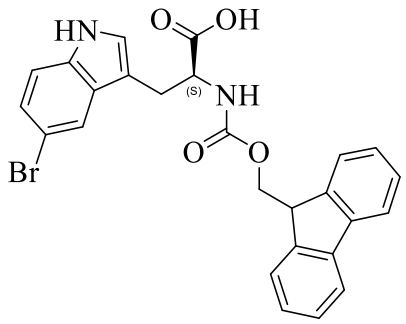
The disassembly of **1.43c** (2.0 g, 2.58 mmol) was carried out using the general procedure, to yield the title compound as a crude mixture. The crude was purified using preparative RP-HPLC **Method 2** and freeze dried to afford the product as white powder (250 mg, 49%); m.p. 261.7 °C (Lit.[205] m.p. 262-263 °C); $[\alpha]_D^{24} = -20.6^o$ (c = 0.10, MeOH) (Lit.[205] $[\alpha]_D^{24} = -19.4^o$ (c = 0.12, MeOH)); ^{1}H-NMR (400 MHz, D_2O): δ = 3.20 (dd, J = 16.23, 8.32 Hz, 1H, CH_ACH$_B$), 3.86 (dd, J = 15.02, 5.30 Hz, 1H, CH_ACH$_B$), 4.42 (dd, J = 8.00, 5.01 Hz, 1H, α-H), 7.08 (t, J = 9.36, 2.91 Hz,1H, CH-2), 7.30 (t, J = 9.30, 2.01 Hz, 1H, CH-6), 7.46 (d, J = 9.48 Hz, 1H, CH-7), ppm; ^{13}C-NMR (100 MHz, D_2O): δ = 26.7, 54.9, 108.1, 111.0, 112.6, 120.8, 124.8, 127.2, 128.5, 135.3 ppm; MS: *m/z* (+ESI) calcd. for $C_{11}H_{12}BrN_2O_2^+$ 283.0077, found 238.0055 [MH^+]; RP-HPLC **Method 2**, t_R 6.58 min.

7.4.3.5 Preparation of Fmoc-L-Tryptophan Derivatives

General procedure

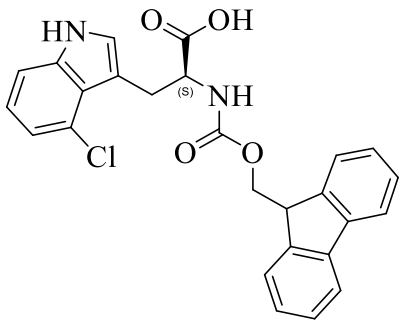
The **1.44** (1 equiv.) was dissolved in aqueous solution of sodium carbonate (3 equiv.). To this, a solution of Fmoc succinimide (1 equiv.), dissolved in anhydrous THF, was added dropwise over 15 min and the resultant reaction mixture was stirred at room temperature for 15 h. The reaction mixture was concentrated under *vacuo*. The crude mixture was dissolved in water and extracted with EtO_2. The aqueous phase was acidified to pH 2 with 1 M aqueous HCl and extracted with EtOAc, dried over $MgSO_4$ and concentrated under *vacuo* to afford the product as brown solid.

(*S*)-2-((((9H-Fluoren-9-yl)methoxy)carbonyl)amino)-3-(5-bromo-1*H*-indol-3-yl)propanoic acid (1.30a)



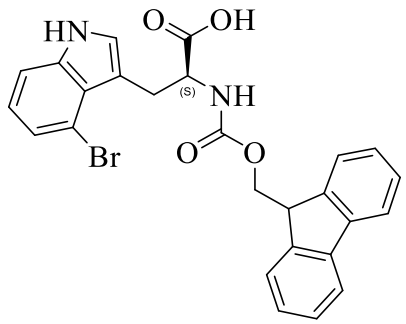
Synthesis was carried out using the general procedure, using **1.44d** (0.141 g, 0.5 mmol) in 10 mL of sodium carbonate (0.16 g, 1.5 mmol) and Fmoc succinimide (0.17 g, 0.5 mmol) dissolved in anhydrous THF (10 mL) to yield the title compound as brown solid (0.13 g, 50% yield); m.p. 130–131 °C; R_f = 0.1 ($CHCl_3$/MeOH, 9:1); $[\alpha]_D^{24}$ = –28.3 (*c* = +1.0, MeOH); ^{1}H-NMR (400 MHz, CD_3OD): δ = 3.29 (dd, *J* = 14, 8 Hz, 1H, CH_AH$_B$), 3.50 (dd, *J* = 14, 5 Hz, 1H, CH$_A$$H_B$), 4.49 (t, *J* = 7 Hz, 1H, Fmoc CH), 4.55 (m, 2H, Fmoc CH_2), 4.61 (m, 1H, α-H), 7.11 (dd, *J* = 14, 8 Hz, 1H, Ar H), 7.28 (m, 2H, Ar Hs), 7.35 (s, 1H, Ar H), 7.36-7.40 (m, 3H, Ar Hs), 7.74 (dd, *J* = 8, 3 Hz, 2H, Ar Hs), 7.81-7.89 (m, 3H, Ar Hs), 10.67 (br, 1H, COOH) ppm; ^{13}C-NMR (100 MHz, CD_3OD): δ = 27.1, 47.1, 54.7, 66.4, 110.3, 111.8, 113.2, 119.9, 120.9, 123.9, 125.1, 125.2, 125.3, 127.1, 127.6, 129.7, 135.2, 141.2, 141.3, 155.9, 172.7 ppm; MS: *m/z* (+ESI) calcd. for $C_{26}H_{22}BrN_2O_4^+$ 505.0763, found 505.0799 [MH^+]; RP-HPLC **Method 1**, t_R 11.77 min.

(*S*)-2-((((9H-fluoren-9-yl)methoxy)carbonyl)amino)-3-(4-chloro-1*H*-indol-3-yl)propanoic acid (1.30b)



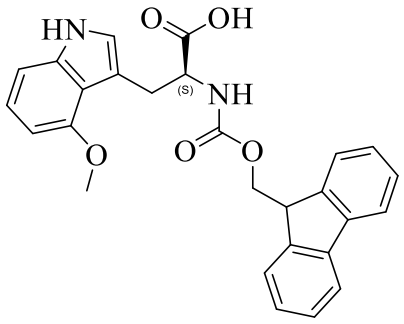
Synthesis was carried out using the general procedure using **1.44b** (0.36 g, 1.50 mmol) in 10 mL aqueous sodium carbonate (0.48 g, 4.5 mmol) and Fmoc succinimide (0.5 g, 1.5 mmol) dissolved in anhydrous THF (10 mL) to yield the title compound as brown solid; (0.311 g, 45% yield); m.p. 103–105 °C (Lit.[205] m.p. 102–104 °C); R_f = 0.1 ($CHCl_3$/ MeOH, 9:1); $[\alpha]_D^{24}$ = –12.3º (*c* = 0.50, MeOH) (Lit.[205] $[\alpha]_D^{24}$ = –10.3º (*c* = 0.55, MeOH)); ^{1}H-NMR (400 MHz, CD_3OD): δ = 3.20 (dd, *J* = 15, 8 Hz, 1H, CH_AH$_B$), 3.30 (dd, *J* = 14, 5 Hz, 1H, CH$_A$$H_B$), 4.46 (t, *J* = 9 Hz, 1H, Fmoc CH), 4.56 (m, 2H, Fmoc CH_2), 4.61 (m, 1H, α-H), 6.63 (d, *J* = 9 Hz, 1H, N*H*), 7.03 (dd, *J* = 9, 2 Hz, 1H, Ar H), 7.29 (m, 2H, Ar Hs), 7.36 (s, 1H, Ar H), 7.38-7.50 (m, 3H, Ar Hs), 7.66 (dd, *J* = 8, 4 Hz, 2H, Ar Hs), 7.70 (d, *J* = 2 Hz, 1H, Ar Hs), 7.86 (d, *J* = 8 Hz, 2H, Ar Hs), 10.99 (br, 1H, CO_2H) ppm; ^{13}C-NMR (100 MHz, CD_3OD): δ = 29.2, 47.0, 53.8, 66.9, 103.9, 111.2, 119.9, 125.1, 127.2, 128.9, 130.1, 133.2, 135.9, 137.5, 141.2, 143.8, 156.1, 174.5 ppm; MS: *m/z* (+ESI) calcd. for $C_{26}H_{22}ClN_2O_4^+$ 461.1263, found 461.1217 [MH^+].

(*S*)-2-((((9H-Fluoren-9-yl)methoxy)carbonyl)amino)-3-(4-bromo-1*H*-indol-3-yl)propanoic acid (1.30 c)



Synthesis was carried out using the general procedure, using **1.44c** (0.72 g, 2.52 mmol) in 10 mL of sodium carbonate (0.8 g, 7.56 mmol) and Fmoc succinimide (0.84 g, 2.52 mmol) dissolved in anhydrous THF (20 mL) to yield the title compound as brown solid (0.64 g, 50%); m.p. 92–94 °C (Lit.[205] m.p. 90–93 °C); R_f = 0.1 ($CHCl_3$/MeOH, 9:1); $[\alpha]_D^{24}$ = –23.3º (*c* = 1.0, MeOH) (Lit $[\alpha]_D^{24}$ = –22.3º (*c* = 1.0, MeOH)); ^{1}H-NMR (400 MHz, CD_3OD): δ = 3.30 (dd, *J* = 14, 8 Hz, 1H, CH_AH$_B$), 3.41 (dd, *J* = 14, 5 Hz, 1H, CH$_A$$H_B$), 4.30 (t, *J* = 7 Hz, 1H, Fmoc CH), 4.41 (m, 2H, Fmoc CH_2), 4.81 (m, 1H, α-H), 7.31 (dd, *J* = 14, 8 Hz, 1H, Ar H), 7.28 (m, 2H, Ar Hs), 7.32 (s, 1H, Ar H), 7.38-7.44 (m, 3H, Ar Hs), 7.74 (dd, *J* = 8, 3 Hz, 2H, Ar Hs), 7.80-7.87 (m, 3H, Ar Hs), 10.39 (br, 1H, COOH) ppm; ^{13}C-NMR (100 MHz, CD_3OD): δ = 27.4, 47.3, 60.3, 67.3, 110.1, 110.8, 112.9, 120.5, 123.0, 123.2, 125.2, 126.8, 135.3, 138.7, 142.7, 143.6, 155.8, 175.6 ppm; MS: *m/z* (+ESI) calcd. for $C_{26}H_{22}BrN_2O_4^+$ 505.3755, found 505.3789 [MH^+]; RP-HPLC **Method 1**, t_R 11.59 min.

(*S*)-2-((((9H-fluoren-9-yl)methoxy)carbonyl)amino)-3-(4-methoxy-1*H*-indol-2-yl)propanoic acid (1.30d)

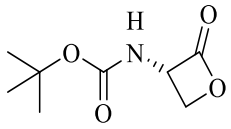


Fmoc protection was carried out using the general procedure using **1.44d** (0.50 g, 2.2 mmol), sodium carbonate (0.68 g, 6.40 mmol) and Fmoc succinimide (0.72 g, 2.14 mmol) to yield the title compound as off-white solid; (0.5 g, 50% yield); m.p. 172.9 ºC (Lit.[205] m.p. 170-172 ºC); R_f = 0.1 ($CHCl_3$/ MeOH, 9:1); $[\alpha]_D^{24}$ = –25.5° (*c* = 1.0, MeOH) (Lit.[205] $[\alpha]_D^{24}$ = –24.5 (*c* = 1.0, MeOH)); ^{1}H-NMR (400 MHz, CD_3OD): δ = 3.28 (dd, *J* = 15, 10 Hz, 1H, CH_AH_B), 3.83 (dd, *J* = 15, 7 Hz, 1H, CH_AH_B), 4.16 (s, 3H, OCH_3), 4.18 (t, *J* = 7 Hz, 1H, Fmoc CH), 4.28 (m, 2H, Fmoc CH_2), 4.32 (m, 1H, α-H), 6.93 (d, *J* = 6 Hz, 1H, NH), 7.02 (d, *J* = 6 Hz, 1H, Ar H), 7.04 (m, 2H, Ar Hs), 7.24 (s, 1H, Ar H), 7.32 (m, 2H, Ar Hs), 7.39 (m, 2H, Ar Hs), 7.60 (m, 2H, Ar Hs), 7.84 (d, *J* = 8 Hz, 2H, Ar Hs), 10.98 (br, 1H, NH) ppm; ^{13}C-NMR (100 MHz, CD_3OD): δ = 29.2, 47.1, 53.8, 55.9, 66.8, 101.9, 103.5, 111.0, 118.6, 119.1, 124.1, 125.1, 127.1, 128.9, 135.1, 135.7, 141.3, 143.6, 153.9, 156.1, 174.5 ppm; MS: *m/z* (+ESI) calcd. for $C_{27}H_{25}N_2O_5^+$ 475.1763, found 475.1799 [MH^+]; RP-HPLC **Method 1**, t_R= 11.90 min.

7.5 Experimental for Chapter 3

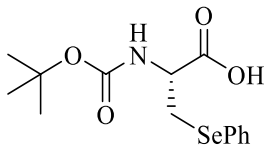
7.5.1 Preparation of Phenylselenocysteine

(*S*)-*tert*-butyl (2-oxooxetan-3-yl)carbamate (1.46)



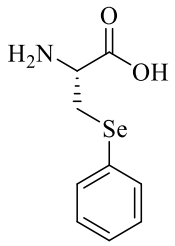
Diethyl azodicarboxylate (1.74 g, 10 mmol) was added to a stirred solution of triphenylphosphine (2.62g, 10 mmol) dissolved in dry THF (40 mL) at -78 °C under nitrogen flow. The resultant solution was stirred for 10 minutes at -78 °C. A solution of Boc-L-serine-OH **1.45** (2.05 g, 10 mmol) dissolved in dry THF (25 mL) was added drop wise over 30 minutes to the stirred solution. The resultant solution was stirred for a further 20 minutes at -78 °C under nitrogen and gradually warmed to room temperature over 2.5 hours. The reaction mixture was concentrated under *vacuo* and the yellow oil was suspended in hexane/ethyl acetate 1:1. The resultant white precipitate was filtered and the yellow filtrate was concentrated under *vacuo* and purified through column chromatography (Hexane/Ethyl acetate, 7:3) to yield the *β*-lactone **1.46** as a white solid (855 mg, 46%). m.p. 118–119 ºC (Lit[205] m.p. 119.5–120.5 ºC); MS: *m/z* (+ESI) calcd for $C_{13}H_{20}N_2O_4S$ Na+ 323.1036, found 323.1044 [MNa^+]. ^{1}H-NMR (400 MHz, $CDCl_3$): δ = 1.47 (s, 9H, C(C*H*$_3$)$_3$), 4.43 (br, 2H, C*H*$_2$), 5.11 (br, 1H, NC*H*), 5.31 (br, 1H, N*H*) ppm. ^{13}C NMR (100 MHz, $CDCl_3$): δ = 28.4, 59.7, 67.3, 83.1, 156.3, 169.7; $[\alpha]_D^{23}$ = -16.1º (c=1.0, CH_3Cl) (Lit[205] $[\alpha]_D^{23}$ = -26.7º (c=1.0, MeOH)

(*R*)-2-((tert-butoxycarbonyl)amino)-3-(phenylselanyl)propanioc acid (1.47)



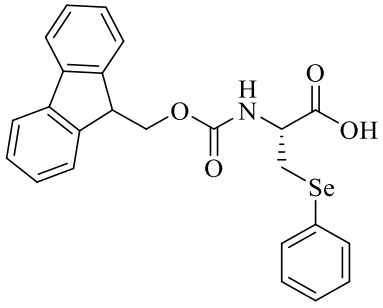
Diphenyl diselenide (758.5 mg, 2.43 mmol) was dissolved in dry ethanol (25 mL) and stirred under nitrogen at room temperature for 10 minutes until a homogenous mixture was obtained. To this sodium trimethylborohydride (622 mg, 4.86 mmol) was added and the resultant mixture was stirred for 1 hour at room temperature. To this, a solution of lactone **1.46** dissolved in dry ethanol (5 mL) was added and the resultant mixture was stirred at room temperature for 4 hours. The reaction mixture was then concentrated under *vacuo* and the dry crude was dissolved in saturated $NaHCO_3$. The aqueous layer was extracted with diethyl ether (4 x 50 mL) to remove the excess amount of diphenyl diselenide. The aqueous layer was acidified with 3M HCl to pH = 2 and extracted with ethyl acetate. The organic layers were combined, dried over sodium sulphate and concentrated under *vacuo*. The resultant crude product was suspended in hexane overnight to obtain the pure product as white solid (819 mg, 70%). m.p. 88–90 ºC (Lit[205] m.p. 89–92 °C) MS: *m/z* (+ESI) calcd for $C_{14}H_{19}NNaO_4Se$ Na+ 368.0377, found 368.0130 [MNa^+], ^1H NMR (400 MHz, $CDCl_3$): δ = 1.44 (s, 9H, $C(CH_3)_3$), 3.39 (br, 2H, CH_2), 4.64 (br, 1H, α-CH), 5.29 (br, 1H, NH), 7.28 (m, 3H, arom. CH), 7.56 (m, 2H, arom. CH) ppm. ^{13}C NMR (100 MHz, $CDCl_3$): δ = 28.3, 30.2, 53.6, 80.50, 127.61, 129.3, 133.65, 156.3, 178.3. $[\alpha]_D^{23}$ = -35.5º (c=1.0, methanol) (Lit[205] $[\alpha]_D^{23}$ = -34.5º (c=1.0, methanol))

(*R*)-2-amino-3-(phenylselenyl)propanoic acid (1.48)



Boc-Phenylselenocysteine **1.47** (735 mg, 2.13 mmol) was dissolved in dichloromethane (15 mL) and stirred at room temperature. To this trifluoroacetic acid (15 mL) was added drop-wise and the resultant solution was stirred under room temperature for 1 hour. Reaction mixture was concentrated under *vacuo* and washed with diethyl ether (3 x 30 mL) to yield the trifluoroacetate salt of the compound **1.48** as white solid (500 mg, 95%). MS: *m/z* (+ESI) calcd for $C_9H_{12}NO_2Se^+$ 246.0033, found 246.0023, ^{1}H NMR (400 MHz, MeOD): δ = 3.12 (dd, *J* = 16, 4 Hz, 1H, C*H*AHB), 3.30 (dd, *J* = 16, 4 Hz, 1H, CHA*H*B), 3.89(dd, *J* = 4, 4 Hz, 1H, α-H), 7.23 (m, 3H, arom. CH), 7.59 (m, 3H, arom. CH) ppm, ^{13}C NMR (100 MHz, $CDCl_3$): δ = 53.6, 80.5, 127.6, 129.3, 133.7, 156.3, 178.3, $[\alpha]_D^{23}$ = -29.9 (c=1.0, methanol); m.p. 166–170 °C (Lit[205] m.p. 166–170 °C).

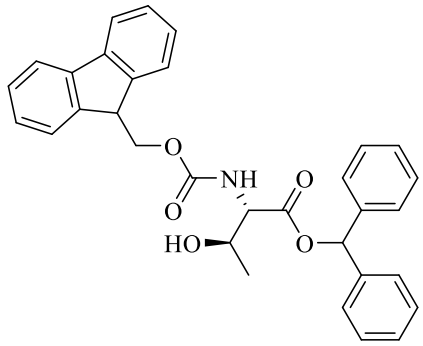
(*R*)-2-((((9H-fluoren-9-yl)methoxy)carbonyl)amino)-3-(phenylselanyl)propanoic acid (1.28)



Phenylselenocysteine **1.48** (361 mg, 1.47 mmol) was dissolved in sodium carbonate solution (496 mg, 4.42 mmol). To this, a solution of Fmoc succinimide (496 mg, 1.47 mmol) dissolved in dry THF (10 mL) was added drop-wise over 20 minutes and stirred at room temperature for 24 hours. The reaction mixture was concentrated under *vacuo*. To this water was added and extracted with diethyl ether (3 x 30 mL). The aqueous phase was acidified to pH 2 with 1 M HCl and extracted with ethyl acetate (3 x 20 mL), dried over sodium sulphate and concentrated under *vacuo* to afford the product as white solid (564 mg, 82%). RP-HPLC **Method 1**, t_R= 10.88 min. MS: *m/z* (+ESI) calcd for $C_{24}H_{21}NO_4Se$ Na+ 490.0528, found 490.0721 [MNa^+]. m.p. 98.1-99.3 °C; ^{1}H NMR (400MHz, $CDCl_3$): δ = 3.32 (dd, *J* = 5, 13 Hz, 1H, C*H*AHB), 3.42 (dd, *J* = 5, 13 Hz, 1H, C*H*AHB), 4.17 (t, *J* = 7 Hz, 1H, OCH_2CH), 4.34 (m, 2H, OCH_2CH), 4.73 (br, 1H, α-H), 5.53 (d, *J* = 8 Hz, 1H, NH), 7.26 (m, 4H, arom. CH), 7.33 (m, 2H, arom. CH), 7.40 (m, 2H, arom. CH), 7.55 (m, 3H, arom. CH), 7.75 (m, 2H, arom. CH) ppm. ^{13}C NMR (100MHz, $CDCl_3$): δ = 29.71, 47.23, 54.64, 67.34, 119.80, 125.20, 127.61, 127.92, 128.65, 129.35, 133.52, 141.30, 143.75, 144.30, 156.90; $[\alpha]_D^{23}$ = -30.9 (c=1.0, methanol) (Lit[205] $[\alpha]_D^{22}$ = –32.4º (*c* = 7.0, EtOAc))

7.5.2 Preparation for Dehydrobutyrine

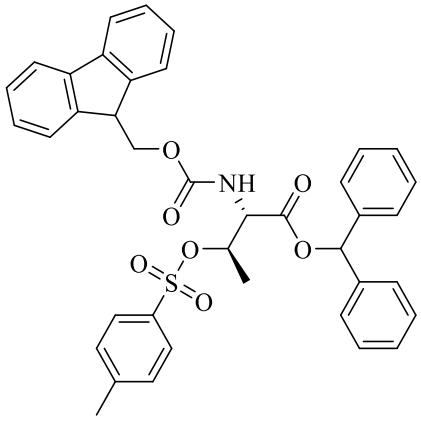
Benzhydryl (((9H-fluoren-9-yl)methoxy)carbonyl)-*L*-threoninate (1.51)



The Fmoc-threonine **1.49**(6.82 g, 20 mmol) and benzophenone hydrazine (5.88 g, 30 mmol) were dissolved in dichloromethane (100 mL). After addition of 1% iodine dichloromethane solution (10 mL), the solution is cooled at -10 °C under continued stirring. (Diacetoxyiodo)benzene (9.66 g, 30 mmol) was then added portion wise over a period of 30 minutes. The reaction mixture was allowed to warm to 0 °C and stirred for a further 30 minutes. The solvent was removed under *vacuo*, the residual material, which contains acetic acid and iodobenzene, dissolved in ethyl acetate (100 mL), and extracted with water (100 mL), 5% aqueous $NaHCO_3$ (80 mL), water until pH about 6 (2 x 80 mL), and brine (100 mL). The organic extract was dried over sodium sulfate and concentrated under *vacuo* to give the crude product. The crude product was crystallization in petroleum ether (40–60 °C) to afford the title compound as white solid (8.11 g, 80%); m.p. 128.1–129.3 °C, (Lit[274] m.p. 130–130.5 °C); $[\alpha]_D^{23} = -22.9$ ºC (c = 1.00, $CHCl_3$), (Lit[274] $[\alpha]_D^{23} = -19.9$ ºC (c = 1.67, $CHCl_3$)); ^{1}H NMR (400 MHz, $CDCl_3$): δ = 1.24 (d, J = 6.50 Hz, 3H, CH_3), 4.22 (t, J = 7.05 Hz, 1H, CH), 4.40 (m, 4H, CH+CH_2), 5.57(bs, 1H, NH), 6.93 (s, 1H, $CH(Ph)_2$), 7.30 (m, 12H, Ph), 7.39 (t, J = 7.10 Hz, 2H, Ph), 7.59 (d, J = 7.4 Hz, 2H, Ph), 7.75 (d, J = 7.4 Hz, 2H, Ph); ^{13}C NMR (100 MHz, $CDCl_3$): δ = 20.2, 47.4, 59.6, 67.5, 68.3, 78.6, 120.30 125.4, 127.3, 128.3, 128.6, 129.0, 139.6, 141.3, 143.6, 144.3, 157.3,

170.3; MS: *m/z* (+ESI) calcd. for $C_{32}H_{29}NO_5Na^+$ 507.2163, found 507.3612 [MNa^+].

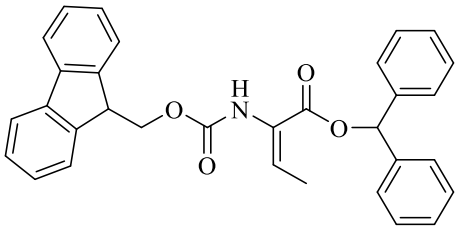
Benzhydryl *N*-(((9H-fluoren-9-yl)-methoxy)-carbonyl)-O-tosyl-L-threoninate (3.32)



The protected amino acid **1.51** (0.825 g, 1.63 mmol) was dissolved in pyridine (6 mL) at 0°C, and TsCl (0.755 g, 4.06 mmol) was added. The reaction was stirred at -10°C. After completion, the mixture was diluted with ethyl acetate and washed with 5% $KHSO_4$. The organic layer was dried with sodium sulphate, concentrated under *vacuo*, and purified through column chromatography (hexane/ethyl acetate, 1:4) to afford product as white solid (0.75 g, 70%). MS: *m/z* (+ESI) calcd for $C_{39}H_{35}NO_7S\ Na^+$ 661.2136, found 661.2369 [MNa^+]. m.p. 60.3-61.3 °C; ^{1}H NMR (400MHz, $CDCl_3$): δ = 1.33 (d, *J* = 6.47 Hz, 3H, CH_3), 2.40 (s, 3H, CH_3), 4.18 (t, *J* = 6.99 Hz, 1H, CH), 4.38 (d, *J* = 7.01 Hz, 2H, CH_2), 4.56 (dd, *J* = 9.54 Hz, 2.48 Hz, 1H, CH), 5.18 (qd, *J* = 6.40 Hz, 2.36 Hz, 1H, CH), 5.20 (d, *J* = 9.39 Hz, 1H, NH), 6.73 (s, 1H, $CH(Ph)_2$), 7.18 (d, *J* = 8.10 Hz, 2H, Ph), 7.33 (m, 14H, Ph), 7.57 (dd, *J* = 7.18 Hz, 2.59 Hz, 4H, Ph), 7.75 (d, J = 5.62 Hz, 2H, Ph); ^{13}C NMR (100MHz, CDCl3): δ = 18.4, 47.6, 58.4, 67.7, 78.2, 79.3, 120.4, 125.6, 127.6, 127.9, 128.1, 128.3, 128.4, 128.6, 129.0, 130.0, 134.3, 138.0, 139.6, 139.9, 142.3, 143.3, 143.9, 145.3, 156.3, 168.9; m.p. 60.3-61.3 °C, (Lit[274] m.p. 60.7–62.0 °C); $[\alpha]_D^{23}$ = –16.6 ºC (*c* = 1.00, $CHCl_3$), (Lit[276]

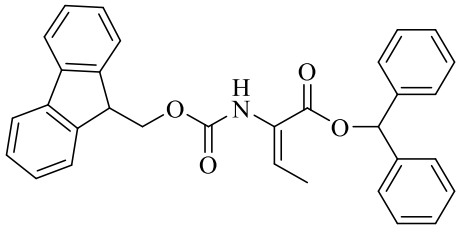
$[\alpha]_D^{23} = -15.4$ ºC (c = 1.93, $CHCl_3$))

Benzhydryl -2-((((9H-fluoren-9-yl)methoxy)carbonyl)amino)but-2-enoate (33)



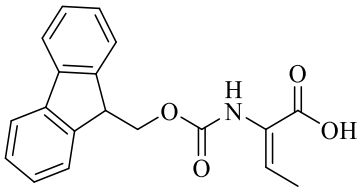
The protected amino acid **31** (0.825 g, 1.63 mmol) was dissolved in pyridine (6 mL) at -10°C, and TsCl (0.755 g, 4.06 mmol) was added. The reaction was stirred at -10°C for 2 days. After that, the reaction temperature was brought up to 50°C and stirred for 10 hours. After completion, the mixture was diluted with ethyl acetate (100 mL) and washed with 5% $KHSO_4$ (3 x 50 mL). The organic layer was dried with sodium sulphate, concentrated under *vacuo*, and purified through column chromatography (hexane/ethyl acetate, 1:4) to afford product as colourless oil (0.40 g, 50%). MS: *m/z* (+ESI) calcd for $C_{32}H_{27}NO_4$ Na^+ 489.1621 [MNa^+], found 5152.239 ^{1}H NMR (400MHz, $CDCl_3$): δ = 1.84 (t, J = 6.47 Hz, 3H, CH_3), 4.20 (br, 1H, CH), 4.40 (br, 2H, CH_2), 6.95 (q, J = 6.47 12.6 Hz, 1H, $CH(Ph)_2$), 7.35 (br, 14H, Ph), 7.60 (m, 2H, Ph), 7.78 (d, J = 7.60 Hz, Ph); ^{13}C NMR (100MHz, $CDCl_3$): δ = 13.5, 68.5, 78.6, 94.7, 126.4, 126.6, 128.1, 128.3, 128.4, 128.6, 129.0, 130.1, 135.3, 137.9, 139.4, 139.9, 142.3, 143.2, 143.9, 145.3, 156.3, 168.9 ppm

Benzhydryl -2-((((9H-fluoren-9-yl)methoxy)carbonyl)amino)but-2-enoate (1.53)



Diphenyl diselenide (87 mg, 0.278 mmol) was dissolved in dry ethanol (5 mL) and stirred under nitrogen at room temperature for 10 minutes until a homogenous mixture obtained. To this, sodium trimethylborohydride (72 mg, 0.557 mmol) was added and the resultant mixture was stirred for 1 hour at room temperature. After that, a solution of protected amino acid **3.32** in dry ethanol (2 mL) was added and the resultant mixture was stirred at room temperature for 4 hours. The reaction mixture was then concentrated under *vacuo* and the dry crude was dissolved in saturated $NaHCO_3$ (100mL). The aqueous layer extracted with ethyl acetate (3 x 10 mL). The organic layer was combined, dried over sodium sulphate, concentrated under *vacuo* and purified through column chromatography (hexane/ethyl acetate, 1:4) to afford **1.53** as colourless oil (99 mg, 60%). MS: *m/z* (+ESI) calcd for $C_{32}H_{27}NO_4\ Na^+$ 489.1621 [MNa^+], found 5152.239 ^{1}H NMR (400MHz, $CDCl_3$): δ = 1.84 (t, *J* = 6.47 Hz, 3H, CH_3), 4.20 (br, 1H, CH), 4.40 (br, 2H, CH_2), 6.95 (q, *J* = 6.47 12.6 Hz, 1H, $CH(Ph)_2$), 7.35 (br, 14H, Ph), 7.60 (m, 2H, Ph), 7.78 (d, *J* = 7.60 Hz, Ph); ^{13}C NMR (100MHz, $CDCl_3$): δ = 13.5, 68.5, 78.6, 94.7, 126.4, 126.6, 128.1, 128.3, 128.4, 128.6, 129.0, 130.1, 135.3, 137.9, 139.4, 139.9, 142.3, 143.2, 143.9, 145.3, 156.3, 168.9 ppm

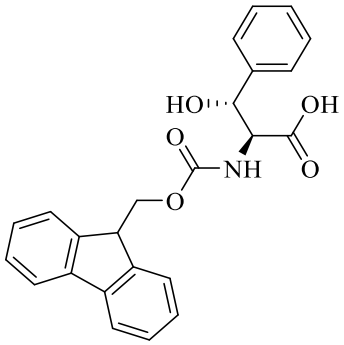
(Z)-2-((((9H-fluoren-9-yl)methoxy)carbonyl)amino)but-2-enoic acid (1.55)



1.53 (1.50 g, 3.07 mmol) was dissolved in 40 mL DCM/TFA/anisole (20/16/4) and stirred at room temperature for 2 h. The solution was then evaporated under *vacuo* to dryness and the residual material was extensively triturated with diethyl ether to afford the **1.55** as a white solid (0.864 g, 87%); m.p. 226.6 - 227.5 °C; R_f = 0.17 (EtOAc/hexane/AcOH, 10:10:0.1); ^{1}H-NMR (400 MHz, DMSO-d_6): δ = 1.74 (d, J = 7 Hz, 3H, CH_3), 4.25 (m, 1H, Fmoc-CH), 4.38 (d, J = 7 Hz, 2H, Fmoc-CH_2), 6.75 (q, J = 14, 7 Hz, 1H, CH), 7.29 (m, 3H, ArHs), 7.37 (m, 2H, ArHs), 7.67 (m, 2H, ArHs), 7.79 (d, J = 7 Hz, 2H, ArHs) ppm; ^{13}C-NMR (100 MHz, DMSO-d_6): δ = 13.7, 47.1, 120.6, 125.7, 127.2, 127.5, 128.1, 128.8, 129.1, 129.5, 129.7, 141.2, 144.2; MS: *m/z* (+ESI) calcd. for $C_{19}H_{18}NO_4^+$ 324.1230, found 324.1237 [MH^+]; RP-HPLC **Method 1**, t_R 9.43 min

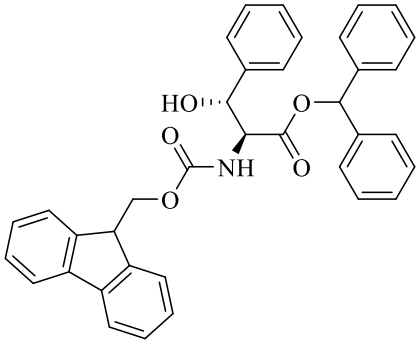
7.5.3 Preparation for Dehydrophenylalanine

2-((((9H-fluoren-9-yl)methoxy)carbonyl)amino)-3-hydroxy-3-phenylpropanoic acid (1.50)



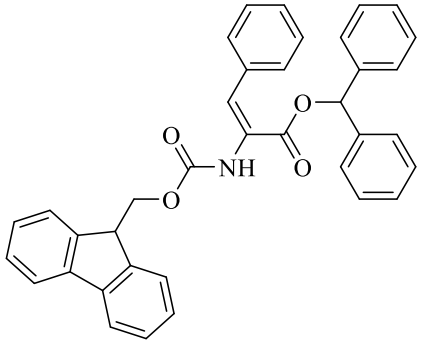
Synthesis was carried out using the procedure described above, using 2-amino-3-hydroxy-3-phenylpropanoic acid (0.91 g, 5 mmol) in 10 mL aqueous sodium carbonate (0.53 g, 15 mmol) and Fmoc succinimide (1.67 g, 5 mmol) dissolved in anhydrous THF (10 mL) to yield the title compound as brown solid; (1.01 g, 50%); m.p. 231-233^{o} C; R_f = 0.1 ($CHCl_3$/ MeOH, 9:1); ^{1}H-NMR (400 MHz, CD_3OD): ^{1}H NMR: δ 4.46 (1H, t, *J* = 3.1 Hz), 4.59-4.62 (2H, 4.61 (d, *J* = 3.1 Hz), 4.61 (d, *J* = 3.1 Hz)), 5.21 (1H, d, *J* = 6.7 Hz), 5.36 (1H, d, *J* = 6.7 Hz), 7.30-7.49 (9H, m, ArH), 7.64-7.70 (2H, m, ArH), 7.83-7.89 (2H, m, ArH), 12.89 (1H, br, COOH). ppm; ^{13}C-NMR (100 MHz, CD_3OD): δ = 47.0, 60.2, 66.9, 73.5, 119.8, 125.1, 126.5, 127.2, 128.5, 128.9, 140.1, 141.2, 143.8, 155.5, 174.9 ppm; MS: *m/z* (+ESI) calcd. for $C_{24}H_{22}NO_5^+$ 404.1492, found 404.1456 [MH^+].

Benzhydryl(2S,3R)-2-((((9H-fluoren-9-yl)methoxy)carbonyl)amino)-3-hydroxy-3-phenylpropanoate (1.52)



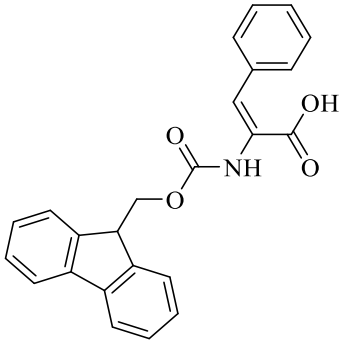
The Fmoc-threonine **1.50** (2 g, 5 mmol) and benzophenone hydrazine (1.47 g, 7.5 mmol) were dissolved in dichloromethane (100 mL). After addition of 1% iodine dichloromethane solution (10 mL), the solution is cooled at -10 °C under continued stirring. (Diacetoxyiodo)benzene (2.42 g, 7.5 mmol) was then added portionwise over a period of 30 minutes. The reaction mixture was allowed to warm to 0 °C and stirred for a further 30 minutes. The solvent was removed under *vacuo*, the residual material, which contains acetic acid and iodobenzene, dissolved in ethyl acetate (100 mL), and extracted with water (100 mL), 5% aqueous $NaHCO_3$ (80 mL), water until pH about 6 (2 x 80 mL), and brine (100 mL). The organic extract was dried over sodium sulfate and concentrated under *vacuo* to give the crude product. The crude product was column chromatography (Hexane/Ethyl acetate, 1:4) to afford the title compound as white solid (2 g, 70%); m.p. 195–197 °C; ^{1}H NMR (400 MHz, $CDCl_3$): δ 4.46 (1H, t, *J* = 3.1 Hz), 4.59-4.62 (2H, m), 5.14 (1H, d, *J* = 6.7 Hz), 5.40 (1H, d, *J* = 6.7 Hz), 6.47 (1H, s), 7.30-7.51 (13H, m, ArH), 7.55-7.61 (4H, m, ArH), 7.64-7.72 (4H, m, ArH), 7.83-7.89 (2H, m, ArH).; ^{13}C NMR (100 MHz, $CDCl_3$): δ = 47.1, 60.2, 66.9, 73.6, 79.1, 119.9, 125.1, 126.5, 127.1, 127.2, 127.3, 128.1, 128.5, 128.6, 128.9, 139.1, 140.1, 141.3, 143.7, 155.5, 171.3; MS: *m/z* (+ESI) calcd. for $C_{37}H_{32}NO_5^+$ 570.2275, found 507.3612 [MH^+].

Benzhydryl (Z)-2-((((9H-fluoren-9-yl)methoxy)carbonyl)amino)-3-phenylacrylate (1.54)



The protected amino acid **1.52** (0.57 g, 1 mmol) was dissolved in pyridine (6 mL) at -10°C, and TsCl (0.19 g, 1 mmol) was added. The reaction was stirred at -10°C for 2 days. After that, the reaction temperature was brought up to 50°C and stirred for 10 hours. After completion, the mixture was diluted with ethyl acetate (100 mL) and washed with 5% $KHSO_4$ (3 x 50 mL). The organic layer was dried with sodium sulphate, concentrated under *vacuo*, and purified through column chromatography (Hexane/Ethyl acetate, 1:4) to afford product as colourless oil (0.26 g, 50%). ^{1}H NMR (400MHz, $CDCl_3$): δ = 4.48 (1H, t, *J* = 3.1 Hz), 4.60-4.62 (3H, m), 5.18 (1H, d, *J* = 6.7 Hz), 5.41 (1H, d, *J* = 6.7 Hz), 6.49 (1H, s), 7.32-7.51 (13H, m, ArH), 7.55-7.64 (4H, m, ArH), 7.66-7.78 (4H, m, ArH), 7.83-7.89 (2H, m, ArH).; ^{13}C NMR (100 MHz, $CDCl_3$): δ = 47.1, 66.9, 79.2, 119.9, 125.2, 127.1, 127.2, 127.3, 128.1, 128.5, 128.7, 128.9, 131.7, 139.1, 140.1, 141.3, 143.7, 154.5, 161.6; MS: *m/z* (+ESI) calcd. for $C_{37}H_{30}NO_4^+$ 552.2169, found 552.2147 [MH^+].

(Z)-2-((((9H-fluoren-9-yl)methoxy)carbonyl)amino)-3-phenylacrylic acid (1.56)



The protected amino **1.54** (0.25 g, 0.45 mmol) was dissolved in 20 mL DCM/TFA/anisole (20/16/4) and stirred at room temperature for 2 h. The solution was then evaporated under *vacuo* to dryness and the residual material was extensively triturated with diethyl ether to afford the **1.56** as a white solid (0.15 g, 87%); m.p. 226.6 - 227.5 °C; R_f = 0.2 (EtOAc/hexane/AcOH, 10:10:0.1); ^{1}H-NMR (400 MHz, DMSO-d_6): δ = 4.46 (m, 1H, Fmoc-CH), 4.70 (d, J = 7 Hz, 2H, Fmoc-CH_2), 6.13 (s, 1H, CH), 7.29 (m, 3H, ArHs), 7.37 (m, 3H, ArHs), 7.67 (m, 3H, ArHs), 7.79 (d, J = 7 Hz, 4H, ArHs), 12.56 (br, 1H, COOH) ppm; ^{13}C-NMR (100 MHz, DMSO-d_6): δ = 47.1, 66.9, 119.2, 125.1, 127.3, 128.6, 130.9, 132.5, 141.5, 143.9, 154.8, 164.3 ; MS: *m/z* (+ESI) calcd. for $C_{24}H_{20}NO_4^+$ 386.1387, found 386.1372 [MH^+], RP-HPLC **Method 1**, t_R 11.96 min.

7.6 Experimental for Chapter 4

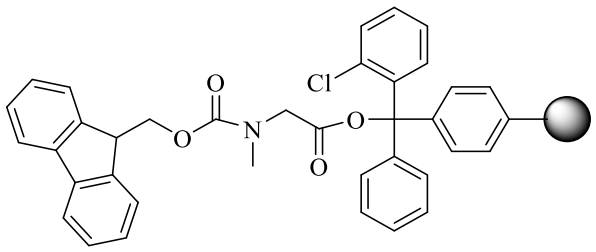
7.6.1 Preparation of Linear Argyrin Precursors

7.6.1.1 General Procedure for Determination of Resin Substitution Based on the Fmoc-Substitution Test

An accurately weight of dry Fmoc-substituted resin was transferred to a vial containing a solution of 20% *v/v* piperidine in DMF (3 mL) and left for 3 hours. 300µL of the reaction solution was diluted to 3 mL of fresh piperidine solution. The UV absorbance reading was taken at 290 nm. The loading was calculated using equation: **Loading (mmol/g) = ($Absorbance_{sample}$)/(weight of sample x 1.75)**

The percentage efficiency of the resin loading was evaluated by equation: loading efficiency (%) = (loading / theoretical loading) x 100

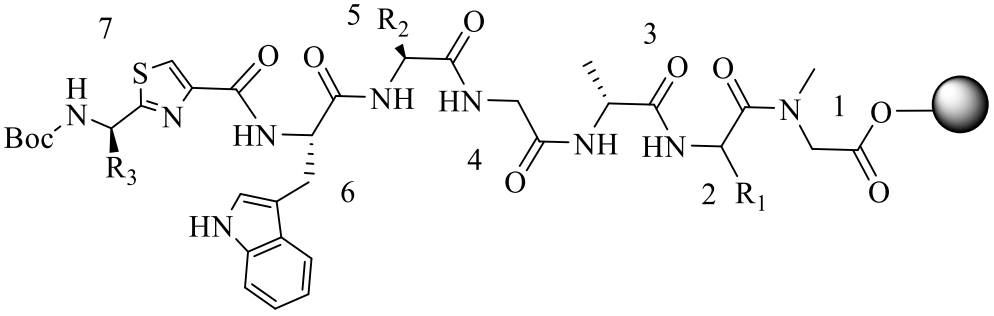
(*S*)-2-Chlorotrityl[*N*-(fluoren-9-ylmethoxycarbonyl)methyl-amino]-aceticacid Polystyrene 1.23



2-chlorotrity resin **4.14** (1g, 1.2 mmol) was placed in a round bottom flask and swollen in 5mL DCM for 2 hours. Fmoc-sar-OH (0.37g, 1.2 mmol) and DIPEA (0.42 mL, 2.4 mmol) were added to the resin containing flask. After stirring for

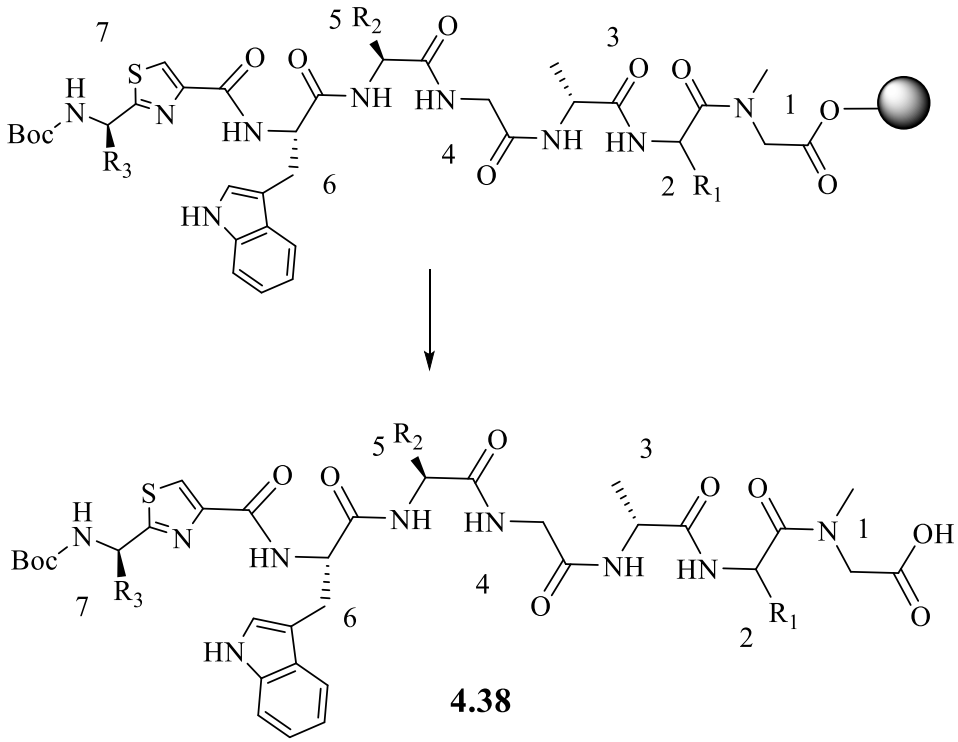
3 hours, methanol (10 mL) was added and stirred for a further 15 minutes. After that, the resin was filtered, washed with DMF, DCM and hexane, and dried under *vacuo* (1.340 g, 85%). The loading of **36** is 0.667 mmol/g.

7.6.1.2 General Procedure for Linear Argyrin Assembly



The resin product **1.23** (1 equiv.) was placed in an Omnifit^{TM} continuous flow glass column (150 x 10 mm) and swollen with a mixture of DMF/DCM 1:1 for 15 h. The resin was washed under continuous flow of DMF (2.8 mL min^{-1}, 10 min). Fmoc deprotection was carried out under continuous flow of 20% *v/v* piperidine in DMF (2.8 mL min^{-1}, 10 min) and washed with DMF (2.8 mL min^{-1}, 10 min). Washing and deprotection steps were carried out using a NOVA SYN® GEM peptide manual synthesiser and the reaction was monitored post column at 344 nM. Sequential acylation reactions were carried out for 4 h at ambient temperature in the reaction column using appropriately *N*α-protected amino acid (4 equiv), carboxyl-activating reagent HATU (3.9 equiv.) and DIPEA (8 equiv.) dissolved in 0.6–1.0 mL of DMF. Each acylation reaction was followed by wash and deprotection step as described above. After the desired sequence Boc-R_3-Thz^7-Trp^6-$R_2{}^5$-Gly^4-$R_1{}^3$-Ph(Se)^2-OH was assembled, the resin was washed with DMF (15 min, 2.5 mL min^{-1}), filtered and washed successively with DMF, DCM and hexane, and dried under *vacuo*.

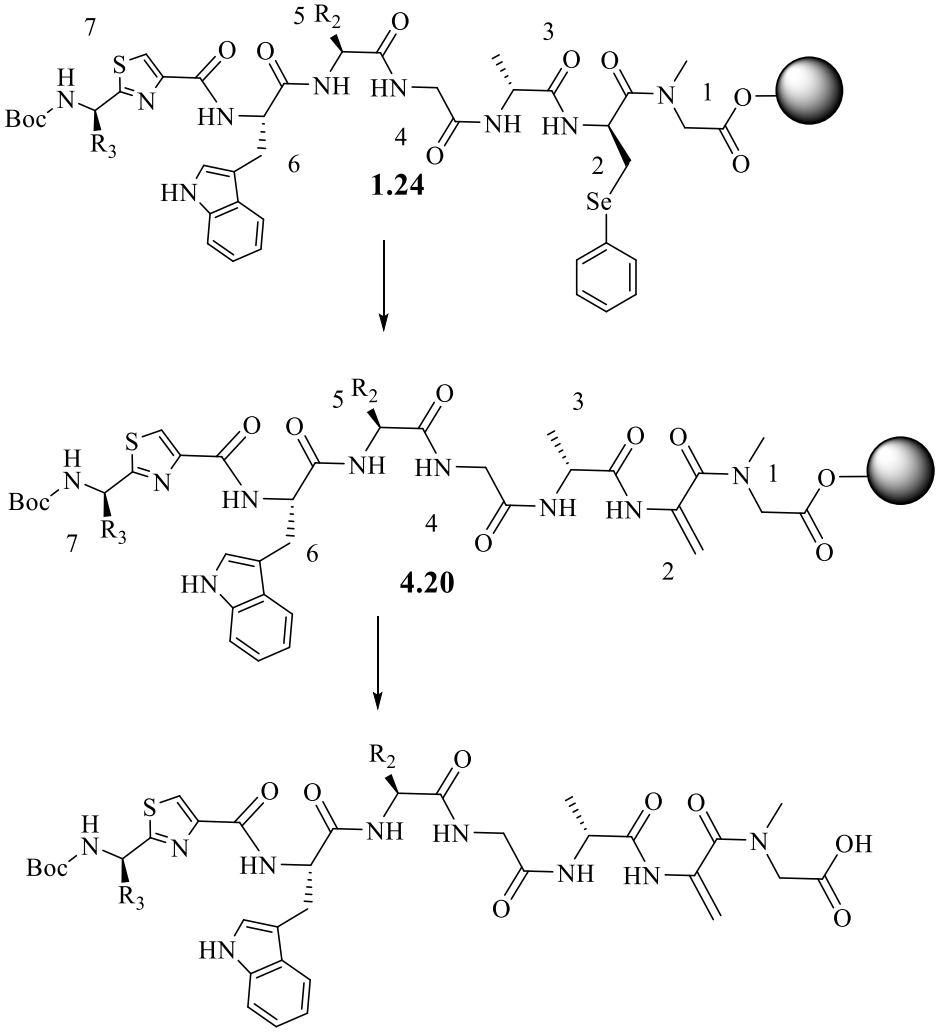
7.6.1.3 General Procedure for Acidolytic Cleavage



4.38

The peptidyl resin was suspended in a mixture of TFA/DCM, 1:1 (10 mL) for 3 h. The resin was filtered, washed with DCM and the filtrate was concentrated under *vacuo*. The residual material was triturated with diethyl ether to afford the crude peptide which was analysed using RP-HPLC. The crude **4.38** was subjected to cyclisation without purification.

7.6.2 General Procedure for On-resin Oxidation Elimination of Phenyl Selenide



The linear peptide on resin was placed in an Omnifit™ continuous flow glass column (150 x 10 mm) and swollen with DMF/DCM 1:1 mixture for 10 h. The resin was washed with DMF (5 mL) and a solution of $NaIO_4$ (2 equiv.) dissolved in DMF/H_2O 1:1 (1 mL) added to the column and stirred intermittently at ambient temperature until the reaction completion was determined by RP-HPLC. Subsequently, the resin was washed successively with DMF (5 mL), H_2O (20 mL) and DMF (15 mL), filtered, washed successively with DCM and hexane, and dried under *vacou*. The peptidyl resin was then suspended in a

mixture of TFA/DCM 1:1 (10 mL) for 2 h. The resin was filtered, washed with DCM and the filtrate was concentrated under *vacou*. The residual material was triturated with cold diethyl ether to afford the crude peptide which was analysed using RP-HPLC. The crude product was subjected to macrocyclisation without purification.

H-D-Ala-Thz-Trp-Thr(Bzl)-Gly-D-Ala-DhA-Sar-OH (4.25)

Crude yield: 39 mg, 40%; MS: *m/z* (+ESI) calcd for $C_{39}H_{48}N_9O_9S^+$ 818.32 [MH^+] found 818.0645; RP-HPLC **Method 1**, t_R 6.72 min.

H-D-Ala-Thz-Trp-Trp(5-Br)-Gly-D-Ala-DhA-Sar-OH (4.30)

Crude yield: 44 mg, 80%; ES-MS *m/z* calcd. for $C_{39}H_{444}BrN_{10}NaO_8S^+$ 891.2242, found 891.2200 [MNa^+]; RP-HPLC **Method 1**, t_R 6.58 min.

H-D-Ala-Thz-Trp-Trp(4-Cl)-D-Allygly-D-Ala-DhA-Sar-OH (4.31)

Crude yield: 49 mg, 84%; ES-MS *m/z* calcd. for $C_{41}H_{45}BrN_{10}O_8S$ 872.28 [MH^+] found 872.9678; RP-HPLC **Method 1**, t_R 6.49 min.

H-D-Ala-Thz-Trp-Trp(4-Br)-Gly-D-Ala-DhB-Sar-OH (4.29)

Crude yield: 39 mg, 84%; ES-MS *m/z* calcd. for $C_{40}H_{45}BrN_{10}NaO_8S^+$ 927.2218, found 927.2190 [MNa^+]; RP-HPLC **Method 1**, t_R 6.58 min.

H-D-Ala-Thz-Trp-Trp(4-Cl)-Gly-D-Ala-DhB-Sar-OH (4.32)

Crude yield: 19.0 mg, 44%; ES-MS *m/z* calcd. for $C_{40}H_{46}ClN_{10}O_8S^+$ 861.2904, found 861.2911 [MH^+]; RP-HPLC **Method 1**, t_R 6.50 min.

H-D-Ser(OMe)-Thz-Trp-Trp(4-Br)-Gly-D-Ala-DhB-Sar-OH (4.33)

Crude yield: 162 mg; ES-MS *m/z* calcd. for $C_{41}H_{47}BrN_{10}NaO_9S^+$ 957.2324, found 957.2304 [MNa^+]; RP-HPLC **Method 1**, t_R 6.30 min.

H-D-Ala-Thz-Trp-Trp(4-MeO)-Gly-D-Ala-DhB-Sar-OH (4.34)

Crude yield: 42 mg, 84%; ES-MS *m/z* calcd. for $C_{41}H_{49}N_{10}O_9S^+$ 857.3399, found 857.3439 [MH^+]; RP-HPLC **Method 1**, t_R 6.58 min.

H-D-Ala-Thz-Trp-Trp(4-Br)-Gly-D-Ala-DhPh-Sar-OH (4.35)

Crude yield: 50 mg, 82%; ES-MS *m/z* calcd. for $C_{45}H_{48}BrN_{10}O_8S^+$ 967.2555, found 967.2553 [MH^+]; RP-HPLC **Method 1**, t_R 7.59 min.

H-D-Ala-Thz-Trp-Trp(4-Br)-Gly-D-Ala-DhVal-Sar-OH (4.36)

Crude yield: 44 mg, 80%; ES-MS *m/z* calcd. for $C_{40}H_{45}BrN_{10}O_8S^+$ 919.2555, found 919.2546 [MH^+]; RP-HPLC **Method 1**, t_R 6.93 min.

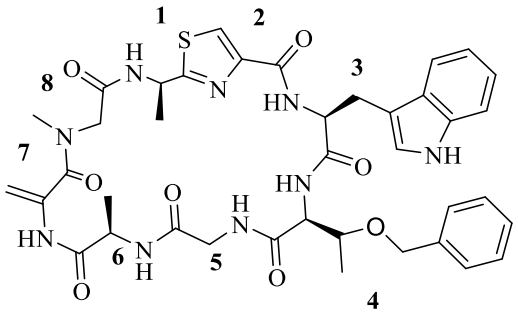
H-D-Ala-Thz-Trp-Trp(4-Br)-Gly-D-Ala-DhLeu-Sar-OH (4.37)

Crude yield: 48 mg, 81%; ES-MS *m/z* calcd. for $C_{42}H_{50}BrN_{10}O_8S^+$ 933.2712, found 933.2725 [MH^+]; RP-HPLC **Method 1**, t_R 7.58 min.

7.6.2 General Procedure for Head-to-Tail Cyclisation

PyBOP (2 equiv.), HOBt (2 equiv.) and DIPEA (9 equiv.) were added successively to a 0.5 mM solution of crude linear peptide (1 equiv.) in DMF:DCM (1:200). The reaction mixture was stirred for 15 h or until completion is determined by RP-HPLC. The crude mixture was concentrated under *vacuo* and purified using semi-preparative RP-HPLC.

***Cyclo*[D-Ala-Thz-Trp-Thr(Bzl)-Gly-D-Ala-DhA-Sar] (4.40)**

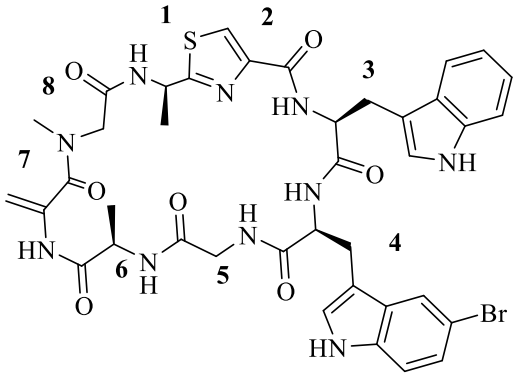


Synthesis was carried out using the general procedure for head-to-tail cyclisation employing PyBOP (24 mg, 0.044 mmol), HOBt (6.8 mg, 0.044 mmol) and DIPEA (29 µL, 0.20 mmol) in a 0.5 mM solution of crude linear peptide (20 mg, 0.023 mmol).The crude mixture was concentrated under *vacuo* and purified using preparative RP-HPLC **method 1** and freeze dried to afford the title peptide as white powder (6 mg, 35% yield); $[\alpha]_D^{22} = +125.97^o$ ($c = 0.1$, MeOH);

^{1}H-NMR (400 MHz, DMSO-d$_6$): δ = 0.79 (d, J = 7 Hz, 3H, 6-CH$_3$),1.16 (d, J = 7 Hz, 3H, 4-CH$_3$), 1.56 (d, J = 7 Hz, 3H, 1-CH$_3$), 1.79 (d, J = 7 Hz, 3H, 7-CH$_3$), 3.19 (s, 3H, 8-CH$_3$), 3.25-3.79 (m, 5H, 3-CH$_2$,, 5-CH_AH$_B$, 8-CH$_2$), 4.23 (m, 1H, 6-α-CH), 4.32 (m, 2H, 3-α-CH, 5-CH$_A$$H_B$), , 4.77 (td, J = 12, 3 Hz, 1H, 4-α-CH), 5.38 (m, 1H, 1-α-CH), 5.40 (s, 2H, 7-CH$_2$), 6.92-7.03, 7.21-7.27 (m,

7H, Ar Hs), 7.38 (d, *J* = 8 Hz, 1H, Ar H), 7.83 (d, *J* = 7 Hz, 1H, Ar H), 8.01 (d, *J* = 9 Hz, 1H, 1-NH), 8.15 (d, *J* = 9 Hz, 1H, 6-NH), 8.46 (m, 1H, 3-NH), 8.55 (s, 1H, 7-NH), 8.69 (m, 2H, 4-NH, 5-NH), 10.73 (s, 1H, indole-NH),ppm; MS: *m/z* (+ESI) calcd. for $C_{39}H_{46}N_9O_8S^+$ 799.3112 [MH^+] found 800.0704; RP-HPLC **Method 1**, t_R 9.42 min.

***Cyclo*[D-Ala-Thz-Trp-Trp(5-Br)-Gly-D-Ala-DhA-Sar] (4.41)**

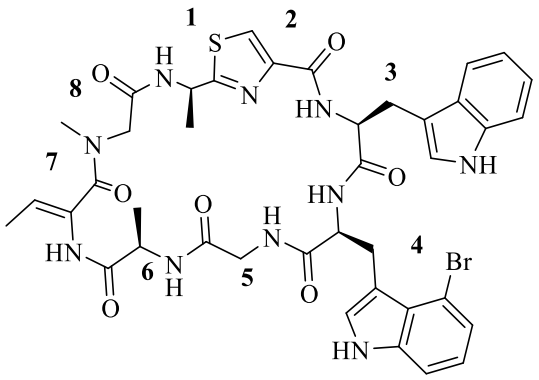


Synthesis was carried out using the general procedure for head-to-tail cyclisation employing PyBOP (26 mg, 0.05 mmol), HOBt (6.8 mg, 0.05 mmol) and DIPEA (38 µL, 0.225 mmol) in a 0.5 mM solution of crude linear peptide (22.6 mg, 0.025 mmol).The crude mixture was concentrated under *vacuo* and purified using preparative RP-HPLC **method 1** and freeze dried to afford the title peptide as white powder (6 mg, 30% yield); $[\alpha]_D^{22}$ = +120.96° (*c* = 0.97, MeOH);

^{1}H-NMR (400 MHz, DMSO-d$_6$): δ = 1.10 (d, *J* = 7 Hz, 3H, 6-CH$_3$), 1.58 (d, *J* = 7 Hz, 3H, 1-CH$_3$), 3.32 (s, 3H, 8-CH$_3$), 3.42 (d, *J* = 7 Hz, 1H, 3-C*H*$_A$H$_B$), 3.43 (d, *J* = 7 Hz, 1H, 8-C*H*$_A$H$_B$), 3.49 (d, *J* = 7 Hz, 1H, 4-CH$_A$H$_B$), 3.53 (m, 2H, 5-C*H*$_A$H$_B$ and 4- CH$_A$*H*$_B$), 3.58 (d, *J* = 6 Hz, 1H, 3-CH$_A$*H*$_B$), 3.62 (m, 1H, 8-CH$_A$*H*$_B$), 3.67 (m, 1H, 5-CH$_A$*H*$_B$), 4.45 (m, 2H, 4 and 6-α-CH), 4.97 (s, 1H, 7-C*H*$_A$H$_B$), 5.10 (m, 1H, 3-α-CH), 5.27 (s, 1H, 7-CH$_A$*H*$_B$), 5.53 (m, 1H, 1-α-CH), 7.06 (m, 2H, Ar Hs), 7.12 (d, *J* = 8, 1 Hz, 1H, Ar H), 7.14 (d, *J* = 2 Hz,

1H, Ar H), 7.26 (m, 2H, Ar Hs), 7.32 (m, 1H, Ar H), 7.36 (d, J = 8 Hz, 1H, Ar H), 7.50 (dd, J = 8 Hz, 1H, Ar H), 7.70 (m, 2H, 4 and 5- NH), 7.84 (d, J = 8 Hz, 1H, 6-NH), 8.02 (s, 1H, 2-CH), 8.58 (d, J = 9 Hz, 1H, 1-NH), 8.91 (d, J = 8 Hz, 1H, 3-NH), 9.21 (s, 1H, 7-NH), 10.44 (s, 1H, indole-NH), 10.58(s, 1H, indole-NH) ppm; MS: *m/z* (+ESI) calcd. for $C_{39}H_{42}BrN_{10}O_7S^+$ 873.2137, found 873.2130 [MH^+]; RP-HPLC **Method 1**, t_R = 9.34 min.

***Cyclo*[D-Ala-Thz-Trp-Trp(4-Br)-Gly-D-Ala-DhA-Sar] (4.42)**

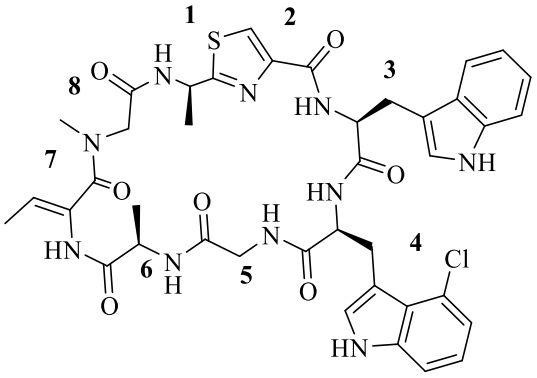


Synthesis was carried out using the general procedure for head-to-tail cyclisation employing PyBOP (26 mg, 0.05 mmol), HOBt (6.8 mg, 0.05 mmol) and DIPEA (38 μL, 0.225 mmol) in a 0.5 mM solution of crude linear peptide (22.6 mg, 0.025 mmol).The crude mixture was concentrated under *vacuo* and purified using preparative RP-HPLC **method 1** and freeze dried to afford the title peptide as white powder (7.76 mg, 35% yield); $[\alpha]_D^{22} = +131.96^o$ ($c = 0.97$, MeOH);

^{1}H-NMR (400 MHz, DMSO-d_6): δ = 0.79 (d, J = 7 Hz, 3H, 6-CH_3), 1.54 (d, J = 7 Hz, 3H, 1-CH_3), 1.78 (d, J = 7 Hz, 3H, 7-CH_3), 3.19 (s, 3H, 8-CH_3), 3.25-3.79 (m, 7H, 3-CH_2, 4-CH_2, 5-CH_AH$_B$, 8-CH_2), 4.23 (m, 1H, 6-α-CH), 4.32 (m, 2H, 3-α-CH, 5-CH$_A$$H_B$), 4.77 (td, J = 12, 3 Hz, 1H, 4-α-CH), 5.38 (m, 1H, 1-α-CH), 5.53 (q, J = 14, 7 Hz, 1H, 7-CH), 6.92-7.03, 7.20-7.27 (m, 7H, Ar Hs), 7.38 (d, J = 8 Hz, 1H, Ar H), 7.83 (d, J = 7 Hz, 1H, Ar H), 7.95 (s, 1H, 2-CH),

8.01 (d, *J* = 9 Hz, 1H, 1-NH), 8.15 (d, *J* = 9 Hz, 1H, 6-NH), 8.46 (m, 1H, 3-NH), 8.55 (s, 1H, 7-NH), 8.69 (m, 2H, 4-NH, 5-NH), 10.73 (s, 1H, indole-NH), 11.25 (d, *J* = 2 Hz, 1H, indole-NH) ppm; MS: *m/z* (+ESI) calcd. for $C_{40}H_{44}BrN_{10}O_7S^+$ 887.2293 and 889.2273, found 887.2287 and 889.2263 [MH^+]; RP-HPLC **Method 1**, t_R 9.87 min.

***Cyclo*[d-Ala-Thz-Trp-Trp(4-Cl)-Gly-d-Ala-DhB-Sar] (4.43)**

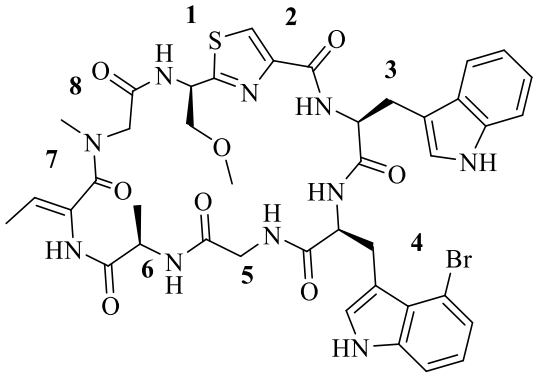


Synthesis was carried out using the general procedure for head-to-tail cyclisation employing PyBOP (12 mg, 0.02 mmol), HOBt (3 mg, 0.02 mmol) and DIPEA (17.5 µL, 0.10 mmol) in a 0.5 mM solution of crude linear peptide **(intermediate 13n)** (10 mg, 0.01 mmol). The crude mixture was concentrated under *vacuo* and purified using preparative RP-HPLC **method 1** and freeze dried to afford the title peptide as white powder (0.5 mg, 15% yield); $[\alpha]_D^{22}$ = +181.82° (*c* = 0.088, MeOH);

^{1}H-NMR (400 MHz, DMSO-d$_6$): δ = 0.81 (d, *J* = 7 Hz, 3H, 6-CH_3), 1.56 (d, *J* = 7 Hz, 3H, 1-CH_3), 1.80 (d, *J* = 7 Hz, 3H, 7-CH_3), 3.20 (s, 3H, 8-CH_3), 3.53-3.75 (m, 7H, 3-CH_2, 4-CH_2, 5-CH_AH$_B$, 8-CH_2), 4.25 (m, 1H, 6-α-CH), 4.33 (m, 2H, 3-α-CH, 5-CH_AH$_B$), 4.78 (m, 1H, 4-α-CH), 5.41 (m, 1H, 1-α-CH), 5.54 (q, *J* = 11, 6 Hz, 1H, 7-CH), 6.99-7.11, 7.20-7.28 (m, 7H, Ar Hs), 7.36 (dd, *J* = 7, 2 Hz , 1H, Ar H), 7.86 (d, *J* = 7 Hz, 1H, Ar H), 7.96 (s, 1H, 2-CH), 8.04 (d, *J* = 9 Hz, 1H, 1-NH), 8.18 (d, *J* = 9 Hz, 1H, 6-NH), 8.46 (m, 1H, 3-NH), 8.58 (s,

1H, 7-NH), 8.73 (m, 2H, 4-NH, 5-NH), 10.75 (s, 1H, indole-NH), 11.27 (s, 1H, indole-NH) ppm; MS: *m/z* (+ESI) calcd. for $C_{40}H_{44}ClN_{10}O_7S^+$ 843.2798 and 845.2769, found 843.2839 and 845.2850 [MH^+]; and calcd. for $C_{40}H_{43}ClN_{10}NaO_7S^+$ 865.2623 and 867.2594, found 865.2650 and 867.2658 [MNa^+]; RP-HPLC **Method 1**, t_R 9.55 min.

***Cyclo*[d-Ser(OMe)-Thz-Trp-Trp(4-Br)-Gly-d-Ala-DhB-Sar] (4.44)**

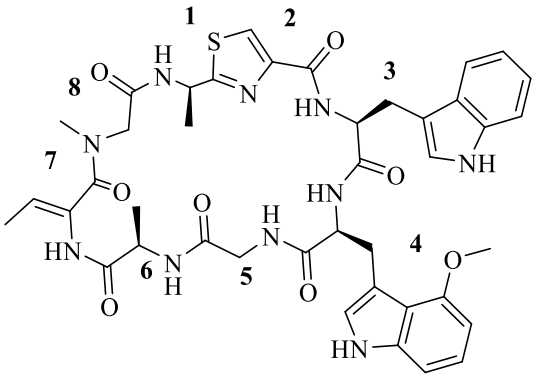


Synthesis was carried out using the general procedure for head-to-tail cyclisation employing PyBOP (22.3 mg, 0.04 mmol), HOBt (5.8 mg, 0.04 mmol) and DIPEA (32.8 µL, 0.193 mmol) in a 0.5 mM solution of crude linear peptide (43 mg, 0.02 mmol).The crude mixture was concentrated under *vacuo* and purified using preparative RP-HPLC **method 1** and freeze dried to afford the title peptide as white powder (3.69 mg, 19% yield); $[\alpha]_D^{22}$ = +103.48 º (*c* = 0.1675, MeOH);

^{1}H-NMR (400 MHz, DMSO-d_6): δ = 0.77 (d, *J* = 7 Hz, 3H, 6-CH_3), 1.78 (d, *J* = 7 Hz, 3H, 7-CH_3), 3.18 (s, 3H, 8-CH_3), 3.22-3.82 (m, 12H, 1-CH_2, 1-CH_3, 3-CH_2, 4-CH_2, 5-CH_AH$_B$, 8-CH_2), 4.26 (m, 1H, 6-α-CH), 4.36 (m, 1H, 5-CH$_A$$H_B$), 4.43 (m, 1H, 3-α-CH), 4.77 (m, 1H, 4-α-CH), 5.39 (m, 1H, 1-α-CH), 5.52 (q, *J* = 14, 7 Hz, 1H, 7-CH), 6.94-7.05, 7.20-7.28 (m, 7H, Ar Hs), 7.40 (d, *J* = 8 Hz, 1H, Ar H), 7.86 (d, *J* = 7 Hz, 1H, Ar H), 7.98 (s, 1H, 2-CH), 8.08 (d, *J* = 9 Hz, 1H, 1-NH), 8.18 (d, *J* = 7 Hz, 1H, 6-NH), 8.51 (m, 1H, 3-NH), 8.60 (s, 1H, 7-

NH), 8.65-8.74 (m, 2H, 4-NH, 5-NH), 10.74 (s, 1H, indole-NH), 11.28 (s, 1H, indole-NH) ppm; MS: *m/z* (+ESI) calcd. for $C_{40}H_{44}BrN_{10}O_7S^+$ 917.2399, found 917.2375 [MH^+]; RP-HPLC **Method 1**, t_R 9.50 min.

***Cyclo*[D-Ala-Thz-Trp-Trp(4-MeO)-Gly-D-Ala-DhB-Sar] (4.45)**

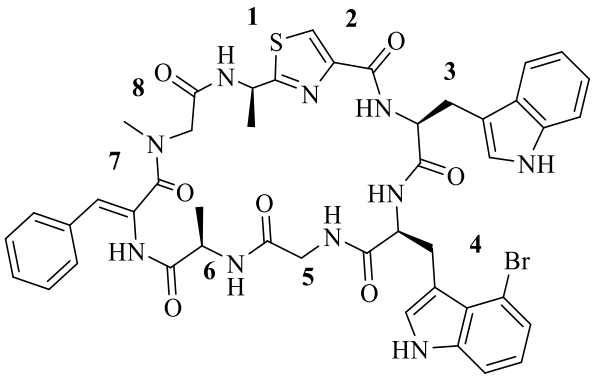


Synthesis was carried out using the general procedure for head-to-tail cyclisation employing PyBOP (26 mg, 0.05 mmol), HOBt (6.8 mg, 0.05 mmol) and DIPEA (38 μL, 0.225 mmol) in a 0.5 mM solution of crude linear peptide (22.6 mg, 0.025 mmol).The crude mixture was concentrated under *vacuo* and purified using preparative RP-HPLC **method 1** and freeze dried to afford the title peptide as white powder (8.2 mg, 40% yield); $[\alpha]_D^{22}$ = +125.16° (*c* = 0.1, MeOH);

^{1}H-NMR (400 MHz, DMSO-d_6): δ = 0.84 (d, *J* = 7 Hz, 3H, 6-CH_3), 1.57 (d, *J* = 7 Hz, 3H, 1-CH_3), 1.81 (d, *J* = 7 Hz, 3H, 7-CH_3), 2.36 (s, 3H, 4-CH_3), 3.19 (s, 3H, 8-CH_3), 3.25-3.79 (m, 7H, 3-CH_2, 4-CH_2, 5-CH_AH$_B$, 8-CH_2), 4.26 (m, 1H, 6-α-CH), 4.44 (m, 2H, 3-α-CH, 5-C$H_A H_B$), 4.74 (td, *J* = 12, 3 Hz, 1H, 4-α-CH), 5.43 (m, 1H, 1-α-CH), 5.56 (q, *J* = 14, 7 Hz, 1H, 7-CH), 6.92-7.03, 7.20-7.27 (m, 7H, Ar Hs), 7.39 (d, *J* = 8 Hz, 1H, Ar H), 7.84 (d, *J* = 7 Hz, 1H, Ar H), 7.96 (s, 1H, 2-CH), 8.06 (d, *J* = 9 Hz, 1H, 1-NH), 8.15 (d, *J* = 9 Hz, 1H, 6-NH), 8.47 (m, 1H, 3-NH), 8.56 (s, 1H, 7-NH), 8.72 (m, 2H, 4-NH, 5-NH), 10.77 (s, 1H, indole-NH), 10.90 (d, *J* = 2 Hz, 1H, indole-NH) ppm; MS: *m/z* (+ESI) calcd.

for $C_{41}H_{47}N_{10}O_8S^+$ 839.3294, found 839.3309 [MH^+]; RP-HPLC **Method 1**, t_R 9.46 min.

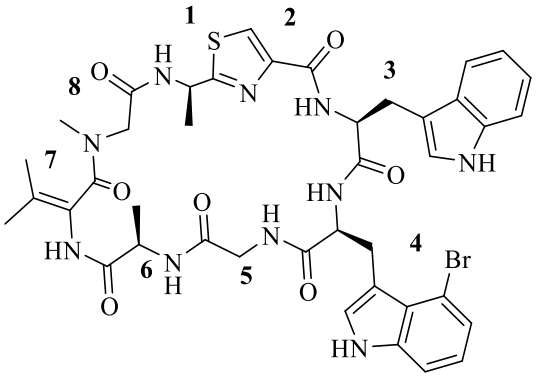
***Cyclo*[D-Ala-Thz-Trp-Trp(4-Br)-Gly-D-Ala-DhPh-Sar] (4.46)**



Synthesis was carried out using the general procedure for head-to-tail cyclisation employing PyBOP (26 mg, 0.05 mmol), HOBt (6.8 mg, 0.05 mmol) and DIPEA (38 μL, 0.225 mmol) in a 0.5 mM solution of crude linear peptide (22.6 mg, 0.025 mmol).The crude mixture was concentrated under *vacuo* and purified using preparative RP-HPLC **method 1** and freeze dried to afford the title peptide as white powder 7.1 mg, 35% yield); $[\alpha]_D^{22}$ = +144.1° (*c* = 0.1, MeOH);

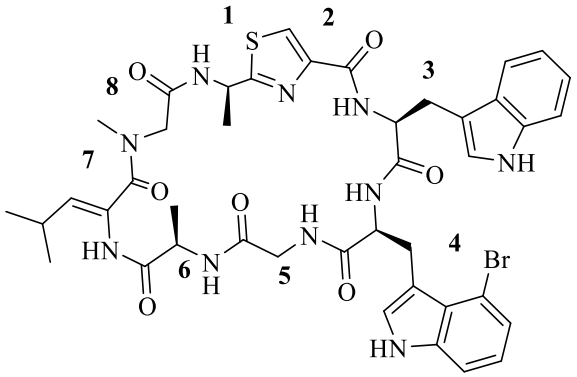
^{1}H-NMR (400 MHz, DMSO-d_6): δ = 0.77 (d, *J* = 7 Hz, 3H, 6-CH_3), 1.51 (d, *J* = 7 Hz, 3H, 1-CH_3), 1.79 (d, *J* = 7 Hz, 3H, 7-CH_3), 3.16 (s, 3H, 8-CH_3), 3.21-3.71 (m, 7H, 3-CH_2, 4-CH_2, 5-CH_AH$_B$, 8-CH_2), 4.22 (m, 1H, 6-α-CH), 4.31 (m, 2H, 3-α-CH, 5-C$H_A$$H_B$), 4.75 (td, *J* = 12, 3 Hz, 1H, 4-α-CH), 5.31 (m, 1H, 1-α-CH), 5.86 (s, 1H, 7-CH), 6.92-7.03, 7.20-7.27 (m, 8H, Ar Hs), 7.38 (m, 3H, Ar H), 7.85 (m, 2H, Ar H), 7.97 (m, 2H, 2-CH), 8.11 (d, *J* = 8 Hz, 1H, 1-NH), 8.18 (d, *J* = 8 Hz, 1H, 6-NH), 8.44 (m, 1H, 3-NH), 8.51 (s, 1H, 7-NH), 8.68 (m, 2H, 4-NH, 5-NH), 10.79 (s, 1H, indole-NH), 11.01 (d, *J* = 2 Hz, 1H, indole-NH) ppm; MS: *m/z* (+ESI) calcd. for $C_{45}H_{46}BrN_{10}O_7S^+$ 949.2450, found 949.2402 [MH^+]; RP-HPLC **Method 1**, t_R 10.90 min.

***Cyclo*[D-Ala-Thz-Trp-Trp(4-Br)-Gly-D-Ala-DhVal-Sar] (4.47)**



Synthesis was carried out using the general procedure for head-to-tail cyclisation employing PyBOP (26 mg, 0.05 mmol), HOBt (6.8 mg, 0.05 mmol) and DIPEA (38 μL, 0.225 mmol) in a 0.5 mM solution of crude linear peptide (22.6 mg, 0.025 mmol).The crude mixture was concentrated under *vacuo* and purified using preparative RP-HPLC **method 1** and freeze dried to afford the title peptide as white powder (9.1 mg, 42%); $[\alpha]_D^{22} = +134.2^o$ ($c = 0.1$, MeOH); ^{1}H-NMR (400 MHz, DMSO-d$_6$): δ = 0.78 (d, J = 7 Hz, 3H, 6-CH$_3$), 1.55 (d, J = 7 Hz, 3H, 1-CH$_3$), 1.70 (s, 3H, 1-CH$_3$), 1.80 (s, 3H, 1-CH$_3$), 3.22 (s, 3H, 8-CH$_3$), 3.26-3.79 (m, 7H, 3-CH$_2$, 4-CH$_2$, 5-CH_AH$_B$, 8-CH$_2$), 4.24 (m, 1H, 6-α-CH), 4.33 (m, 2H, 3-α-CH, 5-CH$_A$$H_B$), 4.80 (td, J = 12, 3 Hz, 1H, 4-α-CH), 5.41 (m, 1H, 1-α-CH), 6.92-7.03, 7.21-7.28 (m, 7H, Ar Hs), 7.39 (d, J = 8 Hz, 1H, Ar H), 7.84 (d, J = 7 Hz, 1H, Ar H), 7.96 (s, 1H, 2-CH), 8.11 (d, J = 9 Hz, 1H, 1-NH), 8.19 (d, J = 9 Hz, 1H, 6-NH), 8.56 (m, 1H, 3-NH), 8.65 (s, 1H, 7-NH), 8.79 (m, 2H, 4-NH, 5-NH), 10.80 (s, 1H, indole-NH), 11.19 (d, J = 2 Hz, 1H, indole-NH) ppm; MS: *m/z* (+ESI) calcd. for $C_{41}H_{46}BrN_{10}O_7S^+$ 901.2450, found 901.2435 [MH$^+$]; RP-HPLC **Method 1**, t_R 10.09 min.

***Cyclo*[D-Ala-Thz-Trp-Trp(4-Br)-Gly-D-Ala-DhLeu-Sar] (4.48)**



Synthesis was carried out using the general procedure for head-to-tail cyclisation employing PyBOP (26 mg, 0.05 mmol), HOBt (6.8 mg, 0.05 mmol) and DIPEA (38 μL, 0.225 mmol) in a 0.5 mM solution of crude linear peptide (22.6 mg, 0.025 mmol).The crude mixture was concentrated under *vacuo* and purified using preparative RP-HPLC **method 1** and freeze dried to afford the title peptide as white powder (6.3 mg, 35% yield); $[\alpha]_D^{22}$ = +136.1° (*c* = 0.1, MeOH)

^{1}H-NMR (400 MHz, DMSO-d_6): δ = 0.84 (d, *J* = 7 Hz, 3H, 6-CH_3), 1.04 (d, *J* = 6 Hz, 3H, 7-CH_3), 1.15 (d, *J* = 6 Hz, 3H, 7-CH_3), 1.58 (d, *J* = 7 Hz, 3H, 1-CH_3), 2.34 (m, 1H, 7-CH), 3.30 (s, 3H, 8-CH_3), 3.25-3.80 (m, 7H, 3-CH_2, 4-CH_2, 5-CH_AH$_B$, 8-CH_2), 4.22 (m, 1H, 6-α-CH), 4.42 (m, 2H, 3-α-CH, 5-CH_AH_B), 4.78 (td, *J* = 12, 3 Hz, 1H, 4-α-CH), 5.29 (m, 1H, 1-α-CH), 5.45 (q, *J* = 14, 7 Hz, 1H, 7-CH), 6.97-7.09, 7.23-730 (m, 7H, Ar Hs), 7.40 (d, *J* = 8 Hz, 1H, Ar H), 7.90 (d, *J* = 7 Hz, 1H, Ar H), 7.96 (s, 1H, 2-CH), 8.06 (d, *J* = 8 Hz, 1H, 1-NH), 8.19 (d, *J* = 8 Hz, 1H, 6-NH), 8.41 (m, 1H, 3-NH), 8.50 (s, 1H, 7-NH), 8.61 (m, 2H, 4-NH, 5-NH), 10.78 (s, 1H, indole-NH), 11.28 (s, 1H, indole-NH) ppm; MS: *m/z* (+ESI) calcd. for $C_{42}H_{48}BrN_{10}O_7S^+$ 915.2606, found 915.2622 [MH^+]; RP-HPLC **Method 1**, t_R 11.30 min.

7.7 Antibacterial Assay

The bacterial strain tested in the antibacterial assay are *Pseudomonas aeruginosa* PAO1, *Burkholderia multivorans* ATCC17616, *Proteus mirabilis* Hauser 1885 (*Pr. Mirabilis*), *Streptococcus pyogene* (*Strep. pyogene*) and *Streptococcus agalactiae* (*Strep. agalactiae*). Upon arrival, all the strains were stored and maintained as frozen stocks at -78 ºC. *P. aeruginosa* and *Pr. Mirabilis* cultures were incubated aerobically in Muller-Hinton (MH) media at 37 ºC in a shaking incubator (200 rpm) overnight. *B. multivorans* culture was incubated aerobically in MH media at 30 ºC in a shaking incubator (200 rpm) overnight. *Step. pyogene* and *Strep. Agalactiae* cultures were incubated aerobically in brain heart infusion (BHI) media at 37 ºC in a static incubator overnight.

IC_{50} determination of *P. aeruginosa* and *Pr. mirabilis*

The IC_{50} of the test compounds against *P. aeruginosa* PAO1 and *Pr. mirabilis* Hauser 1885 were determined in the MH media at 37 ºC. The overnight grown bacterial culture was diluted with MH media to achieve an OD_{610nm} of 0.05. The test compounds dilution was prepared from a 10 mM DMSO stock solution. A volume of 10 µL of the 10 mM solution was added to 990 µL of the bacterial sample in MH media with an OD_{610nm} of 0.05. This 1 mL sample was then serially diluted with 0.05 OD_{610nm} of bacterial culture containing 1 % DMSO.

200 µL of the prepared samples, which contains bacteria and testing compound with desired concentration, were dispensed into a 96-well microtiter plate and incubated at 37 ºC in a Tecan i-control 1.9.17.0 microplate reader. The OD was monitored intermittently at 15 minutes over 17 hours. The IC_{50} was determined by the measurement of OD_{610nm} at 13 h. Each tested compound was evaluated in duplicate at concentration of 100, 50, 25, 12.5, 6.25, 3.125, 1.56, and 0.78

μM. Each experiment was repeated three times.

IC_{50} determination of *B. multivorans*

The IC_{50} of the test compounds against *Burkholderia multivorans* ATCC17616 was determined in the MH media at 30 ºC. The overnight grown bacterial culture was diluted with MH media to achieve an OD_{610nm} of 0.005. The test compounds dilution was prepared from a 10 mM DMSO stock solution. A volume of 2.5 μL of the 10 mM solution was added to 990 μL of the bacterial sample in MH media with an OD_{610nm} of 0.005. This 1 mL sample was then serially diluted with 0.005 OD_{610nm} of bacterial culture containing 1 % DMSO.

200 μL of the prepared samples, which contains bacteria and testing compound with desired concentration, were dispensed into a 96-well microtiter plate and incubated at 30 ºC in a Tecan i-control 1.9.17.0 microplate reader. The OD was monitored intermittently at 15 minutes over 25 hours. The IC_{50} was determined by the measurement of OD_{610nm} at 20 h. Each tested compound was evaluated in duplicate at concentration of 25, 12.5, 6.25, 3.125, 1.56, 0.78, 0.39, and 0.20 μM. Each experiment was repeated three times.

IC_{50} determination of *Step. pyogene* and *Strep. agalactiae*

The IC_{50} of the test compounds against *Streptococcus pyogene* and *Streptococcus agalactiae* were determined in the BHI media at 37 ºC. The overnight grown bacterial culture was diluted with BHI media to achieve an OD_{610nm} of 0.05. The test compounds dilution was prepared from a 10 mM DMSO stock solution. A volume of 10 μL of the 10 mM solution was added to 990 μL of the bacterial sample in MH media with an OD_{610nm} of 0.05. This 1 mL sample was then serially diluted with 0.05 OD_{610nm} of bacterial culture containing 1 % DMSO.

200 μL of the prepared samples, which contains bacteria and testing compound with desired concentration, were dispensed into a 96-well microtiter plate and incubated at 37 ºC in a Tecan i-control 1.9.17.0 microplate reader. The OD was monitored intermittently at 15 minutes over 17 hours. The IC_{50} was determined by the measurement of OD_{610nm} at 13 h. Each tested compound was evaluated in duplicate at concentration of 100, 50, 25, 12.5, 6.25, 3.125, 1.56, and 0.78 μM. Each experiment was repeated three times.

7.8 Chemical Stability of Argyrin Analogues

A 100 μM solution of test compound was prepared in phosphate buffered saline (PBS) with pH 7.4 from a 10 mM DMSO stock solution. The prepared samples were kept at 37 ºC for 24 hours. RP-HPLC was used to determine the stability of the test compounds. The percentage peak area of the sample was determined at 0 hour, 1 h, 2 h, 6 h, and then 24 h. The peak area of above time points was compared. The compounds were also tested with pH adjusted to 1.0 or 7.4. The percentage peak area of the sample was determined at 0 hour, 1 hour, 2 h, 6 h, and then 24 h. The peak area of above time points was compared.

Chapter 8
References

1 S. A. Waksman, *Mycologia*, 1947, **39**, 565–569.

2 C. Nathan and O. Cars, *N. Engl. J. Med.*, 2014, **371**, 1761–1763.

3 N. Rosenblatt-Farrell, *Environ. Health Perspect.*, 2009, **117**, A244–A250.

4 R. J. Fair and Y. Tor, *Perspect. Med. Chem.*, 2014, **6**, 25–64.

5 C. L. Ventola, *Pharm. Ther.*, 2015, **40**, 344–352.

6 Antibiotic Resistance Threats in the United States 2013, https://www.cdc.gov/drugresistance/threat-report-2013/index.html, (accessed 23 September 2017).

7 E. D. Brown and G. D. Wright, *Nature*, 2016, **529**, 336–343.

8 A. Schatz, E. Bugle and S. A. Waksman, *Proc. Soc. Exp. Biol. Med.*, 1944, **55**, 66–69.

9 K. C. Nicolaou and S. Rigol, *J. Antibiot. (Tokyo)*,2011.

10 L. L. Silver, *Clin. Microbiol. Rev.*, 2011, **24**, 71–109.

11 Manager, A Scientific Roadmap for Antibiotic Discovery, http://pew.org/26ZYUqA, (accessed 20 June 2017).

12 D. J. Newman and G. M. Cragg, *J. Nat. Prod.*, 2007, **70**, 461–77.

13 H. C. Neu and K. P. Fu, *Antimicrob. Agents Chemother.*, 1978, **13**, 584–588.

14 G. L. Dunn, *J. Antimicrob. Chemother.*, 1982, **10**, 1–10.

15 M. Jiang, J. Yao, L. I. Zhang, T. Gao, Y. Zhang, X. Weng and G. Feng, *Biomed. Rep.*, 2016, **4**, 40–44.

16 F. D. Lowy, *J. Clin. Invest.*, 2003, **111**, 1265–1273.

17 M. S. Rappé and S. J. Giovannoni, *Annu. Rev. Microbiol.*, 2003, **57**, 369–394.

18 J. Clardy, M. A. Fischbach and C. T. Walsh, *Nat. Biotechnol.*, 2006, **24**, 1541–1550.

19 D. Nichols, N. Cahoon, E. M. Trakhtenberg, L. Pham, A. Mehta, A. Belanger, T. Kanigan, K. Lewis and S. S. Epstein, *Appl. Environ. Microbiol.*, 2010, **76**, 2445–2450.

20 L. L. Ling, T. Schneider, A. J. Peoples, A. L. Spoering, I. Engels, B. P. Conlon, A. Mueller, T. F. Schäberle, D. E. Hughes, S. Epstein, M. Jones, L. Lazarides, V. A. Steadman, D. R. Cohen, C. R. Felix, K. A. Fetterman, W. P. Millett, A. G. Nitti, A. M. Zullo, C. Chen and K. Lewis, *Nature*, 2015, **517**, 455–459.

21 PIXNIO, Free picture, https://pixnio.com/science/microscopy-images/scanning-electron-micrograph-of-burkholderia-cepacia, (accessed 23 September 2017).

22 P. Vandamme, B. Holmes, M. Vancanneyt, T. Coenye, B. Hoste, R. Coopman, H. Revets, S. Lauwers, M. Gillis, K. Kersters and J. R. W. Govan, *Int. J. Syst. Evol. Microbiol.*, 1997, **47**, 1188–1200.

23 P. Vandamme, B. Holmes, T. Coenye, J. Goris, E. Mahenthiralingam, J. J. LiPuma and J. R. W. Govan, *Res. Microbiol.*, 2003, **154**, 91–96.

24 J. L. Jacobs, A. C. Fasi, A. Ramette, J. J. Smith, R. Hammerschmidt and G. W. Sundin, *Appl. Environ. Microbiol.*, 2008, **74**, 3121–3129.

25 E. Yabuuchi, Y. Kosako, H. Oyaizu, I. Yano, H. Hotta, Y. Hashimoto, T. Ezaki and M. Arakawa, *Microbiol. Immunol.*, 1992, **36**, 1251–1275.

26 M. T. G. Holden, H. M. B. Seth-Smith, L. C. Crossman, M. Sebaihia, S. D. Bentley, A. M. Cerdeño-Tárraga, N. R. Thomson, N. Bason, M. A.

Quail, S. Sharp, I. Cherevach, C. Churcher, I. Goodhead, H. Hauser, N. Holroyd, K. Mungall, P. Scott, D. Walker, B. White, H. Rose, P. Iversen, D. Mil-Homens, E. P. C. Rocha, A. M. Fialho, A. Baldwin, C. Dowson, B. G. Barrell, J. R. Govan, P. Vandamme, C. A. Hart, E. Mahenthiralingam and J. Parkhill, *J. Bacteriol.*, 2009, **191**, 261–277.

27 J. H. Leitão, S. A. Sousa, A. S. Ferreira, C. G. Ramos, I. N. Silva and L. M. Moreira, *Appl. Microbiol. Biotechnol.*, 2010, **87**, 31–40.

28 T. Coenye and P. Vandamme, *Environ. Microbiol.*, 2003, **5**, 719–729.

29 S. Compant, J. Nowak, T. Coenye, C. Clément and E. Ait Barka, *FEMS Microbiol. Rev.*, 2008, **32**, 607–626.

30 C. C. Cain, A. T. Henry, R. H. Waldo, L. J. Casida and J. O. Falkinham, *Appl. Environ. Microbiol.*, 2000, **66**, 4139–4141.

31 T. J. McLoughlin, J. P. Quinn, A. Bettermann and R. Bookland, *Appl. Environ. Microbiol.*, 1992, **58**, 1760–1763.

32 S. L. F. Meyer, S. I. Massoud, D. J. Chitwood and D. P. Roberts, *Nematology*, 2000, **2**, 871–879.

33 L. Chiarini, A. Bevivino, C. Dalmastri, S. Tabacchioni and P. Visca, *Trends Microbiol.*, 2006, **14**, 277–286.

34 A. Isles, I. Maclusky, M. Corey, R. Gold, C. Prober, P. Fleming and H. Levison, *J. Pediatr.*, 1984, **104**, 206–210.

35 R. B. Johnston, *Curr. Opin. Hematol.*, **8**, 17–22.

36 F. Ratjen and G. Döring, *The Lancet*, 2003, **361**, 681–689.

37 *Future Microbiol.*, 2007, **2**, 153–164.

38 M. V. Cunha, A. Pinto-de-Oliveira, L. Meirinhos-Soares, M. J. Salgado, J. Melo-Cristino, S. Correia, C. Barreto and I. Sá-Correia, *J. Clin. Microbiol.*, 2007, **45**, 1628–1633.

39 E. Mahenthiralingam, T. A. Urban and J. B. Goldberg, *Nat. Rev. Microbiol.*, 2005, **3**, 144–156.

40 J. L. Bobadilla, M. Macek, J. P. Fine and P. M. Farrell, *Hum. Mutat.*, 2002, **19**, 575–606.

41 M. Dorwart, P. Thibodeau and P. Thomas, *J. Cyst. Fibros.*, 2004, **3**, 91–94.

42 D. F. McAuley and J. S. Elborn, *Paediatr. Respir. Rev.*, 2000, **1**, 93–100.

43 J. R. Govan and V. Deretic, *Microbiol. Rev.*, 1996, **60**, 539–574.

44 S. McClean and M. Callaghan, *J. Med. Microbiol.*, 2009, **58**, 1–12.

45 R. Biddick, T. Spilker, A. Martin and J. J. LiPuma, *FEMS Microbiol. Lett.*, 2003, **228**, 57–62.

46 J. S. Chen, K. A. Witzmann, T. Spilker, R. J. Fink and J. J. LiPuma, *J. Pediatr.*, 2001, **139**, 643–649.

47 D. P. Speert, D. Henry, P. Vandamme, M. Corey and E. Mahenthiralingam, *Emerg. Infect. Dis.*, 2002, **8**, 181–187.

48 R. C. Boucher, *J. Intern. Med.*, 2007, **261**, 5–16.

49 J. Jacquot, O. Tabary, P. Le Rouzic and A. Clement, *Int. J. Biochem. Cell Biol.*, 2008, **40**, 1703–1715.

50 U. Sajjan, Y. Wu, G. Kent and J. Forstner, *J. Med. Microbiol.*, 2000, **49**, 875–885.

51 U. S. Sajjan, M. B. Hershenson, J. F. Forstner and J. J. LiPuma, *Cell. Microbiol.*, 2008, **10**, 188–201.

52 H. C. Krivan, V. Ginsburg and D. D. Roberts, *Arch. Biochem. Biophys.*, 1988, **260**, 493–496.

53 F. A. Sylvester, U. S. Sajjan and J. F. Forstner, *Infect. Immun.*, 1996, **64**, 1420–1425.

54 U. Schwab, M. Leigh, C. Ribeiro, J. Yankaskas, K. Burns, P. Gilligan, P. Sokol and R. Boucher, *Infect. Immun.*, 2002, **70**, 4547–4555.

55 U. S. Sajjan, J. H. Yang, M. B. Hershenson and J. J. LiPuma, *Cell. Microbiol.*, 2006, **8**, 1456–1466.

56 C. Duff, P. G. Murphy, M. Callaghan and S. McClean, *Microb. Pathog.*, 2006, **41**, 183–192.

57 G. Marioni, R. Rinaldi, G. Ottaviano, R. Marchese-Ragona, M. Savastano and A. Staffieri, *J. Infect.*, 2006, **53**, e219-222.

58 M. B. Miller and B. L. Bassler, *Annu. Rev. Microbiol.*, 2001, **55**, 165–199.

59 S. Lewenza, B. Conway, E. P. Greenberg and P. A. Sokol, *J. Bacteriol.*, 1999, **181**, 748–756.

60 V. Venturi, A. Friscina, I. Bertani, G. Devescovi and C. Aguilar, *Res. Microbiol.*, 2004, **155**, 238–244.

61 R. J. Malott and P. A. Sokol, *J. Bacteriol.*, 2007, **189**, 3006–3016.

62 R. J. Malott, A. Baldwin, E. Mahenthiralingam and P. A. Sokol, *Infect. Immun.*, 2005, **73**, 4982–4992.

63 R. J. Malott, E. P. O'Grady, J. Toller, S. Inhülsen, L. Eberl and P. A. Sokol, *J. Bacteriol.*, 2009, **191**, 2447–2460.

64 Y. Deng, C. Boon, L. Eberl and L.-H. Zhang, *J. Bacteriol.*, 2009, **191**, 7270–7278.

65 F.G. Christine C., H. Tammy M.-H. and V. Miguel A., *Microb. Pathog.*, 2002, **32**, 249–254.

66 P. W. Whitby, T. M. VanWagoner, A. A. Taylor, T. W. Seale, D. J. Morton, J. J. LiPuma and T. L. Stull, *J. Med. Microbiol.*, 2006, **55**, 11–21.

67 M. Tomich, A. Griffith, C. A. Herfst, J. L. Burns and C. D. Mohr, *Infect. Immun.*, 2003, **71**, 1405–1415.

68 D. F. Aubert, R. S. Flannagan and M. A. Valvano, *Infect. Immun.*, 2008, **76**, 1979–1991.

69 S. U. Sajjan, L. A. Carmody, C. F. Gonzalez and J. J. LiPuma, *Infect. Immun.*, 2008, **76**, 5447–5455.

70 R. Zhang, J. J. LiPuma and C. F. Gonzalez, *Microbiology*, 2009, **155**, 4005–4013.

71 T. Mullen, K. Markey, P. Murphy, S. McClean and M. Callaghan, *Eur. J. Clin. Microbiol. Infect. Dis. Off. Publ. Eur. Soc. Clin. Microbiol.*, 2007, **26**, 869–877.

72 S. Gingues, C. Kooi, M. B. Visser, B. Subsin and P. A. Sokol, *J.*

Bacteriol., 2005, **187**, 8247–8255.

73 C. Kooi, B. Subsin, R. Chen, B. Pohorelic and P. A. Sokol, *Infect. Immun.*, 2006, **74**, 4083–4093.

74 M. S. Thomas, *BioMetals*, 2007, **20**, 431–452.

75 P. W. Whitby, T. M. VanWagoner, J. M. Springer, D. J. Morton, T. W. Seale and T. L. Stull, *J. Med. Microbiol.*, 2006, **55**, 661–668.

76 C. R. H. Raetz and C. Whitfield, *Annu. Rev. Biochem.*, 2002, **71**, 635–700.

77 A. D. Vinion-Dubiel and J. B. Goldberg, *J. Endotoxin Res.*, 2003, **9**, 201–213.

78 H. Shimomura, M. Matsuura, S. Saito, Y. Hirai, Y. Isshiki and K. Kawahara, *Infect. Immun.*, 2003, **71**, 5225–5230.

79 A. D. Welman and I. S. Maddox, *Trends Biotechnol.*, 2003, **21**, 269–274.

80 J. E. A. Zlosnik, T. J. Hird, M. C. Fraenkel, L. M. Moreira, D. A. Henry and D. P. Speert, *J. Clin. Microbiol.*, 2008, **46**, 1470–1473.

81 J. A. Richau, J. H. Leitão, M. Correia, L. Lito, M. J. Salgado, C. Barreto, P. Cescutti and I. Sá-Correia, *J. Clin. Microbiol.*, 2000, **38**, 1651–1655.

82 J. Bylund, L.-A. Burgess, P. Cescutti, R. K. Ernst and D. P. Speert, *J. Biol. Chem.*, 2006, **281**, 2526–2532.

83 K. L. Tomlin, O. P. Coll and H. Ceri, *Can. J. Microbiol.*, 2001, **47**, 949–954.

84 B. A. D. Conway, V. Venu and D. P. Speert, *J. Bacteriol.*, 2002, **184**, 5678–5685.

85 J. J. LiPuma, *Clin. Chest Med.*, 1998, **19**, 473–486.

86 J. L. Burns, C. D. Wadsworth, J. J. Barry and C. P. Goodall, *Antimicrob. Agents Chemother.*, 1996, **40**, 307–313.

87 J. L. Burns, D. M. Lien and L. A. Hedin, *Antimicrob. Agents Chemother.*, 1989, **33**, 1247–1251.

88 S. C. Aronoff, *Antimicrob. Agents Chemother.*, 1988, **32**, 1636–1639.

89 J. L. Burns, L. A. Hedin and D. M. Lien, *Antimicrob. Agents Chemother.*,

1989, **33**, 136–141.

90 S. P. Conway, K. G. Brownlee, M. Denton and D. G. Peckham, *Am. J. Respir. Med.*, 2003, **2**, 321–332.

91 R. Ball, K. G. Brownlee, A. J. A. Duff, M. Denton, S. P. Conway and T. W. R. Lee, *J. Cyst. Fibros.*, 2010, **9**, 73–74.

92 C. A. O'Malley, *Respir. Care*, 2009, **54**, 641–657.

93 Pseudomonas aeruginosa, enteric, SEM - Stock Image F017/4009 Science Photo Library, http://www.sciencephoto.com/media/816537/view, (accessed 24 September 2017).

94 A. Peix, M.H. Ramírez-Bahena and E. Velázquez, *Infect. Genet. Evol.*, 2009, **9**, 1132–1147.

95 A. J. Spiers, A. Buckling and P. B. Rainey, *Microbiology*, 2000, **146**, 2345–2350.

96 J. M. Meyer, *Arch. Microbiol.*, 2000, **174**, 135–142.

97 S. L. Gellatly and R. E. W. Hancock, *Pathog. Dis.*, 2013, **67**, 159–173.

98 J. B. Lyczak, C. L. Cannon and G. B. Pier, *Microbes Infect.*, 2000, **2**, 1051–1060.

99 B. J. Williams, J. Dehnbostel and T. S. Blackwell, *Respirology*, 2010, **15**, 1037–1056.

100 A. Mena, E. E. Smith, J. L. Burns, D. P. Speert, S. M. Moskowitz, J. L. Perez and A. Oliver, *J. Bacteriol.*, 2008, **190**, 7910–7917.

101 S. Furukawa, S. L. Kuchma and G. A. O'Toole, *J. Bacteriol.*, 2006, **188**, 1211–1217.

102 P. Ghosh, *Microbiol. Mol. Biol. Rev.*, 2004, **68**, 771–795.

103 J. Pizarro-Cerdá and P. Cossart, *Cell*, 2006, **124**, 715–727.

104 L. L. Burrows, *Annu. Rev. Microbiol.*, 2012, **66**, 493–520.

105 E. A. Miao, E. Andersen-Nissen, S. E. Warren and A. Aderem, *Semin. Immunopathol.*, 2007, **29**, 275–288.

106 E. Kipnis, T. Sawa and J. Wiener-Kronish, *Médecine Mal. Infect.*, 2006,

36, 78–91.

107 A. T. Y. Yeung, E. C. W. Torfs, F. Jamshidi, M. Bains, I. Wiegand, R. E. W. Hancock and J. Overhage, *J. Bacteriol.*, 2009, **191**, 5592–5602.

108 A. Filloux, *Front. Microbiol.*, 2011, **2**, 155.

109 A. R. Hauser, *Nat. Rev. Microbiol.*, 2009, **7**, 654–665.

110 C. M. Shaver and A. R. Hauser, *Infect. Immun.*, 2004, **72**, 6969–6977.

111 M. Galle, S. Jin, P. Bogaert, M. Haegman, P. Vandenabeele and R. Beyaert, *PLoS One*, 2012, **7**, e41547.

112 A. J. Laarman, B. W. Bardoel, M. Ruyken, J. Fernie, F. J. Milder, J. A. G. van Strijp and S. H. M. Rooijakkers, *J. Immunol. Baltim. Md 1950*, 2012, **188**, 386–393.

113 B. W. Bardoel, S. van der Ent, M. J. C. Pel, J. Tommassen, C. M. J. Pieterse, K. P. M. van Kessel and J. A. G. van Strijp, *PLOS Pathog.*, 2011, **7**, e1002206.

114 D. S. Toder, S. J. Ferrell, J. L. Nezezon, L. Rust and B. H. Iglewski, *Infect. Immun.*, 1994, **62**, 1320–1327.

115 D. Leduc, N. Beaufort, S. de Bentzmann, J.-C. Rousselle, A. Namane, M. Chignard and D. Pidard, *Infect. Immun.*, 2007, **75**, 3848–3858.

116 L. S. Engel, J. M. Hill, J. M. Moreau, L. C. Green, J. A. Hobden and R. J. O'Callaghan, *Invest. Ophthalmol. Vis. Sci.*, 1998, **39**, 662–665.

117 J. L. Malloy, R. A. W. Veldhuizen, B. A. Thibodeaux, R. J. O'Callaghan and J. R. Wright, *Am. J. Physiol. Lung Cell. Mol. Physiol.*, 2005, **288**, L409-418.

118 J. D. King, D. Kocíncová, E. L. Westman and J. S. Lam, *Innate Immun.*, 2009, **15**, 261–312.

119 J. S. Lam, V. L. Taylor, S. T. Islam, Y. Hao and D. Kocíncová, *Front. Microbiol.*, 2011, **2**, 118.

120 S. Akira, S. Uematsu and O. Takeuchi, *Cell*, 2006, **124**, 783–801.

121 R. K. Ernst, S. M. Moskowitz, J. C. Emerson, G. M. Kraig, K. N. Adams, M. D. Harvey, B. Ramsey, D. P. Speert, J. L. Burns and S. I. Miller, *J.*

Infect. Dis., 2007, **196**, 1088–1092.

122 A. Teghanemt, D. Zhang, E. N. Levis, J. P. Weiss and T. L. Gioannini, *J. Immunol.*, 2005, **175**, 4669–4676.

123 A. Deep, U. Chaudhary and V. Gupta, *J. Lab. Physicians*, 2011, **3**, 4.

124 J. P. Pearson, K. M. Gray, L. Passador, K. D. Tucker, A. Eberhard, B. H. Iglewski and E. P. Greenberg, *Proc. Natl. Acad. Sci. U. S. A.*, 1994, **91**, 197–201.

125 E. C. Pesci, J. B. J. Milbank, J. P. Pearson, S. McKnight, A. S. Kende, E. P. Greenberg and B. H. Iglewski, *Proc. Natl. Acad. Sci. U. S. A.*, 1999, **96**, 11229–11234.

126 J. M. Brint and D. E. Ohman, *J. Bacteriol.*, 1995, **177**, 7155–7163.

127 M. J. Gambello and B. H. Iglewski, *J. Bacteriol.*, 1991, **173**, 3000–3009.

128 S. Heeb, M. P. Fletcher, S. R. Chhabra, S. P. Diggle, P. Williams and M. Cámara, *Fems Microbiol. Rev.*, 2011, **35**, 247–274.

129 T. Bjarnsholt, T. Tolker-Nielsen, N. Høiby and M. Givskov, *Expert Rev. Mol. Med.*, 2010, **12**, e11.

130 H.-C. Flemming and J. Wingender, *Nat. Rev. Microbiol.*, 2010, **8**, 623–633.

131 L. Hall-Stoodley and P. Stoodley, *Cell. Microbiol.*, 2009, **11**, 1034–1043.

132 O. Lieleg, M. Caldara, R. Baumgärtel and K. Ribbeck, *Soft Matter*, 2011, **7**, 3307–3314.

133 K. Sauer, A. K. Camper, G. D. Ehrlich, J. W. Costerton and D. G. Davies, *J. Bacteriol.*, 2002, **184**, 1140–1154.

134 M. J. Franklin, D. E. Nivens, J. T. Weadge and P. L. Howell, *Front. Microbiol.*, 2011, **2**.

135 J. B. Kaplan, *J. Dent. Res.*, 2010, **89**, 205–218.

136 T. Rasamiravaka, Q. Labtani, P. Duez and M. El Jaziri, *BioMed Res. Int.*, 2015, **2015**, 759348.

137 H. Mikkelsen, M. Sivaneson and A. Filloux, *Environ. Microbiol.*, 2011, **13**, 1666–1681.

138 M. Bejerano-Sagie and K. B. Xavier, *Curr. Opin. Microbiol.*, 2007, **10**, 189–198.

139 P. Cornelis, *Appl. Microbiol. Biotechnol.*, 2010, **86**, 1637–1645.

140 S. Wagner, R. Sommer, S. Hinsberger, C. Lu, R. W. Hartmann, M. Empting and A. Titz, *J. Med. Chem.*, 2016, **59**, 5929–5969.

141 Y. Carmeli, N. Troillet, G. M. Eliopoulos and M. H. Samore, *Antimicrob. Agents Chemother.*, 1999, **43**, 1379–1382.

142 H. P. Schweizer, *Genet. Mol. Res. GMR*, 2003, **2**, 48–62.

143 S. Tamber and R. E. W. Hancock, *Front. Biosci. J. Virtual Libr.*, 2003, **8**, s472-483.

144 R. E. W. Hancock and D. P. Speert, *Drug Resist. Updat.*, 2000, **3**, 247–255.

145 E. B. M. Breidenstein, C. de la Fuente-Núñez and R. E. W. Hancock, *Trends Microbiol.*, 2011, **19**, 419–426.

146 H. Pai, J.-W. Kim, J. Kim, J. H. Lee, K. W. Choe and N. Gotoh, *Antimicrob. Agents Chemother.*, 2001, **45**, 480–484.

147 J. R. Aeschlimann, *Pharmacother. J. Hum. Pharmacol. Drug Ther.*, 2003, **23**, 916–924.

148 D. M. Livermore, *Clin. Infect. Dis.*, 2002, **34**, 634–640.

149 T. R. Walsh, M. A. Toleman, L. Poirel and P. Nordmann, *Clin. Microbiol. Rev.*, 2005, **18**, 306–325.

150 C. Juan, M. D. Maciá, O. Gutiérrez, C. Vidal, J. L. Pérez and A. Oliver, *Antimicrob. Agents Chemother.*, 2005, **49**, 4733–4738.

151 G. F. Weldhagen, L. Poirel and P. Nordmann, *Antimicrob. Agents Chemother.*, 2003, **47**, 2385–2392.

152 Y. Matsuo, S. Eda, N. Gotoh, E. Yoshihara and T. Nakae, *FEMS Microbiol. Lett.*, 2004, **238**, 23–28.

153 M. M. Ochs, M. P. McCusker, M. Bains and R. E. W. Hancock, *Antimicrob. Agents Chemother.*, 1999, **43**, 1085–1090.

154 D. C. Hooper, *Emerg. Infect. Dis.*, 2001, **7**, 337–341.

155 M. Barber and P. M. Waterworth, *Br. Med. J.*, 1966, **1**, 203–205.

156 L. Fernández, E. B. M. Breidenstein and R. E. W. Hancock, *Drug Resist. Updat.*, 2011, **14**, 1–21.

157 H. Mouneimné, J. Robert, V. Jarlier and E. Cambau, *Antimicrob. Agents Chemother.*, 1999, **43**, 62–66.

158 J. T. Zobell, D. C. Young, C. D. Waters, K. Ampofo, J. Cash, B. C. Marshall, J. Olson and B. A. Chatfield, *Pediatr. Pulmonol.*, 2011, **46**, 987–990.

159 J. T. Zobell, D. C. Young, C. D. Waters, C. Stockmann, K. Ampofo, C. M. T. Sherwin and M. G. Spigarelli, *Pediatr. Pulmonol.*, 2012, **47**, 1147–1158.

160 L. M. Rose and R. Neale, *Sci. Transl. Med.*, 2010, **2**, 63mr4-63mr4.

161 C. Stockmann, C. M. T. Sherwin, J. T. Zobell, D. C. Young, C. D. Waters, M. G. Spigarelli and K. Ampofo, *Pediatr. Pulmonol.*, 2013, **48**, 211–220.

162 W. Couet, N. Grégoire, S. Marchand and O. Mimoz, *Clin. Microbiol. Infect.*, 2012, **18**, 30–39.

163 M. S. Oliveira, G. V. B. Prado, S. F. Costa, R. S. Grinbaum and A. S. Levin, *Diagn. Microbiol. Infect. Dis.*, 2009, **65**, 431–434.

164 S. Faruqi, J. McCreanor, T. Moon, R. Meigh and A. H. Morice, *Int. J. Antimicrob. Agents*, 2008, **32**, 461–463.

165 A. Mirakhur, M. J. Gallagher, M. J. Ledson, C. A. Hart and M. J. Walshaw, *J. Cyst. Fibros.*, 2003, **2**, 19–24.

166 E. Selva, L. Gastaldo, G. S. Saddler, G. Toppo, P. Ferrari, G. Carniti and B. P. Goldstein, *J. Antibiot. (Tokyo)*, 1996, **49**, 145–149.

167 F. Sasse, H. Steinmetz, T. Schupp, F. Petersen, K. Memmert, H. Hofmann, C. Heusser, V. Brinkmann, P. von Matt, G. Höfle and H. Reichenbach, *J. Antibiot. (Tokyo)*, 2002, **55**, 543–551.

168 L. Vollbrecht, H. Steinmetz, G. Hofle, L. Oberer, G. Rihs, G. Bovermann and P. von Matt, *J. Antibiot. (Tokyo)*, 2002, **55**, 715–721.

169 I. Nickeleit, S. Zender, F. Sasse, R. Geffers, G. Brandes, I. Sorensen, H.

Steinmetz, S. Kubicka, T. Carlomagno, D. Menche, I. Gutgemann, J. Buer, A. Gossler, M. P. Manns, M. Kalesse, R. Frank and N. P. Malek, *Cancer Cell*, 2008, **14**, 23–35.

170 B. Nyfeler, D. Hoepfner, D. Palestrant, C. A. Kirby, L. Whitehead, R. Yu, G. Deng, R. E. Caughlan, A. L. Woods, A. K. Jones, S. W. Barnes, J. R. Walker, S. Gaulis, E. Hauy, S. M. Brachmann, P. Krastel, C. Studer, R. Riedl, D. Estoppey, T. Aust, N. R. Movva, Z. Wang, M. Salcius, G. A. Michaud, G. McAllister, L. O. Murphy, J. A. Tallarico, C. J. Wilson and C. R. Dean, *PLoS One*, 2012, **7**, e42657.

171 V. Ramakrishnan, *Cell*, 2002, **108**, 557–572.

172 T. M. Schmeing and V. Ramakrishnan, *Nature*, 2009, **461**, 1234–1242.

173 S. Shoji, S. E. Walker and K. Fredrick, *ACS Chem. Biol.*, 2009, **4**, 93–107.

174 H. R. Bourne, D. A. Sanders and F. McCormick, *Nature*, 1991, **349**, 117–127.

175 T. E. Dever, M. J. Glynias and W. C. Merrick, *Proc. Natl. Acad. Sci. U. S. A.*, 1987, **84**, 1814–1818.

176 E. Salsi, E. Farah and D. N. Ermolenko, *J. Mol. Biol.*, 2016, **428**, 2248–2258.

177 M. V. Rodnina, A. Savelsbergh, V. I. Katunin and W. Wintermeyer, *Nature*, 1997, **385**, 37–41.

178 A. AEvarsson, E. Brazhnikov, M. Garber, J. Zheltonosova, Y. Chirgadze, S. al-Karadaghi, L. A. Svensson and A. Liljas, *EMBO J.*, 1994, **13**, 3669–3677.

179 E. D. Brown, *Biochem. Cell Biol.*, 2005, **83**, 738–746.

180 K. Nagai, C. Oubridge, T. H. Jessen, J. Li and P. R. Evans, *Nature*, 1990, **348**, 515–520.

181 S. Al-Karadaghi, A. Ævarsson, M. Garber, J. Zheltonosova and A. Liljas, *Structure*, 1996, **4**, 555–565.

182 J. Zhou, L. Lancaster, J. P. Donohue and H. F. Noller, *Science*, 2013, **340**,

1236086.

183 R. K. Agrawal, A. B. Heagle, P. Penczek, R. A. Grassucci and J. Frank, *Nat. Struct. Biol.*, 1999, **6**, 643–647.

184 H. Stark, M. V. Rodnina, H.-J. Wieden, M. van Heel and W. Wintermeyer, *Cell*, 2000, **100**, 301–309.

185 Y. Chen, S. Feng, V. Kumar, R. Ero and Y.-G. Gao, *Nat. Struct. Mol. Biol.*, 2013, **20**, 1077–1084.

186 Y.G. Gao, M. Selmer, C. M. Dunham, A. Weixlbaumer, A. C. Kelley and V. Ramakrishnan, *Science*, 2009, **326**, 694–699.

187 C. E. Cunha, R. Belardinelli, F. Peske, W. Holtkamp, W. Wintermeyer and M. V. Rodnina, *Translation*, 2013, **1**, e24315.

188 G. R. Willie, N. Richman, W. O. Godtfredsen and J. W. Bodley, *Biochemistry (Mosc.)*, 1975, **14**, 1713–1718.

189 A. Okura, T. Kinoshita and N. Tanaka, *J. Antibiot. (Tokyo)*, 1971, **24**, 655–661.

190 A. Borg, M. Holm, I. Shiroyama, V. Hauryliuk, M. Pavlov, S. Sanyal and M. Ehrenberg, *J. Biol. Chem.*, 2015, **290**, 3440–3454.

191 W. Wintermeyer, A. Savelsbergh, Y. P. Semenkov, V. I. Katunin and M. V. Rodnina, *Cold Spring Harb. Symp. Quant. Biol.*, 2001, **66**, 449–458.

192 Y. Chen, R. K. Koripella, S. Sanyal and M. Selmer, *FEBS J.*, 2010, **277**, 3789–3803.

193 C. Ticu, M. Murataliev, R. Nechifor and K. S. Wilson, *J. Biol. Chem.*, 2011, **286**, 21697–21705.

194 D. Dobie and J. Gray, *Arch. Dis. Child.*, 2004, **89**, 74–77.

195 I. Nagaev, J. Björkman, D. I. Andersson and D. Hughes, *Mol. Microbiol.*, 2001, **40**, 433–439.

196 K. A. Martemyanov, A. Liljas, A. S. Yarunin and A. T. Gudkov, *J. Biol. Chem.*, 2001, **276**, 28774–28778.

197 A. J. O'Neill, F. McLaws, G. Kahlmeter, A. S. Henriksen and I. Chopra, *Antimicrob. Agents Chemother.*, 2007, **51**, 1737–1740.

198 T. Norström, J. Lannergård and D. Hughes, *Antimicrob. Agents Chemother.*, 2007, **51**, 4438–4446.

199 P. Bielecki, P. Lukat, K. Hüsecken, A. Dötsch, H. Steinmetz, R. W. Hartmann, R. Müller and S. Häussler, *ChemBioChem*, 2012, **13**, 2339–2345.

200 J. Heitman, N. R. Movva and M. N. Hall, *Science*, 1991, **253**, 905–909.

201 P. Smits, J. Smeitink and L. van den Heuvel, *J. Biomed. Biotechnol.*, 2010, **2010**, 737385.

202 S. V. Ley and A. Priour, *Eur. J. Org. Chem.*, 2002, **2002**, 3995–4004.

203 W. B. Wu, Z. Li, G. B. Zhou and S. Jiang, *Tetrahedron Lett.*, 2011, **52**, 2488–2491.

204 L. Bülow, I. Nickeleit, A.-K. Girbig, T. Brodmann, A. Rentsch, U. Eggert, F. Sasse, H. Steinmetz, R. Frank, T. Carlomagno, N. P. Malek and M. Kalesse, *ChemMedChem*, 2010, **5**, 832–836.

205 C.-H. Chen, S. Genapathy, P. M. Fischer and W. C. Chan, *Org. Biomol. Chem.*, 2014, **12**, 9764–9768.

206 E. Aguilar and A. I. Meyers, *Tetrahedron Lett.*, 1994, **35**, 2473–2476.

207 K. Harada, *Nature*, 1963, **200**, 1201–1201.

208 D. S. Nielsen, H. N. Hoang, R.-J. Lohman, F. Diness and D. P. Fairlie, *Org. Lett.*, 2012, **14**, 5720–5723.

209 Z. Xia and C. D. Smith, *J. Org. Chem.*, 2001, **66**, 3459–3466.

210 R. A. Hughes, S. P. Thompson, L. Alcaraz and C. J. Moody, *J. Am. Chem. Soc.*, 2005, **127**, 15644–15651.

211 Z. Wang, *Comprehensive Organic Name Reactions and Reagents*, John Wiley & Sons, Inc., 2010.

212 U. Schmidt, P. Gleich, H. Griesser and R. Utz, *Synthesis*, 1986, **1986**, 992–998.

213 Y. Hamada, M. Shibata, T. Sugiura, S. Kato and T. Shioiri, *J. Org. Chem.*, 1987, **52**, 1252–1255.

214 S. Fenner, Z. E. Wilson and S. V. Ley, *Chem. Eur. J.*, 2016, **22**, 15902–

15912.

215 S. Scheibye, B. S. Pedersen and S.-O. Lawesson, *Bull. Sociétés Chim. Belg.*, 1978, **87**, 229–238.

216 G. Lajoie, F. Lépine, L. Maziak and B. Belleau, *Tetrahedron Lett.*, 1983, **24**, 3815–3818.

217 M. Jesberger, T. P. Davis and L. Barner, *Synthesis*, 2003, **2003**, 1929–1958.

218 M. W. Bredenkamp, C. W. Holzapfel and W. J. van Zyl, *Synth. Commun.*, 1990, **20**, 2235–2249.

219 S. V. Ley, A. Priour and C. Heusser, *Org. Lett.*, 2002, **4**, 711–714.

220 C.H. Chen, Thesis, University of Nottingham, 2013.

221 B. Meseguer, D. Alonso-Díaz, N. Griebenow, T. Herget and H. Waldmann, *Chem. Eur. J.*, 2000, **6**, 3943–3957.

222 V. R. Pattabiraman, J. L. Stymiest, D. J. Derksen, N. I. Martin and J. C. Vederas, *Org. Lett.*, 2007, **9**, 699–702.

223 The Nobel Prize in Chemistry 2001, https://www.nobelprize.org/nobel_prizes/chemistry/laureates/2001/, (accessed 26 September 2017).

224 Y. Jia and J. Zhu, *J. Org. Chem.*, 2006, **71**, 7826–7834.

225 J. M. Padrón, G. Kokotos, T. Martín, T. Markidis, W. A. Gibbons and V. S. Martín, *Tetrahedron Asymm.* , 1998, **9**, 3381–3394.

226 Y. N. Belokon, A. G. Bulychev, S. V. Vitt, Y. T. Struchkov, A. S. Batsanov, T. V. Timofeeva, V. A. Tsyryapkin, M. G. Ryzhov and L. A. Lysova, *J. Am. Chem. Soc.*, 1985, **107**, 4252–4259.

227 V. A. Soloshonok, C. Cai and V. J. Hruby, *Tetrahedron Lett.*, 2000, **41**, 135–139.

228 A. Popkov, V. Langer, P. A. Manorik and T. Weidlich, *Transit. Met. Chem.*, 2003, **28**, 475–481.

229 A. E. Sorochinsky, J. L. Aceña, H. Moriwaki, T. Sato and V. A. Soloshonok, *Amino Acids*, 2013, **45**, 691–718.

230 A. Popkov and B. D. Spiegeleer, *Dalton Trans.*, 2012, **41**, 1430–1440.

231 V. A. Soloshonok, D. V. Avilov and V. P. Kukhar, *Tetrahedron Asymm.*, 1996, **7**, 1547–1550.

232 V. A. Soloshonok, C. Cai and V. J. Hruby, *Tetrahedron Lett.*, 2000, **41**, 9645–9649.

233 J. Wang, T. Shi, G. Deng, H. Jiang and H. Liu, *J. Org. Chem.*, 2008, **73**, 8563–8570.

234 V. A. Soloshonok, X. Tang, V. J. Hruby and L. V. Meervelt, *Org. Lett.*, 2001, **3**, 341–343.

235 A. Vilsmeier and A. Haack, *Berichte Dtsch. Chem. Ges. B Ser.*, 1927, **60**, 119–122.

236 Y. Basel and A. Hassner, *J. Org. Chem.*, 2000, **65**, 6368–6380.

237 J. Thesing, *Chem. Ber.*, 1954, **87**, 692–699.

238 H. Brückner and C. Keller-Hoehl, *Chromatographia*, 1990, **30**, 621–629.

239 P. Marfey, *Carlsberg Res. Commun.*, 1984, **49**, 591.

240 A. Paquet, *Can. J. Chem.*, 1982, **60**, 976–980.

241 D. Siodłak, *Amino Acids*, 2015, **47**, 1–17.

242 A. T. R. Mattick and A. Hirsch, *Lancet Lond. Engl.*, 1947, **2**, 5–8.

243 G. Bierbaum and H.G. Sahl, *Curr. Pharm. Biotechnol.*, 2009, **10**, 2–18.

244 C. Chatterjee, M. Paul, L. Xie and W. A. van der Donk, *Chem. Rev.*, 2005, **105**, 633–684.

245 J. Dischinger, I. Wiedemann, G. Bierbaum and H.-G. Sahl, in *Handbook of Biologically Active Peptides (Second Edition)*, ed. A. J. Kastin, Academic Press, Boston, 2013, pp. 119–128.

246 H. E. Hasper, B. de Kruijff and E. Breukink, *Biochemistry (Mosc.)*, 2004, **43**, 11567–11575.

247 T. J. Oman and W. A. van der Donk, *ACS Chem. Biol.*, 2009, **4**, 865–874.

248 K. Hosoda, M. Ohya, T. Kohno, T. Maeda, S. Endo and K. Wakamatsu, *J. Biochem. (Tokyo)*, 1996, **119**, 226–230.

249 J. Béahdy, in *Advances in Applied Microbiology*, ed. D. Perlman,

Academic Press, 1974, vol. 18, pp. 309–406.

250 L. C. W. Brown, M. G. Acker, J. Clardy, C. T. Walsh and M. A. Fischbach, *Proc. Natl. Acad. Sci.*, 2009, **106**, 2549–2553.

251 W. L. Kelly, L. Pan and C. Li, *J. Am. Chem. Soc.*, 2009, **131**, 4327–4334.

252 K. Engelhardt, K. F. Degnes, M. Kemmler, H. Bredholt, E. Fjaervik, G. Klinkenberg, H. Sletta, T. E. Ellingsen and S. B. Zotchev, *Appl. Environ. Microbiol.*, 2010, **76**, 4969–4976.

253 R. Liao, L. Duan, C. Lei, H. Pan, Y. Ding, Q. Zhang, D. Chen, B. Shen, Y. Yu and W. Liu, *Chem. Biol.*, 2009, **16**, 141–147.

254 X. Baringo, F. Albericio and M. Álvarez, *Mar. Drugs*, 2014, **12**, 317–351.

255 J. D. Walter, M. Hunter, M. Cobb, G. Traeger and P. C. Spiegel, *Nucleic Acids Res.*, 2012, **40**, 360–370.

256 A. Parmeggiani and P. Nissen, *FEBS Lett.*, 2006, **580**, 4576–4581.

257 C. H. McGinnis, C. A. Johnson and J. E. Fox, *Poult. Sci.*, 1978, **57**, 1641–1645.

258 J. M. Humphrey and A. R. Chamberlin, *Chem. Rev.*, 1997, **97**, 2243–2266.

259 D. Ranganathan, K. Shah and N. Vaish, *J. Chem. Soc. Chem. Commun.*, 1992, **0**, 1145–1147.

260 C. Bonauer, T. Walenzyk and B. König, *Synthesis*, 2006, **2006**, 1–20.

261 K. Goodall and A. F. Parsons, *Tetrahedron Lett.*, 1995, **36**, 3259–3260.

262 R. J. Cherney and L. Wang, *J. Org. Chem.*, 1996, **61**, 2544–2546.

263 I. Photaki, *J. Am. Chem. Soc.*, 1963, **85**, 1123–1126.

264 R. F. Cunico and L. Bedell, *J. Org. Chem.*, 1980, **45**, 4797–4798.

265 D. H. Strumeyer, W. N. White and D. E. Koshland, *Proc. Natl. Acad. Sci.*, 1963, **50**, 931–935.

266 Y. Nakagawa, T. Tsuno, K. Nakajima, M. Iwai, H. Kawai and K. Okawa, *Bull. Chem. Soc. Jpn.*, 1972, **45**, 1162–1167.

267 P. M. T. Ferreira, H. L. S. Maia, L. S. Monteiro and J. Sacramento, *J. Chem. Soc. [Perkin 1]*, 1999, **0**, 3697–3703.

268 H. Tanaka, A. M. Sawayama and T. J. Wandless, *J. Am. Chem. Soc.*, 2003,

125, 6864–6865.

269 D. P. Galonić, W. A. van der Donk and D. Y. Gin, *Chem. Eur. J.*, 2003, **9**, 5997–6006.

270 K. Nakamura, T. Isaka, H. Toshima and M. Kodaka, *Tetrahedron Lett.*, 2004, **45**, 7221–7224.

271 Z. Miao and J. P. Tam, *Org. Lett.*, 2000, **2**, 3711–3713.

272 K. Nakamura, Y. Ohnishi, E. Horikawa, T. Konakahara, M. Kodaka and H. Okuno, *Tetrahedron Lett.*, 2003, **44**, 5445–5448.

273 R. Walter and J. Roy, *J. Org. Chem.*, 1971, **36**, 2561–2563.

274 H. Zhou and W. A. van der Donk, *Org. Lett.*, 2002, **4**, 1335–1338.

275 N. M. Okeley, Y. Zhu and W. A. van der Donk, *Org. Lett.*, 2000, **2**, 3603–3606.

276 O. Mitsunobu and M. Yamada, *Bull. Chem. Soc. Jpn.*, 1967, **40**, 2380–2382.

277 S. Fletcher, *Org. Chem. Front.*, 2015, **2**, 739–752.

278 S. G. Nelson, K. L. Spencer, W. S. Cheung and S. J. Mamie, *Tetrahedron*, 2002, **58**, 7081–7091.

279 N. D. Smith and M. Goodman, *Org. Lett.*, 2003, **5**, 1035–1037.

280 D. Liotta, W. Markiewicz and H. Santiesteban, *Tetrahedron Lett.*, 1977, **18**, 4365–4367.

281 M. L. Pedersen and D. B. Berkowitz, *J. Org. Chem.*, 1993, **58**, 6966–6975.

282 R. B. Merrifield, *J. Am. Chem. Soc.*, 1963, **85**, 2149–2154.

283 The Nobel Prize in Chemistry 1984, https://www.nobelprize.org/nobel_prizes/chemistry/laureates/1984/, (accessed 25 September 2017).

284 R. B. Merrifield, *Biochemistry (Mosc.)*, 1964, **3**, 1385–1390.

285 S. Sakakibara, Y. Shimonishi, Y. Kishida, M. Okada and H. Sugihara, *Bull. Chem. Soc. Jpn.*, 1967, **40**, 2164–2167.

286 L. A. Carpino and G. Y. Han, *J. Am. Chem. Soc.*, 1970, **92**, 5748–5749.

287 G. R. Matsueda and J. M. Stewart, *Peptides*, 1981, **2**, 45–50.

288 S.-S. Wang, *J. Am. Chem. Soc.*, 1973, **95**, 1328–1333.

289 M. Verlander, *Int. J. Pept. Res. Ther.*, 2007, **13**, 75–82.

290 G. Barany and R. B. Merrifield, *J. Am. Chem. Soc.*, 1977, **99**, 7363–7365.

291 C. D. Chang and J. Meienhofer, *Int. J. Pept. Protein Res.*, 1978, **11**, 246–249.

292 H. M. Geysen, R. H. Meloen and S. J. Barteling, *Proc. Natl. Acad. Sci. U. S. A.*, 1984, **81**, 3998–4002.

293 R. A. Houghten, *Proc. Natl. Acad. Sci.*, 1985, **82**, 5131–5135.

294 M. Mergler, R. Tanner, J. Gosteli and P. Grogg, *Tetrahedron Lett.*, 1988, **29**, 4005–4008.

295 H. Rink, *Tetrahedron Lett.*, 1987, **28**, 3787–3790.

296 P. Sieber, *Tetrahedron Lett.*, 1987, **28**, 2107–2110.

297 K. Barlos, D. Gatos, J. Kallitsis, G. Papaphotiu, P. Sotiriu, Y. Wenqing and W. Schäfer, *Tetrahedron Lett.*, 1989, **30**, 3943–3946.

298 M. Schnölzer, P. Alewood, A. Jones, D. Alewood and S. B. H. Kent, *Int. J. Pept. Res. Ther.*, 2007, **13**, 31–44.

299 W. Bannwarth, in *Combinatorial Chemistry*, eds. W. Bannwarth and E. Felder, Wiley-VCH Verlag GmbH, 2000, pp. 47–208.

300 T. Wöhr and M. Mutter, *Tetrahedron Lett.*, 1995, **36**, 3847–3848.

301 M. Brandt, S. Gammeltoft and K. J. Jensen, *Int. J. Pept. Res. Ther.*, 2006, **12**, 349–357.

302 P. White, J. W. Keyte, K. Bailey and G. Bloomberg, *J. Pept. Sci. Off. Publ. Eur. Pept. Soc.*, 2004, **10**, 18–26.

303 R. Sheppard, *J. Pept. Sci.*, 2003, **9**, 545–552.

304 I. Coin, M. Beyermann and M. Bienert, *Nat. Protoc.*, 2007, **2**, 3247–3256.

305 B. Merrifield, *Science*, 1986, **232**, 341–347.

306 V. K. Sarin, S. B. H. Kent and R. B. Merrifield, *J. Am. Chem. Soc.*, 1980, **102**, 5463–5470.

307 F. I. Auzanneau, M. Meldal and K. Bock, *J. Pept. Sci. Off. Publ. Eur. Pept. Soc.*, 1995, **1**, 31–44.

308 G. A. Acosta, M. del Fresno, M. Paradis-Bas, M. Rigau-DeLlobet, S. Côté, M. Royo and F. Albericio, *J. Pept. Sci. Off. Publ. Eur. Pept. Soc.*, 2009, **15**, 629–633.

309 W. Chan and P. White, Eds., *Fmoc Solid Phase Peptide Synthesis: A Practical Approach*, Oxford University Press, Oxford, New York, 1999.

310 J. C. Sheehan and G. P. Hess, *J. Am. Chem. Soc.*, 1955, **77**, 1067–1068.

311 S. L. Pedersen, A. P. Tofteng, L. Malik and K. J. Jensen, *Chem. Soc. Rev.*, 2012, **41**, 1826–1844.

312 J. Coste, D. Le-Nguyen and B. Castro, *Tetrahedron Lett.*, 1990, **31**, 205–208.

313 D. Hudson, *J. Org. Chem.*, 1988, **53**, 617–624.

314 R. Subirós-Funosas, R. Prohens, R. Barbas, A. El-Faham and F. Albericio, *Chem. Eur. J.*, 2009, **15**, 9394–9403.

315 V. Dourtoglou, J.-C. Ziegler and B. Gross, *Tetrahedron Lett.*, 1978, **19**, 1269–1272.

316 L. A. Carpino, A. El-Faham and F. Albericio, *Tetrahedron Lett.*, 1994, **35**, 2279–2282.

317 L. A. Carpino, H. Imazumi, B. M. Foxman, M. J. Vela, P. Henklein, A. El-Faham, J. Klose and M. Bienert, *Org. Lett.*, 2000, **2**, 2253–2256.

318 P. Athanassopoulos, K. Barlos, D. Gatos, O. Hatzi and C. Tzavara, *Tetrahedron Lett.*, 1995, **36**, 5645–5648.

319 K. Barlos, D. Gatos, S. Kapolos, C. Poulos, W. Schäfer and Y. Wenqing, *Int. J. Pept. Protein Res.*, 1991, **38**, 555–561.

320 M. Malesevic, U. Strijowski, D. Bachle and N. Sewald, *J. Biotechnol.*

321 J. Hachmann and M. Lebl, *Pept. Sci.*, 2006, **84**, 340–347.

322 Sivaneswary Genapathy, Thesis, University of Nottingham, 2015

323 M. A. Larkin, G. Blackshields, N. P. Brown, R. Chenna, P. A. McGettigan, H. McWilliam, F. Valentin, I. M. Wallace, A. Wilm, R. Lopez, J. D. Thompson, T. J. Gibson and D. G. Higgins, *Bioinformatics*, 2007, **23**, 2947–2948.

324 E. Lacey, J. A. Edgar and C. C. J. Culvenor, *Biochem. Pharmacol.*, 1987, **36**, 2133–2138.

325 N. Shimada, K. Morimoto, H. Naganawa, T. Takita, M. Hamada, K. Maeda, T. Takeuchi and H. Umezawa, *J. Antibiot. (Tokyo)*, 1981, **34**, 1613–1614.

326 Y. Yasuno, M. Hamada, T. Yamada, T. Shinada and Y. Ohfune, *Eur. J. Org. Chem.*, 2013, **2013**, 1884–1888.

327 J. C. Jiménez, B. Chavarría, À. López-Macià, M. Royo, E. Giralt and F. Albericio, *Org. Lett.*, 2003, **5**, 2115–2118.

328 I. Wiegand, K. Hilpert and R. E. W. Hancock, *Nat. Protoc.*, 2008, **3**, 163–175.

329 D. M. Hacek, D. C. Dressel and L. R. Peterson, *J. Clin. Microbiol.*, 1999, **37**, 1881–1884.

330 G. A. Pankey and L. D. Sabath, *Clin. Infect. Dis.*, 2004, **38**, 864–870.

331 Y. N. Belokon', V. I. Tararov, V. I. Maleev, T. F. Savel'eva and M. G. Ryzhov, *Tetrahedron Asymm.*, 1998, **9**, 4249–4252.

332 Y. N. Belokon, I. E. Zel'tser, V. I. Bakhmutov, M. B. Saporovskaya, M. G. Ryzhov, A. I. Yanovskii, Y. T. Struchkov and V. M. Belikov, *J. Am. Chem. Soc.*, 1983, **105**, 2010–2017.